Diesel Exhaust Particles and Macrophage Function:

Relevance to COPD

By

Gurpreet Sehra

A Thesis Submitted to Imperial College London

For the Degree of Doctor of Philosophy in the Faculty of Medicine

September, 2013

National Heart and Lung Institute, Imperial College London

Dovehouse Street, London, SW3 6LY

Abstract

Atmospheric pollution is a global problem with a significant health risk. For example, inhalation of diesel exhaust particles (DEP), a major component of atmospheric pollution, increases the incidence of exacerbations in patients with chronic obstructive pulmonary disease (COPD). DEP comprise a carbon core with adsorbed chemical compounds, metals and endotoxin. Inhaled DEP deposit in the lung and are targets for macrophages. Macrophages normally clear inhaled DEP and maintain lung sterility. However, macrophages also drive COPD pathophysiology by releasing inflammatory mediators. DEP heighten chronic inflammatory processes and induce cytotoxicity in macrophages. However the effects of DEP on macrophages from COPD patients remain unclear. The hypothesis underlying the present thesis was that 'DEP modulate macrophage pro-inflammatory mediator release and phagocytosis, and this is more prominent in COPD. To address this hypothesis, monocyte-derived macrophages (MDM) from non-smokers, smokers and patients with COPD were exposed to three types of DEP, termed DEP-N (generated from a light engine), standard reference material (SRM)-1650B, SRM-2975 and control inert beads, and MDM viability, mediator release and phagocytosis were examined. Characterisation of the DEP showed each sample to be heterogeneous in size, and subject to aggregation. Fe and Cu metals were associated with the DEP-N sample but not with SRM-1650B or SRM-2975. DEP at concentrations ≤ 100μg/ml did not induce cytotoxicity in MDM from non-smokers, smokers and patients with COPD, as determined by MTT. DEP-N, but not SRM-2975, SRM-1650B or inert beads, stimulated CXCL8 release by MDM compared with non-stimulated controls. This was not due to endotoxin in the DEP-N samples. MDM from non-smokers and COPD patients were twice as responsive to DEP-N as cells from smokers. DEP-N-treated

MDM activated p38 and ERK 1/2 MAPK pathways. A p38 inhibitor (PF-755616) or MEK inhibitor (PD98059) suppressed DEP-N-induced MDM activation of p38 or ERK 1/2 respectively, with associated inhibition of CXCL8 release, with no effect on viability. DEP-N inhibited MDM phagocytosis of beads from all subject groups in a concentration-dependent manner, which was to some extent, associated with decreased cell viability.

In conclusion, DEP-N, but not SRM, stimulated MDM CXCL8 release and suppressed phagocytosis, possibly as a result of differences in surface-adsorbed metals. The combined, opposite functional effects of DEP may, at least in part, contribute to the association between DEP exposure and incidence of exacerbations in patients with COPD. DEP-induced CXCL8 release was mediated *via* p38 and ERK 1/2 MAPK pathways, which suggests that inhibition of p38 or ERK 1/2 signalling may have therapeutic potential in COPD.

Acknowledgements

I am grateful to my supervisors Professor Louise Donnelly and Dr Duncan Rogers for giving me the opportunity to undertake this PhD in their laboratory. I am thankful for their continuous support, guidance and mentoring throughout the duration of this course. I would like to express my gratitude to Mr Peter Fenwick for teaching me everything I need to know in the laboratory and for his kind support over the years. I would also like to thank Ms Sally Meah who has constantly provided blood samples to complete experiments.

A special thank you also goes to all my friends past and present, who have offered their support in numbers during the highs and lows of the PhD. A special mention goes to Vikram, Purvi, Jen, Harpal, Julie, Nadia, Kiran, Catherine and Patricia; I've always enjoyed having our chats over a cup of tea and a slice of cake. I would also like to thank the rest of 'Team Donnelly' and 'Team Rogers' - Rebecca, Kylie, Joanne, Amy Turner, Amy Day, Tankut and Natasha for their help over the years.

Last but not least, I would like to thank my family for their constant supply of support, patience, encouragement and wise words. They have always told me that anything is possible as long you work hard and are dedicated, these wise words have seen me to the end of this PhD. Thank you.

Declaration

I declare that this thesis is entirely my own work.

Gurpreet Sehra.

Table of Contents **Page Number**

List of Figures — Page Number

List of Tables Page Number

Abbreviations

AHR	Airway hyper-responsiveness
AM	Alveolar macrophages
ANOVA	Analysis of variance
AP.1	Activator protein 1
BAL	Bronchial alveolar lavage
BSA	Bovine serum albumin
CAPs	Concentrated ambient particles
CB	Carbon black
CD	Cluster of differentiation
CO	Carbon monoxide
CO_2	Carbon dioxide
COPD	Chronic obstructive pulmonary disease
CR	Complement receptors
CRP	C-reactive protein
CSF	Colony stimulating factor
CXC	C-X-C motif
CXCR	C-X-C chemokine receptor
DAPI	4',6-diamidino-2-phenylindole
ddH_20	Double-distilled water
DEP	Diesel exhaust particles
DEP-E	Diesel exhaust particle extract
DEP-N	Diesel exhaust particles used by Nightingale, *et al*, 2000
DEP-W	Washed diesel exhaust particles
DMSO	Dimethyl sulfoxide
DNA	Deoxyribonucleic acid

DOFA	Desferrioxamine
D-PBS	Dulbecco's phosphate buffered saline
ECL	Enhanced chemiluminescence
ECM	Extracellular matrix
EDTA	Ethylene-diamine-tetra-acetic-acid
EFW	Endotoxin free water
EGF	Epidermal growth factor
EGTA	Ethylene glycol tetra-acetic acid
ELISA	Enzyme-linked immunosorbant assays
ERK 1/2	Extracellular signal regulated kinase 1/2
FACS	Fluorescence activated cell sorter
FCS	Foetal calf serum
FEV_1	Forced expiratory volume in 1 sec
FVC	Forced vital capacity
GOLD	Global initiative for chronic obstructive lung diseases
GM-CSF	Granulocyte macrophage colony stimulating factor
H_2O	Water
H_2SO_4	Sulphuric acid
HBSS	Hanks balanced salt solution
HEPES	4-(2-hydroxyethyl)-1-piperazineethanesulfonic acid
HLA-DR	Human leukocyte antigen DR
HRA	Health research authority
HRP	Horse radish peroxidase
HSP27	Heat shock protein 27
IC_{50}	Inhibitory concentration at 50%
ICP-OES	Inductively coupled plasma atomic emission spectroscopy

IFN	Interferon
Ig	Immunoglobulin
IL	Interleukin
IP-10	Interferon inducible protein-10
JNK	c-Jun N-terminal kinases
LAL	Limolas amebocyte lysate
LG	L-glutamine
LOS	Lipooligosacchride
LPS	Lipopolysaccharide
MAPK	Mitogen activated protein kinases
MARCO	Macrophage receptor with collagenous structure
MDM	Monocyte derived macrophages
MEK 1/2	Mitogen activate protein kinase kinase 1/2
MIG	Monokine induced by interferon gamma
MMP	Matrixmetalloproteases
MOPS	3-(N-morpholino)propanesulfonic acid
MTT	3-(4,5-Dithiazol-2-yl)-2,5-Diphenyltetrazolium
NAC	N-acetylcysteine
NFkB	Nuclear factor kappa light chain enhancer of activated B cells
NIST	National institute of standards and technology
Nitro-PAH	Nitro-polycyclic aromatic hydrocarbons
NHLI	National heart and lung institute
NO_2	Nitrogen oxides
NTHI	Non-typeable *H.influenzae*
OMP	Outer membrane protein
PAH	Polycyclic aromatic hydrocarbons

PAMP	Pathogen associated molecular patterns
PBMC	Peripheral blood mononuclear cells
PE	Phycoerythrin
PFA	Paraformaldehyde
PM	Particulate matter
$PM_{0.1}$	Particles with a diameter of 0.1μm
$PM_{2.5}$	Particles with a diameter of 2.5μm
PM_{10}	Particles with a diameter of 10μm
PRR	Pattern recognition receptors
PS	Penicillin/streptomycin
RBC	Red blood cells
RBH	Royal Brompton Hospital
ROS	Reactive oxygen species
RPMI-1640	Roswell park memorial institute-1640
RT	Room temperature
SAD	Small airways disease
SAPK	Stress activated protein kinase
SDS	Sodium dodecyl sulphate
SRM	Standard reference material
SO_2	Sulphur dioxide
SO_3	Sulphur trioxide
SP	Surfactant protein
SR	Scavenger receptors
TBS	Tris buffered saline
TEM	Transmission electron microscopy
TGF-β	Transforming growth factor β

TLR	Toll like receptor
TMB	Tetramethylbenzinidine
TNF	Tumour necrosis factor
TRIS	Tris(hydroxymethyl)aminomethane
TWEEN-20	Polysorbate 20
7-AAD	7-amino-actinomycin

Publications/Abstracts

1. **Sehra G.,** Barnes, P. J., Rogers, D. F., and Donnelly, L. E., (2013) Effect of Diesel Exhaust Particles on Monocyte-Derived Macrophage Mediator Release and Phagocytosis in Chronic Obstructive Pulmonary Disease. European Respiratory Society Conference, (Barcelona, Spain). Accepted.

2. **Sehra, G**., Rogers, D. F., and Donnelly, L. E., (2011). Differential Effects of Diesel Exhaust Particles and Endotoxin on Phagocytosis and Cytokine Release by Monocyte-Derived Macrophages. Eur Respir J. 38; Suppl 55, 700s.

3. **Sehra, G.,** Rogers, D. F., and Donnelly, L. E., (2011). Differential Effects of Diesel Exhaust Particles and Endotoxin on Phagocytosis and Cytokine Release by Monocyte-Derived Macrophages. European Respiratory Society Lung Science Conference (Estoril, Portugal).

4. **Sehra, G.,** Fenwick, P., Rogers, D. F., and Donnelly, L. E., (2010). Differential Effects of Diesel Exhaust Particles and Endotoxin on Phagocytosis and Cytokine Release by Monocyte-Derived Macrophages. Eur Respir J. 36; Suppl 54, 791s.

5. **Sehra, G.,** Rogers, D. F., and Donnelly, L. E., (2010). Differential Effects of Diesel Exhaust Particles and Endotoxin on Phagocytosis and Cytokine Release by Monocyte-Derived Macrophages. British Association of Lung Research Summer Meeting (Swansea, UK).

Chapter 1:

General Introduction

1.1 Introduction

Air pollution is increasing worldwide and has adverse effects on respiratory health (Dockery & Pope 1994; Kampa & Castanas 2008). Chronic obstructive pulmonary disease (COPD) is a respiratory condition affecting 200 million individuals globally, and is currently the fourth leading cause of death worldwide (Barnes 2004; Vermaelen & Brusselle 2013). COPD patients are susceptible to deleterious effects to their health caused by elevations in atmospheric pollution. In urban environments, a major contributor of atmospheric pollution is diesel exhaust particles (DEP), and inhalation of these particles are associated with increased respiratory symptoms in patients with COPD (Sunyer et al. 1993; Anderson et al. 1997; Sunyer et al. 2000). The small diameter (<0.1μm - <10μm) of DEP favour their deposition within the lung. Large particles deposit in the upper respiratory tract (>6μm) or nasal passages (Dockery & Pope 1994) and smaller particles (<2.5μm) deposit in terminal airways and become targets for alveolar macrophages, which, in turn, have been implicated in the pathophysiology of COPD (Donaldson & Stone 2003; Barnes 2004). DEP deposited in the alveolar compartment of the lung may stimulate inflammatory responses by pulmonary cells. The coupled effect of DEP-induced inflammation and macrophage activation in patients with COPD may contribute to the adverse health effects associated with elevations in atmospheric pollution. The present thesis describes research work aimed at understanding some of the effects of DEP on macrophage function.

1.2 Air Pollution

Atmospheric pollution is the contamination of indoor or outdoor air by biological, chemical and/or physical pollutants, in amounts sufficient to cause adverse effects in humans and/or animals, or to the natural environment (Olmo et al. 2011; Bell & Davis 2001). Pollutants generally have a complex composition and are emitted or formed by primary or secondary routes (Sonibare 2011). Primary pollutants, for example carbon monoxide (CO), sulfur dioxide (SO_2) or nitrogen oxides (e.g NO_2), are released directly into the atmosphere (Wanner 1993). Secondary pollutants are formed by interaction between primary pollutants in the atmosphere, for example the production of ozone or acid rain (Sonibare 2011). Atmospheric pollutants encompass heterogeneous liquid or solid particles, the latter including pollen, dust and soot. These particles are commonly referred to as particulate matter (PM) and are classified according to their aerodynamic diameter. For example, particles with diameters of approximately 0.1μm, 2.5μm or 10μm are referred to as $PM_{0.1}$, $PM_{2.5}$ or PM_{10} respectively (Backes et al. 2013).

1.2.1 Diesel Exhaust Particles

PM_{10} have been studied extensively and elevations in levels of atmospheric PM_{10} are associated with adverse effects on respiratory health, such as reduced lung function, disease exacerbations, increased hospitalisations and mortality, as determined by epidemiological studies (Bell & Davis 2001; Dockery & Pope 1994; Park et al. 2011). A major contributor to PM_{10} are vehicle exhaust emissions, including diesel exhaust (Murphy & Richards 1999; Mcclellan 1987). Diesel exhaust consists of gaseous and particulate components formed by the combustion of diesel fuel (Ono-Ogasawara & Smith 2004). The particulate component, termed diesel

exhaust particles (DEP), comprises an elemental carbon core 'soot', to which semi-volatile or low-volatile organic compounds are adsorbed, including polycyclic aromatic hydrocarbons (PAH) and nitro-PAHs (Table 1.1), endotoxin and metals, including Na, Mg, Si, Fe, Cu and Ca (Figure 1.1) (Saitoh et al. 2003; Sehlstedt, *et al*, 2010). Individual DEP invariably aggregate, and sulphite, water and sulphuric acid condense on the particle surface.

Table 1.1 Aromatic Hydrocarbons Adsorbed on Diesel Soot

PAHs	**Nitro-PAHs**
Phenathrene	1-Nitropyrene
Fluoranthene	1,6-Dinitropyrene
Pyrene	3-Nitrophenantherene
Benzo[*a*]anthracene	4-Nitropyrene
Benzo[*e*]pyrene	6-Nitrochrysene
Benzo[*ghi*]perylene	6-Nitrobenzo[*a*]pyrene
Benzo[*k*]fluoranthene	7-Nitrobenz[*a*]anthracene
Chrysene	9-Nitroanthracene

Adsorbed polycyclic aromatic hydrocarbons (PAHs) and nitro-PAHs on the surface of DEP. Table adapted from Chen & Cahill n.d., 2000 and National Institute of Standards and Technology (NIST) certificates (See Appendix III).

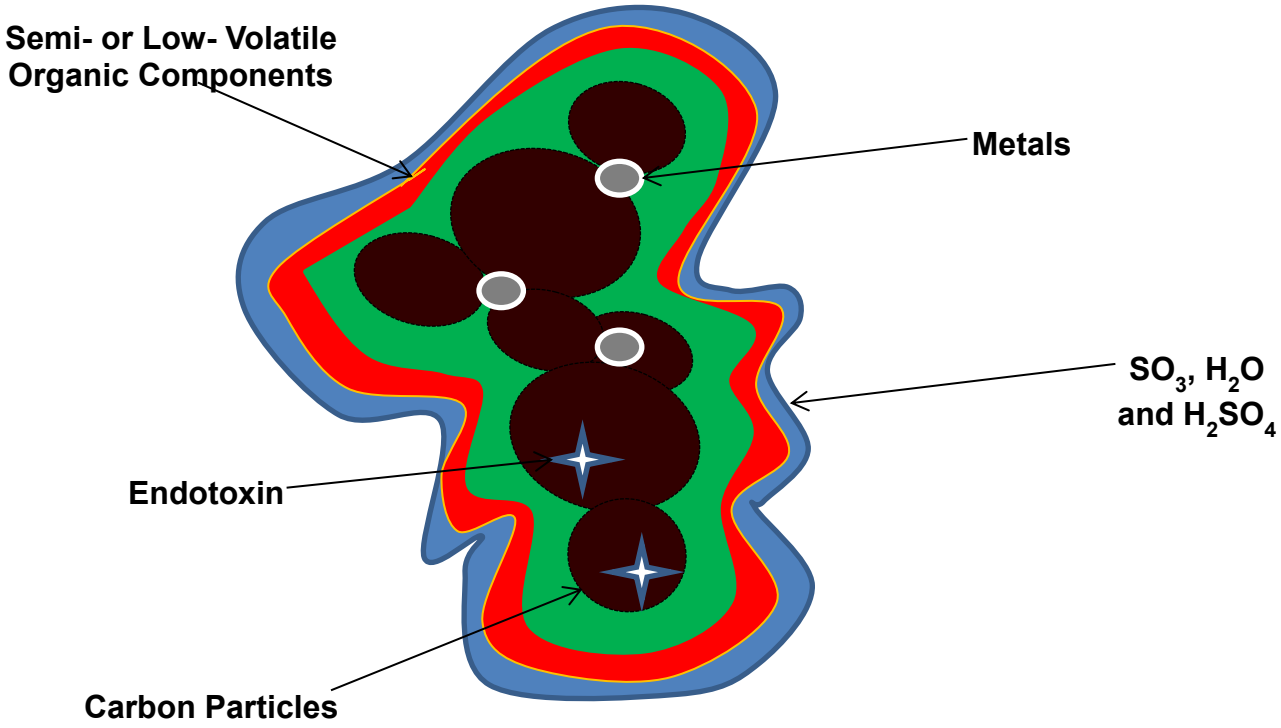

Figure 1.1 Diagram of DEP Aggregate

DEP are composed of carbon particle aggregates which adsorb semi- or low-volatile organic components, metals or endotoxin, in addition to a layer of condensed SO_3, H_2O and H_2SO_4. Image adapted from Twigg and Phillips et al. 2009.

The mechanisms associated with particle formation in diesel exhaust typically involve two 'modes', namely the nucleation mode and the accumulation mode (Schneider et al. 2005). The nucleation mode is considered to be liquid particles which consist of sulfate, water or semi-volatile organic compounds (Schneider et al. 2005). These particles are between 5-50nm, and are formed by the high temperatures created in the exhaust-pipe of vehicles. At high temperatures, organic substances are vaporised and, on cooling, the low-volatile organic components are condensed on to the surface of existing carbonaceous particles, leading to the formation of particles in the accumulation mode (Ono-Ogasawara & Smith 2004). Accumulation mode particles are between 30-500nm, and typically consist of carbonaceous soot particles with adsorbed semi-volatile condensates (Figure 1.2)

(Kittelson et al. 2006; Kittelson et al. 1999; Ma et al. 2008). The chemical composition of DEP, is therefore, complex, and is influenced by the formation of nucleation mode particles. This is because particles in nucleation mode are indirectly dependent on fuel type, engine type (heavy or light) or engine running conditions (Rönkkö et al. 2006; Saitoh et al. 2003).

The physical features of DEP, including size, shape and composition, govern their behaviour on respiratory health. DEP are major contributors to $PM_{10,}$ however, significant proportions of DEP are typically found in the range $PM_{0.1}$ - $PM_{2.5}$ (Ono-Ogasawara & Smith 2004). The size of DEP enables them to penetrate and deposit in the alveolar compartment of the lung, where they impact on the thin alveolar epithelium and pass into the circulation (Wichmann 2007). In addition, DEP readily bind together forming aggregates of various sizes. Furthermore, the complex shape of DEP aggregates may inhibit appropriate phagocytosis, and hence clearance, by alveolar macrophages (Champion & Mitragotri 2009). Interference with macrophage function could, therefore, have deleterious effects on health, for example in patients with COPD.

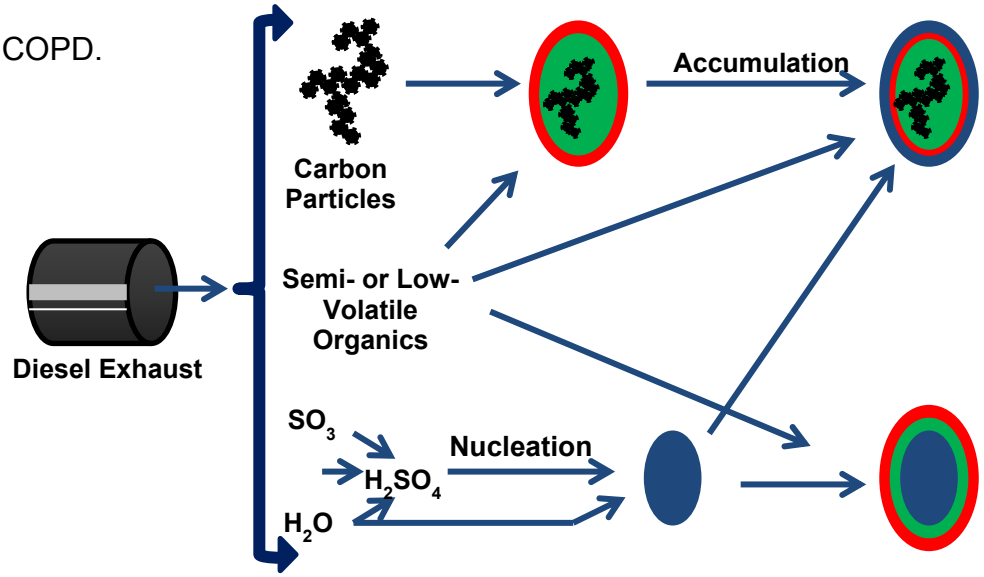

Figure 1.2 Mechanism of DEP Formation by Nucleation and Accumulation Modes

Primary emissions of diesel exhaust consist of carbon soot particles, semi- or low-volatile organic components, SO_3, H_2O and H_2SO_4. Semi- or low-volatile organic components, SO_3, H_2O and H_2SO_4 condense on to the surface of existing carbon soot particles. During the nucleation process SO_3, H_2O and H_2SO_4 also bind to form liquid particles. Diagram adapted from Schneider et al. 2005.

1.3 Chronic Obstructive Pulmonary Disease

COPD is an irreversible chronic inflammatory respiratory condition. COPD affects the large airways, the peripheral small airways, and the lung parenchyma, leading to airway obstruction (Vestbo et al. 2012; GOLD, 2014). Airflow obstruction is measured using spirometry, and decreases in forced expiratory volume in 1 sec (FEV_1), and the ratio of FEV_1 to forced vital capacity (FVC), are indicative of abnormalities in lung function. For example, FEV_1 <80% and FEV_1/FVC <0.7 reflect impaired lung function in patients with COPD. In addition, lung function reduces steadily with disease progression (Figure 1.3). The severity of COPD is correlated with a number of factors including length of smoking history, muscle weakness and exacerbations (MacNee 2005a; Dourado, et al. 2006; O'Donnell & Parker 2006; Barnes 2010).

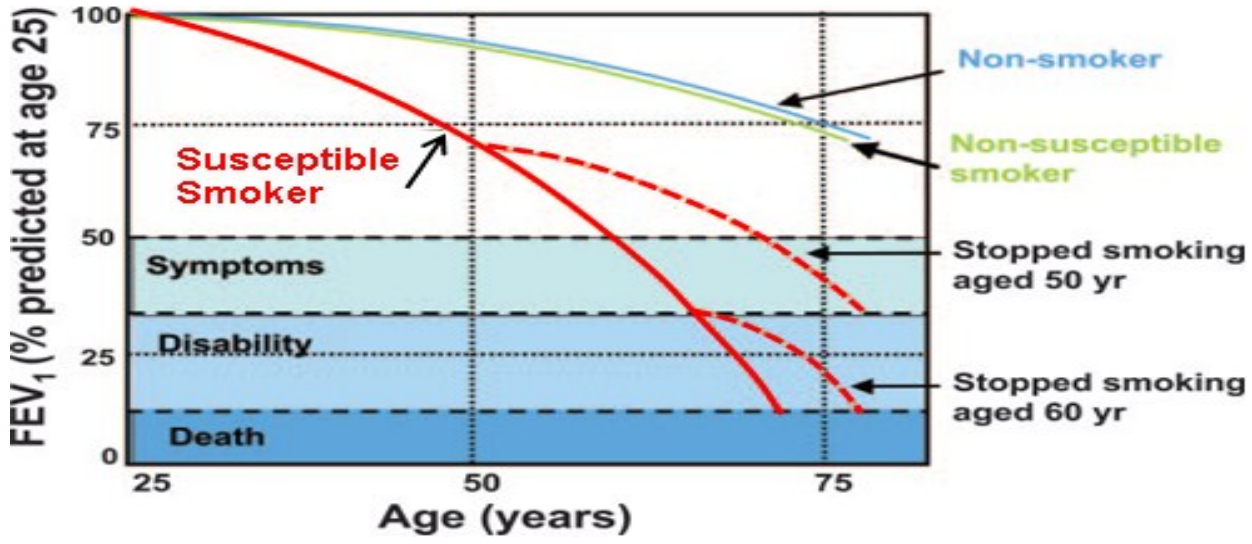

Figure 1.3 Accelerated Decline in Airflow in Patients with COPD compared with Non-smokers and Smokers

Declined airflow is a normal feature of ageing (blue line). However, 10–20% of smokers who are susceptible to COPD, have an accelerated decline in airflow (red line) compared to non-smokers and non-susceptible smokers (green line). The length of smoking history further declines airflow, and leads to onset of symptoms, disability and eventually death. Cessation of smoking slows the rate of decline in airflow reduction, but does not reverse it. Diagram adapted from Barnes 2004.

COPD is primarily associated with long-term cigarette smoking, as well as inhalation of toxic gases/irritants and atmospheric pollutants including DEP (Løkke et al. 2006; Hart et al. 2012; Ulvestad et al. 2000). However, only 10-20% of chronic smokers develop COPD, and cessation of smoking is associated with lowered disease progression (Figure 1.3). Cigarette smoke contains ~4,700 chemicals, many of which are noxious, including free-radicals and other oxidants (Rahman 2005). Cigarette smoke exposure induces inflammatory responses in the lung and is associated with COPD pathophysiology, which comprises chronic bronchitis, small airways disease (SAD) and emphysema (Figure 1.4).

1.3.1 Chronic Bronchitis

Chronic bronchitis is the term used for the hyper-secretion of mucus in the airways (Kim & Criner 2013) (Figure 1.4A). Excess mucus production is associated with hyperplasia or hypertrophy of goblet cells and submucosal glands (Kim & Criner 2013; Vestbo, et al. 2006; Saetta, et al. 2000). Excess mucus obstructs the airway lumen leading to reduced airflow (Figure 1.3A). The mechanism(s) of cigarette smoke-induced increases in mucus secreting tissue is not fully understood, but appears to involve upregulation of epidermal growth factor (EGF) signalling pathways resulting in the transcription and synthesis of mucins (Kim & Criner 2013). Clearance of mucus in chronic bronchitis is suppressed by ineffective mucocilliary clearance, which contributes to the characteristic 'cough' observed in many COPD patients.

1.3.2 Small Airways Disease

Peripheral (i.e. 'small') airways permit laminar movement of inspired air to the alveolar compartment of the lung to facilitate effective gas exchange (Burgel 2011). Small airways in healthy individuals typically have thin walls and are <2mm in diameter and provide no resistance to the flow of air (Burgel 2011). Reduced airflow in COPD is associated particularly with structural changes in the small airways (Figure 1.4B). These changes include thickening of the airway wall, increased smooth muscle mass, peri-bronchial fibrosis and luminal occlusion by mucus plugs.

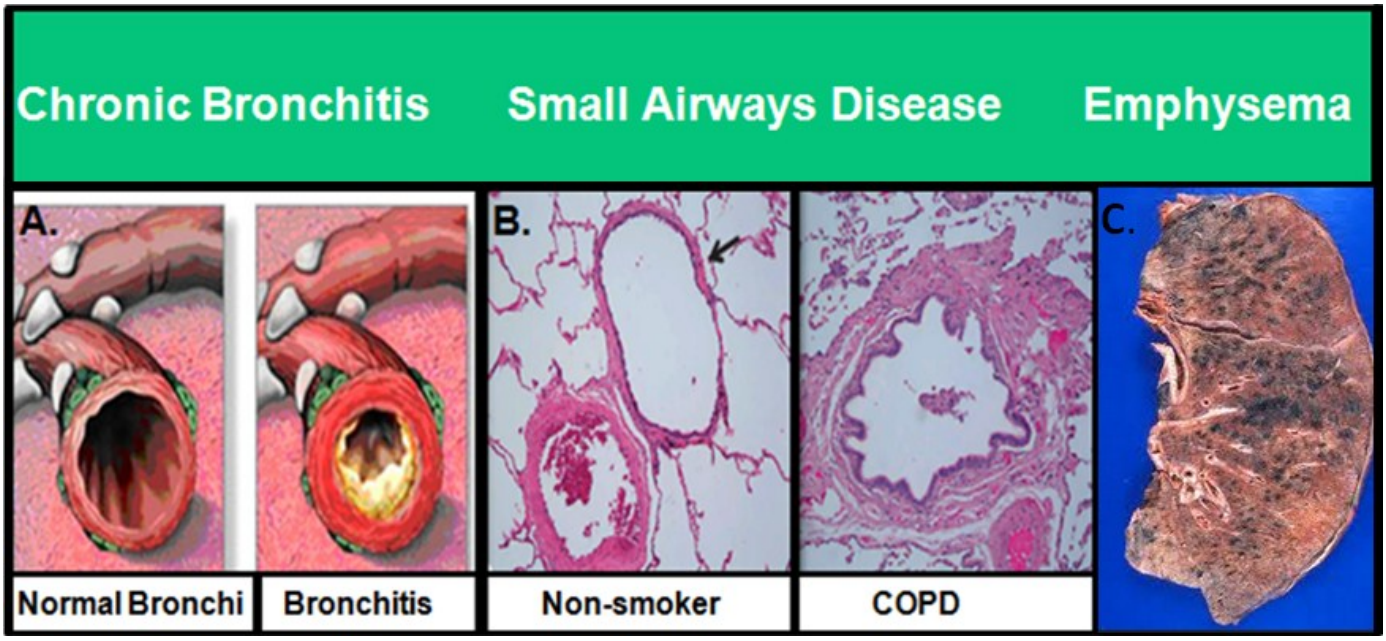

Figure 1.4 Key Features of COPD Pathophysiology

COPD is a respiratory disorder, characterised by three key features, these include, chronic bronchitis, small airways disease and emphysema. (A) Airways from healthy non-smokers do not secrete excess mucus compared to airways from patients with COPD. (B) Small airways from non-smokers (black arrow) have thin airway walls and are not thickened by fibrosis. The airways are held open by alveolar attachments. In COPD the airway walls are thickened by fibrosis, resulting in the occlusion of the airway lumen. (C) Emphysema is the destruction of the lung parenchyma by proteases produced by inflammatory cells for example neutrophils and macrophages. Individual images are adapted from Baraldo et al. 2012; http://www.pennmedicine.org/encyclopedia/em_PrintArticle.aspx?gcid=001087; http://www.flickr.com/photos/30950973@N03/4858474968.

Cigarette smoking is a major contributor to development of small airways disease (Churg et al. 2006; Yoshida & Tuder 2007). Inhalation of cigarette smoke triggers an inflammatory response by pulmonary cells against the noxious chemicals or debris deposited in the peripheral airways (MacNee 2005a). Smoking initiates migration of mononuclear cells and lymphocytes into the airway walls, and of macrophages into the luminal space (Hogg et al. 2004). Histological examination of lung tissue shows that small airways from smokers without COPD have a modest infiltration of immune cells compared to patients with disease (Hogg et al. 2004). Cigarette smoke activates immune cells and stimulates release of inflammatory mediators which are also implicated in small airways disease pathology. For example, activated macrophages release transforming growth factor (TGF)-β or fibroblast growth factors, which both contribute to fibrosis of airways (Barnes 2008).

1.3.3 Emphysema

Emphysema is the destruction of lung parenchyma (Figure 1.4C) leading to enlargement of distal airspaces *via* degradation of small airway walls and capillary beds. Emphysema is characterised by decreased elastic recoil of the lung, thereby preventing appropriate expulsion of air. The pathophysiology of emphysema involves protease-antiprotease and/or oxidant-antioxidant imbalances (MacNee 2005b; Abboud & Vimalanathan 2008). Proteases are released from macrophages and activated neutrophils that migrate to sites of tissue inflammation or pathogenic stimuli. Macrophages and neutrophils release proteases to digest lung tissue components such as collagen or elastin, to facilitate movement to sites of inflammation (Thorley & Tetley 2007). In addition to secreting proteases, these cells also secrete antiproteases to prevent excess damage to the lung tissue. However, in COPD this balance is shifted, and levels of proteases overwhelm the level of anti-

proteases present in the lung. The abundance of proteases in the pulmonary environment is thought to lead to the digestion of alveolar attachments, thereby causing pre-mature closure of peripheral airways (Abboud & Vimalanathan 2008; MacNee 2005a).

In addition to the protease burden in COPD, levels of oxidants are also elevated and overwhelm endogenous anti-oxidants (MacNee 2005b). A major contributor to oxidative stress is the oxidant nitric oxide, released from cigarette smoke and inflammatory cells (Rytilä et al. 2006). Oxidative stress may perpetuate emphysema by inactivating anti-proteases, sequestrating neutrophils, degrading extracellular matrix (ECM) and inducing pro-inflammatory mediator release (Rahman 2005).

1.4 DEP and COPD

DEP appear to be involved in aggravating the hallmark features of COPD (Lopes et al. 2009; Sagai et al. 1996; Churg et al. 2006; Macnee & Donaldson 2003). Inhaled DEP deposit on the the airway epithelium leading to the onset of airway hyper-responsiveness (AHR), emphysematous damage, respiratory toxicity and generation of reactive oxygen species (ROS) (Behndig et al. 2006; Nordernhall et al. 2001). As well as inducing lung injury and augmenting inflammation, DEP are also involved in impairment of cellular defences against respiratory pathogens by inhibiting secretion of pro-inflammatory cytokines by alveolar macrophages (Castranova et al. 2001; Yin et al. 2005a). The detrimental effects induced by DEP maybe a consequence of the noxious composition of these particles (Amakawa et al. 2003). One area where DEP appear to be particularly relevant to COPD is in their association with exacerbations of the disease.

1.4.1 Exacerbations of COPD

COPD patients are susceptible to exacerbations characterised by augmentation of symptoms such as dyspnoea, airway inflammation, mucus purulence and cough (Makris & Bouros 2009). The heightened inflammation associated with exacerbations leads to a progressive decline in FEV_1, resulting in high rates of hospitalization, poor quality of life and premature mortality (Wedchiza & Donaldson 2003). Respiratory micro-organisms such as viruses (e.g. rhinovirus or respiratory synticial virus) and bacteria (e.g. *Haemophilus influenzae* or *Streptococcus pnuemoniae*), colonise the lung and are major causative agents associated with exacerbations (McManus et al. 2008; Seemungal et al. 2001). In addition, the incidence of COPD exacerbations is increased during episodes of high atmospheric pollution (Lundborg et al. 2006; Medina-Ramón et al. 2006; Zanobetti, et al. 2008; Sint, et al. 2008).

1.5 Pulmonary Inflammation in COPD

Chronic airway and lung inflammation is a characteristic feature of COPD, and is initiated by cigarette smoking (Figure 1.5). Cigarette smoke exposure causes the infiltration of a variety of immune cells into the airways and lung, including macrophages, neutrophils and $CD8^+$ T-lymphocytes. Activated immune cells release pro-inflammatory mediators which are implicated in the pathophysiology of COPD.

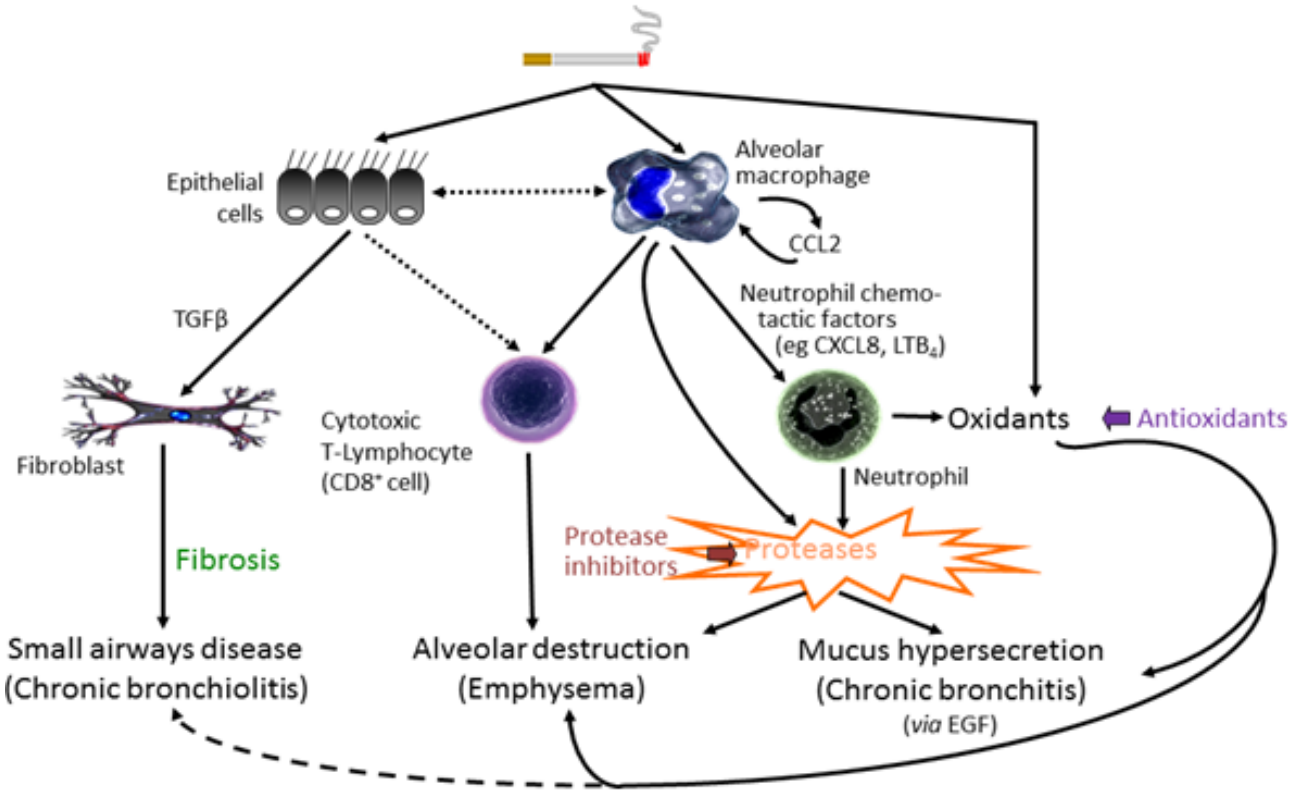

Figure 1.5 Inflammatory Mechanisms Associated with Cigarette Smoke Exposure Contributes to COPD Pathophysiology

Cigarette smoke stimulates alveolar macrophages to release chemokines for example CXCL8, LTB_4 and CCL2, which mediate recruitment of neutrophils, $CD8^+$ T-lymphocytes and monocytes. Neutrophils and $CD8^+$ T-lymphocytes release proteases which degrade lung parenchyma and thereby are associated with mucus hypersecretion (chronic bronchitis) and alveolar destruction (emphysema). In addition, oxidants released by these cells also contribute to mucus hypersecretion, alveolar destruction and small airways disease (chronic bronchiolitis). Cigarette smoke also stimulates epithelial cells to release TGF-β, which is associated with the thickening of airway walls by fibrosis. Diagram adapted from Barnes 2004.

1.5.1 Alveolar Macrophages

Alveolar macrophages (AM) are resident at the blood-alveolus interface and are pivotal in innate and adaptive immunity (Barnes, 2004; Twigg 2004). These cells are placed in the alveolar spaces to maintain sterility of the lungs by engulfing inhaled particles, debris, apoptotic cells and pathogens (Barnes, 2004). In addition to their phagocytic functions, these cells also release inflammatory mediators (e.g. CXCL8, interleukin (IL)-6 or tumour necrosis factor (TNF)α), generate oxidative species

involved in microbial killing, and secrete proteases (Russell et al. 2002; Culpitt et al. 2003; Barnes, 2004). The role of macrophages in COPD is discussed in more detail below (Section 1.6).

1.5.2 Neutrophils

Neutrophils are important in defence against infection. In healthy airways, tissue invasion by bacterial or viral pathogens is suppressed by non-specific mechanisms, for example, the mucocilliary transport system (Sethi 2000). Evasion of these barriers results in recruitment of inflammatory cells, including neutrophils from the bone marrow, to the site of inflammation (van Eeden et al. 2000; Donnelly & Barnes 2012). Activation of neutrophils *via* interaction of surface pattern recognition receptors (PRRs) and pathogen-associated molecular patterns (PAMPs) on micro-organisms, initiates the respiratory burst process which is involved in killing of pathogens (Parker et al. 2005).

In COPD, neutrophils are increased in bronchoalveolar lavage (BAL) and sputum samples from patients, although only moderate numbers are observed in lung parenchyma or bronchioles (Barnes 2004). The difference in numbers of neutrophils between BAL or sputum and lung tissue may indicate the transient nature of these cells (Barnes 2004). The movement of neutrophils through lung tissue involves secretion of proteases, including matrixmetalloproteases (MMP)-8, MMP-9, cathepsin and neutrophil elastase, which digest lung tissue and facilitate migration of these cells to sites of inflammation or pathogenic stimuli (Di Stefano et al. 1994). Excessive production of neutrophil proteases, such as neutrophil elastase, is associated with induction of mucus metaplasia and destruction of alveolar

attachments leading to emphysema (Baraldo et al. 2012; O'Donnell & Parker 2006; Barnes 2004).

1.5.3 Lymphocytes

B and T-Lymphocytes are associated with adaptive immunity, antigenic specificity, expansion of antigenic specific daughter cells and immunologic 'memory' (Gadgil & Duncan 2008). T-lymphocytes are sub-divided into helper or cytotoxic lymphocytes, and are discriminated by the expression of $CD4^+$ or $CD8^+$ glycoproteins respectively (Barceló et al. 2008). $CD8^+$ T-lymphocytes, are one of the predominant cell types, along with macrophages, in peripheral airways of patients with COPD (Finkelstein et al. 1995; Majo et al. 2001; Hodge et al. 2007; Gadgil & Duncan 2008; Baraldo et al. 2012).

Cigarette smoke or irritants stimulate type II pneumocytes to release chemokines such as interferon inducible protein (IP)-10 (CXCL10) or monokine induced by interferon gamma (MIG) (CXCL9) (Gadgil & Duncan, 2008; Barnes 2008). These chemokines are involved in the recruitment of $CD8^+$ T-lymphocytes to the airways, by binding to the receptor CXCR3 which is highly expressed on these cells. In turn, $CD8^+$ T-cells release interferon (IFN)-ɣ, which further stimulates the release of the CXCL9 and CXCL10 (Barnes 2008). In addition to releasing inflammatory mediators, $CD8^+$ T-lymphocytes are also involved in the destruction of alveolar wall by releasing the cytotoxic enzymes perforin and granzyme B (Barnes 2008).

B-lymphocytes are observed in severe COPD (GOLD stage IV) and are found in peripheral small airways. These cells are present in lymphoid follicles and surround T-lymphocytes (Hogg et al. 2004; Barnes 2008). B-lymphocytes are associated with production of auto-antibodies in severe stages of COPD (Agusti et al. 2003).

1.6 Alveolar Macrophages in COPD

Macrophages occupy a pivotal role in the pathophysiology of COPD (Figure 1.5), and may be considered 'orchestrators' of the disease (Donnelly & Barnes 2012). The number of macrophages is increased in BAL fluid and sputum of patients with COPD (Retamales et al. 2001; Barnes et al. 2003). They are also increased at sites of emphysema and in peripheral airways (Barnes 2004).

The lung environment of healthy non-smokers is usually sterile. However, in COPD patients the lung is often colonised by bacterial pathogens, for example *H. influenzae* or *S.pneumoniae* (Sethi 2011; Taylor et al. 2010). AM from COPD patients show a reduced ability to clear inhaled pathogens compared to non-smoker and smoker controls (Berenson et al. 2006; Taylor et al. 2010; Berenson et al. 2013). Parallel experiments conducted on primary alveolar macrophages and blood macrophages from COPD patients (ex-smokers and current smokers), exposed to respiratory pathogens, display inconsistent findings in the clearance of phagocytic prey. For example, AM from ex-smoker and current smoking COPD patients, displayed reduced clearance of three different strains of *non-typeable H.influenzae* (NTHI), compared with AM from non-smokers. However, identical experiments conducted on blood macrophages did not display this defect (Berenson, *et al*, 2006). In contrast to this finding, other *in-vitro* studies have shown that blood monocyte-derived macrophages (MDM) from patients with COPD, are also defective in the clearance of NTHI, but not *S..pnuemoniae* compared to control groups (Berenson, et al. 2006). Similar findings are observed in tissue AM, with cells from COPD patients being defective in the uptake of NTHI and *Moraxella Catarrhalis* but not *S..pnuemoniae* (Berenson, et al. 2013). The inability to appropriately clear inhaled pathogens may

be responsible for continued colonisation of the airways, a propensity to more frequent exacerbations and aggravation of the underlying inflammation seen in COPD.

It has been determined that the extent of defective macrophage phagocytosis is not limited to specific respiratory pathogens, but also extends to the ineffective clearance of apoptotic cells i.e. airway epithelial cells. Inadequate clearance of apoptotic cells may lead to release of intracellular contents which are injurious to surrounding tissue; and may be associated with emphysema and pulmonary fibrosis (Hodge et al. 2003). BAL macrophages from non-smokers or COPD patients incubated with apoptotic epithelial cells or fluorescent beads showed that cells from COPD patients were defective in the clearance of apoptotic epithelial cells compared to non-smoker macrophages. In contrast, macrophages from COPD patients still retained their ability to internalise fluorescent beads.

The mechanism associated with reduced phagocytosis in macrophages is unclear. *In-vitro* studies looking at the effects of MDM from non-smokers, smokers and patients with COPD on the clearance of NTHI and *S.pnuemoniae*, showed a reduction in the uptake of pathogens. However, this effect was not associated with alterations in macrophage receptor expression for e.g. Toll like receptor (TLR) -2, TLR 4, macrophage receptor with collagenous structure (MARCO), cluster of differentiation (CD) 163, CD36 or mannose receptors; other studies have showed that primary AM from COPD patients and healthy smokers display a reduction in CD31, CD91, CD44 and CD71 (Taylor, et al, 2010; Hodge, et al. 2007). Therefore it is suggested that impaired macrophage phagocytosis maybe associated with alterations in macrophage receptor expression.

1.6.1 Mechanisms of Phagocytosis

Phagocytosis is the actin-dependent process of internalising prey which is >0.5μm in diameter (Aderem & Underhill 1999). The phagocytic process can occur *via* a number of mechanisms, but relies on discriminating 'non-self' molecules from 'self' molecules. This process involves recognising highly conserved PAMPs, for example lipopolysacchrides and formylated peptides by PRRs (Taylor et al. 2005; Ishii et al. 2008; Rovina et al. 2013). The most common phagocytic process, involves coating pathogens or particles with soluble serum proteins, termed 'opsonins', which include immunoglobulins (Ig) or complement. The recognition of immunoglobulins or complement by macrophage Fc-receptors (e.g. Fc-ɣRIII) or complement receptors (e.g. C3b) respectively, increases the susceptibility of phagocytosis (Aderem & Underhill 1999; Donnelly & Barnes 2012). In addition, other receptors, namely the scavenger receptors (SR) are associated with non-opsonised phagocytosis (Donnelly & Barnes 2012; Greenberg & Grinstein 2002).

Opsonised-mediated phagocytosis involves activation of the Fc-receptor or the complement receptor (CR), leading to the rearrangement of the macrophage cytoskeleton and finally resulting in particle internalisation. The internalisation of particles by macrophages, can occur by two different processes, the first process is mediated by the Fc-receptors and involves pseudopodia extending from the surface of the cell which encapsulates the particle in a zippering manner (Donnelly & Barnes 2012). The second process is mediated by CRs and involves the particle 'sinking' into the cell with only small protrusions of the cell membrane surrounding the particle (Aderem & Underhill 1999; Donnelly & Barnes 2012). The internalised particle is then held within a phagosome, to which endosomes bind by a series of fusion and fission

processes. Maturation of the phagosome eventually leads to the binding of lysosomes, thereby creating phagolysosomes. Pathogens contained within the phagolysosomes are degraded by reactive oxygen intermediates (Aderem & Underhill 1999; Donnelly & Barnes 2012).

The lung is not a serum-rich environment, for this reason, the primary means of engulfing inhaled pathogens or particles is *via* non-opsonised phagocytosis (Donnelly & Barnes 2012). SRs are implicated with non-opsonised phagocytosis, with the major SR on the surface of alveolar macrophages being macrophage receptor with collagenous structure (MARCO) (Arredouani et al. 2004; Arredouani et al. 2005; Donnelly & Barnes 2012). However, the mechanism associated with non-opsonised phagocytosis by alveolar macrophages is not fully understood (Arredouani et al. 2004).

As mentioned earlier (Section 1.6), alveolar macrophages are defective in the clearance of inhaled pathogens and in addition also display reduced efferocytosis, which is the clearance of apoptotic cells. Exact mechanisms associated with the reduced efferocytosis are not clear, however, it is considered that recognition receptors on the surface of cells may play a part. For example, alveolar macrophages from smokers and patients with COPD display reduced expression of CD receptors including CD31, CD91, CD44 and CD71, suggesting that smoking may be correlated to impaired macrophage function (Hodge et al. 2007). However, other groups have shown no difference in the mentioned receptors, but have shown reductions in the expression of CD80, the human leukocyte antigen DR (HLA-DR), CD86 and CD11a (Löfdahl et al. 2006; Pons et al. 2005). It is unclear whether defective macrophage phagocytosis is associated with reduced recognition receptor expression, or is a feature of cells becoming replete following exposure to inhaled

debris or particles such as DEP. The satiation of macrophages may prevent further internalisation of other inhaled particles for example respiratory pathogens leading to bacterial colonisation of the lung.

1.6.2 Macrophages and Mediators

In addition to ingestion of microbes and other particles, macrophages also have a secretory role involving release of mediators. Release of mediators serves as a means of communicating with other cells to initiate either an inflammatory or anti-inflammatory response. Activation of macrophages release several mediators, of which CXCL8, IL-6 and TNFα predominate, particularly in COPD (Barnes 2009). In COPD, these mediators contribute and amplify existing immune responses associated with the pathophysiology of the disease.

Cigarette smoke or pathogenic stimuli such as endotoxin, are responsible for stimulating release of macrophage mediators. Stimulation of macrophages activate transcription factors that are typically associated with the expression of inflammatory genes, for example nuclear factor kappa light chain enhancer of activated B cells (NF-κB) or activator protein 1 (AP.1) (Renda et al. 2008). In COPD, activation of NF-κB in macrophages is associated with the increased release of CXCL8, IL-6 and TNFα, this is determined by the localisation of cytoplasmic p65 to the nucleus (Barnes 2004; Libermann & Baltimore 1990). Activation of these transcription factors is associated with the phosphorylation of mitogen activated protein kinases (MAPK) (Renda et al. 2008). The MAPKs are serine/threonine protein kinases which are a complex network of interacting proteins involved in the communication of extracellular signals that lead to phosphorylation of intracellular transcription factors to initiate cellular processes (Figure 1.6) (Seger & Krebs 1995).

In macrophages, p38, extracellular signal regulated kinase (ERK)-1/2 or c-jun N-terminal kinases (JNK) signalling are associated with mediator release (Barnes 2004). In COPD, phosphorylation of p38 is reported to be increased in alveolar macrophages compared to non-smoking or smoker controls (Renda et al. 2008). p38 MAPK has four isomers, namely p38α, p38β, p38ɣ or p38δ (Smith et al. 2006; Nebreda & Porras 2000). These isoforms are encoded by different genes and expression of the different isoforms is tissue-dependent. In alveolar macrophages, the p38α and p38δ isoforms are abundantly expressed (Smith et al. 2006). The isoforms of p38 phosphorylate different substrates, although the effect of the individual isoforms on inflammation are unknown (Smith et al. 2006).

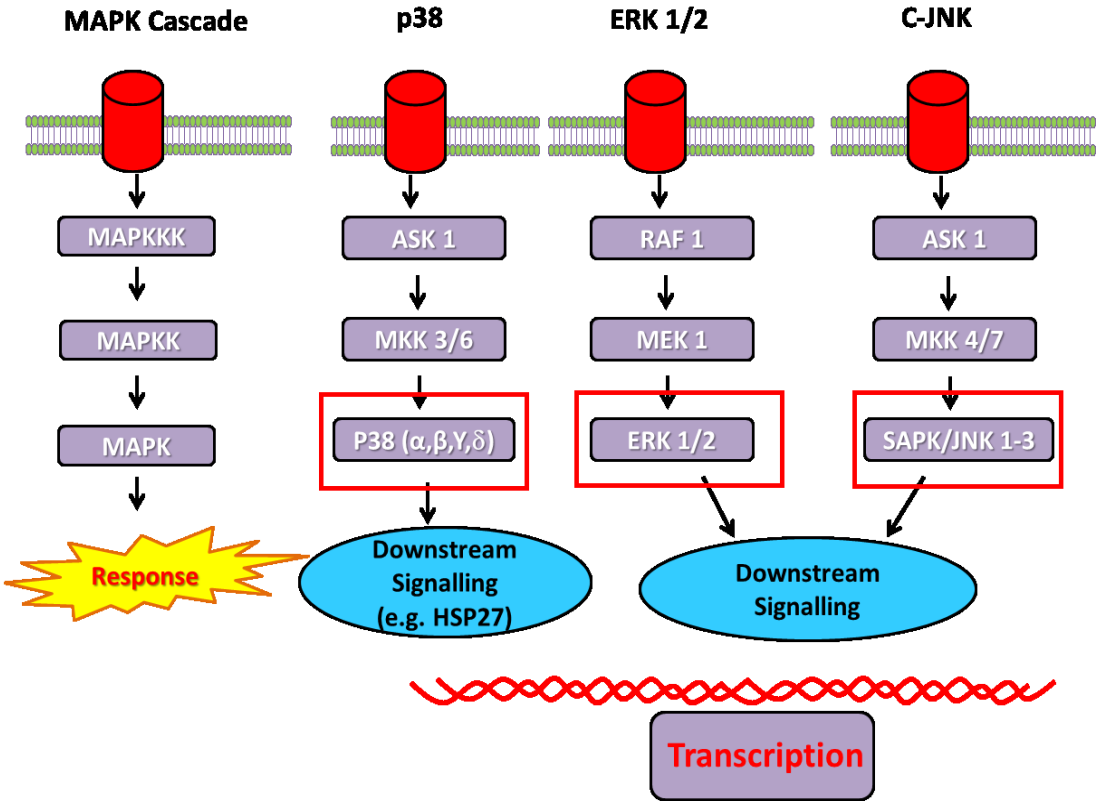

Figure 1.6 MAPK Signalling Pathway

MAPK are serine threonine kinases and include p38, ERK 1/2 and JNK. The MAPK pathway involve enzymes which initiate downstream signalling by regulating substrates in a consecutive manner, resulting in the phosphorylation of transcription factors which leads to cellular responses.

The following mediators have distinct roles in COPD pathophysiology and are released *via* activation of MAPK pathways:

CXCL8: CXCL8 is a chemokine involved in the recruitment of neutrophils and cells that express the G-protein coupled CXCR1 and CXCR2 receptors, to sites of tissue injury, inflammation or pathogenic stimuli. CXCL8 is released by numerous pulmonary cells including alveolar macrophages. Macrophages from patients with COPD, release higher levels of CXCL8 compared to non-smoker and smoker controls as determined by levels of chemokine measured in induced sputum (Keatings et al. 1996; Culpitt et al. 2003; Nocker et al. 1996). The elevated level of CXCL8 is correlated to neutrophil recruitment in the airways of patients with COPD. The increased release of TNFα by macrophages in patients with COPD is also responsible for the activation of recruited neutrophils. The accumulation and activation of neutrophils at sites of inflammation in the peripheral airways may perpetuate underlying inflammation in COPD by stimulating mucus hypersecretion and releasing proteases thereby prompting tissue destruction (Quint & Wedzicha 2007).

Stimulation of macrophages by cigarette smoke or pathogenic stimuli triggers downstream signalling events culminating in the activation of the transcription factor NF-κB or AP.1, which is associated with CXCL8 production (Drost et al. 2005; Murugan & Peck 2009). The activation of these transcription factors are regulated by the phosphorylation of the MAPK p38, ERK-1/2 or JNK (Renda et al. 2008).

IL-6: IL-6 is a pleiotropic cytokine which has been highlighted to mediate several inflammatory effects in the respiratory system. Levels of IL-6 are increased in BAL samples from patients with COPD and are associated with amplifying inflammation

by working in concert with other cytokines (Barnes 2009). IL-6 provides a link between innate and adaptive immunity in COPD *via* the release of acute phase proteins from the liver, and has been implicated in fibrotic remodelling in peripheral airways. In addition, the increased release of IL-6 has also been linked to airway space enlargement, airway inflammation and may mediate systemic co-morbidities associated with COPD including diabetes and bone disease (Ochoa et al. 2011; Barnes 2010).

TNFα: In COPD, levels of TNFα are increased and have been implicated in cachexia 'weight loss' in patients. TNFα, along with IL-6 is responsible for the release of acute phase proteins and C-reactive proteins (CRP) from the liver, therefore driving systemic inflammation and the activation of immune cells. In addition, acute phase proteins are also associated with the activation of complement (Schleimer 2005). The release of TNFα by AM, is associated with cigarette smoke induced emphysema by increasing the production of MMPs by neutrophils (Cosio et al. 2009; Churg et al. 2004). The effects of TNFα are mediated on pulmonary cells including macrophages, by activating p38 MAPK pathways which activates NF-κB to initiate the transcription of inflammatory genes (Barnes 2004).

The effect of DEP on release of these mediators was investigated in the present thesis, using macrophage-like cells, termed, monocyte-derived macrophages (MDM).

1.7 Monocyte-Derived Macrophages

Understanding the effect of DEP on the respiratory system is incomplete. The current thesis attempted to extend previous findings to further understand the interrelationship between DEP and macrophage function. The effect of DEP on AM

function will be examined on blood macrophages, namely MDM. Comparison of primary AM and blood macrophages (Table 1.2), show that despite some differences in receptor expression e.g. CD80, CD86, CD163 and CD62L, this does not appear to alter the functioning of macrophages to clear respiratory pathogens (Berenson et al. 2006; Berenson et al. 2013; Taylor et al. 2010, Winkler et al. 2008; Lacey et al. 2012). Although differences between primary and blood macrophages are evident, as described in Table 1.2, the similarities between AM and blood macrophages cells outweigh the differences (Taylor et al. 2010). It is reasonable to use MDM in this investigation, as these cells are more readily available compared to primary AM, are minimally invasive to acquire and allow comparison of the effect of DEP on macrophage function from patients with COPD, and non-smoker and smoker controls.

1.8 Inhibitor Compounds Used

The study herein involved assessing the contribution of MAPK pathways to inflammatory mediator release. As part of that investigation, inhibitors of different MAPK signalling molecules were used. The characteristics of the inhibitors are outlined below:

p38, ERK 1/2 and c-JNK are involved in the release of mediators by alveolar macrophages in COPD. To determine whether DEP stimulate MDM release of CXCL8, IL-6 or TNFα by MAPK signalling, the p38 inhibitor, PF755616 and MEK inhibitor, PD98059 were used. PF755616 is selective for the p38α and p38β isoforms, and have a half-maximal inhibitory concentration (IC_{50}) of 27nM (Iain Kilty personal communication). PD98059 inhibits the ERK 1/2 upstream signalling

component MEK 1/2. PD98059 has an IC_{50} of 2μM (Alessi et al. 1995; Tudhope, Finney-Hayward, et al. 2008).

1.9 Hypothesis and Aims

From the above, the following hypothesis was proposed: 'DEP modulate macrophage and pro-inflammatory mediator release and phagocytosis, and this is more prominent in COPD'.

To examine this hypothesis, the following aims were investigated:

- **Chapter 3**: Examination of the physical characteristics and metal composition of three different DEP samples.
- **Chapter 4:** Examination of the effect of three DEP samples on non-smoker, smoker or COPD MDM viability.
- **Chapter 5:** Examination of the effect of three DEP samples on non-smoker, smoker or COPD MDM release of CXCL8, IL-6 or TNFα.
- **Chapter 6**: Examination of the mechanism of DEP on MDM mediator release from non-smokers, smokers or patients with COPD.
- **Chapter 7:** Examine the effect of DEP on MDM phagocytosis of fluorescent beads in non-smokers, smokers or patients with COPD.

Table 1.2 Evidence of Similarities between Blood Derived Macrophages and Primary Alveolar Macrophages

Function/Marker	Alveolar Macrophages	Blood Macrophages	References
Morphology	√	√	Becker et al. 1987
Markers:			
• FCγ: - CD14, CD32, CD64	√	√	
• Scavenger Receptors: - MARCO, CD36, CD206 - CD163	√ X	√ X	
• Adhesion Molecule: - CD11b, CD11c, CD164 - CD62L	√ X	√ X	
• Inflammatory Receptors: - CD14	√	√	Winkler et al. 2008
• Co-Stimulatory Molecules: - CD80 - CD86	X X	X X	
• Cigarette Smoke Activates: - ERK MAPK - p38 MAPK	√ √	√ √	
• Cigarette Smoke Induces: - CXCL8 release	√	√	
• Gene Expression	√	√	
Phagocytosis:			
• Fluorescently-Labelled: - *H.influenzae* - *S.pnuemoniae*	√ √	√ √	Taylor et al. 2010
• Fluorescent Beads	√	√	

Evidence from different studies highlighting the similarities and differences between blood derived macrophages and primary alveolar macrophages.

Chapter 2:

Materials and Methods

2.1 Materials

Material	Supplier
Albumin, Bovine Fraction V solution (BSA)	Sigma-Aldrich, Poole, UK
Anti-Mouse IgG HRP-Linked Antibody	New England BioLabs, Hitchen, UK
Anti-Rabbit IgG HRP-Linked Antibody	New England BioLabs, Hitchen, UK
Bio-Rad™ Protein Assay	BioRad, Munich, Germany
Cell Dissociation Solution	Sigma-Aldrich, Poole , UK
Cell Lysis Buffer (10 X)	New England BioLabs, Hertfordshire, UK
Cell Scrapers	Sarstedt, Leicester, UK
Cell-Tracker™ Red	Invitrogen, Paisley, UK
Centrifuge Tubes (50ml)	Sarstedt, Leicester, UK
Centrifuge Tubes (15ml)	Sarstedt, Leicester, UK
Costar 96-Well Black Plates (flat bottom)	Costar, Fisher Scientific, Leicester, UK
Costar 96-Well Clear Plates (flat bottom)	VWR, Leicester, UK
Costar 24-Well Clear Plates (flat bottom)	VWR, Leicester, UK
Coverslips	Thermo Fisher Scientific, Leicester, UK

Dextran from *Leuconostoc spp*.	Sigma-Aldrich, Poole, UK
Diesel Exhaust Particles-N (DEP-N)	Kindly Donated By The Department of Mechanical Engineering, Imperial College, London, UK
Dimethyl Sulphoxide (DMSO)	Sigma-Aldrich, Poole, UK
Dulbecco's Phosphate Buffered Saline (D-PBS)	Sigma-Aldrich, Poole, UK
10X Dulbecco's Phosphate Buffered Saline (10 X D-PBS)	Invitrogen, Paisley, UK
Hycult Limolas Amebocyte Lysate Endotoxin Kit	Cambridge Bioscience, Cambridge, UK
Enhanced Chemiluminesence Substrate reagent (ECL)	GE Healthcare, Chalfont St. Giles, UK
Ethylene-diamine-tetra-acetic Acid (EDTA)	Sigma-Aldrich, Poole, UK
Ethanol	BDH, Poole, UK
Eppendorf Tubes (0.5ml)	Sarstedt, Leicester, UK
Eppendorf Tubes (1.5ml)	Sarstedt, Leicester, UK
Eppendorf Tubes (2.0ml)	Sarstedt, Leicester, UK
FACScanto II flow cytometer	Becton Dickinson, Oxford, UK
FACSClean	Becton Dickinson, Oxford, UK
FACSFlo	Becton, Dickinson, Oxford, UK
FACSRinse	Becton, Dickinson, Oxford, UK
Filters (0.2µm pore)	Sarstedt, Leicester, UK

Fluospheres ® Carboxylate Modified Microspheres (Yellow-green, 2.0µm)	Molecular Probes, Invitrogen, Paisley, UK
Fluostar Optima Fluorimeter	BMG LabTech, Aylesbury, UK
Foetal Calf Serum	Gibco, Invitrogen, Paisley , UK
Full-range Rainbow Molecular Weight Marker	GE Healthcare, Chalfont St. Giles, UK
Formvar Coated Copper Grids	Agar Scientific, Stanstead, UK
Glucose	Sigma-Aldrich, Poole, UK
Haemacytometer Neubauer counting chamber	Fisher Scientific, Leicester, UK
Hanks Balanced Salt Solution	Sigma-Aldrich, Poole, UK
Hybond ECL	Amersham Pharmacia Biotech, GE Healthcare, Chalfont St. Giles, UK
Hyperfilm ^{TM} ECL	Amersham Pharmacia Biotech, GE Healthcare, Chalfont St. Giles, UK
Hybond Nitrocellulose Membrane	Amersham Pharmacia Biotech, GE Healthcare, Chalfont St. Giles, UK
Lab-Tek Permanox 8-Well Chamber Slides	Costar, Fisher Scientific, Leicester, UK
Laemelli Buffer	Sigma-Aldrich, Poole, UK
Launch Vision Works LS (Densitometer Software)	UVP, Cambridge, UK
L-Glutamine	Sigma-Aldrich, Poole, UK
Light Green	Sigma-Aldrich, Poole, UK
Limolas Amebocyte Assay	Hycult Biotech, Cambridge Bioscience, Cambridge, UK
LPS from *Salmonella enterica* Serotype: enteritidis (LPS)	Sigma-Aldrich, Poole, UK

MEK 1/2 Inhibitor (PD98059)	Sigma-Aldrich, Poole, UK
Methanol	Sigma-Aldrich, Poole, UK
Mini Complete Protease Inhibitor Cocktail Tablets	Roche, Mannheim, Germany
Mouse (Monoclonal) Anti-Human CXCL8 Biotin Conjugate	Invitrogen, Paisley, UK
Mouse (Monoclonal) Anti-Human IL-6 Biotin Conjugate	Invitrogen, Paisley, UK
Mouse (Monoclonal) Anti-Human TNFα Biotin Conjugate	Invitrogen, Paisley, UK
Mouse (Monoclonal) Anti-Human CXCL8 Capture Antibody	Invitrogen, Paisley, UK
Mouse (Monoclonal) Anti-Human IL-6 Capture Antibody	Invitrogen, Paisley, UK
Mouse (Monoclonal) Anti-Human TNFα Capture Antibody	Invitrogen, Paisley, UK
MTT(3-(4,5-dimethythiazol2-yl)-2,5-diphenyltetrazolium bromide	Sigma-Aldrich, Poole, UK
NUNC Maxisorp Flat Bottomed Plates	Fisher Scientific, Leicester, UK
NuPage 4-12% BIS-TRIS Electrophoresis Gels	Invitrogen, Paisley, UK
NuPage MOPS SDS Running Buffer (20X)	Invitrogen, Paisley, UK
p38 Inhibitor (PF755616)	Pfizer, Kent, UK
Paraformaldehyde (PFA)	Sigma-Aldrich, Poole, UK
PE Annexin V: Apoptosis Detection Kit I	Beckton Dickinson, Oxford, UK
Penicillin	Sigma-Aldrich, Poole, UK
Percoll	GE Healthcare, Buckinghamshire, UK

Pippette Tips With Microcapillary for Loading Gels	VWR, Leicester, UK
Phosphatase Inhibitor II	Sigma-Aldrich, Poole, UK
Phosphatase Inhibitor III	Sigma-Aldrich, Poole, UK
Phosphate Buffered Saline Tablets (PBS)	Sigma-Aldrich, Poole, UK
Phospho-HSP27 Primary Antibody	New England BioLabs, Hitchen, UK
Phospho-p38α Primary Antibody	New England BioLabs, Hitchen, UK
Phospho-p42/44 (ERK 1/2) Primary Antibody	New England BioLabs, Hitchen, UK
Phospho-SAPK/JNK Primary Antibody	New England BioLabs, Hitchen, UK
Polyoxyethylene-Sorbitan Monolaurate (Tween-20)	Sigma-Aldrich, Poole, UK
Polymyxin B	Sigma-Aldrich, Poole, UK
Polystyrene Round Bottomed (5ml) FACS Tubes	Becton Dickinson, Oxford, UK
Recombinant Human GM-CSF	R&D systems, Oxford, UK
Recombinant Human CXCL8 Standard	R&D systems, Oxford, UK
Recombinant Human IL-6 Standard	R&D systems, Oxford, UK
Recombinant Human TNFα Standard	R&D systems Oxford, UK
Roswell Park Memorial Institute media (RPMI) – 1640	Sigma-Aldrich, Poole, UK
Saponin	Sigma-Aldrich, Poole, UK
Sodium Azide	Sigma-Aldrich, Poole, UK

Sodium Chloride (0.9%)	Baxter Healthcare, Northampton, UK
Sodium Chloride	VWR, Leicester, UK
Sonicator	Fisher Scientific, Leicester, UK
Streptavidin-conjugated horseradish peroxidise	Invitrogen, Paisley, UK
SRM-1650B	National Institute of Standards & Technology, Gaithersburg MD, USA
SRM–2975	National Institute of Standards & Technology, Gaithersburg MD, USA
Streptomycin	Sigma Aldrich, Poole, UK
Sucrose	Fisher Scientific, Leicester, UK
Syringes	3S Healthcare, London, UK
Toludine blue	Sigma-Aldrich, Poole, UK
Total- ERK 1/2 primary antibody	New England BioLabs, Hitchen, UK
Total- HSP27 primary antibody	New England BioLabs, Hitchen, UK
Total-p38α primary antibody	New England BioLabs, Hitchen, UK
Total-SAPK/JNK MAPK primary antibody	New England BioLabs, Hitchen, UK
Trizma base (TRIS)	Sigma-Aldrich, Poole, UK
Trypan blue	Sigma-Aldrich, Poole, UK
Tetramethylbenzine Solution (TMB)	B.D Optima, Oxford, UK
UVP GelDoc-IT Imaging System (Densitometer)	UVP, Cambridge, UK

β-Mercaptoethanol	Sigma-Aldrich, Poole, UK
4',6-Diamidino-2-phenylindole dihydrochloride (DAPI)	Sigma-Aldrich, Poole, UK
0.2μm Sized Inert Beads	Sigma-Aldrich, Poole, UK
10μm Sized Inert Beads	Sigma-Aldrich, Poole, UK
30μm Sized Inert Beads	Sigma-Aldrich, Poole, UK

2.2 Methods

2.2.1 Subject Selection: Blood Sampling and Lung Function Measurements

Whole blood was collected by venepuncture from healthy non-smoker, smoker and COPD volunteers recruited from the National Heart & Lung Institute (NHLI), London, Royal Brompton Hospital (RBH), London and Wexham Park Hospital, Slough, Berkshire. All volunteers gave written and informed consent as approved by the Health Research Authority (HRA) Ethics Committee, Chelsea, London (previously known as NHS Royal Brompton, Harefield and the NHLI Research Ethics Committee) (See Appendix I).

2.2.1.1 Non-smokers

Non-smokers aged between 45 - 80 years had normal lung function as predicted by age, sex and height, with normal bronchial reactivity (see section 2.2.1.6). Volunteers had no history of respiratory disease, no history of cigarette smoking and were not taking regular medication.

2.2.1.2 Smokers

Smokers aged between 45 - 80 years had normal lung function as predicted by age, sex and height, with normal bronchial reactivity, no history of respiratory disease and were not taking regular medication. Smokers had a smoking history of at least 10 pack years (a pack year defined as 20 cigarettes per day for one year).

2.2.1.3 COPD Patients

COPD patients were aged between 45 - 80 years. Inclusion criteria for patients with COPD were in accordance with the Global Initiative for Chronic Obstructive Lung Disease guidelines (Vestbo et al. 2012). Patients with COPD had a forced expiratory value (FEV_1): forced vital capacity (FVC) ratio of <0.7, a post-bronchodilator FEV_1 % predicted of <85%, and no previous history of other respiratory diseases. Patients with COPD also had a smoking history of at least 10 pack years. Patients were excluded from the study if they presented with significant findings in medical records, or upon examination, apart from symptoms associated with COPD.

2.2.1.4 Clinical Measurements

Lung function measurements were undertaken by respiratory nursing staff located at the Royal Brompton, Harefield and Wexham Park hospitals.

2.2.1.5 Spirometry

FEV_1 and FVC were measured using a spirometer. Readings were expressed as absolute values or as a percentage of predicted values for age, sex and height. Baseline readings were recorded by taking the highest reading following three attempts; each attempt was separated by 1min intervals. Predicted values were based on calculations derived from Crapo tables, which assign predicted values by correlating age, sex and height (Crapo et al. 1981).

2.2.1.6 Bronchial Reactivity

Volunteers underwent a bronchial reactivity challenge to assess airway responsiveness. The challenge involved inhaling methacholine chloride at increasing

doses between 0.0625 - 64mg/ml diluted in 0.9% ($^{W}/_{V}$) sodium chloride (saline). FEV_1 was measured (Section 2.2.1.5), following inhalation of each individual dose of methacholine chloride.

On arrival volunteers were asked to rest for 15 min before baseline spirometry was measured. Following baseline assessment, volunteers inhaled five deep breaths of nebulised saline, delivered via a breath-activated dosimeter (Mefar Dosimeter MB3, Brescia, Italy) and held their breath for 6 s. Following inhalation of saline, each dose of methacholine was inhaled and FEV_1 measurements were recorded at 30 and 180 s. If FEV_1 fell by 20% and was reversible using a bronchodilator (salbutamol), the challenge was stopped and the volunteer was excluded from the study. This is because any suggested airway hyper-responsiveness is consistent with a diagnosis of asthma rather than COPD (Cockroft 2010).

2.2.2 Isolation of PBMC

Peripheral blood mononuclear cells (PBMC) were isolated from 60ml whole blood obtained from non-smokers, smokers and COPD patients. Blood was collected in 0.5M of the chelating agent ethylene-diamine-tetra-acetic acid (EDTA), and divided into 3 x 20ml aliquots. Red blood cells (RBC) were sedimented using 6% ($^{W}/_{V}$) dextran diluted in 0.9% ($^{W}/_{V}$) sodium chloride, and further diluted in Hank's balanced salt solution (HBSS) to isolate PBMC. In brief, 3 x 20ml aliquots of blood were transferred into separate 3 x 50ml centrifuge tubes and mixed with 20ml HBSS and 10ml of 6% ($^{W}/_{V}$) dextran solution, giving a total volume of 50ml. Blood was sedimented at room temperature (RT) for 20 min, after which the PBMC-rich layer was collected and transferred to clean 3 x 50ml centrifuge tubes. PBMC were washed twice with 15ml HBSS by centrifuging for 5 min at 400 x *g* at 22°C.

PBMC were separated from granulocytes using a discontinuous Percoll density gradient. The discontinuous gradient was prepared by diluting neat Percoll (1:10) with 9% ($^{W}/_{V}$) sodium chloride solution to obtain a 100% working concentration. The working concentration of Percoll was further diluted with 0.9% ($^{W}/_{V}$) sodium chloride to obtain the following density fractions: 81% ($^{V}/_{V}$), 67% ($^{V}/_{V}$) and 55% ($^{V}/_{V}$). These fractions were prepared by diluting 8.1ml, 6.7ml and 5.5ml Percoll with 1.9ml, 3.3ml and 4.5ml of 0.9% ($^{W}/_{V}$) sodium chloride, respectively. Once prepared, 4ml of the 81% ($^{V}/_{V}$) fraction was transferred to 15ml centrifuge tubes, followed by carefully over-laying 4ml of the 67% ($^{V}/_{V}$) fraction. The discontinuous Percoll gradient was completed by re-suspending pelleted PBMC in 4ml of the 55% ($^{V}/_{V}$) fraction and carefully layering the cells upon the 67% ($^{V}/_{V}$) fraction. The discontinuous Percoll gradient was centrifuged at 750 x *g* for 30 min at 22°C to separate PBMC from granulocytes. PBMC were collected from the 55%/67% interface and were washed in 50ml HBSS by centrifuging at 400 x *g* for 5 min at 22°C. PBMC were then re-suspended in 10ml MDM 'complete media' (Roswell Park Memorial Institute (RPMI)-1640, containing 10% ($^{V}/_{V}$) foetal calf serum (FCS), 10mg/ml (1% ($^{V}/_{V}$) penicillin/streptomycin (PS), 2mM (1% ($^{V}/_{V}$)) L-glutamine (LG)), and an aliquot withdrawn to perform a cell count. The aliquot of PBMC were diluted 1:10 in Kimura dye (0.05% ($^{V}/_{V}$) toluidine blue, 0.03% ($^{V}/_{V}$) light green, 10% ($^{V}/_{V}$) saponin, 0.07M phosphate buffer pH 6.4) and cells were counted on a haemocytometer. Once the cells had been counted the PBMC were centrifuged at 300 x *g* for 5 min at 22°C and re-suspended at 1 x 10^6 cell/ml in MDM media.

2.2.3 Monocyte Differentiation to MDM

PBMC were seeded onto 96-well clear-bottom, black plates at 1 x 10^5 cells/well and incubated for 2h at 37°C, 5% ($^{v}/_{v}$) CO_2 to allow monocytes to adhere to the plastic

surface (Tudhope, Finney-hayward, et al. 2008). Following incubation, non-adherent cells were aspirated and the attached monocytes were cultured in MDM media containing 2ng/ml granulocyte macrophage-colony stimulating factor (GM-CSF). Monocytes were incubated for 12d to allow full differentiation into MDM; cells were replenished with fresh MDM media containing GM-CSF on days 4 and 7 (Taylor et al. 2010).

2.2.4 DEP Sample Collection

Three different samples of DEP were used in this project, namely DEP used by Nightingale et al. 2000, termed DEP-N herein, and standard reference material (SRM)-1650B and SRM-2975 purchased from the National Institute of Standards and Technology (NIST) (Gaithersburg, MD, USA). DEP-N was prepared by placing cyclone collectors on the exhaust of a stationary diesel engine. The engine was run at 3,000 rpm with break pressure applied at 300-500-kPa, with a 20% exhaust-gas re-circulation fraction. A heat-exchanger, four cyclones and a standard gas recirculation route were used to mimic the use of a light-duty vehicle. DEP-N were collected and passed through a 20μm sieve and stored in a tight-lidded container. DEP-N were representative of the emissions of a light-duty engine.

SRM-1650B and SRM - 2975 were reported by NIST to have an average particulate diameter of 0.18μm and 11.2μm respectively. SRM-1650B and SRM-2975 particles are representative of the emissions from an industrial-forklift truck and a heavy-duty engine, respectively. SRM-1650B material was generated by several direct four-stroke engines operating under different conditions which were representative of heavy-duty engine emissions. SRM-1650B were collected from heat exchangers of a dilution tube facility following 200 hr of particulates accumulating. SRM-2975 material

was collected from a filter system designed for diesel-powered fork-lifts. SRM-2975 was received by NIST in a 55-gal drum and homogenised using a V-blender before packaging in polyethylene bags. Both samples were analysed for adsorbed PAH and nitro-PAH constituents, with values given on reference certificates (See Appendix III).

2.2.5 Metal Composition of DEP Samples

The composition of metals adsorbed to the surface of the DEP samples was identified by inductively coupled plasma atomic emission spectroscopy (ICP-OES). This assay was kindly performed by Dr J Seiffert and Mr P Maguire, Imperial College London. In brief, DEP samples were introduced into flowing argon to form plasma, which contained a rich source of both excited and ionized atoms. Light emitted by elements in the samples was measured. To determine the elemental composition of DEP-N, SRM-1650B or SRM-2975 samples, emission intensities were compared to the intensities of five standard solutions of known concentrations.

2.2.6. Detection of Endotoxin on DEP samples

DEP and lipopolysaccharide (LPS) were each re-suspended in sterile HBSS (pH 7.5) to obtain a concentration range of 1-100µg/ml for DEP and 0.01-100ng/ml for LPS. Endotoxin concentrations used to produce the standard curve were prepared by diluting 50µl reconstituted stock endotoxin standard (50 EU/ml) with 35µl endotoxin free water (EFW) to obtain a concentration of 30EU/ml. 50µl of EFW was pipetted in duplicate into wells on the microtitre plate provided with the kit, to which 33µl of the 30EU/ml concentration was pippetted into the assigned wells to obtain the highest concentration for the standard curve of 10EU/ml (Figure 2.1). Serial dilutions were then performed by transferring 33µl of the 10EU/ml concentration of endotoxin and

pipetting it into subsequent wells; 33µl from this well was then transferred to the next well and so on to obtain a range of endotoxin concentrations from 10EU/ml - 0EU/ml. 50µl DEP (with unknown concentrations of endotoxin), or LPS samples, were pipetted to assigned wells on the microtitre plate, followed by 50µl limolas amebocyte lysate (LAL) reagent, and incubated for 45 min at RT to enable the reagent to bind to the endotoxin (successful binding of LAL reagent to endotoxin produces a yellow colour). Colour formation was closely monitored and the reaction was stopped by pipetting 50µl of 'stop' solution (50% ($^{V}/_{V}$) acetic acid diluted in 15ml distilled water). Absorbance was read on a plate reader at λ 405nm. The lower limit of detection of the assay was 0.04EU/ml.

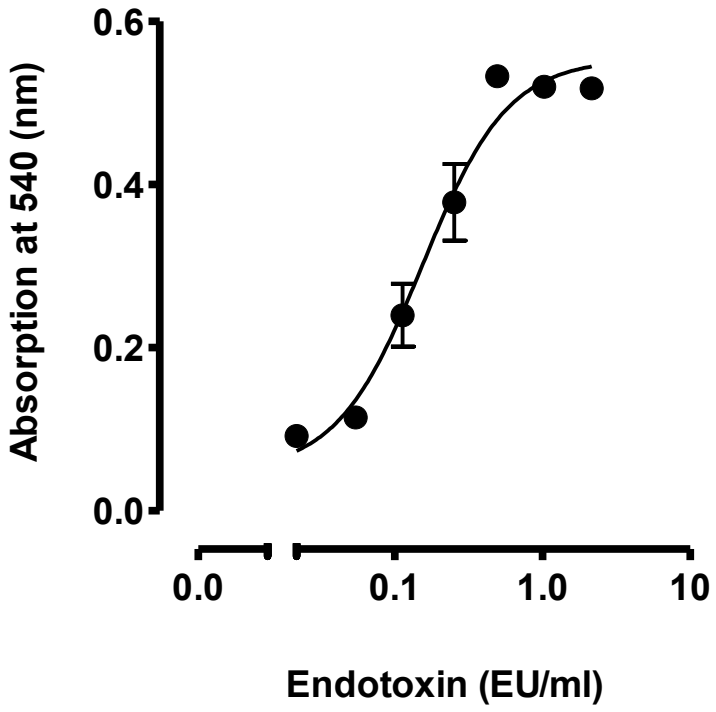

Figure 2.1 Endotoxin Standard Curve

Standard curve used to interpolate unknown concentrations of endotoxin on DEP and LPS samples. Data are in triplicate and are mean ± SEM, n =1.

2.2.7 MDM Treatments

2.2.7.1 Treatment of MDM with Inert Beads

Inert, polystyrene-based beads of different sizes (30μm, 10μm or 0.2μm) were commercially brought as a suspension in aqueous solution. The beads were further suspended in 10x D-PBS to obtain an isotonic solution. Beads were sonicated for 2 min and aliquoted into 1.5ml Eppendorf tubes and stored at -20˚C until required. Prior to MDM treatment, inert beads were sonicated and 300μl of inert beads were diluted in 700ml of RPMI-1640 serum-free cell culture media to obtain a stock concentration of 30mg/ml. Inert beads were further diluted in cell culture media to obtain the concentration range of 1-300 μg/ml (Figure 2.2). MDM were treated with the beads (1-300 μg/ml) and incubated for 24h at 37˚C in 5% ($^{V}/_{V}$) CO_2.

2.2.7.2 Treatment of MDM with DEP Samples

DEP-N, SRM-1650B or SRM-2975 were reconstituted in warmed HBSS at a stock concentration of 30mg/ml. DEP-N, SRM-1650B or SRM-2975 were then sonicated for 2 min to disaggregate particles, and aliquotted into 0.5ml Eppendorf tubes and stored at -20°C until required. Prior to treatment of MDM, DEP were again sonicated for 2 min and diluted in RPMI-1640 serum-free cell culture media to give a concentration range of 1-300μg/ml (Figure 2.2). MDM treated with DEP were incubated for 24h at 37˚C in 5% ($^{V}/_{V}$) CO_2.

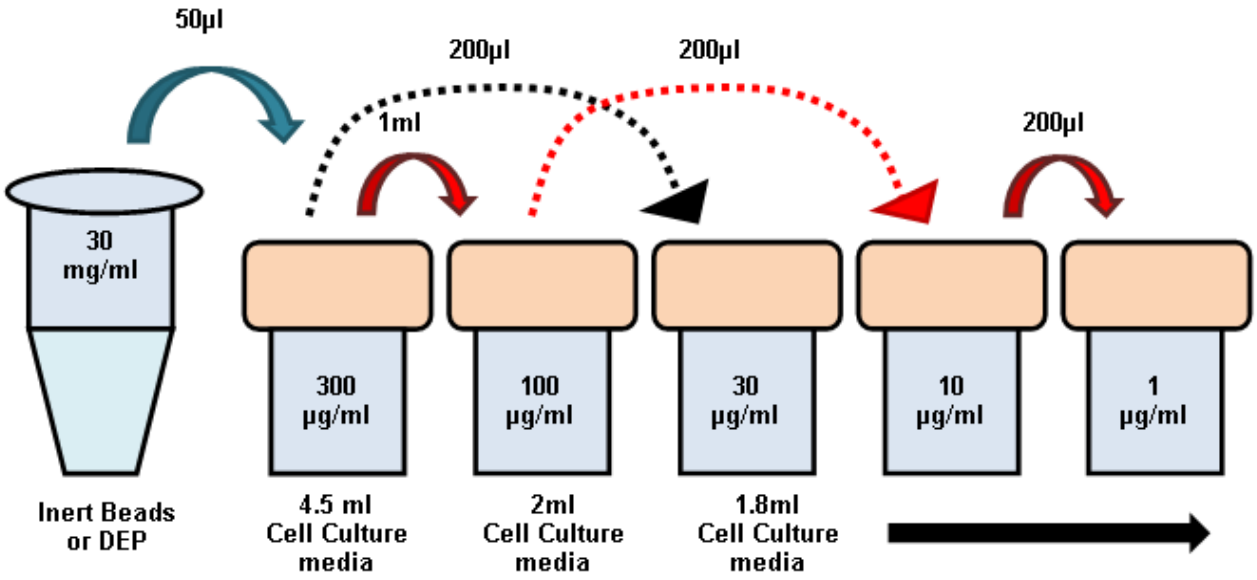

Figure 2.2 Dilution of Inert-Beads or DEP Samples

MDM were treated with increasing concentrations of inert beads or DEP (1-300µg/ml), to determine their effect on MDM function. To prepare these concentrations, particles (30mg/ml) were diluted 1:100 by transferring 50µl of particles (30mg/ml) to 4.50ml of cell culture media to obtain the top concentration of 300µg/ml (blue arrow). Subsequently, a 1:3 dilution of the 300µg/ml concentration was prepared by pipetting 1ml particles (300µg/ml) to 2ml cell culture media, to obtain a concentration of 100µg/ml (red arrow). In addition, a further 1:10 dilution was prepared from the 300µg/ml of particles to obtain a concentration of 30µg/ml (black dashed arrow). Serial dilutions were performed by diluting particles (100µg/ml) 1:10 by transferring 200µl particles (100µg/ml) to 1.8ml of media (black solid arrow) to obtain the following concentrations: 10µg/ml (red dashed arrow) and 1µg/ml (red arrow).

2.2.7.3 Treatment of MDM with DEP or LPS, With or Without Polymyxin B

In order to determine the contribution, if any, of LPS to any MDM responses observed, polymyxin B was used to inhibit the activity of LPS via its LPS-binding and neutralising activity. Polymyxin B (120mg/ml) was diluted in 12ml filter-sterilised double-distilled water (ddH_2O), to obtain a stock concentration of 10mg/ml. 50µl polymyxin B was aliquoted into 0.5ml Eppendorf tubes and stored at 4°C until

required. Polymyxin B treatment was prepared by diluting polymyxin B 1:1000 in serum-free RPMI-1640 cell culture media to obtain a working concentration of 10µg/ml. DEP-N (1-100µg/ml) (Section 2.2.7.2) or LPS (10ng/ml) (Section 2.2.7.4) was prepared in cell culture media with or without polymyxin B and incubated for 1hr at RT. Following incubation, 150µl DEP (1-100µg/ml) or LPS (10ng/ml), diluted with or without polymyxin B, was pipetted onto MDM. Cells treated with only media or media containing polymyxin B (10µg/ml) were used as non-stimulated baseline controls and were incubated at 37C, 5% ($^{V}/_{V}$) CO_2 for 24h. Following incubation, supernatants were harvested and analysed for release of CXCL8 using enzyme-immunosorbant assays (ELISA) (Section 2.2.10).

2.2.7.4 Preparation and Treatment of MDM with LPS with or without Polymyxin B

Lyphophilised LPS was reconstituted by pipetting 1ml of D-PBS to obtain a stock concentration of 1mg/ml. 5µl of LPS was then aliquotted into 0.5ml Eppendorf tubes and stored at -20℃ until required. LPS was diluted 1:10,000 to obtain a concentration of 100ng/ml by pipetting 2.2µl LPS (1mg/ml) into 18.8ml RPMI-1640 cell culture media. This was then further diluted 1:10 by adding 200µl of 100ng/ml LPS to 1.8ml cell culture media to obtain a concentration of 10ng/ml. For polymyxin B experiments MDM cultured at $1x10^5$ cells/well were treated with 100µl LPS (10ng/ml) prepared with or without polymyxin B and incubated for 1h as described in Section 2.2.7.3. In addition to the polymyxin B experiments, LPS (10ng/ml) was also used as a positive control for western blot experiments, including DEP-N concentration response (Section 2.2.7.5) and time-course (Section 2.2.7.6) experiments.

2.2.7.5 Western Blot: DEP-N Concentration-Response

MDM were cultured on a 24-well plate at a density of $5x10^5$ cells/well as described in Section 2.2.3. Cells were treated with 500µl of either increasing concentrations of DEP-N (1-100µg/ml) or LPS (10ng/ml) and incubated at 37℃, 5% ($^V/_V$) CO_2 for 1hr as described in Section 2.2.7.2 and Section 2.2.7.4 respectively. Following incubation, media was removed and cells were washed using 500µl ice-cold D-PBS. The D-PBS was then removed and 15µl lysis buffer containing 10µl protease and phosphatase inhibitors was pipetted onto cells as described in Section 2.2.11.1. Cell membranes and total protein were collected using a cell scraper and transferred to pre-chilled 0.5ml Eppendorf tubes. Phosphorylation of either p38 MAPK, or ERK 1/2, or JNK was determined by western blotting as described in Section 2.2.11.6.

2.2.7.6 Western Blot: DEP-N Time-Course Study

MDM were cultured on 24-well plates at a density of $5X10^5$ cells/well as described in Section 2.2.3. MDM were incubated at 37℃, 5% ($^V/_V$) CO_2 with 500µl DEP-N at 0, 5, 10, 20, 40 and 60 min, or in LPS (10ng/ml) for 60 min. Following incubation, supernatants were removed and cells were immediately placed on ice. Cells were washed with 1ml ice-cold PBS, and 15µl 1x lysis buffer was pipetted onto MDM as described in Section 2.2.11.1. Cell membranes and total protein was collected using a cell scraper and transferred to pre-chilled 0.5ml Eppendorf tubes. Phosphorylation of p38 or ERK 1/2 was determined by western blotting as described in Section 2.2.11.6.

2.2.7.7 Western Blot: Treatment of MDM with p38 Inhibitor

Lyphophilised p38 inhibitor (PF755616) was reconstituted in neat dimethyl sulfoxide (DMSO) to obtain a stock concentration of 10mM and stored at -20^{o}C until required. The p38 inhibitor was diluted in 1:1000 in RPMI-1640 cell culture media to obtain the top concentration of 10μM (10^{-5}M) (Figure 2.3). This was performed by transferring 2μl of the p38 inhibitor to 1.98ml of cell culture media. The top concentration of the p38 inhibitor was further diluted to obtain a concentration range of 10^{-5} - 10^{-10}M, performed as serial dilutions. In brief, 200μl of 10^{-5}M was transferred to 1.8ml cell culture media, and diluted by 1:10 serial dilutions to obtain a concentration range of 10^{-5} - 10^{-10}M. MDM were cultured on 96-well black plates and were treated with 100μl of 10^{-5} – 10^{-10}M inhibitor and incubated at 5% ($^{V}/_{V}$) CO_2, 37^{o}C for 1h. Following incubation, supernatants were removed and DEP-N (100μg/ml) was transferred to cells and further incubated in 5% ($^{V}/_{V}$) CO_2, 37^{o}C for 24h. Following incubation, supernatants were harvested and stored at -20℃ until required for ELISA (Section 2.2.10). For western blot experiments, MDM were cultured on 24-well plates at a density of 5X10^{6} cells/well as described in Section 2.2.3. MDM were treated with 500μl increasing concentrations of p38 inhibitor (10^{-5} - 10^{-10}M) and incubated in 5% ($^{V}/_{V}$) CO_2, 37^{o}C for 30min. Supernatants were removed and 500μl DEP-N was applied and further incubated for 1h in 5% ($^{V}/_{V}$) CO_2, 37^{o}C for 30min. Following incubation, cells were lysed and proteins were separated by western blotting as described in Section 2.2.11. To determine functionally whether or not p38 had been inhibited, phosphorylation of the downstream signalling component heat shock protein 27 (HSP27) was examined as described in Section 2.2.11.6.

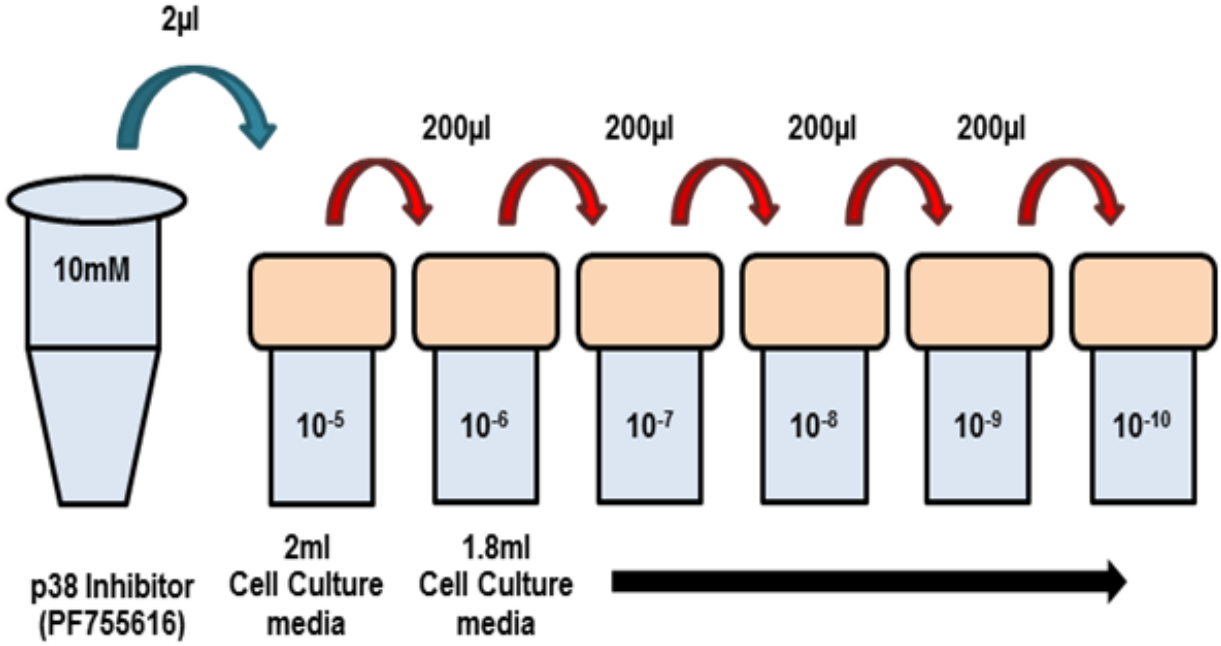

Figure 2.3 Serial Dilution of Stock p38 Inhibitor (PF755616)

The stock concentration of the p38 inhibitor (10mM) was diluted 1:10 (blue arrow) in 2ml serum-free cell culture media to obtain a working concentration of 10^{-5} M. Serial dilutions (red arrows) were performed on the working concentration of the p38 inhibitor by transferring 200µl 10^{-5} M concentration to 1.8ml cell culture media (black arrow); this was repeated to obtain a concentration range of 10^{-5} – 10^{-10}M.

2.2.7.8 Western Blot: Treatment of MDM with MEK 1/2 Inhibitor

The MEK 1/2 inhibitor (PD98059) was reconstituted in neat DMSO to obtain a stock concentration of 30mM and stored at -20℃ until required. The MEK 1/2 inhibitor was diluted 1:1000 in RPMI-1640 serum-free cell culture media to obtain the top concentration of 30µM, by pipetting 3µl stock solution of inhibitor to 2.97ml media. The top concentration of the MEK 1/2 inhibitor was further diluted in media as shown in Figure 2.4 to obtain the concentration range 30µM - 0.1µM. In brief, 1ml of the 30µM concentration of MEK 1/2 inhibitor was diluted in 2ml media to obtain a concentration of 10µM. The 30µM concentration was again diluted 1:10 by transferring 200µl inhibiter to 1.8ml media to obtain the 3µM concentration. Serial

dilutions were then performed on the 10μM inhibitor concentration to obtain the 1μM and 0.1μM concentrations. In brief, 200μl of the 10μM concentration was pipetted into 1.8ml cell culture media to obtain the 1μM concentration, and subsequently 200μl of the 1μM concentration was diluted in 1.8ml media to obtain the 0.1μM concentration. Once the required concentrations were prepared, 100μl of MEK 1/2 inhibitor (30μM - 0.1μM) was pipetted on to MDM cultured on 96-well black plates and incubated in 5% ($^{V}/_{V}$) CO_2, 37^{o}C for 1h. Supernatants were aspirated and 150μl of DEP-N (100μg/ml) was transferred to MDM and further incubated in 5% ($^{V}/_{V}$) CO_2, 37^{o}C for 24h. Following incubation, supernatants were harvested and stored at -20^{o}C until required for ELISA experiments (Section 2.2.10). For western blot experiments, MDM were cultured on 24-well plates at a density of $5X10^6$ cells/well as described in Section 2.2.3. MDM were treated with 500μl PD98059 (0.1μM - 30μM) and incubated at 37^{o}C, 5% ($^{V}/_{V}$) CO_2 for 30 min. Following incubation, supernatants were aspirated and 500μl DEP-N (100μg/ml) was pipetted on to cells and further incubated at 37^{o}C, 5% ($^{V}/_{V}$) CO_2 for 1 hr. Supernatants were removed and cells were lysed and proteins were separated by western blotting as described in Section 2.2.11. To determine whether the ERK 1/2 pathway was inhibited by the MEK 1/2 inhibitor, phosphorylation of ERK 1/2 was examined as described in Section 2.2.11.6.

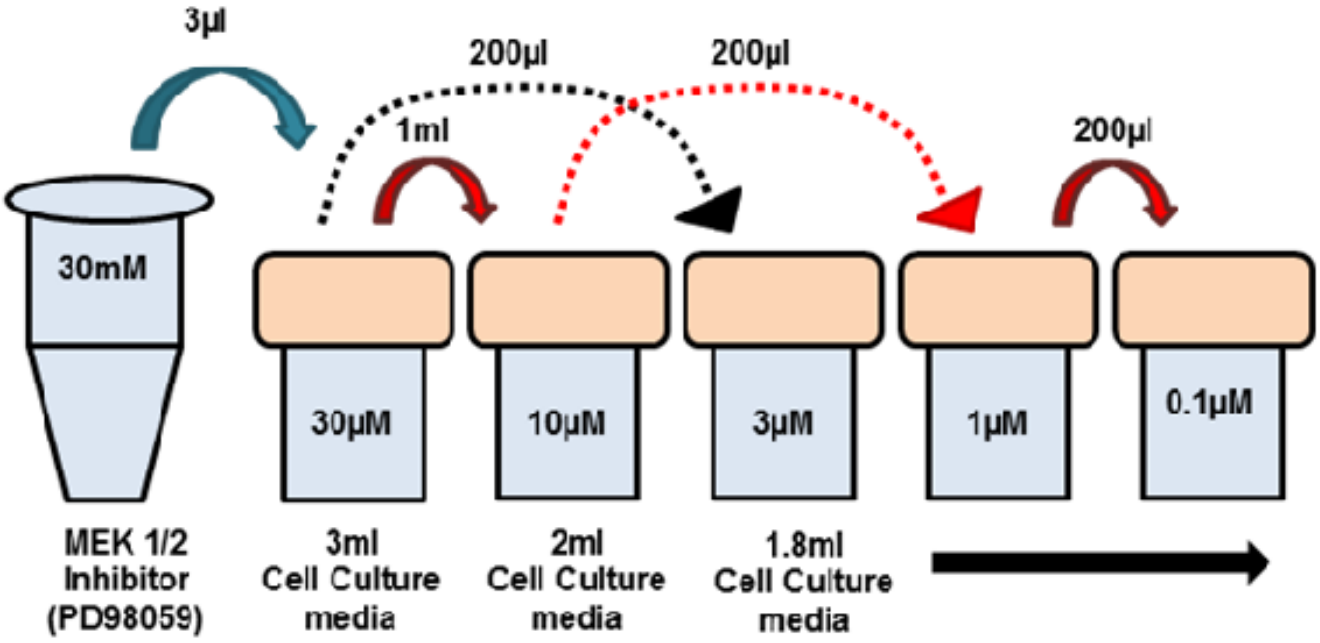

Figure 2.4 Dilution of Stock MEK 1/2 Inhibitor (PD98059)

The concentration range of the MEK 1/2 inhibitor (PD98059) required to treat MDM was between 0.1µM - 30µM. To prepare these concentrations, the stock concentration of MEK 1/2 inhibitor (30mM), was diluted 1:10 (blue arrow) in serum-free cell culture media to obtain a working concentration of 30µM. The 30µM concentration was further diluted 1:3 by transferring 1ml of the 30µM inhibitor to 2ml of media to obtain the 10µM concentration (red arrow). 200µl of the 30µM concentration of inhibitor was further diluted in 1.8ml of media to obtain a concentration of 3µM (black dashed arrow). 200µl of the 10µM concentration was pipetted to 1.8ml cell culture media (black solid arrow) to obtain a concentration of 1µM (red dashed arrow); subsequently 200µl from the 1µM concentration was pipetted to 1.8ml of cell culture media to obtain the final 0.1µM concentration (red arrow).

2.2.7.9 Measurement of Phagocytosis by MDM

The phagocytic capacity of MDM treated with inert beads of different sizes or DEP was assessed by further exposing MDM to carboxylate-based fluorescent beads (size: 2µm). Fluorescent beads were suspended in serum free RPMI-1640 cell culture media at a concentration of $50x10^6$ beads/ml. 100µl fluorescent beads was pipetted onto DEP or inert bead-treated MDM and incubated for 4h at 37˚C in 5% ($^V/_V$) CO_2 (Taylor et al. 2010).

2.2.7.9.1 Quantification of Phagocytosis

MDM were washed with 100µl PBS and any extracellular fluorescence was quenched using 1% ($^{V}/_{V}$) trypan blue for 2 min. Trypan blue was aspirated and phagocytosis of fluorescent beads by MDM was measured using fluorimetery (Fluostar Optima BMG LabTech, Aylesbury, Buckinghamshire) at excitation λ 480nm and emission λ 520nm. Data were expressed as relative fluorescent units (RFU).

2.2.8 Cell viability

2.2.8.1 MTT Assay

MDM viability was determined by the MTT assay which measures mitochondrial function. MDM were incubated with 0.1% ($^{W}/_{V}$) 3-(4,5-Dimethylthiazol-2-yl)-2,5-diphenyltetrazolium (MTT) and incubated at 37°C, 5% ($^{V}/_{V}$) CO_2 for 1 h at RT. During incubation, MTT is reduced to formazan by mitochondrial dehydrogenases of metabolically active cells, and is visualised by the formation of an insoluble purple precipitate. The MTT was aspirated and cells were lysed by 100µl neat DMSO. To avoid interference with the assay by DEP that had been phagocytosed by cells, plates were centrifuged at 400 *x g* for 5 min and lysates were transferred to separate clear 96-well plates. Absorbance was measured at λ 570nm by spectrophotometry. Results were expressed as a percentage of non-stimulated cells, which were considered 100% viable.

2.2.8.2 Detection of Apoptosis and Necrosis

Apoptosis and necrosis of DEP-N-treated MDM were determined by staining cells with annexin V conjugated to the flurochrome phycoerythrin (PE) and 7-Amino-

Actinomycin (7-AAD). The Annexin V PE and 7-AAD kit was purchased from BD Biosciences, Oxford, UK and the protocol was followed according to manufacturer's instructions. In brief, 100µl DEP-N-treated MDM (1-100µg/ml; $1X10^6$ cells/ml) were pipetted directly into FACS tubes and washed with ice-cold D-PBS by centrifugation at 400 x *g*. The cell pellet was re-suspended in 1 X binding buffer (10mM Hepes/NaOH (pH 7.4), 140mM NaCl, 25mM $CaCl_2$) and 5µl Annexin PE and 5µl 7-AAD were pipetted into corresponding FACS tubes. Cells were incubated in the dark for 15 min at RT. Following incubation, cells were washed with D-PBS by centrifugation at 400 x *g* and re-suspended in 4% ($^V/_V$) paraformaldehyde (PFA). Samples were analysed using flow cytometry (BD FACScanto II flow cytometer, UK). For each sample processed, doublets (cells stuck together) were selected out from the population of single cells being analysed. Doublets were removed by identifying where the cells had distributed on a forward and side scatter height *vs* width dot-plot. If cells had distributed away from the main cell population, gates were applied to prevent the former data being collected (Figure 2.5). For each sample processed, 10,000 events were recorded. The Annexin V kit, quantified the percentage of cells undergoing apoptosis or necrosis according to their distribution on a dot plot (Figure 2.6). Cells which had stained positive with Annexin-PE were considered to be undergoing early apoptosis, whereas cells which had stained positive with 7-AAD were considered to be undergoing necrosis. Cells which had stained positively for both Annexin-PE or 7-AAD were undergoing necrosis, whilst unstained cells were considered to be viable (Figure 2.6). Data were analysed using CellQuest software.

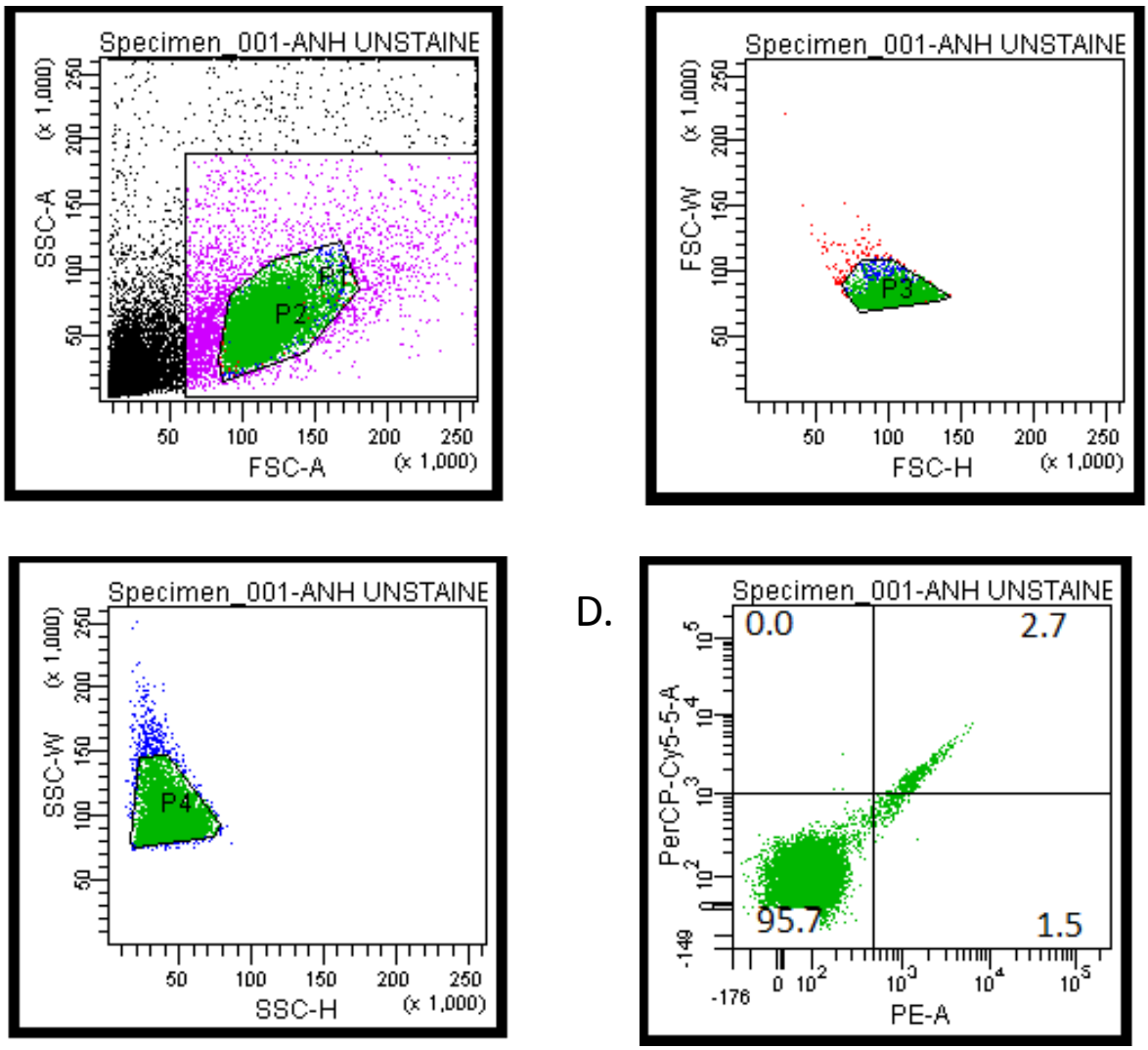

Figure 2.5 Removing Doublets from Single Cell Suspensions

MDM were treated with 1-100µg/ml DEP and incubated for 24h at 37ºC in 5% CO_2. To determine whether DEP induced cell apoptosis or necrosis, MDM were analysed using flow cytometry. (A) MDM from a smoker were selected by 'gating' around the main cell population to avoid inclusion of monocytes or debris. To prevent two or more cells from being processed at the same time, gates were applied to cells and assessed according to their size and granularity on a forward- and side-scatter dot-plot; these cells were termed 'doublets'. (B) Cells were examined on a forward-scatter dot-plot according to their height and width and large cells were removed by applying a gate on the discrete single-cell population and any large cells were excluded. (C) A side-scatter dot-plot was also used, to exclude any cells which had an excess granularity according to the height or width of the cell, as this was representative of doublets. (D) Following removal of doublets the suspension of single cells was processed.

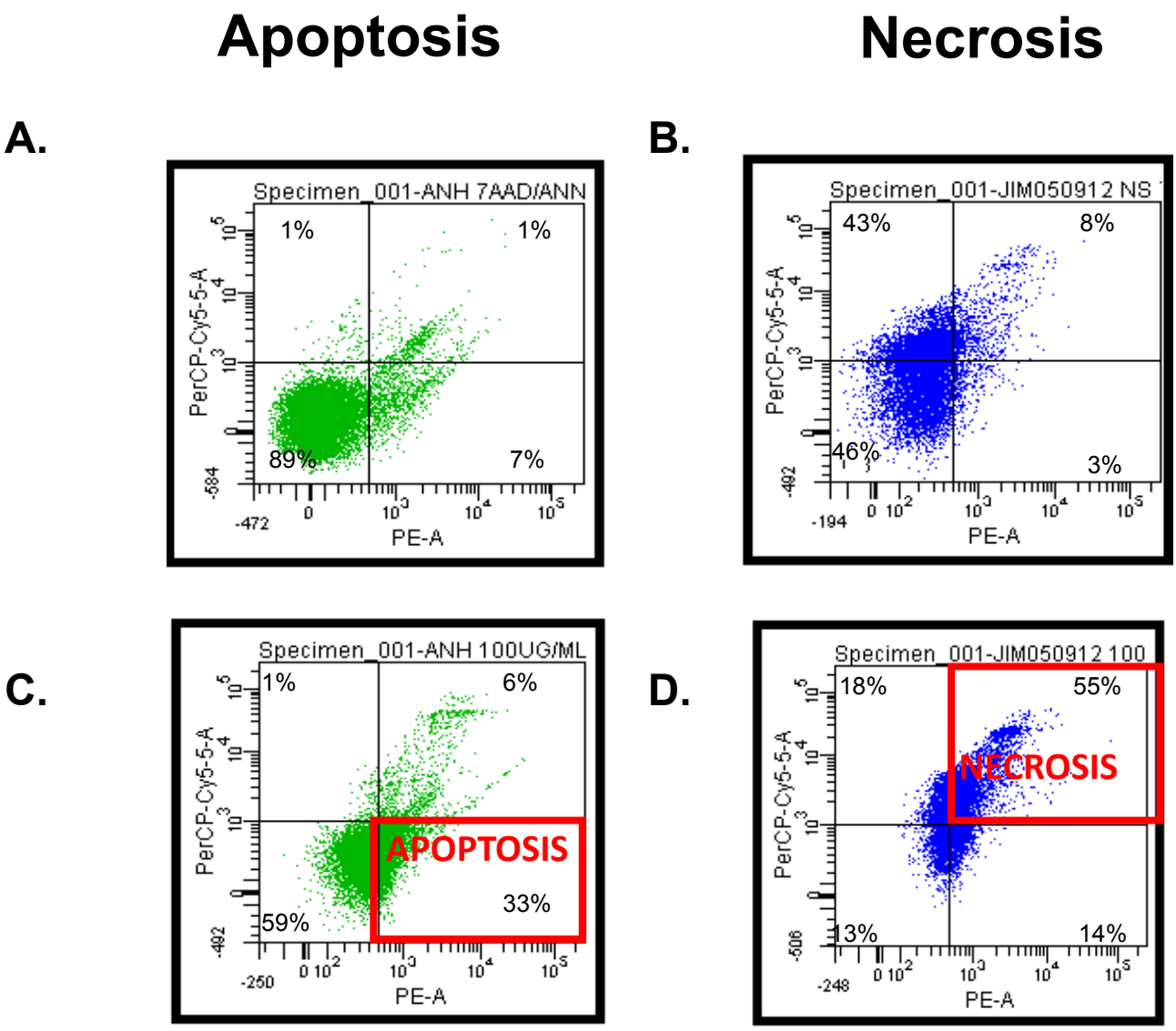

Figure 2.6 Dot-Plots of DEP-N-Treated MDM Undergoing Apoptosis or Necrosis

To differentiate whether DEP or inert bead-treated cells underwent apoptosis or necrosis, cells were stained using PE (marker of apoptosis) or 7AA-D (marker of necrosis) and analysed according to their location on flow cytometry dot-plots. (A-B) Non-stimulated viable cells from a non-smoker and smoker were located in the lower left quadrant. (C) Apoptotic cells that had stained positively for PE only, were located in the lower right quadrant, whereas necrotic MDM that had stained positively for 7-AAD only, were located in the upper left quadrant. (D) Cells which had stained positive for both PE and 7-AAD were located in the upper right quadrant and were considered to be undergoing necrosis.

2.2.9 Imaging of DEP

2.2.9.1 Light Microscopy Imaging of DEP

Stock concentration of DEP-N, SRM-1650B and SRM-2975 (30mg/ml) were sonicated for 5 min and diluted in RPMI-1640 media or double-distilled water (ddH_2O) to obtain a concentration of 300µg/ml. 100µl of each sample was pipetted onto a 48-well flat bottom clear plate and viewed under an inverted light microscope using a X20 objective lens. Images were captured using an Olympus SLR camera fitted with a microscope-compatible adaptor.

2.2.9.2 Light Microscopy Imaging of MDM Incubated with DEP or Inert Beads

MDM (1 x 10^5 cells/well) cultured on 96-well flat bottom black plate were treated with 150µl of DEP or inert bead (1-100µg/ml) samples and incubated at 37°C, 5% ($^V/_V$) CO_2 for 24h as described in Section 2.2.7.1 and Section 2.2.7.2 respectively. Images of MDM treated with DEP or inert beads were captured using a X20 objective lens on via an Olympus SLR camera fitted with a microscope-compatible adaptor.

2.2.9.3 Fluorescent Microscopy Imaging of DEP-Treated or Inert-Bead-Treated MDM Incubated with Fluorescent Beads

MDM were treated with 150µl of increasing concentrations of DEP or inert beads (1-100µg/ml) samples as described in Section 2.2.7.1 and Section 2.2.7.2 respectively. Following treatments, MDM were incubated at 37°C, 5% ($^V/_V$) CO_2 for 24h and, subsequently, supernatants were collected and stored at -20°C until required. DEP- or inert-bead-treated MDM were subsequently incubated with 100µl fluorescent

beads ($50x10^6$ beads/ml) at 37°C, 5% ($^V/_V$) CO_2 for 4h as described in Section 2.2.7.9. Following incubation, supernatants were removed and cells were washed with 100µl D-PBS, and extracellular fluorescence was quenched using 100µl 1% ($^V/_V$) trypan blue. DEP-treated or inert bead-treated MDM were viewed under an inverted light microscope using a fluorescent lamp. Images were captured using a X20 objective lens via an Olympus SLR camera fitted with a microscope-compatible adaptor.

2.2.9.4 Transmission Electron Microscopy (TEM)

2.2.9.4.1 TEM: Particle Characterisation

DEP samples were diluted in ddH_2O to obtain a concentration of 300µg/ml. DEP were sonicated for 30 min and 15µl of each sample was transferred to formvar-coated copper grids and incubated overnight at RT. Particles were stained using 1% ($^V/_V$) uranyl acetate and incubated for 10 min. Grids were washed with ddH_2O and excess moisture was removed using filter paper. Grids were air dried for 15 min and particle morphology and geometric diameters were analysed using TEM.

2.2.9.4.2 TEM: Internalisation of DEP-N by MDM

MDM cultured on 24-well plates were treated with 1ml DEP-N at 1-100µg/ml and were incubated for 24h at 37°C, 5% ($^V/_V$) CO_2. Cells were washed three times with 500µl 0.9% ($^W/_V$) $NaCl_2$ and fixed using 2.5% ($^V/_V$) glutaraldehyde in (0.05M) cacodylate buffer (pH 5.0-7.4). Following dehydration, cells were incubated at 4°C for 2h. Glutaraldehyde was removed and cells were rinsed in cacodylate buffer three times prior to overnight incubation at 4°C. Cells were post-fixed in osmium tetroxide and incubated for 1h at 4°C. Cells were then washed twice with distilled water and

dehydrated by submerging in a series of graded ethanol solutions. Briefly, cells were incubated in 70% ($^{V}/_{V}$) ethanol twice for 10 min each, followed by incubation in 90% ($^{V}/_{V}$) ethanol twice for 10 min and finally incubation in 100% ($^{V}/_{V}$) ethanol three times for 10 min each. Once cells were fixed, ethanol was removed and replaced with araldite resin diluted 50:50 in neat ethanol and incubated for 24h at RT. Tissue culture plates were placed on a rotator to facilitate equal infiltration of araldite resin between samples. Following incubation, the diluted resin was removed and replaced with 100% ($^{V}/_{V}$) resin and further incubated for 2h. Using a pastette, epoxy resin was transferred to wells and precision-moulded embedding capsules (Beem capsules), that allow preparation of uniform, pre-shaped blocks, were filled with fresh resin. The capsules were inverted and affixed over the wells. Tissue culture plates were placed in the oven for 72h at 60^{o}C to harden.

2.2.9.4.3 TEM: Sectioning

Once the resin had hardened, the Beem capsules were removed and sections were cut on a microtome. Glass knives were aligned to cut 1µm thick sections to determine the area of confluent cells. This was done by transferring the 1µm section to a glass slide and staining with toulene blue. The area of confluent cells was further reduced in size and ultra-thin sections of 75nm were taken. These sections were transferred to copper grids and stained using uranyl acetate for 7 min followed by washing with methanol. Sections were than submersed in lead citrate for 5 min and washed with methanol. Grids were placed on hardened wax paper to remove excess methanol before viewing by TEM.

2.2.9.5 Confocal Microscopy

2.2.9.5.1 DEP-N Treatment of MDM

Peripheral blood monocytes monocytes (2 X 10^5/well) were cultured on Lab-tek permanox 8-well chamber slides in the presence of GMCSF (2ng/ml) for 12 days to enable differentiation towards the MDM phenotype (Section 2.2.3). MDM were exposed to 200µl DEP-N (1-100µg/ml) and incubated for 24h in 5% CO_2 at 37°C. MDM incubated in only RPMI-1640 cell culture media served as non-stimulated controls. Fluorescent beads were transferred to MDM and incubated for a further 4h. Particles which had not been phagocytosed were aspirated and extracellular fluorescence was quenched by 1% ($^V/_V$) trypan blue followed by repeated washing with D-PBS as described in Section 2.2.7.9.1.

2.2.9.5.2 Staining

MDM cytoplasm was stained using a working concentration of 12.5mM Cell Tracker™ red, diluted in D-PBS by incubating for 45 min at 37°C. Following incubation, cells were further incubated in pre-warmed RPMI-1640 cell culture media for 30 min at 37°C. Cells were fixed by incubating with 200µl 4% ($^W/_V$) PFA for 10 min at RT, followed by repeated washing with D-PBS. The cell nuclei were stained with 2µM DAPI and incubated for 3 min at RT. Cells were washed again with D-PBS and chambers were removed from the microscope slide. Cover-slips were affixed over the cells using citifluo and sealed with clear nail varnish. Slides were stored in the dark at 4°C.

2.2.9.5.3 Visualisation

Microscope slides were viewed on a Leica SP2 upright confocal microscope. A series of 40 sequential, cross-sectional images of cells were taken to visualise the internalisation of DEP-N and fluorescent beads. Images were overlaid and remodelled using the Volocity ® 3D Imaging Analysis Software (PerkinElmer Inc., Massachusetts, USA).

2.2.10 ELISA

CXCL8, IL-6 and TNFα were measured by ELISA according to manufacturer's instructions (R&D systems, Oxford, UK). Briefly, capture antibody was coated onto Nunc Maxisorp flat-bottom 96-well plates overnight RT. Plates were washed three times with wash buffer (0.05% ($^{V}/_{V}$) Tween-20 in PBS pH 7.1-7.5). Non-specific binding was blocked with 100µl blocking buffer (5% ($^{W}/_{V}$) sucrose, 1% ($^{W}/_{V}$) BSA and 0.01% ($^{W}/_{V}$) azide pH 7.4) and incubated for 1h at room temperature. Standards and supernatants were diluted in reagent diluent (1% BSA ($^{W}/_{V}$) in PBS) and were transferred to the plate and incubated for 2h at RT. Following incubation, plates were washed with wash buffer and 100µl detection antibody was transferred to wells and incubated for 2h at RT. Plates were washed, and 100µl streptavidin-conjugated-horse radish peroxidase (HRP) was transferred to wells and incubated at RT for 20 min. Following incubation, 100µl tetramethybenzinidine substrate (1:1 colour substrate A (H_2O_2) and colour substrate B (TMB)) solution was applied and incubated until sufficient colour had developed. The reaction was stopped by adding 50µl 1M sulphuric acid. Absorbance was set at λ 450nm with wavelength correction at λ 570nm to determine optical density of each well. To determine the concentrations of mediators in unknown samples, readings of individual wells were

interpolated from the standard curve (Figure.2.7). The lower limit of detection for TNFα and CXCL8 was 31.3pg/ml, and for IL-6 was 15.6pg/ml.

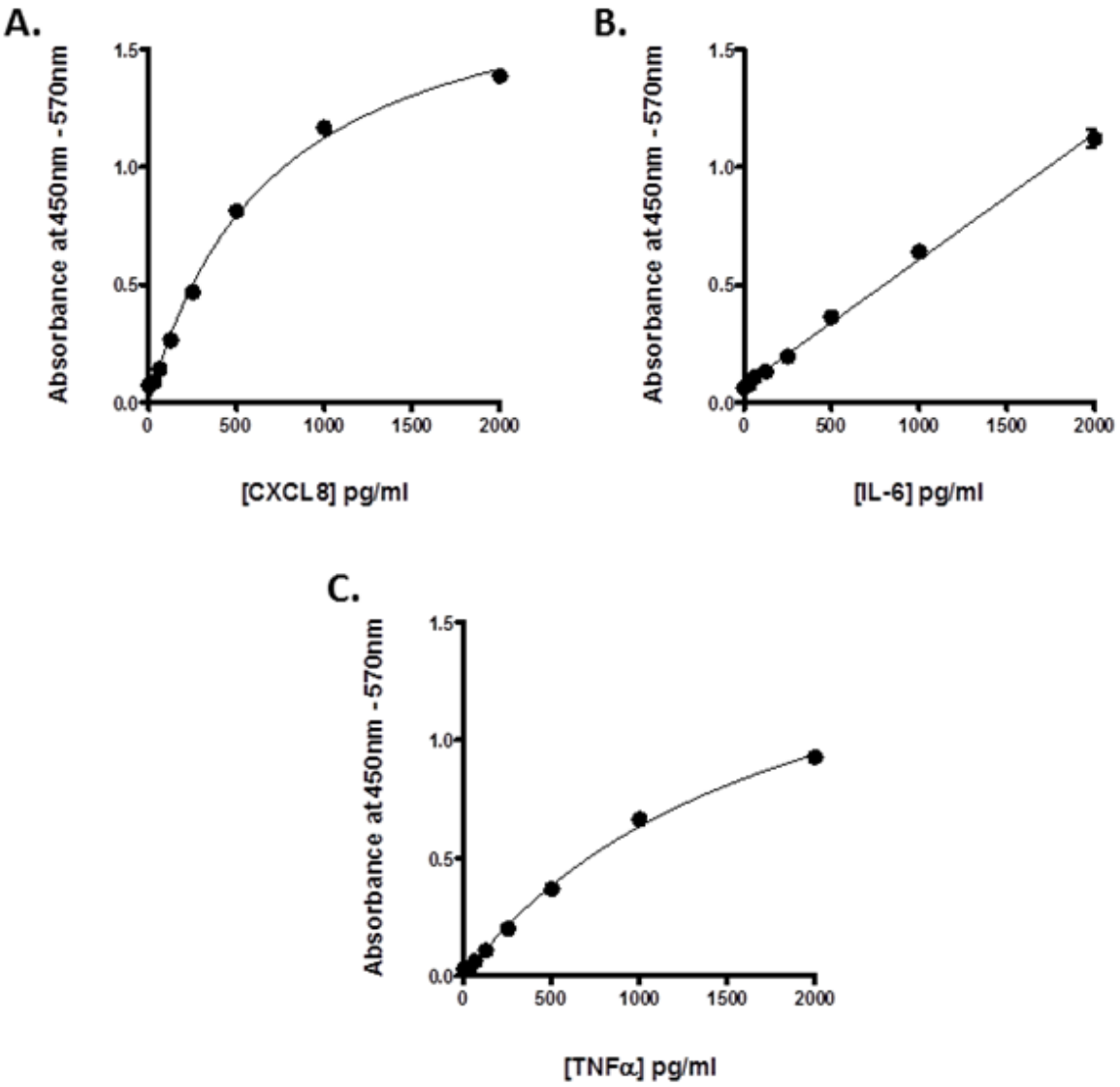

Figure 2.7 ELISA Standard Curves for CXCL8, IL-6 and TNFα

Representative standard curves for (A) CXCL8 (B) TNFα or (C) IL-6. Unknown concentrations of mediators released by DEP- or inert bead-treated MDM were interpolated from the curves. Mediator standards were processed in duplicate and data are expressed as medians or mean ± SEM, n=1.

2.2.11 Western Blotting

2.2.11.1 Protein Extraction

Following differentiation, MDM were exposed to various treatments (Section 2.2.7.5; Section 2.2.7.6; Section 2.2.7.7; Section 2.2.7.8). Media was removed and cells were washed with 500µl ice-cold D-PBS. The D-PBS was then removed and cells were lysed by addition of lysis buffer (150mM NaCl, 20mM Tris-HCl (pH 7.5), 1mM Na_2EDTA,1mM EGTA, 1% ($^{w}/_{v}$) Triton X-100, 2.5mM sodium pyrophosphate, 1mM beta-glycerophosphate, 1mM Na_3VO_4, 1µg/ml leupeptin) containing 10µl of protease and phosphatase inhibitors. Lysates were collected in pre-chilled Eppendorf tubes and centrifuged at 10000 x *g,* for 10 min at 4˚C. Following centrifugation, supernatants were removed from sedimented debris and placed directly on ice.

2.2.11.2 Protein Assay

To determine protein levels in each sample, a BioRad protein assay was performed. In brief, 1mg/ml BSA was used to produce a standard curve in the range 0 - 1mg/ml. Samples were transferred in triplicate to a 96-well clear plate and treated with 200µl BioRad protein reagent (diluted 1:4 in distilled water). Absorbance was measured at ʎ 590nm with a spectrophotometer. Unknown protein concentrations of samples were interpolated from the standard curve (Figure 2.8).

2.2.11.3 Preparation of Samples

20µg/ml protein from each sample was transferred to Eppendorf tubes and diluted with Laemelli sample buffer (62.5mM Tris-HCl, 10% ($^{v}/_{v}$) glycerol, 1% ($^{w}/_{v}$) SDS, 1%

($^{v}/_{v}$) β-mercaptoethanol, 0.01% ($^{w}/_{v}$) bromophenol blue (pH 6.8)) to obtain a final volume of 30µl. These were then boiled for 5 min at 95˚C to denature proteins.

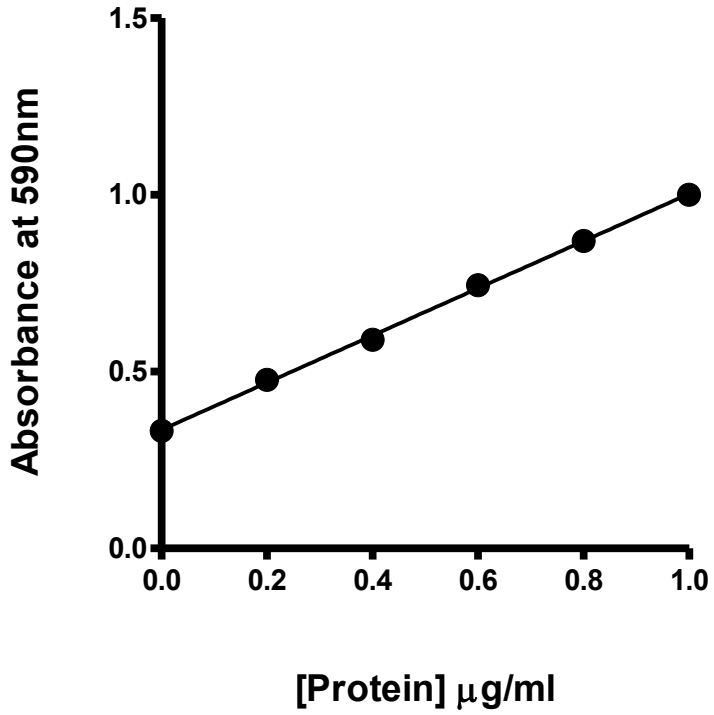

Figure 2.8 BSA Standard Curve for Protein Assay

Representative BSA protein standard curve used to interpolate the concentration of protein in DEP-treated cell lysates. BSA standard samples were processed in duplicate. Data are mean ± SEM, n=1.

2.2.11.4 Gel Electrophoresis

4-12% bis-tris polyacrylamide gels (Invitrogen, Paisley, UK) were used to separate proteins according to size. Gels were secured within a glass tank filled with MOPS running buffer (250mM MOPS, 250mM Tris, 5mM EDTA, 1% ($^{w}/_{v}$) SDS, (pH 7.7)). Using loading micro-capillary pipette tips, 5µl of a molecular weight marker was transferred to gels along with 22µl sample to individual wells. The lid of the tank was

firmly secured and connected to a power source, and 100V was applied for 2h allowing the proteins to resolve.

2.2.11.5 Transfer of Proteins to Hybond Nitrocellulose Membrane

Proteins separated by gel electrophoresis were transferred to a Hybond nitrocellulose membrane. This involved assembling a transfer cassette containing sponge and blotting paper (3MM Chr chromatography paper) soaked in transfer buffer (0.191M glycine, 0.02M Tris-HCl, 20% ($^{v}/_{v}$) methanol, (pH7.4)). The gel and nitrocellulose membrane were then placed in between the stacked sponge and blotting paper and the cassette was closed. The cassette was then placed within a transfer tank along with an ice-pack to prevent the gel from over-heating. Transfer buffer was poured into the tank and connected to a power source. Proteins were transferred at 200mA and 200mV for 1h.

2.2.11.6 Immunodetection

The nitrocellulose membrane was incubated in 12ml blocking buffer (5% ($^{w}/_{v}$) non-fat dried milk dissolved in TBS-Tween 20 (0.5M Tris Base, 9% ($^{w}/_{v}$) NaCl, 0.5% ($^{v}/_{v}$) Tween-20, pH 7.4)) for 1h at RT to prevent non-specific antibody binding. The primary antibody, against the protein of interest, was diluted 1:1000 in blocking buffer and poured over the membrane. The membrane was placed on a rotator and incubated at 4˚C overnight. The membrane was washed repeatedly with TBS-Tween-20 buffer to remove unbound antibody followed by transferring the membrane to blocking buffer containing HRP conjugated secondary antibody (1:1000) and incubating for 1h at RT.

The membrane was then washed with TBS-Tween-20 buffer and incubated in 10ml enhanced chemiluminescence (ECL) detection solution (GE Healthcare, Buckinghamshire, UK) for 2 min at RT. The membrane was then wrapped in cling film and exposed to photographic film for 1-10 min. The film was developed using an AFP imaging developer (New York, USA) and the density of bands of interest was analysed using UVP GelDoc-IT Imaging System and Labworks Software.

2.2.12 Statistical Analysis

Data were compared for statistical significance between subject groups by one-way ANOVA followed by Dunnett's test for multi-group comparisons. Data expressing a P value of <0.05, were considered to be statistically significant. Statistical differences were calculated using Prism V.5 (GraphPad, San Diego, USA).

2.2.13 Overarching Timeline of Experiments

See Figure 2.9.

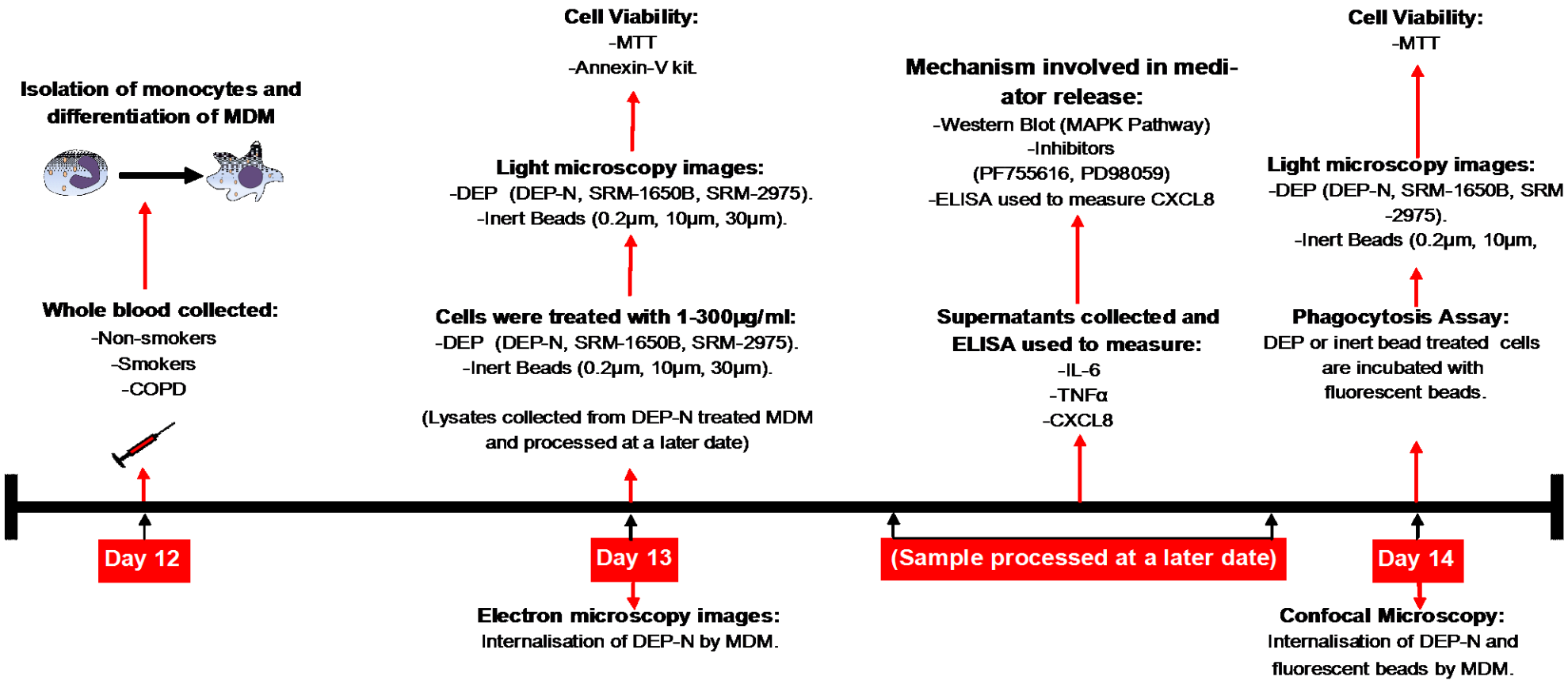

Figure 2.9 Overarching Timeline of Experiments Conducted Throughout the Study

Peripheral whole blood was collected from non-smokers, smokers and patients with COPD. Monocytes were isolated by adherence and incubated with granulocyte-macrophage colony-stimulating factor for 12d to derive MDM. Following incubation cells were treated with 1-300µg/ml DEP or inert beads and incubated for 24h. Supernatants were removed and analysed for pro-inflammatory mediators. DEP or inert bead treated-MDM were further treated with fluorescent beads for 4h and internalisation of beads was determined using fluorimetry. Cell viability of DEP or inert bead treated MDM was examined before and after the addition of fluorescent beads; the effect of DEP-N on the induction of apoptosis or necrosis was examined using the Annexin-V-kit and assessed using flow cytometry. Separate experiments involved lysing DEP-N treated MDM (with or without PF755616 or PD98059 inhibitors) and examining the mechanism of mediator release using western blot and ELISA. Light Microscopy images were taken following DEP or inert bead treatment and after the addition of fluorescent beads. Internalisation of DEP-N by MDM was examined using electron microscopy and internalisation of DEP-N and fluorescent beads by MDM was examined using confocal microscopy.

Chapter 3:

Characterisation of DEP

3.1 Introduction

Atmospheric pollution consists of a complex mixture of heterogeneous particles such as soot, dust, pollen and vehicle exhaust emissions. These particles are known as PM and are classified according to their size (Backes et al. 2013). For example, particles with a diameter <0.1μm, <2.5μm or <10μm are termed $PM_{0.1}$, $PM_{2.5}$ and PM_{10} respectively. Epidemiological studies show that increases in PM are associated with adverse respiratory health (Bell & Davis 2001; Dockery & Pope 1994). A major contributor to PM_{10} are DEP which are formed by incomplete combustion of diesel fuel. DEP consist of an elemental carbon core which binds a number of organic compounds, including PAHs and nitro-PAHS, endotoxin and metals including B, Ca, Fe and Zn (Wichmann 2007).

The mechanism involved in the formation of DEP involve two 'modes', referred to as the nucleation mode and accumulation mode (Schneider et al. 2005). During the nucleation mode, liquid particles consisting of sulfate, water or semi-volatile organic components are formed by high temperatures created in the exhaust-pipe, and are typically between 5-50nm (Schneider et al. 2005). At high temperatures semi-volatile organic components are vaporised and on cooling they condense on to the surface of existing carbon particles (Ono-Ogasawara & Smith 2004). These particles aggregate leading to the formation of particles in the accumulation mode, and are typically between 30-500nm (Kittelson et al. 1999; Kittelson et al. 2006; Ma et al. 2008). The chemical composition of DEP is complex and is influenced by particles in the nucleation mode as they are indirectly dependent on fuel type, engine type (heavy, light or industrial fork-lift) or engine operating conditions (Rönkkö et al. 2006; Saitoh et al. 2003).

Diesel exhaust emissions represent a mixture of fine (<2.5μm) and ultrafine particles (<0.1μm). Ultrafine particles are short-lived in the atmosphere and undergo rapid aggregation, but remain <2.5μm in diameter (Dockery & Pope 1994; Oberdöster 2001). The small size of DEP enables them to be inhaled and deposited deep within the respiratory tract. In addition, the large surface area of these particles enables toxic compounds to condense or bind to their surface. Once inhaled, DEP are in direct contact with biological molecules and cells of the lung, and therefore, influence respiratory health. It is for this reason that the physical and chemical properties of DEP ought to be examined.

The physical and chemical composition of DEP is dependent on engine type (light duty, heavy duty or industrial fork-lift), engine running conditions (idling, accelerating or de-accelerating) and fuel type. Standard reference material (SRM), namely diesel exhaust matter obtained from the National Institute of Standard and Technology (NIST, USA), has been previously characterised. SRM has been examined for average size of particles and proportions of organic and inorganic constituents adsorbed to the surface of the carbon core (Table 3.1 and Table 3.2). However, levels of adsorbed metals on SRM particles have not been characterised. SRM-1650B is a particle sample from a heavy-duty engine with an average particle size of 0.18μm. In contrast, SRM-2975 is a particle sample from an industrial fork-lift engine with an average size of 11.2μm. SRM-1650B has more PAHs and nitro-PAHs compared to SRM-2975 (Table 3.1 and 3.2). The DEP sample used by Nightingale et al. 2000 (DEP-N), was obtained from a light duty engine and has not been previously characterised. In the present investigation, the physical characteristics of DEP-N, SRM-1650B and SRM-2975 were visualised using light and electron

microscopy, and the metals adsorbed to their surface were examined using inductively-coupled plasma atomic emission spectroscopy (ICP-OES).

From the above, the following hypothesis was proposed: 'The three DEP samples used herein (DEP-N, SRM-1650B and SRM-2975) will display differences in their physical and chemical characteristics'. To examine this hypothesis, the following aims were applied:

- Examine the effect of cell culture media and ddH_2O on the aggregation of DEP samples using light microscopy
- Examine particle morphology of DEP samples using TEM
- Examine metal composition of DEP samples using ICP-OES

Table 3.1 Concentrations of PAHs on the surface of SRM-1650B and SRM-2975

Concentrations of Selected PAHs	SRM-1650B (mg/kg)	SRM-2975 (mg/kg)
Phenantherene	70 ± 2	17 ± 3
1-Methylphenanthrene	28 ± 2	1 ± 0.1
2-Methylphenanthrene	71 ± 3	2 ± 0.2
3-Methylphenanthrene	55 ± 2	1+ 0.2
9-Methylphenanthrene	35 ± 2	-
Fluoranthene	47 ± 1	27 ± 5
Pyrene	43 ± 2	1 ± 0.2
Benzo[*ghi*]fluoranthene	11 ± 1	-
Chrysene	13 ± 1	5 ± 0.2

Concentrations of selected PAHs were analysed on the surface of SRM-1650B and SRM-2975 by using two or more analytical techniques (NIST certificate) (See Appendix III).

Table 3.2 Concentrations of Nitro-PAHs on the surface of SRM-1650B and SRM-2975

Concentrations of Selected nitro-PAHs	SRM-1650B (mg/kg)	SRM-2975 (mg/kg)
9-Nitroanthracene	5890 ± 310	3 ± 0.5
1-Nitropyrene	18200 + 200	35 ± 5
7-Nitrobenz[*a*]anthracene	967 ± 42	3 ± 1
6-Nitrochrysene	46 ± 2	2 ± 0.5
6-Nitrobenzo[*a]*pyrene	1390 + 100	1 ± 0.3
1,6-Dinitropyrene	84 ± 3	2 ± 0.4

Concentrations of selected nitro-PAHs were analysed on the surface of SRM-1650B and SRM-2975 by using two or more analytical techniques (NIST certificate) (See Appendix III).

3.2 Methods

3.2.1 Imaging of DEP by Light Microscopy

Stock concentrations of DEP-N, SRM-1650B and SRM-2975 (30mg/ml) were sonicated for 5 min and diluted in serum-free cell culture media or ddH_2O to obtain a concentration of 300µg/ml. 100µl of each sample was pipetted on to 48-well plate and viewed under an inverted light microscope using a X20 objective lens. Images were captured using an Olympus SLR camera fitted with a microscope compatible adaptor.

3.2.2 Imaging of DEP by TEM

DEP samples were diluted in ddH_2O to obtain a concentration of 300µg/ml and sonicated for 30 min. 15µl of each sample was transferred to formvar-coated copper grids and incubated overnight at RT. Particles were stained with 1% ($^{V}/_{V}$) uranyl acetate and incubated for 10min (Section 2.2.9.4.1). Grids were washed with ddH_2O and air-dried for 15 min. Particle morphology and geometric diameters were analysed using TEM.

3.2.3 Metal Composition of DEP

The composition of metal ions adsorbed to the surface of DEP was identified by ICP-OES. This assay was kindly performed by Dr J Seiffert and Mr P Maguire, Imperial College London. In brief, DEP samples were projected into flowing argon to form plasma which contained a rich source of both excited and ionized atoms. Light emitted by the elements in samples was measured. To determine element

concentrations of DEP samples, emission intensities were compared to the intensities of five standard solutions of known concentrations.

3.3 Results

3.3.1 Examination of DEP Samples Using Light Microscopy

DEP have complex physical geometrics and are composed of numerous chemical species. Cell culture media is composed of inorganic salts and metabolites. Dilution of DEP in cell culture media may lead to the surface chemistry of particles reacting with components present in the media, thereby modifying particulate morphology. For this reason, it is important to examine DEP morphology when diluted in cell culture media and ddH_2O (control). DEP morphology was assessed using light microscopy.

DEP-N, SRM-1650B and SRM-2975 were diluted in serum-free cell culture media or ddH_2O and sonicated prior to visual examination using light microscopy. DEP-N (Figure 3.1A) and SRM-1650B (Figure 3.1B) samples diluted in media or ddH_2O appeared as black solid aggregates held together in various shapes and sizes. SRM-2975 (Figure 3.1C) sample contained aggregates of smaller size compared to DEP-N or SRM-1650B.

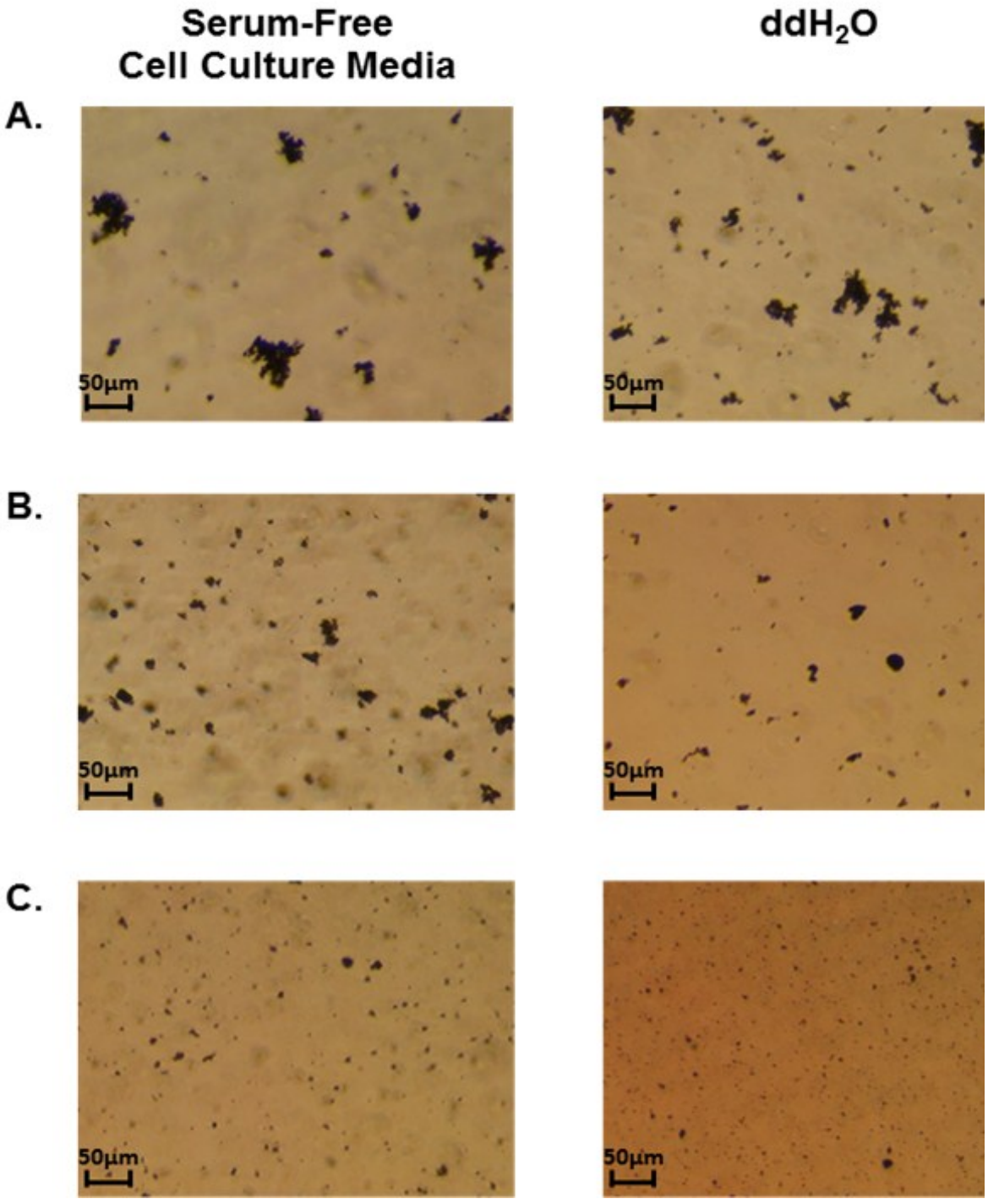

Figure 3.1 Physical Characterisation of DEP Samples in Serum-Free Cell Culture Media or ddH_2O

DEP samples were sonicated for 5min and diluted in serum-free cell culture media or ddH_2O to obtain a concentration of 300µg/ml. Physical characteristics of (A) DEP-N (B) SRM-1650B and(C) SRM-2975 samples were examined using a light microscope at X20 magnification.

3.3.2 Examination of DEP Samples Using TEM

Having established that there was no difference in the morphology of DEP samples following dilution in cell culture media and ddH_2O, the samples were further assessed by TEM. Samples were re-suspended in ddH_2O to avoid interference of carbon compounds present in cell culture media during examination of DEP. TEM was used to determine the morphology and size of individual particles to determine how these characteristics may mediate biological effects.

Analysis of DEP-N showed that primary (non-aggregated) particles encompassed a range of sizes between ~30-60nm, were of an irregular shape, and formed aggregates of various size (Figure 3.2A). Similar findings were also observed following examination of SRM-1650B (Figure 3.2B) and SRM-2975 (Figure 3.2C) samples, with individual particles in the size range ~40-60nm.

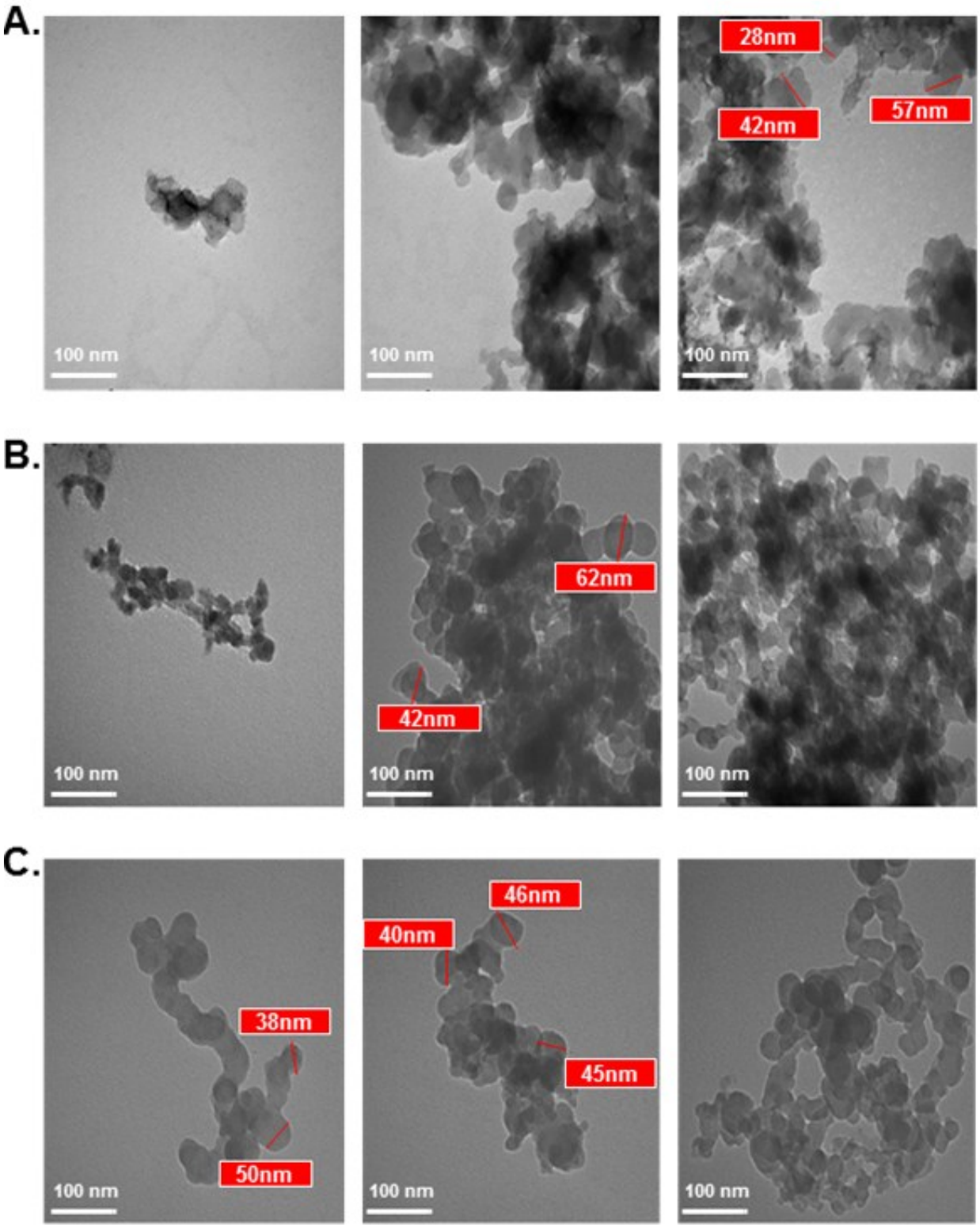

Figure 3.2 TEM of DEP

DEP (300µg/ml) were diluted in ddH_2O and sonicated for 30 min. The DEP solution was then pipetted on formvar copper grids. Particles were stained using 1% ($^{V}/_{V}$) aqueous uranyl acetate and incubated for 10 min at RT. (A) DEP-N (left-right), (B) SRM-1650B (left-right) and (C) SRM-2975 (left-right).

3.3.3 Metal Composition of DEP

Having determined the physical characteristics of DEP samples, the composition of adsorbed metals on the surface of these particles was examined. ICP-OES analysis showed that DEP-N had a 5% ($^{W}/_{W}$) and 20% ($^{W}/_{W}$) mass of Cu and Fe metals whereas SRM-1650B and SRM-2975 did not (Figure 3.3). DEP-N also had higher mass of Ca, Ni and Zn metals compared to the other DEP samples. In contrast, SRM-1650B and SRM-2975 particles had ~2% mass of B adsorbed to their surface compared to DEP-N.

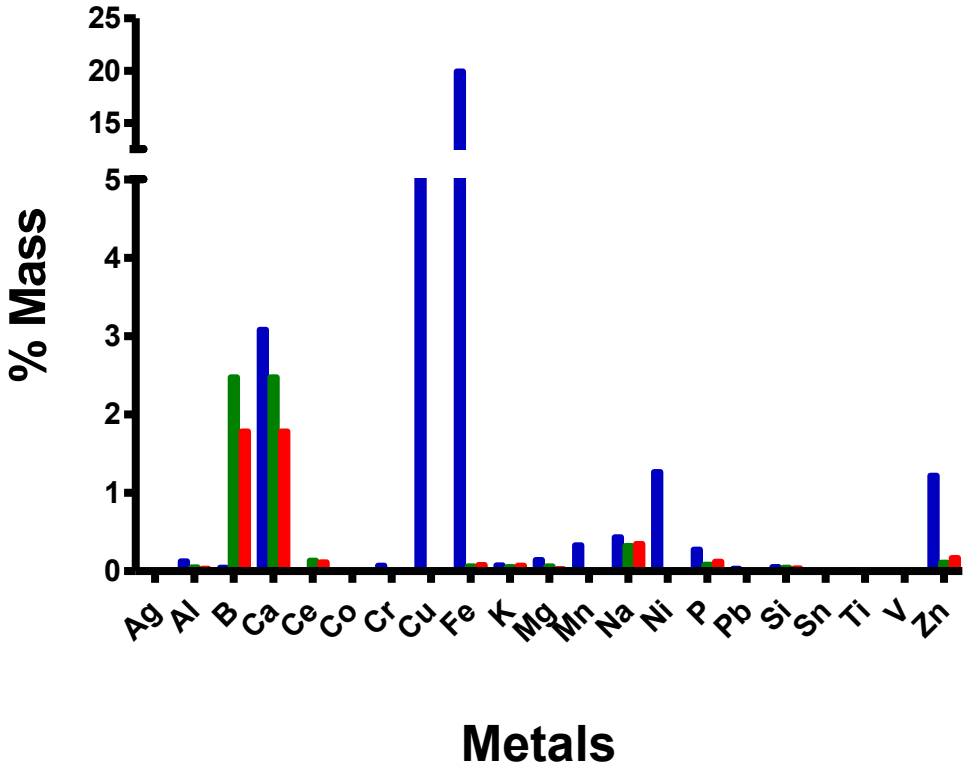

Figure 3.3 Percentage Mass of Metals Adsorbed to the Surface of DEP

DEP, SRM-1650B and SRM-2975 were analysed for the presence of adsorbed metals on the surface of combustion particles by ICP-OES analysis (n=1). This analysis was conducted by Dr J Seiffert and Pierce Maguire, Imperial College London, UK.

3.4 Discussion

The laboratory-generated DEP-N used by Nightingale et al. 2000 were not previously characterised, but were used as a surrogate of the type of particle produced by a light-duty engine, typically found in cars and vans. The standardised samples SRM-1650B and SRM-2975 used herein were obtained from NIST and were acquired from a heavy-duty engine and an industrial forklift engine respectively. The present chapter showed that primary particles from all the three samples formed aggregates of various sizes and shapes when diluted in both cell culture media and ddH_2O despite sonication. No differences were observed between the physical characteristics of the three DEP samples obtained from the different engines types. Similar findings have been reported by others showing that DEP readily aggregates in cell culture media and distilled water as determined by light microscopy and TEM (Saxena et al. 2008; Holder et al. 2008). In addition, Müller et al. 2010, used TEM to examine lung cells (epithelial cells, MDM and monocyte-derived dendritic cells) exposed to DEP (diluted in cell culture media) and observed DEP aggregation, similar to the observation herein.

It was initially speculated that DEP may have aggregated in the cell culture media as an effect mediated by the high content of salts. However, DEP diluted in ddH_2O also aggregated into clumps of variable size and shape. Therefore, it is unlikely that media composition alone is involved in particle aggregation but, rather, the surface chemistry of particles may drive this effect (Murphy et al. 1999). Layahe & Ehrburger-Dolle 1994 describe aggregation of carbon black particles as a process of particle collision by Brownian motion and interactions between acetylene and unsaturated hydrocarbons, which are responsible for growth of particles. Since DEP

consist of carbon, similar mechanisms may be involved in DEP aggregation as observed in the present chapter.

The physical and chemical properties of SRM-1650B and SRM-2975 have been characterised by NIST. The average particle size of SRM-1650B and SRM-2975 is reported as 0.18μm and 11.2μm respectively, as determined by light scattering techniques. Analyses from TEM in the current investigation are in contrast to the findings of NIST. TEM analyses showed an average primary particle size for SRM-1650B and SRM-2975 of ~40-60nm and ~40-50nm respectively. According to Kittelson, et al. 2001, DEP are heterogeneous in size, with most particles existing in either the nucleation mode (5-50nm), composed of carbon, semi-volatile and metallic compounds, and in the accumulation mode (0.05-1.0μm) composed of carbon aggregates and adsorbed material. These observations support the data herein as individual particulates and aggregates from DEP samples were found to be within the range of the nucleation mode.

ICP-OES analysis indicated that all DEP samples herein had a distinct range of trace metals adsorbed on the surface of the DEP carbon core. The samples differed in the content of metal ions, which may be an effect of the different engine type, fuel, operating conditions and temperature used to generate the samples (Taylor et al. n.d.; Mcdonald et al. 2011). Adsorption of metal ions on to DEP are associated with differential biological effects on human health, as determined by human exposure studies or *in-vitro* studies on primary cells and cells lines (Chen & Lippmann 2009). Baulig et al. 2004 found that exposure of the 16-HBE bronchial epithelial cell line to different DEP samples with contrasting levels of Fe and Cu content, stimulated pro-inflammatory cytokine release and were correlated with hydroxyl radical production. A human exposure study by Ghio et al. 2000 revealed that 2h inhalation of

concentrated ambient particles (CAPs) in Chapel Hill, North Carolina, resulted in pulmonary neutrophillic inflammation and increased blood fibrinogen levels. Further examination of the analyses by Huang et al. 2003 showed that sulphate, Fe and Se were responsible for increases in neutrophils found in bronchial alveolar lavage (BAL) samples, and Cu, Zn and V were related to increased fibrinogen levels (Chen & Lippmann 2009). Becker et al. 2005 showed that variations in composition of DEP during different seasons were related to different biological responses in human alveolar macrophages and bronchial epithelial cells. Exposure of cells to equal amounts of coarse (particles >1μm), fine and ultrafine DEP obtained during different seasons in Chapel Hill, NC resulted in the differential release and production of CXCL8 and IL-6. Analysis of DEP constituents by mass spectroscopy and plasma atomic emission spectroscopy indicated that variations in seasonal responses were correlated with the metal ions adsorbed to the surface of particles. For example, IL-6 release was correlated with Fe and Si, whilst CXCL8 release was related to Cr. Soluble metals on DEP may also mediate pro-inflammatory effects by depositing in the airways and reacting with lung lining fluid. The interaction between soluble metal ions and biological molecules present in the airway lining fluid generate reactive oxygen species (ROS) which may mediate these biological effects (Park et al. 2006).

Taken together, the data in this chapter reveal that DEP encompass a wide range of particle sizes and readily form aggregates whether diluted in cell culture media or ddH_2O. The DEP-N, SRM-1650B and SRM-2975 all had particles in the range ~15-60nm, and formed aggregates of similar sizes. It was also determined that even though the different DEP samples were physically similar they differed in metal ion composition, with DEP-N having more Cu, Fe, Ca, Ni and Zn, and the SRM samples having more B than DEP-N. In regards to the findings of this investigation, the

proposed hypothesis: ‘The three DEP samples used herein (DEP-N, SRM-1650B and SRM-2975) will display differences in their physical and chemical characteristics’ was rejected, but still requires further examination in regards to the chemical characteristics of DEP.

Chapter 4:

Effect of DEP on MDM Viability

4.1 Introduction

The previous chapter (Chapter 3) established that DEP-N, SRM-1650B and SRM-2975 were physically similar, but differed in metal ion composition. The detrimental effects of DEP on respiratory health may reflect the noxious composition of these particles (Amakawa et al. 2003). As discussed previously, DEP are composed of a carbon core and various by-products of incomplete combustion, including PAHs, Nitro-PAHs and metals (Cu, B, Fe, Ca and Ni). These by-products have carcinogenic effects on human health as determined by both human and animal exposure studies. *In-vitro* studies in cell lines, show that DEP induce oxidative DNA damage (Mcclellan 1987; Krivoshto et al. 2008; Vattanasit et al. 2013; Attfield et al. 2012). Table 4.1, highlights individual components of DEP and the biological effects they may mediate.

Table 4.1. Classification of Biological Effects Produced by Adsorbed Chemical Species on DEP

Components of DEP		Biological effect
Components of Gas-Phase Emission	Nitrogen & sulphuric oxides Carbon dioxide Carbon monoxide	Respiratory tract irritant Respiratory tract irritant Asphyxiation
Hydrocarbons	Alkanes Alkenes	Respiratory tract irritant Respiratory tract irritant, mutagenic and carcinogenic
Aldehydes	Formaldehydes Monocyclic aromatic hydrocarbons Benzene	Carcinogenic Carcinogenic Mutagenic and carcinogenic
Components of Particle-Phase Emission	Elemental carbon Inorganic sulphate and nitrate PAH (Nitro-PAH)	Adsorbs organic/inorganic compounds Respiratory tract irritant Mutagenic and carcinogenic

Classification of components adsorbed on the elemental carbon core of DEP and their biological effect (adapted by Krivoshto et al. 2008).

Inhaled particles are normally cleared by AM (Warheit & Hartsky 1993). Therefore, understanding the effects of DEP on macrophage function is important. It is unclear whether the toxic effects of DEP are mediated by soluble chemical species adhered to the surface of the particle such as PAHs and toxic metals, or whether the particles mediate their effects following internalisation by cells (Boland et al. 1999). Inhalation and penetration of DEP in the lung leads to apoptosis, inflammation and up-regulation of antioxidant enzymes, as seen in human exposure studies (Salvi et al. 1999; Behndig et al. 2006; Nordenhall et al. 2000) and *in-vitro* studies using primary human cells and cell lines (Hiura et al. 2000; Hiura et al. 1999).

Cell culture studies on human AM, murine macrophage RAW 264.7 and human monocyte THP.1 cell lines, established that treatment of cells with DEP compromised cell viability *via* generation of ROS (Hiura et al. 1999). The increase in ROS disrupts the intracellular anti-oxidant/oxidant balance and leads to oxidative stress, culminating in cellular apoptosis (Hiura et al. 1999). The decline in cell viability may be limited to the organic constituents adsorbed to the surface of DEP. This is because particulates treated with methanol to extract organic constituents from the surface of DEP, do not induce ROS or cellular apoptosis (Hiura et al. 1999; Hiura et al. 2000; Li et al. 2002; Ma & Ma 2002;). In contrast, cells treated with the extract of DEP reduced cell viability by the induction of ROS (Hiura et al. 1999).

Increases in atmospheric DEP contribute to increased hospital admissions and mortality in individuals with COPD (Atkinson et al. 2001). To date, the effects of DEP in COPD comprise epidemiological studies. Most studies look at the risk associated with developing COPD in an occupational setting, or worsening of COPD-related symptoms following exposure to DEP. For example, retrospective studies show that occupational exposure of individuals to DEP increases risk of developing COPD

compared to non-exposed individuals (Anderson et al. 1997; Sunyer et al. 2000). In addition, the case-control study conducted by Hart et al. 2006 looking at the effects of occupational DEP exposure on rail-road workers, demonstrated the link between DEP exposure and COPD-related mortality. However there is a scarcity of information on the effects of DEP on pulmonary macrophages, the important innate immune cells involved in lung homeostasis, which are also implicated in the pathophysiology of lung diseases such as COPD (Barnes 2004). Thus, it is important to determine the effects of DEP-related toxicity on macrophages obtained from an environment of persistent inflammation, as seen in smokers or patients with COPD (Overbeek et al. 2013; Holloway & Donnelly 2013). Primary AM from resected lung tissue or cell lines such as RAW 264.7 have been used for *in-vitro* studies, but these studies have not investigated whether disease alters DEP-related toxicity in macrophages (Hiura et al. 2000). Hiura et al. 1999 and Kafoury et al. 2005 have modelled the effect of DEP on alveolar macrophage toxicity, by using the mouse RAW 264.7 macrophage cell line. Hiura et al. 1999 found that DEP induced cellular apoptosis which was attributed to PAH compounds bound to DEP. In contrast Kafoury et al. 2005 found that DEP treatment did not induce apoptosis in RAW 264.7 cells, this response was associated to the absence of active PAH bound to DEP.

The above findings suggest that the relationship between DEP and their effects on cellular toxicity are not well understood. In this chapter, the toxicity of the three DEP samples was examined on macrophages and the following hypothesis was proposed: 'DEP-N, SRM-1650B and SRM-2975 will reduce macrophage viability by inducing apoptosis and this effect will be more prominent in macrophages from patients with COPD'. To examine this hypothesis the following aims were applied:

- The cytotoxic effects of DEP will be examined on human MDM as a model of macrophages.
- The effects of DEP-related cytotoxicity will be examined in MDM from patients with COPD and compared to MDM from non-smokers and smoker controls.
- The effect of DEP on the induction of apoptosis or necrosis in MDM will be examined by flow cytometry.

4.2 Methods

4.2.1 Isolation of PBMC

PBMC were obtained from non-smokers, smokers and patients with COPD as described in Section 2.2.2. PBMC were cultured in MDM complete media (RPMI-1640, containing 10% ($^{V}/_{V}$) foetal calf serum (FCS), 10mg/ml (1% ($^{V}/_{V}$)) penicillin/streptomycin (PS), 2mM (1% ($^{V}/_{V}$)) L-glutamine (LG)) and seeded onto a 96-well black plate ($1x10^{5}$ cell/well). Cells were incubated for 2h at 37°C, 5% ($^{V}/_{V}$) CO_2 to isolate monocytes by adherence to the plastic tissue culture plate. Monocytes were cultured in MDM complete media containing 2ng/ml GM-CSF and incubated for a further 12 days at 37°C, 5% ($^{V}/_{V}$) CO_2 to derive MDM (Section.2.2.3).

4.2.2 Treatment of MDM with Inert Beads

Inert beads of 0.2µm, 10µm or 30µm diameter were re-suspended in 10X D-PBS at a concentration of 30mg/ml. Beads were sonicated for 2 min to disaggregate them and were diluted in RPMI-1640 media in the concentration range 1-300µg/ml. MDM were treated with 1-300µg/ml inert beads and incubated for 24h at 37°C, 5% ($^{V}/_{V}$) CO_2. Non-stimulated MDM were incubated in media alone and were used as baseline controls (Section 2.2.7.1).

4.2.3 Treatment of MDM with DEP

DEP-N, SRM-1650B and SRM-2975 were suspended in warmed HBSS at a stock concentration of 30mg/ml. DEP samples were sonicated for 2 min to break up large aggregates of particles and were diluted in RPMI-1640 media at the concentration range 1-300µg/ml. MDM were treated with these particles at 1-300µg/ml and

incubated for 24h at 37°C, 5% ($^{V}/_{V}$) CO_2. Non-stimulated (NS) cells were incubated in media alone and were used as baseline controls (Section 2.2.7.2).

4.2.4 Light microscopy of Inert-Bead- and DEP-Treated-MDM

Images of MDM treated with increasing concentrations (1-100µg/ml) of inert beads or DEP samples, were captured on an inverted light microscope using X20 objective lens. Pictures were taken with an Olympus SLR camera fitted with a microscope compatible adaptor.

4.2.5 Cell Viability

Cell viability was assessed as described in Section 2.2.8.1

4.2.6 Assessment of MDM internalisation of DEP-N by TEM

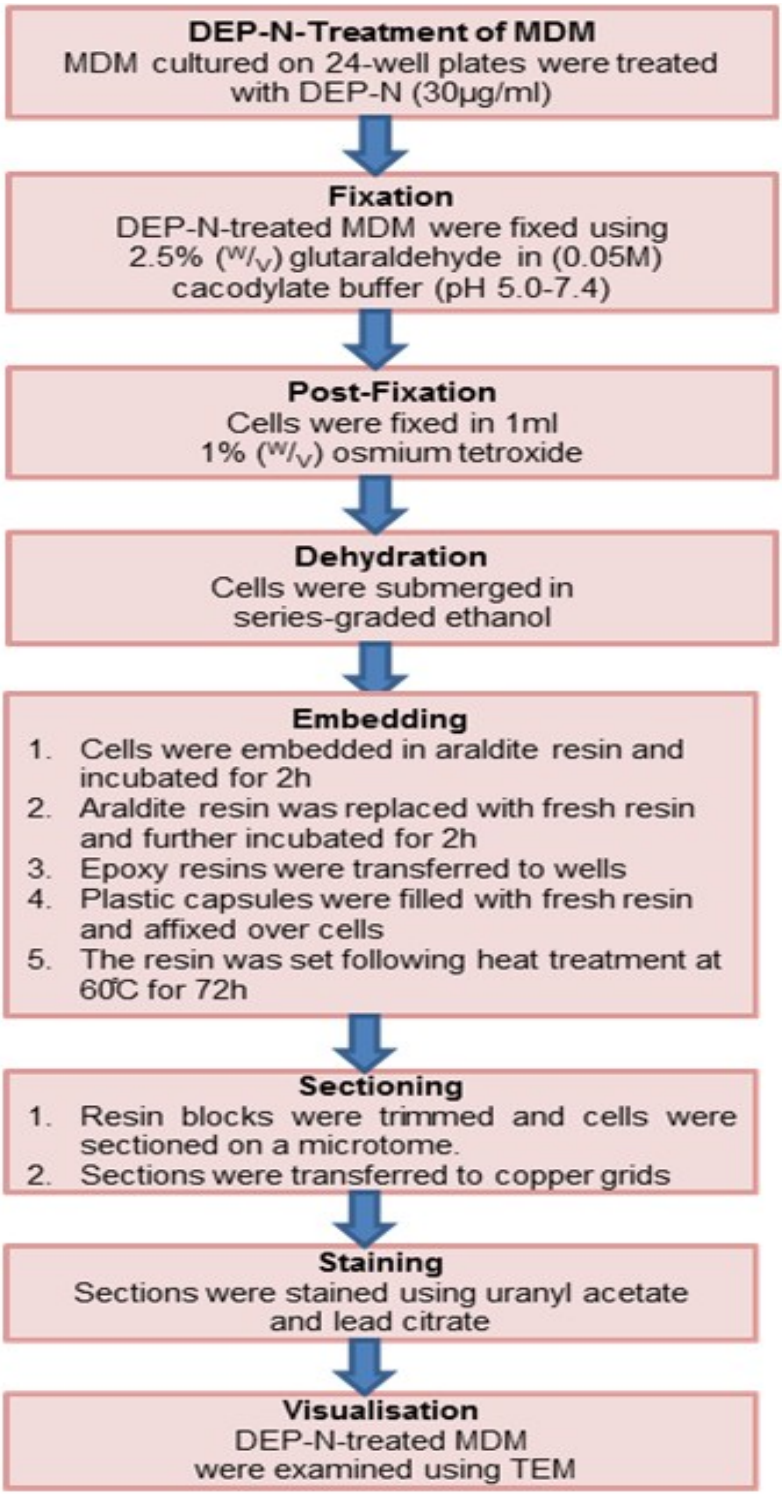

Figure 4.1 Flow Chart of TEM Methodology, to Examine DEP-N Internalisation by MDM

The methodology of preparing DEP-N-treated MDM samples, prior to TEM examination.

4.2.7 Detection of Apoptosis and Necrosis

MDM were treated with DEP-N (1-100µg/ml) as described in Section 2.2.7.2. Non-stimulated (NS) cells were used as baseline controls. Cells were transferred to polystyrene FACS tubes at 100µl and stained with 5µl of Annexin-PE and 7-AAD as described in Section 2.2.8.2. Cells staining positive with either Annexin-PE/7-AAD flurochromes were analysed using FACS Diva software (Figure 4.2). The percentage of apoptotic or necrotic cells were analysed as described in Section 2.2.8.2.

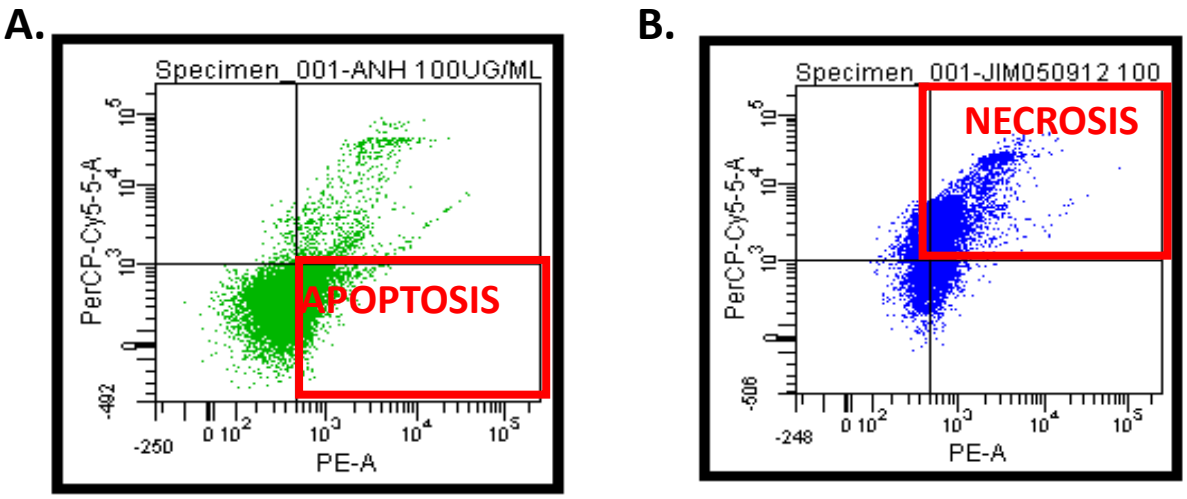

Figure 4.2. Distribution of DEP-N-Treated MDM Stained with Annexin-PE and 7-AAD

DEP-N-treated MDM (1-100µg/ml) were stained with Annexin-PE and 7-AAD, and analysed using flow cytometry. Cells undergoing (A) apoptosis had stained positively with Annexin-PE and were present in the lower right quadrant of the dot plot. Cells undergoing (B) necrosis had stained positively with 7-AAD and were present in the upper right quadrant of the dot plot.

4.2.8 Statistics

Data were compared for statistical significance between subject groups by one-way ANOVA followed Dunnett's test for multi-group comparisons. Data expressing a P value of <0.05, were considered to be statistically significant. Statistical differences were calculated using Prism V.5 (GraphPad, San Diego, USA).

4.3 Results

4.3.1 Volunteer Demographics

Characteristics of volunteers recruited for the study are shown in Table 4.2. Patients with COPD were significantly older than either non-smoker or smoker volunteers; however there were no differences in smoking history between smokers and COPD patients. Patients with COPD had significantly reduced FEV_1, FEV_1 % predicted, FVC and FEV_1: FVC ratio compared to either non-smokers or smokers. There were no differences in lung function between non-smokers and smokers.

Table 4.2 Volunteer Demographics

	Non-Smokers n=28	Smokers n=18	COPD n=49
Age (Years)	57 ± 2	58 ± 2	67 ± 1*** ##
Gender (M:F)	12:16	7:11	27:22
FEV_1 (L)	2.9 ± 0.2	2.7 ± 0.2	1.3 ± 0.1***###
FEV_1 (% Predicted)	100 ± 3	98 ± 4	51 ± 3***###
FVC (L)	4 ± 0.2	4 ± 0.3	3 ± 0.1***##
FEV_1:FVC	0.8 ± 0.02	0.7 ± 0.02	0.5 ± 0.02***###
Smoking History (Pack Years)	-	34 ± 5***	39 ± 4***

Data are mean ± S.E.M. **p<0.01, ***p<0.001 *vs* non-smokers, # p<0.05, ## p<0.01 *vs* smokers, ### p<0.001 *vs* smokers.

4.3.2 Monocyte Differentiation to MDM

To examine the interaction of DEP-N, SRM-1650B or SRM-2975 on macrophage function, it was necessary to establish an acute exposure model. MDM were

selected as a replacement for macrophages due to their availability, acquisition through minimally-invasive techniques, ability to compare effects in individuals with different health status, and similarities to primary AM (Winkler et al. 2008).

MDM were derived by isolating monocytes and culturing these cells in the presence of GM-CSF for 12d. To determine whether these cells had fully differentiated into MDM, photomicrographs were taken at days 0, 3, 6, 9 and 12 to assess their morphology (Figure 4.3). Monocytes at day 0 were small and round compared to cells which had been incubated in GM-CSF at day 3-12. Other morphological changes observed throughout the incubation time period included cells becoming flatter and having a larger cytoplasmic volume (compared to monocytes on day 0). Cells undergoing differentiation also had a granular appearance and extending pseudopodia (indicated by red arrows in Figure 4.3), suggesting a macrophage-like phenotype.

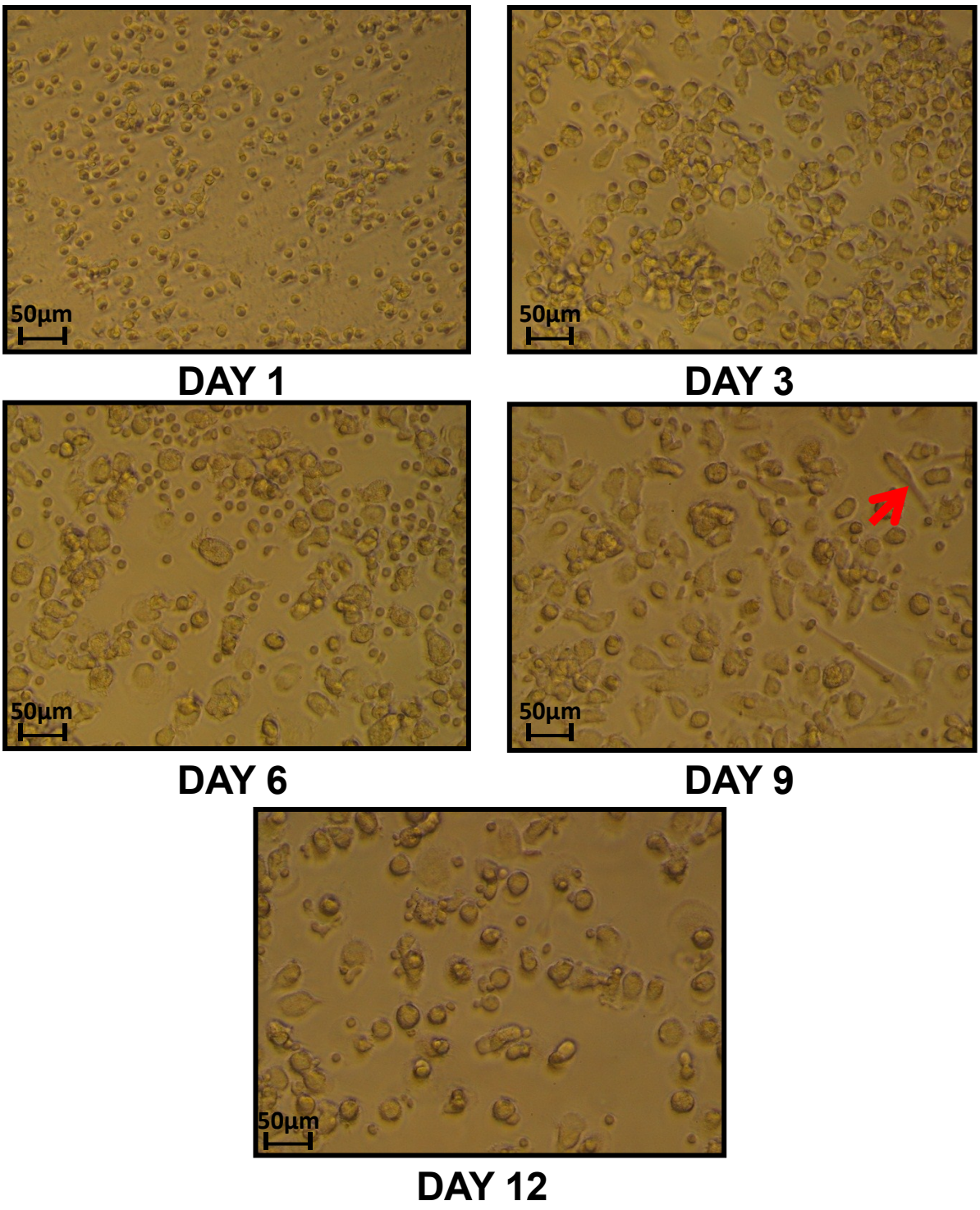

Figure 4.3 Effect of GM-CSF on Monocyte Differentiation into MDM

Whole blood monocytes from a smoker subject were isolated by adherence. Cells were incubated in the presence of GM-CSF (2ng/ml) for 12 days to enable differentiation of monocytes into MDM. Photomicrographs of cells undergoing differentiation were taken at days 1, 3, 6, 9 and 12. Red arrows indicate extending pseudopodia by MDM. Cells were viewed using light microscopy at X 20 magnification.

4.3.3 Effect of DEP on MDM Viability and Morphology

MDM from non-smokers, smokers and COPD patients were exposed to increasing concentrations of DEP-N, SRM-1650B and SRM-2975 for 24h and changes in cell viability and morphology were assessed. Increasing concentrations of DEP-N decreased cell viability in a concentration-dependent manner, with a significant decrease in cell viability of ~50% at 300µg/ml for MDM from non-smokers and COPD patients (Figure. 4.4A). Similar data was observed from MDM from smokers, but did not reach statistical significance. Cell viability was not reduced when cells were exposed to either SRM-1650B (Figure. 4.4B) or SRM-2975 (Figure 4.4C). However, there was a significant reduction of viability by ~35% in MDM from COPD patients exposed to 300µg/ml SRM-1650B (Figure. 4.4B). As 300µg/ml of DEP decreased cell viability, this concentration was excluded from further analyses.

The next question was whether or not MDM from different subject groups internalised DEP (1-100µg/ml). In order to address this, photomicrographs of cells exposed to the different DEP were examined. MDM from non-smokers, smokers and COPD patients appeared to show internalisation of DEP-N at concentrations of 10 – 100 µg/ml, with no difference between subject groups (Figure 4.5). Similar data were seen with MDM exposed to SRM-1650B and SRM-2975, with internalisation of particles seen at concentrations of 30–100µg/ml (Figures 4.6 and Figure 4.7).

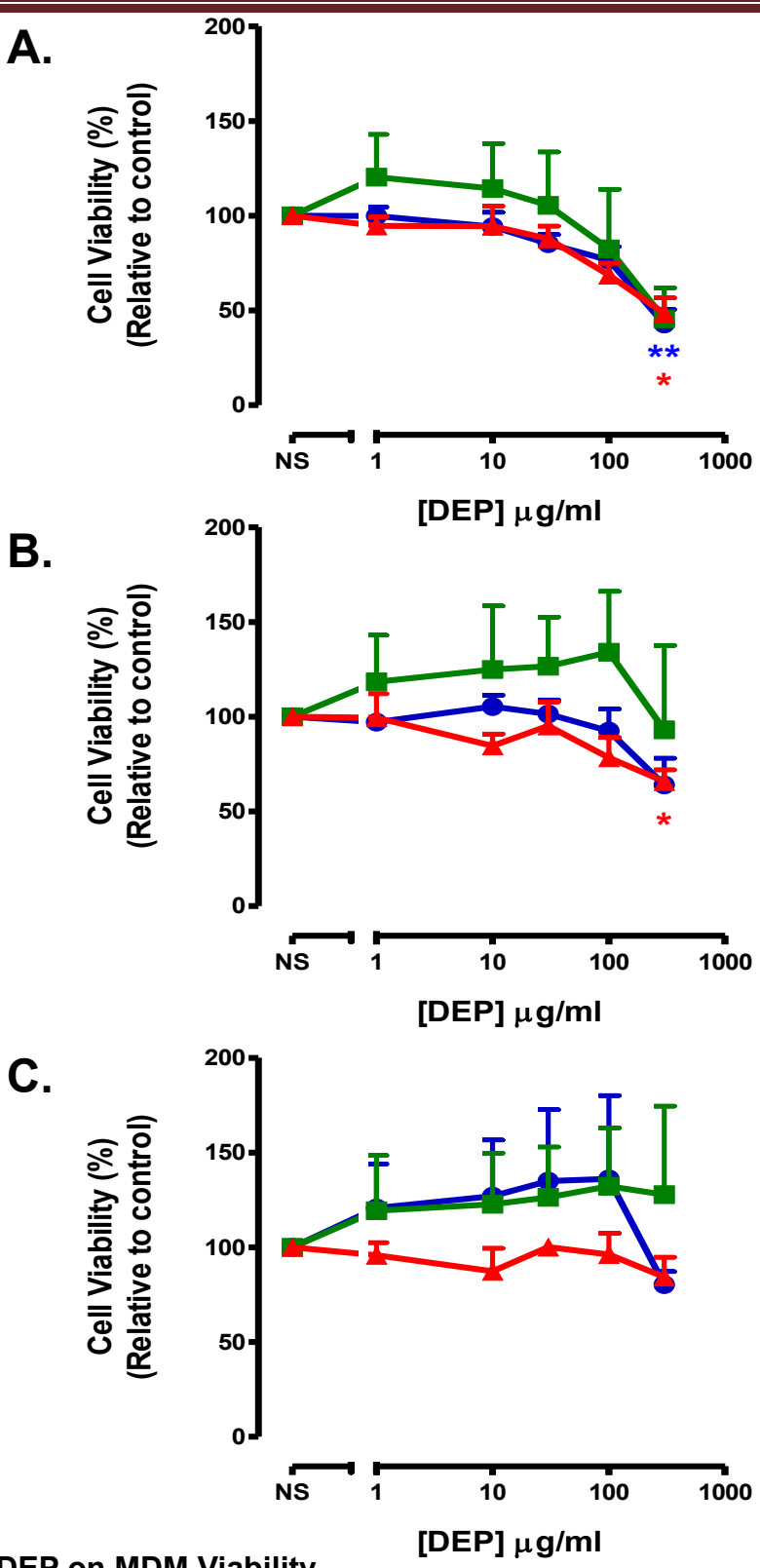

Figure. 4.4 Effect of DEP on MDM Viability.

MDM from non-smokers (●) (n=5), smokers (■) (n=3) and patients with COPD (▲) (n=4; ex-smoker n=2, current smoker n=1, unknown n=1) were treated with 1-100µg/ml of (A) DEP-N, (B) SRM-1650B or (C) SRM-2975. DEP-treated cells were incubated for 24h followed by treatment with MTT to determine cell viability. Non-stimulated (NS) cells were used as baseline controls and represented 100% cell viability (normalised data). Data are mean ± SEM % cell viability (relative to control). *p<0.05, **p<0.01 *vs* NS.

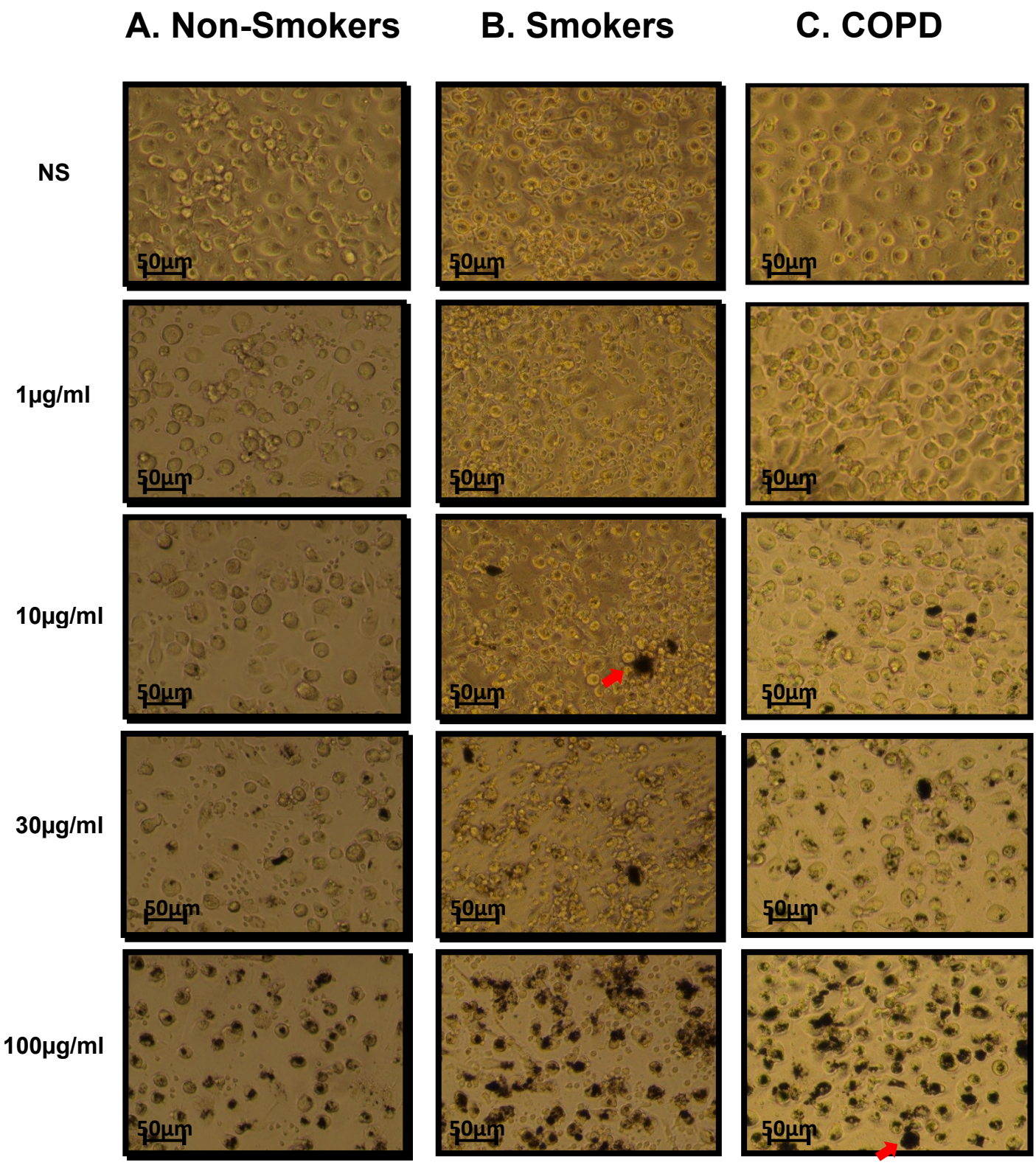

Figure 4.5 Photomicrographs of DEP-N-Treated MDM

MDM from Non-smokers (A), Smokers (B) and COPD (C) patients were treated with DEP-N (1-100µg/ml) and incubated for 24h. Non-stimulated (NS) cells were used as a baseline control. Red arrows indicate DEP aggregates. Cells were viewed by light microscopy and images were taken at X 20 magnification.

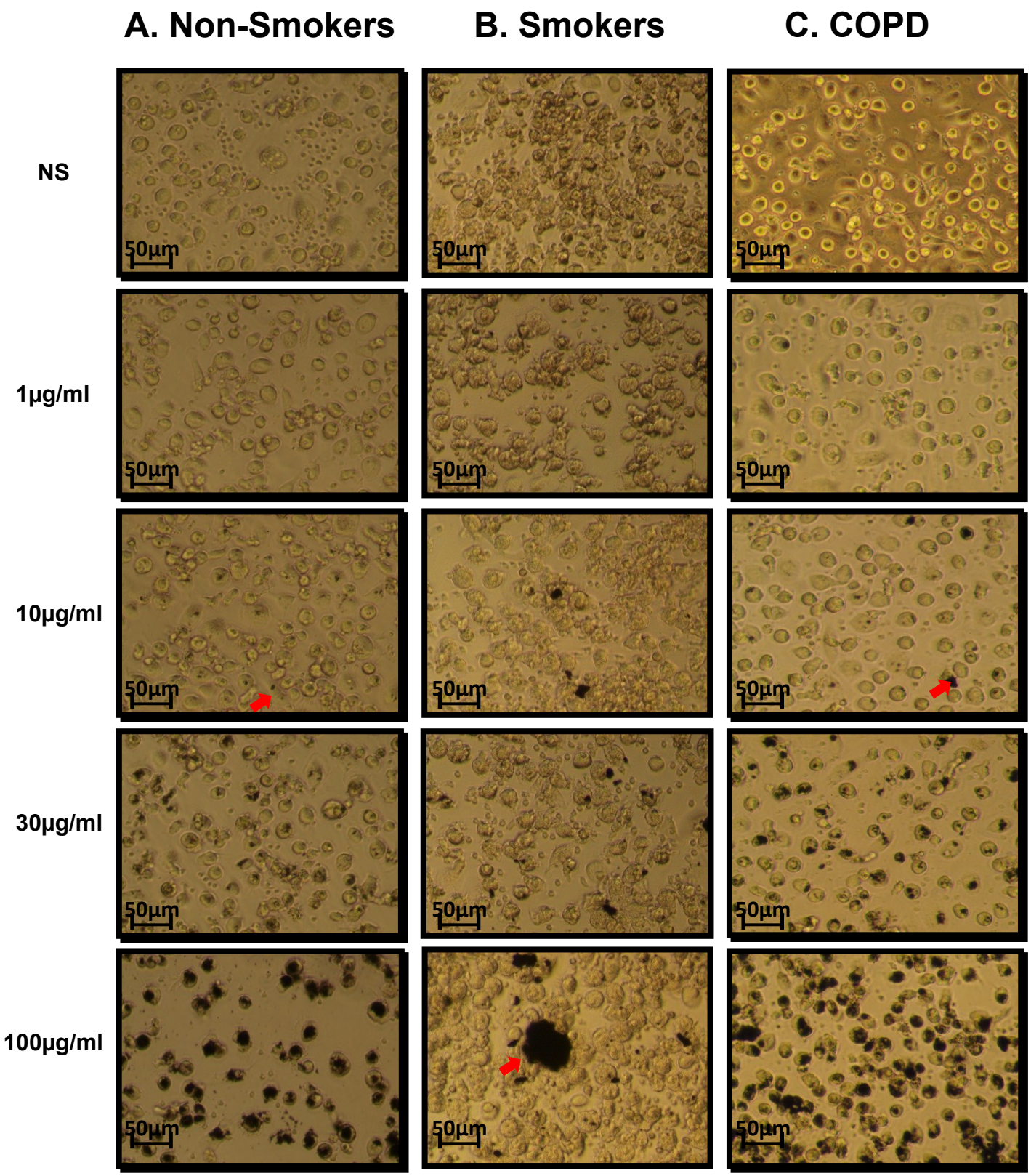

Figure 4.6 Photomicrographs of SRM-1650B-Treated MDM

MDM from Non-smokers (A), Smokers (B) and COPD (C) patients were treated with SRM-1650B (1-100µg/ml) and incubated for 24h. Non-stimulated (NS) cells were used as a baseline control. Red arrows indicate DEP aggregates. Cells were viewed by light microscopy and images were taken at X 20 magnification.

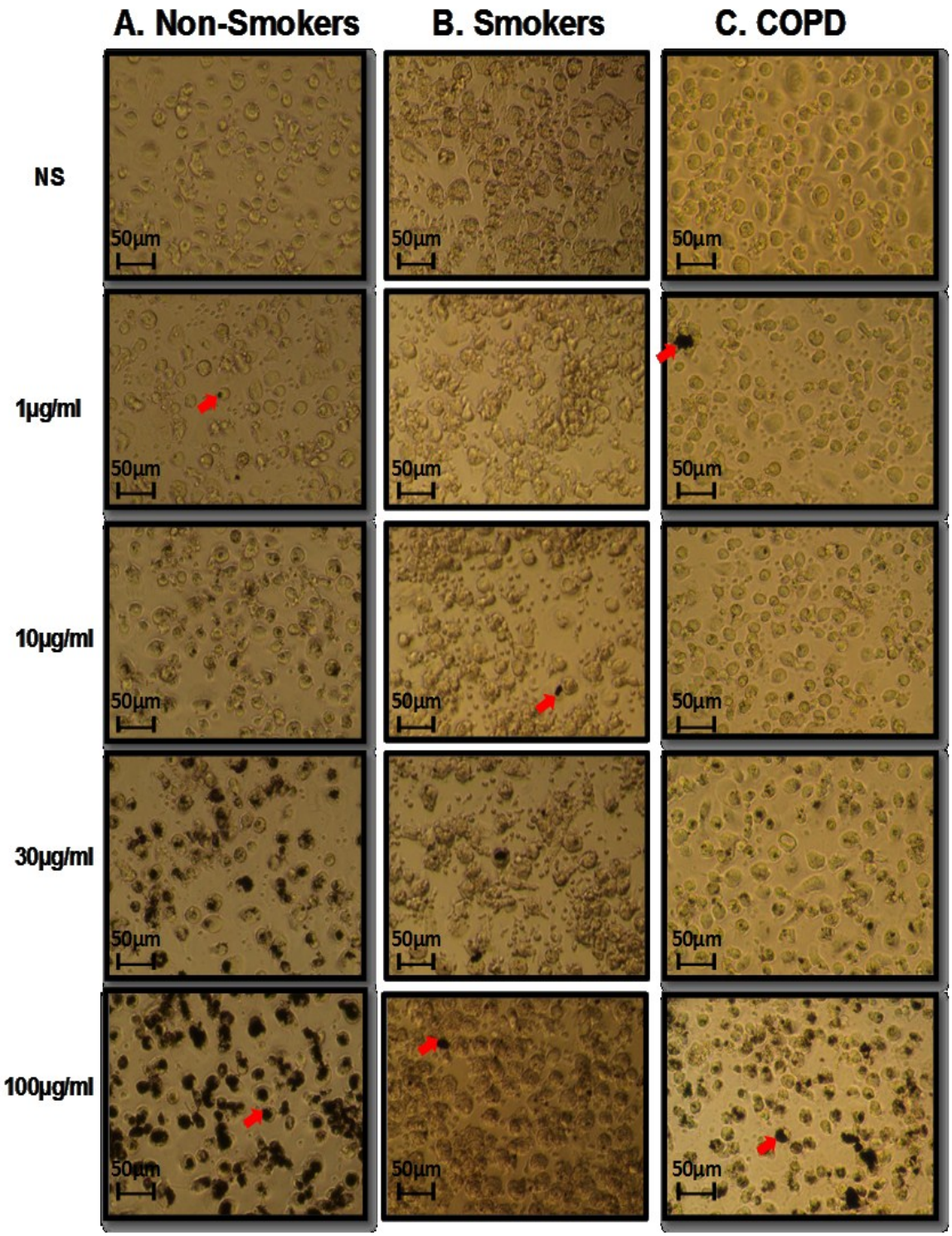

Figure 4.7 Photomicrographs of SRM-2975-Treated MDM

MDM from Non-smokers (A), Smokers (B) and COPD (C) patients were treated with SRM-2975 (1-100µg/ml) and incubated for 24h. Non-stimulated (NS) cells were used as a baseline control. Red arrows indicate DEP aggregates. Cells were viewed by light microscopy and images were taken at X 20 magnification.

4.3.4 Effect of Inert Beads on MDM Viability and Morphology

The effect of DEP on MDM viability and morphology might be due merely to ingestion of particles rather than elemental composition. To determine whether particle size altered viability and morphology, MDM were exposed to inert beads of different sizes in order to mimic the size distribution of the samples of DEP used herein.

MDM from non-smokers, smokers and COPD patients were exposed to inert beads with diameters of 0.2μm, 10μm or 30μm. Increasing concentrations of beads of any size did not significantly decrease cell viability of MDM from the different subject groups (Figure 4.8), although MDM from COPD patients treated with the highest concentration of 0.2μm beads showed decreased cell viability by ~30%, albeit not significant (Figure 4.8A). MDM from COPD patients treated with 300μg/ml of 30μm beads significantly increased viability compared to non-smoker MDM (Figure 4.8C).

Having demonstrated that inert beads did not reduce MDM viability, it was unclear whether cells had actually internalised the beads, which may be responsible for the lack of effect on cell viability. It was also important to determine whether the size distribution of particles altered cellular morphology. Photomicrographs of MDM from non-smokers, smokers and COPD patients exposed to increasing concentrations of 0.2μm beads, did not show any alteration of cellular morphology (Figure 4.9). Internalisation of the 0.2μm beads by MDM was not visible, although aggregates were observed at 30 - 100μg/ml concentrations (indicated by red arrows in Figure 4.9).

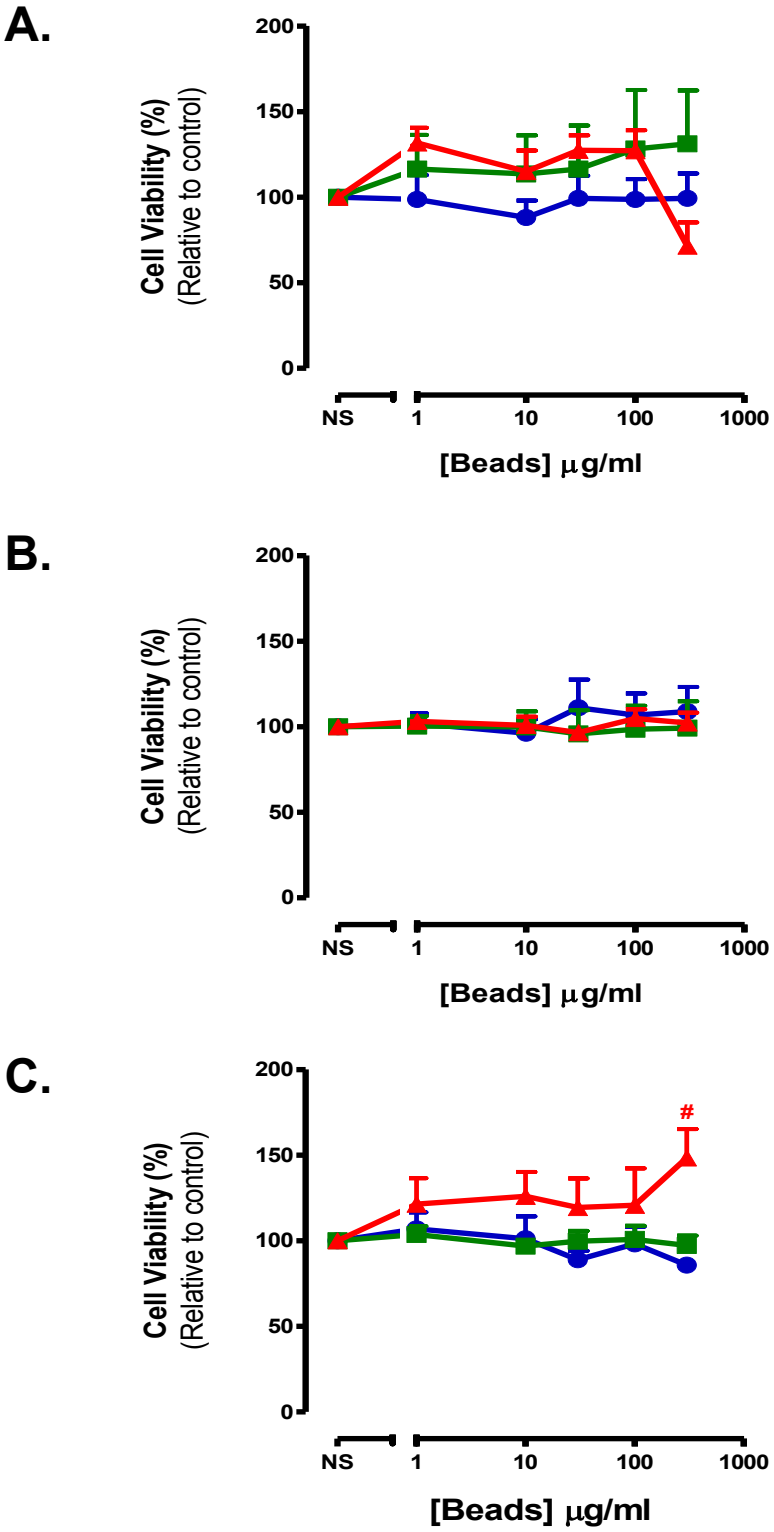

Figure. 4.8 Effect of Inert beads on MDM Viability.

MDM from non-smokers (●) (n=4), smokers (■) (n=2-4) and patients with COPD (▲) (n=3-4; ex-smokers n=2, current-smokers n=1, unknown n=1) were treated with 1-100μg/ml of (A) 0.2μm beads, (B) 10μm beads or (C) 30μm beads. MDM were incubated at 5% ($^{V}/_{V}$) CO_2, 37°C for 24h, followed by treatment with MTT to determine cell viability. Non-stimulated (NS) cells were used as baseline controls and represented 100% cell viability (normalised data). Data are mean ± SEM of % cell viability (relative to NS). # $p<0.05$ non-smokers *vs* COPD

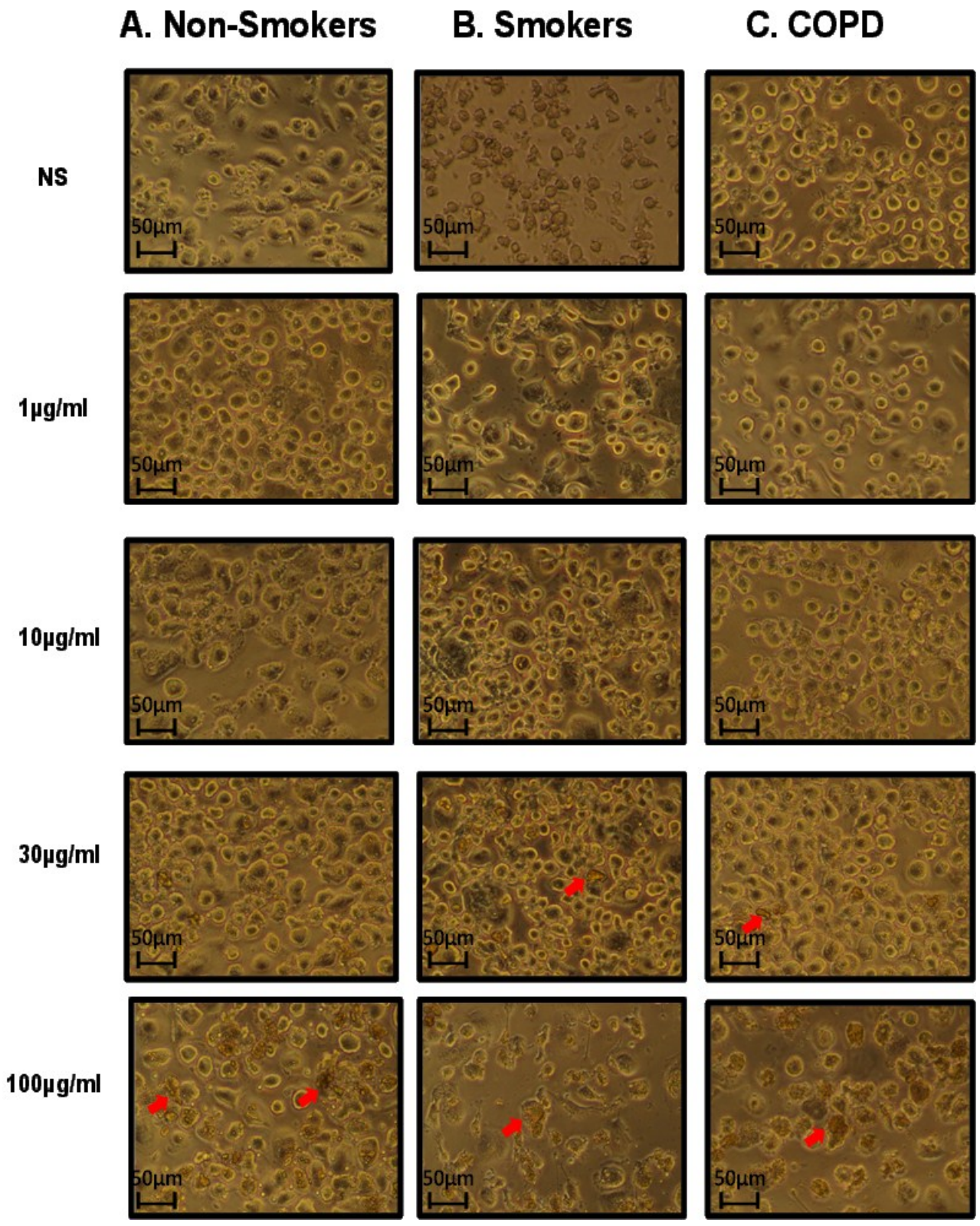

Figure 4.9 Photomicrographs of 0.2µm Inert Bead-Treated MDM

MDM from Non-smokers (A), Smokers (B) and COPD patients (C) were treated with 0.2µm polystyrene beads (1-100µg/ml) and incubated for 24h. Non-stimulated (NS) cells were used as a baseline control. Red arrows indicate artefacts. Cells were viewed by light microscopy and images were taken at X 20 magnification.

The 10μm and 30μm inert beads were spherical and were observed across 1-100μg/ml concentrations (indicated by red arrows in Figure 4.10 and Figure 4.11). MDM exposed to increasing concentrations of 10μm beads did not alter cellular morphology in the different subject groups when compared to non-stimulated controls. The 10μm beads appeared to have been ingested by cells at 10-100μg/ml concentration, with some cells displaying internalisation of two beads (Figure 4.10). MDM exposed to increasing concentrations of 30μm sized inert beads, altered cellular morphology. MDM treated with the 30μm beads had aggregated around the bead, which appeared as a 'group effort' by the cells, to internalise the prey (indicated by white arrows in Figure 4.11).

4.3.5 TEM: Internalisation of DEP-N by MDM

Since MDM were more susceptible to DEP-N related toxicity, it was still unclear whether the decrease in viability was an effect of particle ingestion or chemical composition. In order to further determine whether particulates were being internalised by cells, TEM was used.

The TEM images show that MDM have characteristic features typical of macrophages, such as extending pseudopodia (indicated by red arrows) and the presence of cellular vesicles (indicated by yellow arrows) (Figure 4.12A, Figure 4.12B). It also confirms that MDM were capable of ingesting DEP-N, as particulates were seen in membrane-bound vesicles located in the cytoplasm of the cell (Figure 4.12B).

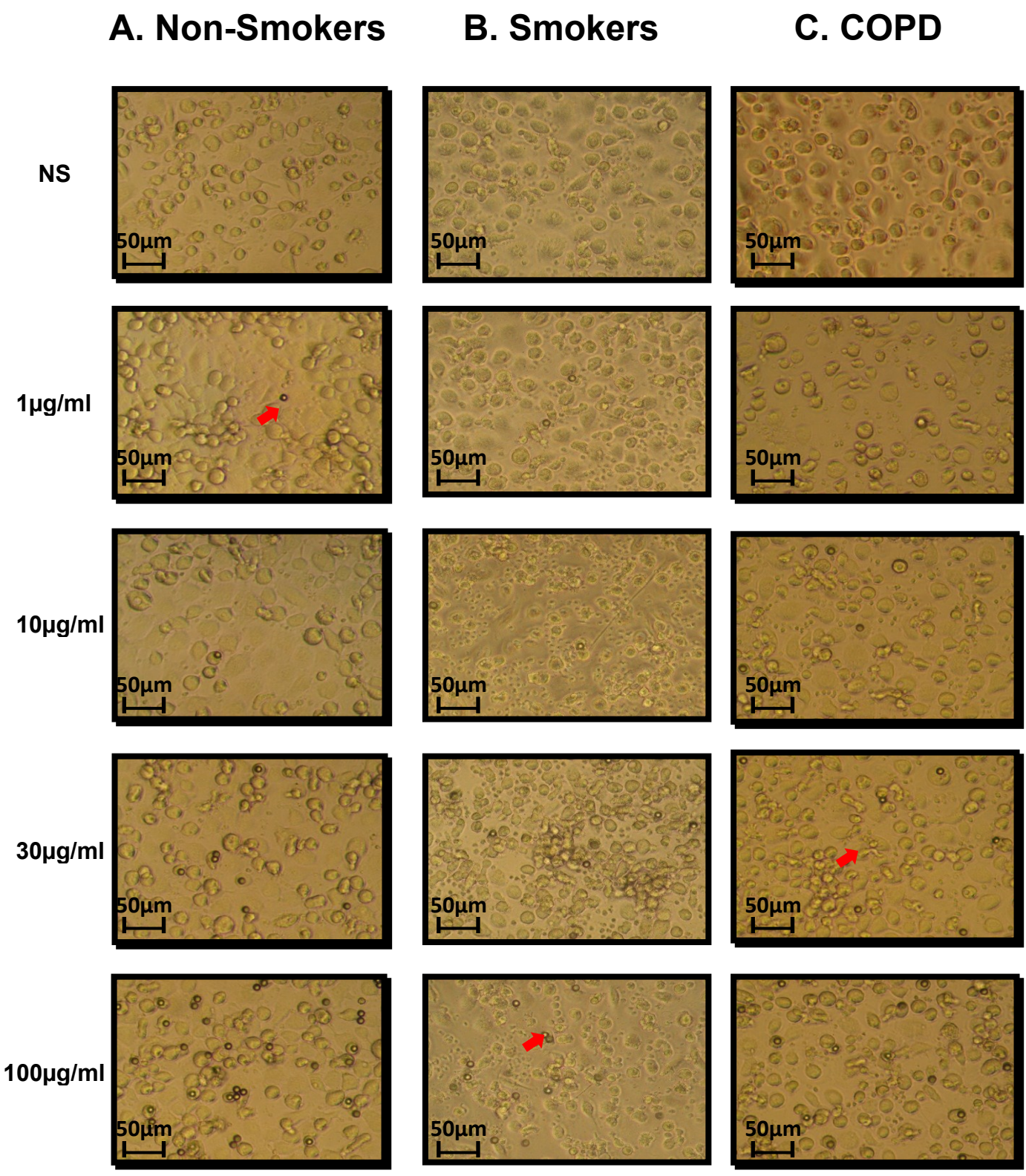

Figure 4.10 Photomicrographs of 10µm Inert Bead-Treated MDM

MDM from Non-smokers (A), Smokers (B) and COPD patients (C) were treated with 10µm polystyrene beads (1-100µg/ml) and incubated for 24h. Non-stimulated (NS) cells were used as a baseline control. Red arrows indicate inert beads bound/internalised by MDM. Cells were viewed by light microscopy and images were taken at X 20 magnification.

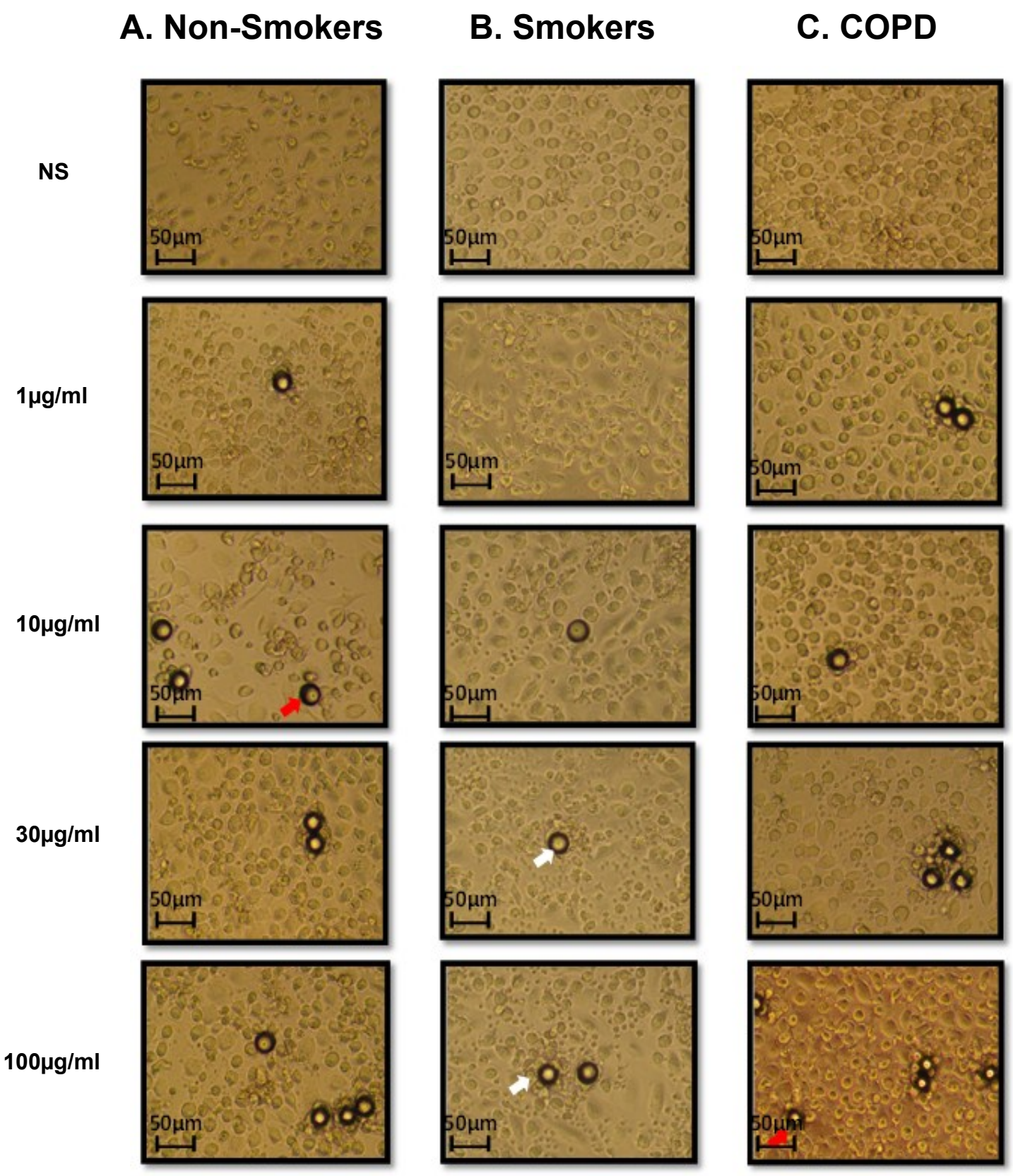

Figure 4.11 Photomicrographs of 30µm Inert Bead-Treated MDM

MDM from Non-smokers (A), Smokers (B) and COPD (C) patients were treated with 30µm polystyrene beads (1-100µg/ml) and incubated for 24h. Non-stimulated (NS) cells were used as a baseline control. Red arrows indicate the 30µm inert bead and white arrows indicate the assembly of cells around the inert beads. Cells were viewed by light microscopy and images were taken at X 20 magnification.

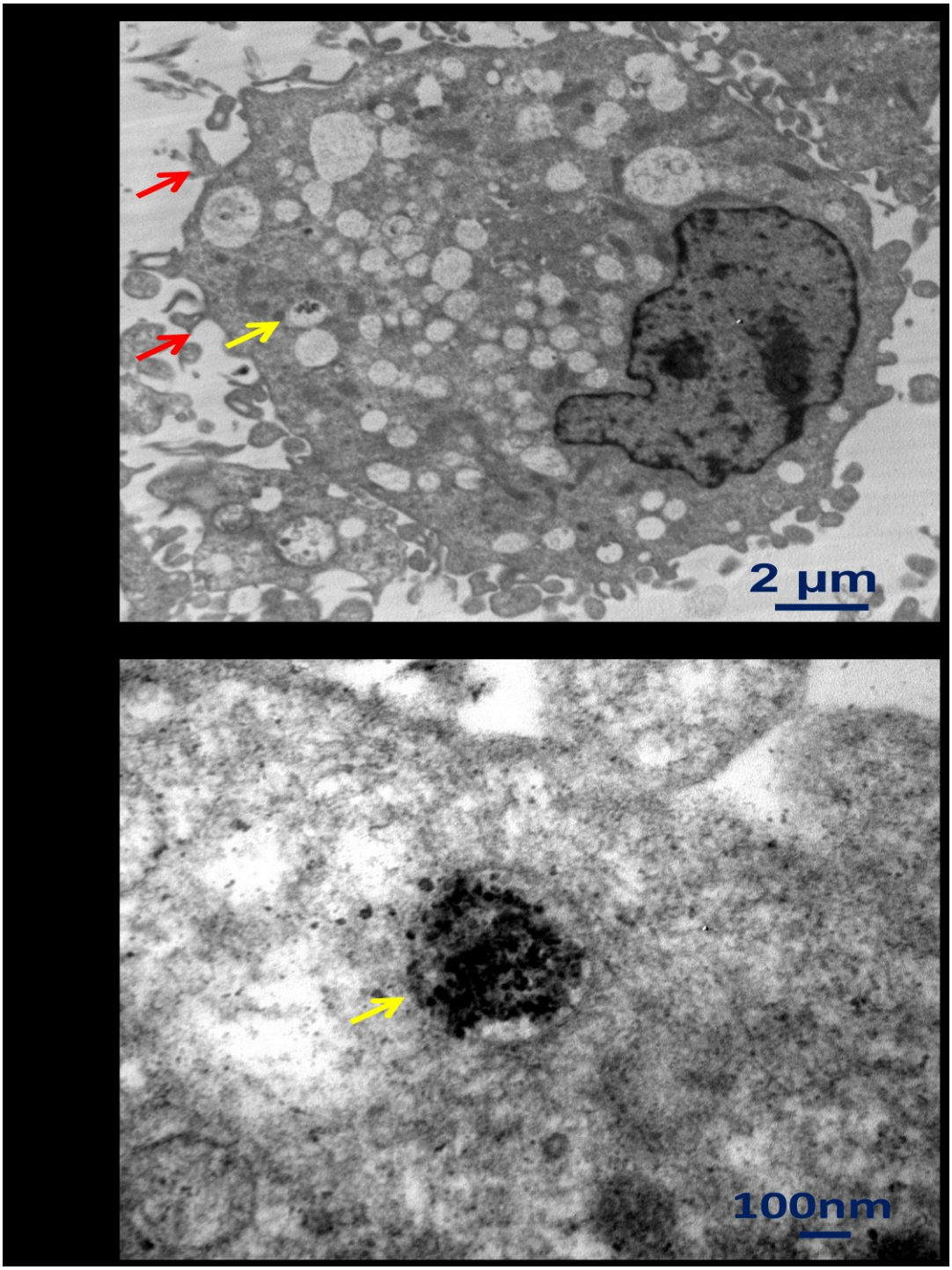

Figure 4.12. TEM: Internalisation of DEP-N by MDM

MDM from a non-smoker subject was treated with DEP-N (30µg/ml) for 24h. TEM image shows typical features of MDM such as pseudopodia (red arrow) and cellular vesicles (yellow arrow). (A) TEM image of MDM showing DEP-N internalised by MDM (B) Detailed view of DEP-N internalised within membrane bound vesicles.

4.3.6 Effect of DEP-N on MDM Apoptosis and Necrosis

Since MDM were susceptible to DEP-N related toxicity, it was unclear whether DEP-N treatment induced cellular apoptosis or necrosis. To assess this further, DEP-N treated cells were stained with Annexin-V and 7-AAD as markers of apoptosis or necrosis respectively and analysed using flow cytometry.

Flow cytometry plots show that DEP-N induced both apoptosis and necrosis in MDM from all subject groups as indicated by the shift of unstained viable cells to the upper and lower right quadrant (Figure 4.1A and Figure 4.1B in section 4.2.7). The shift in viable cells undergoing necrosis was greater in MDM from non-smokers and patients with COPD (Figure 4.13A and Figure 4.13C); however cells from smokers were resilient to this effect and ~34% of these cells were apoptotic (Figure 4.13B). Data from the flow cytometry plots were translated to graphs and, from these analyses, it was observed that DEP-N significantly induced apoptosis in a concentration-dependent manner in MDM from non-smokers and smokers by ~20% and ~13% respectively, at the highest concentration. Cells from patients with COPD were also apoptotic at 100µg/ml DEP-N by ~15%; however statistical significance was not reached (Figure 4.14A). DEP-N significantly induced necrosis in a concentration-dependent manner in MDM from non-smokers and smokers by ~66% and ~27% at 100µg/ml respectively. Cells from patients with COPD also showed a trend towards concentration-dependent necrosis following DEP-N treatment. MDM from patients with COPD were ~55% necrotic at the highest concentration of DEP-treatment (Figure 4.14B). Despite data being significant, MDM from smokers appeared less susceptible to the effects of DEP-N induced necrosis at 1-100µg/ml compared to non-smokers and patients with COPD.

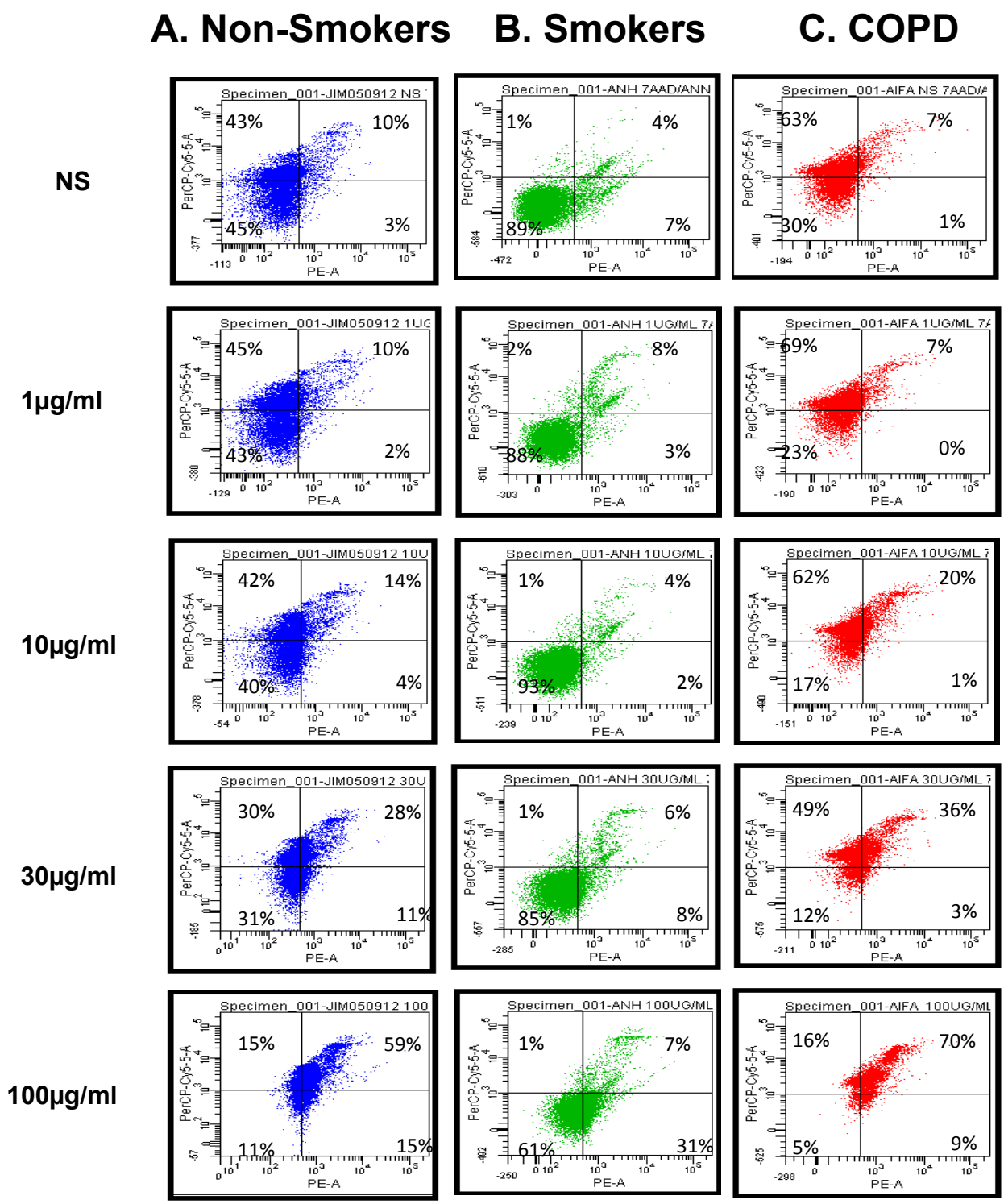

Figure 4.13. Flow Cytometry Dot Plots Showing the Effect of DEP-N on Apoptosis and Necrosis of MDM.

MDM from (A) non-smokers, (B) smokers and (C) COPD were treated with 1-100µg/ml DEP-N and incubated at 37°C, 5% ($^{V}/_{V}$) CO_2 for 24h. Following incubation, cells were stained with Annexin-V and 7-AAD (bind cells undergoing apoptosis or necrosis) for 15 min at RT. Data are dot plots from a individual experiments.

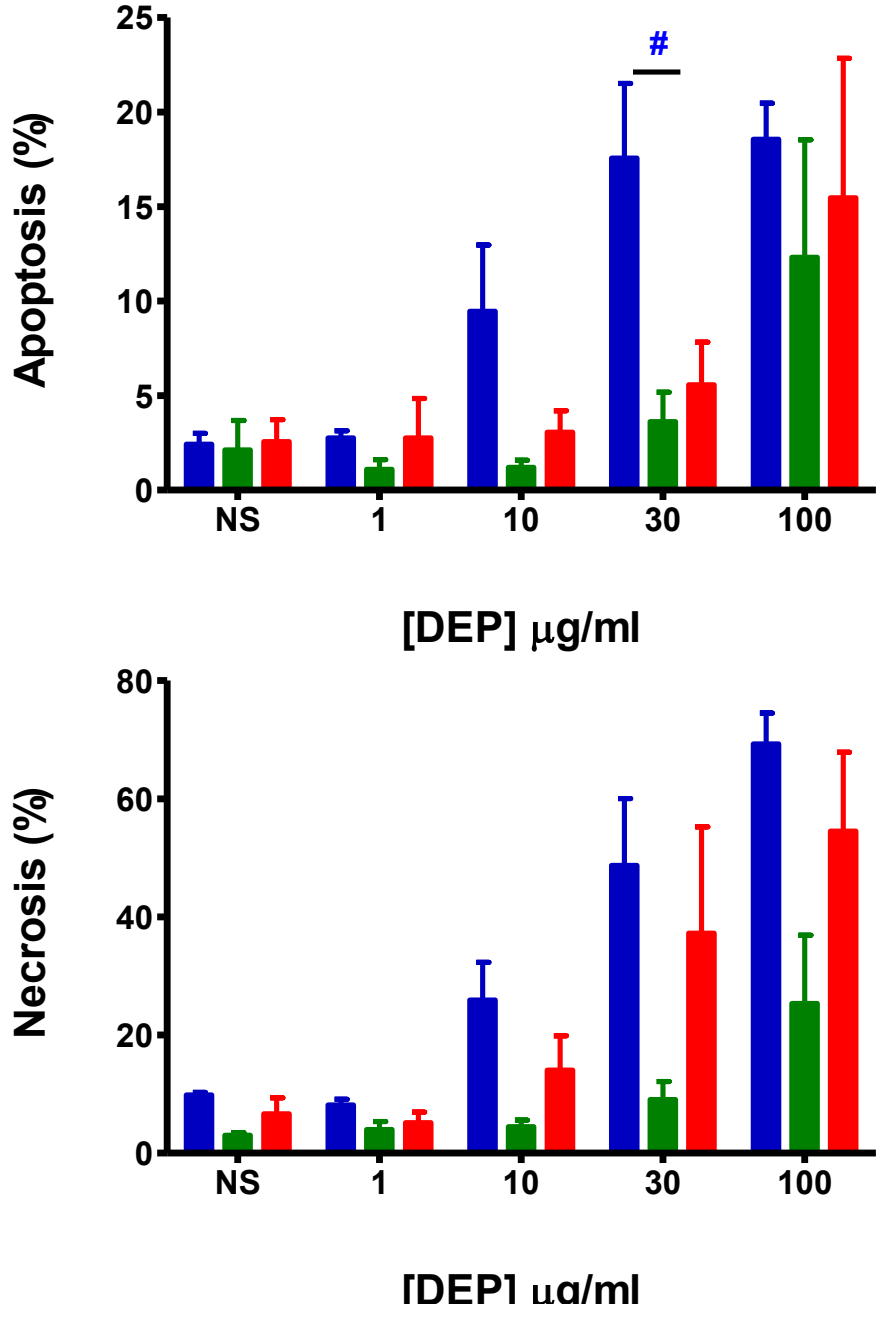

Figure 4.14 Distribution of MDM Undergoing Apoptosis or Necrosis Induced by DEP-N

MDM from non-smokers (■) (n=3), smokers (■) (n=4) and patients with COPD (■) (n=3; ex-smoker n=2, current smoker n=1) were treated with 1-100μg/ml DEP and incubated for 24h. Following incubation DEP-N-treated MDM were stained with Annexin-V and 7-AAD, and then analysed by flow cytometry to determine whether cells underwent (A) apoptosis or (B) necrosis. Data are mean ± SEM. # p< 0.05 non-smokers *vs* smokers.

4.4 Discussion

MDM were used in the present chapter to model alveolar macrophages due to their ready availability, acquisition through minimally-invasive techniques, and ability to compare effects in individuals with different health status. Monocytes were incubated in the presence of GM-CSF for 12 days and had differentiated into macrophage-like cells (Winkler et al. 2008; Taylor et al. 2010; Tudhope et al. 2008).

In this investigation the toxicity of three different DEP samples were examined using MDM viability and morphology as outputs and compared to the effects of cells treated with commercial inert beads of different sizes. The DEP samples had variable effects on cell viability, with DEP-N being more toxic than SRM-1650B or SRM-2975 at high concentrations, with no visible effect on cellular morphology. It was unclear whether composition or ingestion of particles by cells was driving toxicity, therefore inert beads with a size distribution of 0.2μm - 30μm were used. The inert beads did not reduce viability, as seen with DEP-N and SRM-1650B, suggesting that the effects of DEP on MDM may have been driven by their composition, and not size.

The *in-vitro* study conducted by Xia et al. 2004, showed similar findings to the present data, highlighting that composition of DEP may be responsible for cytotoxicity. In this study the RAW 264.7 macrophage cell line was exposed to different chemicals fractionated from DEP such as aliphatic, aromatic and polar organic components. Fractionated chemicals induced variable toxic effects on RAW 264.7 cells, with quinone-enriched polar chemicals being potent inducers of ROS, thereby perturbing mitochondrial function and initiating apoptosis. Hiura et al. 2000 also showed that treatment of primary alveolar macrophages and RAW 264.7 cells

with DEP extracts perturbed mitochondrial function via ROS generation, leading to cellular apoptosis. These observations may explain the increased susceptibility of MDM to DEP-N related toxicity compared to the SRM-1650B or SRM-2975 samples. For instance, DEP-N has trace metals (chapter 3) and may also have a higher content of adsorbed aromatic organic compounds such as quinones which are ROS generators that may initiate mitochondrial damage leading to cellular apoptosis and necrosis (Park et al. 2011; Hiura et al. 1999; Castranova et al. 2001; Block et al. 2004). This could be determined by pre-treating MDM with anti-oxidants such as N'-acetylcysteine (NAC) or glutathione to reverse ROS production, thereby preserving viability. Detection of anti-oxidant transcription factor up-regulation, such as Nrf2, may also confirm whether DEP is an inducer of oxidative stress, as DEP stimulates anti-oxidant and cytoprotective responses at low concentrations of exposure in macrophages (Xiao et al. 2003; Li et al. 2000).

Even though MDM were more susceptible to DEP-N-related toxicity, SRM-1650B also reduced cell viability at the highest concentration of treatment, whereas SRM-2975 exposure did not. The variability between these samples may be reflected in the increased number of PAH and nitro-PAH adsorbed on the surface of SRM-1650B compared to SRM-2975 (Chapter 3). Taken together with the findings mentioned above, the increased toxicity of SRM-1650B may be associated with the increased number of adsorbed chemicals on the surface of the particles.

MDM from smokers, despite being significant, appeared less susceptible to DEP-N-induced necrosis when compared to cells obtained from non-smokers or COPD patients. Data from flow cytometric analyses shows that MDM from smokers may already have cytoprotective responses (such as anti-oxidants) in place to protect cells against exposure to noxious chemicals. The study conducted by McCusker &

Hoidal 1990, showed that BAL macrophages from smokers have a higher level of superoxide dismutase and catalase activity compared to macrophages from non-smokers. This may be similar in MDM from smokers and may explain why MDM from different subject groups are inclined to undergo different processes culminating in cell death, as MDM from smokers may have a number of anti-oxidant defences in place to balance oxidants released in the circulatory system by cigarette smoke. Therefore increases in ROS production by DEP exposure may be counteracted by the excess anti-oxidative enzymes in smoker macrophages.

In summary, the current chapter reveals that DEP-N treated MDM show reduced viability in non-smokers and patients with COPD. DEP-N related toxicity initiated necrosis in MDM from non-smokers and patients with COPD; however MDM from smokers appeared less susceptible to this form of cell death. Findings from this chapter supported the hypothesis, suggesting that DEP will reduce macrophage cell viability; however mechanism of cellular demise requires further examination.

Chapter 5:

Effect of DEP on Cytokine Release by MDM

5.1 Introduction

Findings from Chapters 3 and 4 established that the DEP samples (DEP-N, SRM-1650B and SRM-2975) used herein were physically and morphologically similar, but displayed differences in their surface chemistry. It was also established that the composition of the DEP samples induced cytotoxicity in MDM from non-smokers and COPD patients at 100μg/ml as determined by flow cytometric analyses. Having determined the physical properties, metal composition and toxicity of DEP, the next step was to determine the effect of these particles on macrophage function, including pro-inflammatory cytokine release and phagocytosis. In this chapter, the effect of DEP on cytokine release from MDM will be examined, comparing the effects of DEP between MDM from non-smokers, smokers and patients with COPD.

Macrophages are the 'janitors' of the lung with their overall function being to maintain pulmonary homeostasis. Macrophages respond to inflammatory cues which initiate these cells to phagocytose inhaled particles or pathogens and secrete mediators (Barnes 2004). In COPD, macrophages are implicated in the inflammatory processes associated with the disease, and are activated by a number of stimuli including, DEP, endotoxin, and inflammatory cytokines (Barnes 2004; Vogel et al. 2005). Macrophages from COPD patients release pro-inflammatory cytokines such as CXCL8, IL-6 and TNFα which are associated with perpetuation of airway inflammation typically seen in COPD. These cytokines are increased in COPD as determined by analysis of sputum or BAL (Keatings et al. 1996). As mentioned previously, DEP comprise an elemental carbon core which binds a number of components including organic and inorganic compounds, metals (Cu and Fe) and

endotoxin. The composition of DEP has been reported to mediate pro-inflammatory cytokine release from macrophages (Imrich et al. 2007).

In addition, metals bound to the surface of these DEP may also have a role. Huang et al. 2003 exposed the airway epithelial cell line BEAS-2B and mouse macrophages, RAW 264.7, with ultrafine particles, fine and coarse PM samples and cytokine release was measured. BEAS-2B treated with ultrafine particles released higher levels of CXCL8 compared to cells exposed to fine and coarse PM. The increase in CXCL8 release from BEAS-2B cells was associated with Cr and Mn adsorbed to the surface of ultrafine particles. In contrast, RAW 264.7 cells released significantly higher levels of TNFα when exposed to ultrafine particles compared to particles of larger diameters.

Endotoxin is found in the environment and is adsorbed on the surface of DEP. Endotoxin is a microbial stimulus and inhalation is associated with changes in lung function and exacerbation of pulmonary diseases (Arimoto et al. 2005). Administration of DEP in combination with endotoxin (lipopolysacchride) is associated with neutrophillic lung inflammation and increased chemokine release in mice (Takano et al. 2002). The *in-vitro* study conducted by Huang et al. 2002 examined the effect of fine or coarse DEP on the release of TNFα from RAW 264.7 cells. Coarse DEP significantly increased TNFα release, and also contained a higher content of endotoxin than fine particles. Polymyxin B is as antibiotic that binds to and inactivates endotoxin (Cardoso et al. 2007). Treatment of DEP with polymyxin B reduced TNFα release in RAW 264.7 cells by 32% and 42% in the coarse and fine fraction of DEP samples. For this reason it was suggested that the endotoxin component of DEP, was in part involved in the stimulation of TNFα release by macrophages.

From the above discussion, it is hypothesised that 'Treatment of MDM with DEP-N, SRM-1650B or SRM-2975 will stimulate release of CXCL8, IL-6 and TNFα, and release of these mediators will be more profound in MDM from patients with COPD'.

To examine this hypothesis, the following aims were investigated:

- Determine whether particle size and/or surface chemistry stimulated CXCL8, IL-6 and TNFα release by MDM treated with 0.2μm, 10μm and 30μm inert beads.
- Determine whether DEP surface chemistry stimulated CXCL8, IL-6 and TNFα release by MDM treated with DEP-N, SRM-1650B or SRM-2975.
- Determine the involvement of endotoxin in DEP induced cytokine release by using the limolas amebocyte lysate (LAL) assay and the endotoxin 'scavenger' polymyxin B.

5.2 Methods

5.2.1 Treatment of MDM with DEP or Inert Beads

MDM were treated with DEP (DEP-N, SRM-1650B or SRM-2975) or inert beads with different size diameters (0.2µm, 10µm and 30µm) and incubated at 37℃, 5% ($^{V}/_{V}$) CO_2 for 24h as described in Section 2.2.7.1 and Section 2.2.7.2. Following incubation, supernatants were harvested and stored at -80℃ until assayed.

5.2.2 Measuring Release of Cytokines from DEP- or Inert Bead-Treated MDM

Concentrations of CXCL8, IL-6 and TNFα were measured in supernatants collected from DEP-or inert bead-treated MDM. Cytokines were measured using ELISA as described in section 2.2.10. The limit of detection for CXCL8 or TNFα was 31.3pg/ml and IL-6 was 15.6pg/ml.

5.2.3 Measuring Endotoxin Content of DEP Samples

5.2.3.1 Measuring Endotoxin Content on DEP Samples Using Limolas Amebocyte Lysate Assay

The endotoxin content of the DEP-N, SRM-1650B and SRM-2975 samples was measured using the LAL assay. LPS was used as a positive control. Reagents provided in the assay kit were prepared as described in Section 2.2.6. DEP (1-00µg/ml) samples (with unknown amounts of endotoxin content) were diluted in HBSS (pH 7.5).

To determine the endotoxin content of the DEP samples, a series of endotoxin concentrations (provided in the kit) were used to produce a standard curve (Figure 5.1). Serial dilutions of standard endotoxin concentrations were prepared in the range 0-10 EU/ml (Figure 5.1). 50µl of DEP samples (1-100µg/ml) with unknown concentrations of endotoxin were pipetted on to a micro-titre plate (provided with kit) followed by addition of 50µl of LAL. Samples were incubated for 45 min at room temperature to allow the LAL reagent to bind to endotoxin to produce a yellow colour. This reaction was stopped by pipetting 50µl of 'Stop solution' (50% ($^{V}/_{V}$) acetic acid diluted in 15ml distilled water) and the absorbance was read on a plate reader at λ 405nm. The limit of detection of the assay was 0.04EU/ml.

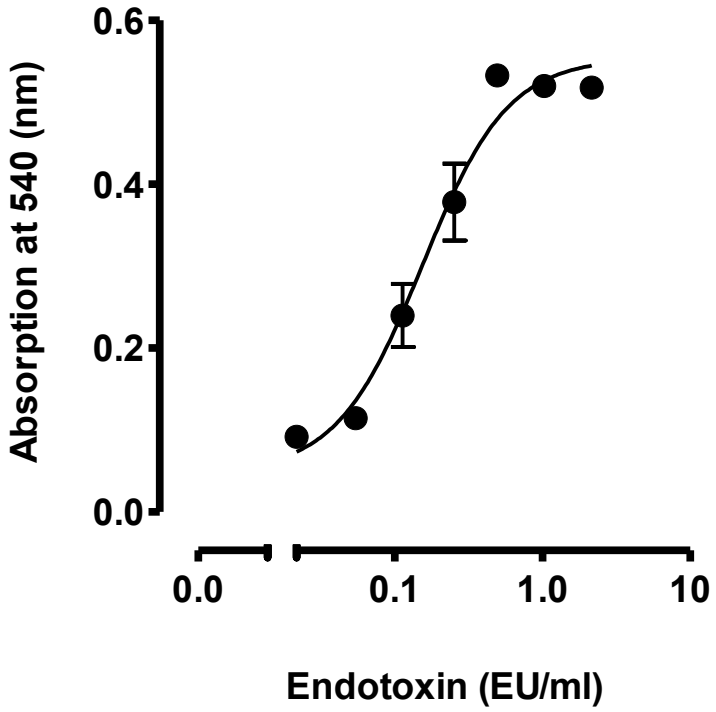

Figure 5.1 Endotoxin Standard Curve

Standard curve used to interpolate unknown concentrations of endotoxin on DEP and LPS samples. Data are in triplicate and are mean ± SEM, n =1.

5.2.3.2 Treatment of DEP-N with Polymyxin B

To determine if the antibiotic, polymyxin B, would inhibit LPS activity in DEP-induced MDM release of CXCL8, DEP-N and the positive control LPS was prepared in polymyxin B treated media. In brief, DEP-N (1-100µg/ml) and the positive control LPS (10ng/ml) were prepared in cell culture media as described in Section 2.2.7.2 and Section 2.2.7.4. DEP-N (1-100µg/ml) and LPS (10ng/ml) were also prepared in cell culture media containing the antibiotic polymyxin B (10mg/ml). MDM were treated with DEP-N or LPS with or without polymyxin B as described in Section 2.2.7.2 and Section 2.2.7.4. Cells were incubated at 37°C, 5% ($^{V}/_{V}$) CO_2 for 24h and supernatants were collected. Supernatants were analysed for release of CXCL8 from MDM treated with DEP-N or LPS samples with or without polymyxin B.

5.2.4 Cell Viability

Cell viability of MDM treated with DEP-N or LPS, with or without polymyxin B was assessed by MTT assay as described in section 2.2.8.1.

5.2.5 Statistics

Data sets were compared for statistical significance between subject groups by one-way ANOVA followed by Dunnett's test for multi-group comparisons. A P value <0.05, was considered statistically significant. Data were analysed using Prism V.5 (GraphPad, San Diego, USA).

5.3 Results

5.3.1 Effect of Inert Beads on MDM Cytokine Release

To determine whether the composition or size of particles were associated with the release of pro-inflammatory mediators, namely CXCL8, IL-6 or TNFα, MDM were treated with inert beads of different sizes.

MDM from non-smokers, smokers and patients with COPD treated with 0.2μm, 10μm or 30μm diameter beads did not significantly stimulate release of CXCL8 (Figure 5.2), IL-6 (Figure 5.3) or TNFα (Figure 5.4) compared to non-stimulated controls, and were below the limit of detection for these assays.

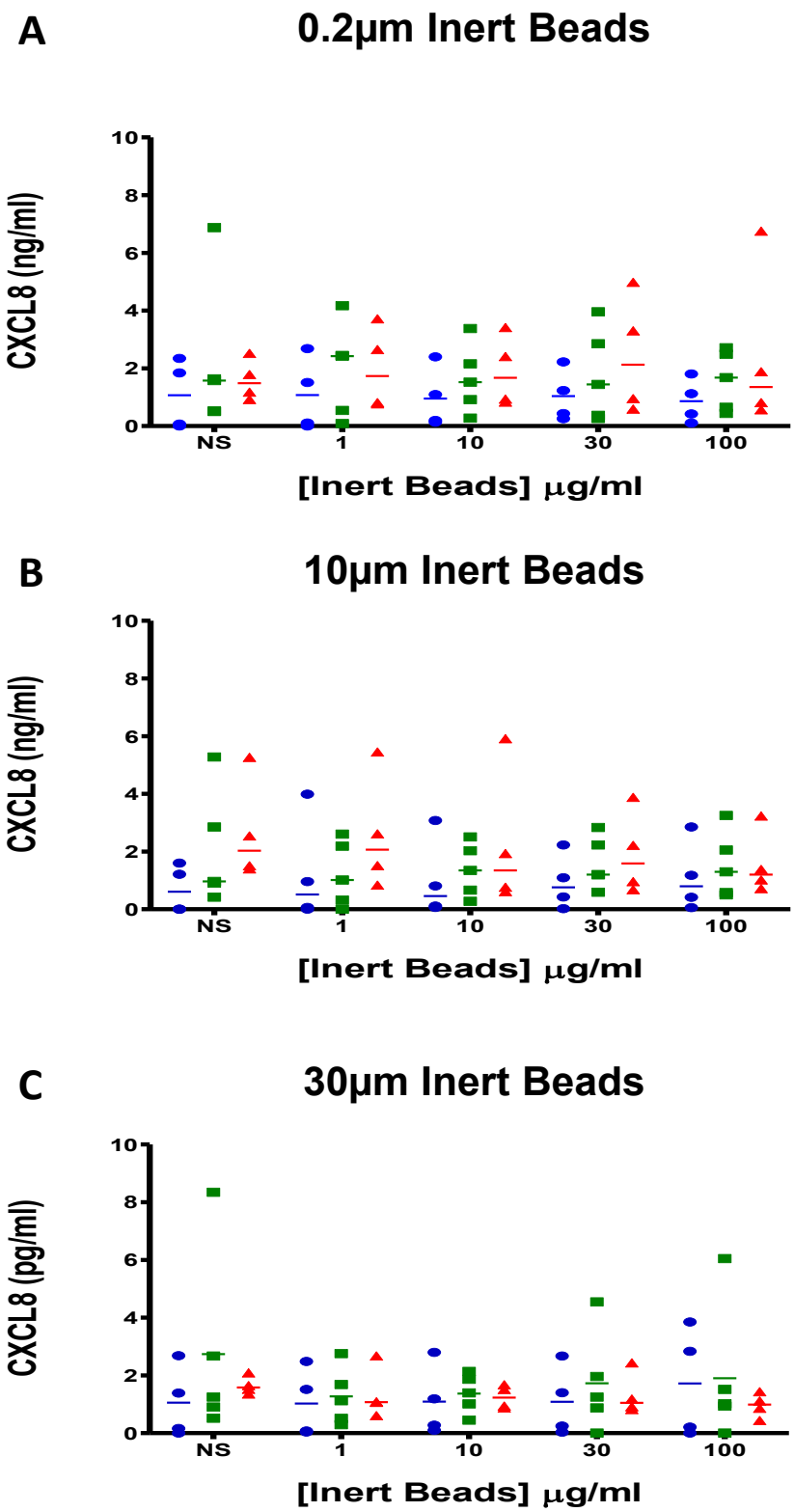

Figure 5.2. Effect of Inert Bead-Treated MDM on CXCL8 Release.

MDM from non-smokers (●) (n=4), smokers (■) (n=5) and patients with COPD (▲) (n=4; ex-smokers n=1; current-smokers n=1; unknown n=2) were treated with 1-100µg/ml of (A) 0.2µm, (B) 10µm or (C) 30µm inert beads and incubated at 5% ($^{V}/_{V}$) CO_2, at 37℃ for 24h. Following incubation, supernatants were harvested and CXCL8 release was measured using ELISA. Data are expressed as medians. No significant differences were found.

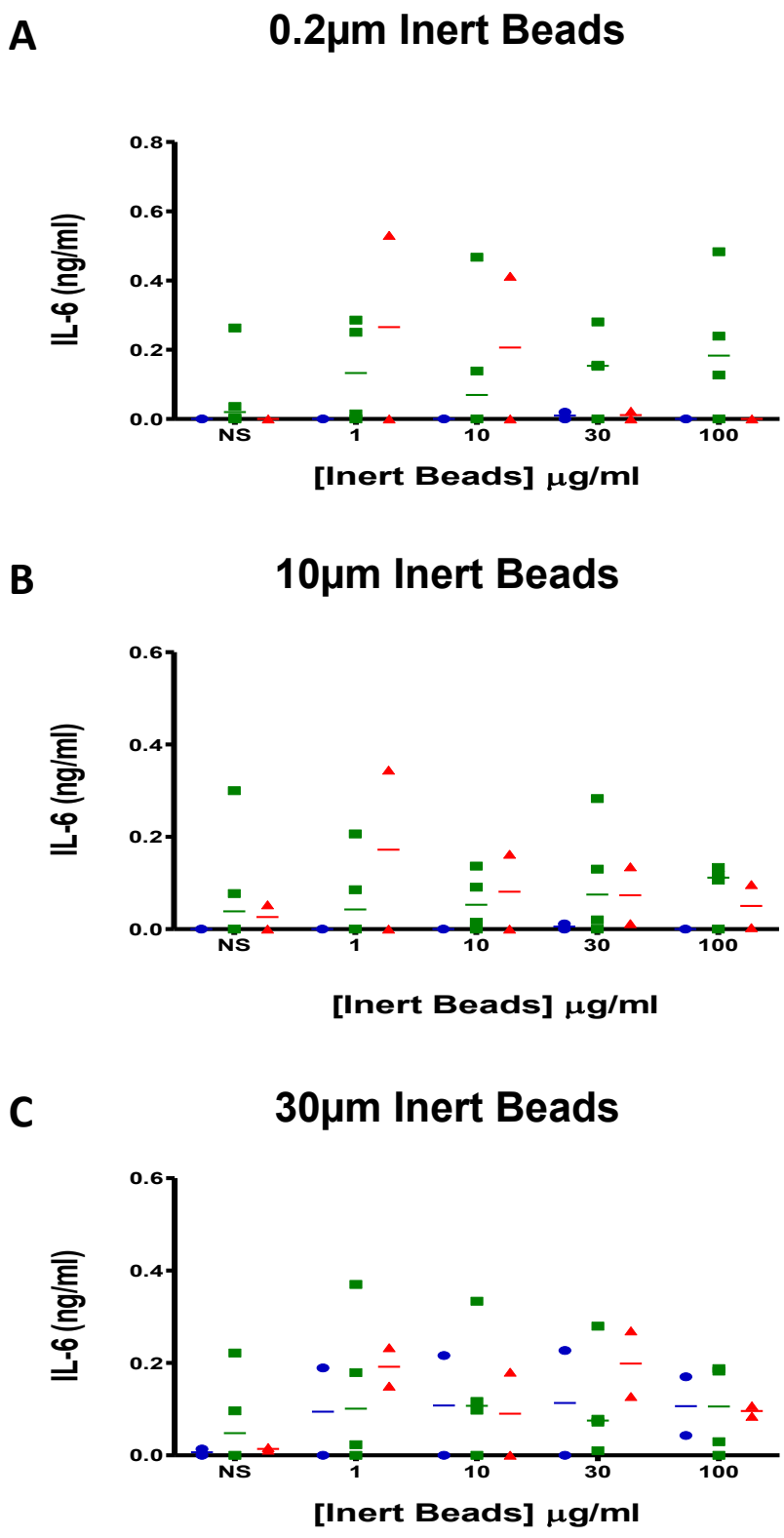

Figure 5.3. Effect of Inert Bead-Treated MDM on IL-6 Release.

MDM from non-smokers (●) (n=2), smokers (■) (n=4) and patients with COPD (▲) (n=2; ex-smokers n=1; current-smokers n=1) were treated with 1-100µg/ml of (A) 0.2µm, (B) 10µm or (C) 30µm inert beads and incubated at 5% ($^{V}/_{V}$) CO_2, at 37°C for 24h. Following incubation, supernatants were harvested and IL-6 release was measured using ELISA. Data are expressed as medians. No significant differences were found.

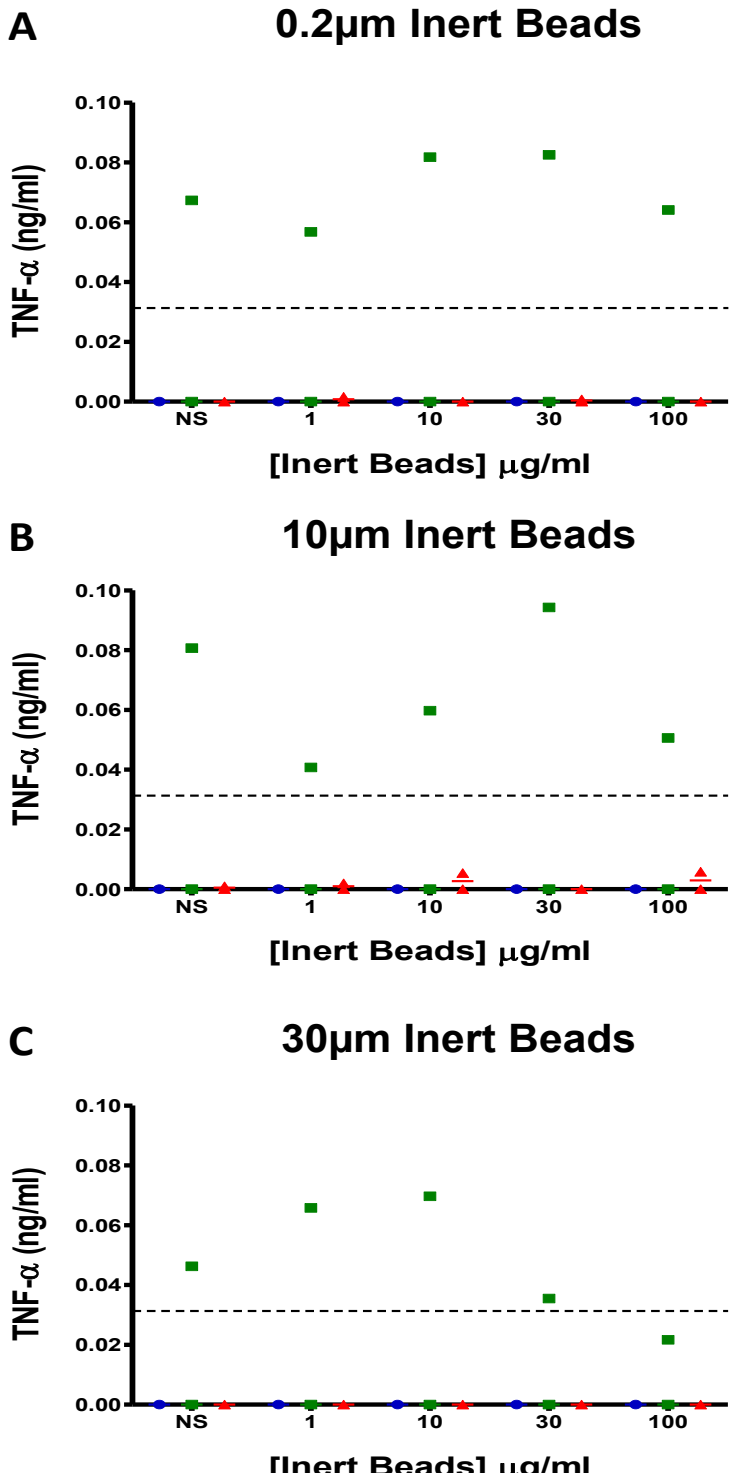

Figure 5.4. Effect of Inert Bead-Treated MDM on TNFα Release.

MDM from non-smokers (●) (n=1), smokers (■) (n=4) and patients with COPD (▲) (n=2; ex-smokers n=1; current-smokers n=1) were treated with 1-100µg/ml of (A) 0.2µm, (B) 10µm or (C) 30µm inert beads and incubated at 5% ($^{V}/_{V}$) CO_2, at 37°C for 24h. Following incubation, supernatants were harvested and TNFα release was measured using ELISA. Dotted line represents limit of detection. Data are expressed as medians. No significant differences were found.

5.3.2 Effect of DEP on MDM Cytokine Release

Having determined that inert beads did not stimulate cytokine release, the next step was to determine whether the three DEP samples (DEP-N, SRM-1650B and SRM-2975) would induce MDM release of CXCL8, IL-6 or TNFα. MDM treated with DEP-N released CXCL8 in a concentration-dependent manner, with cells from smokers releasing less CXCL8 than non-smokers, or patients with COPD. The maximal release of CXCL8 from smoker MDM was ~8ng/ml compared to cells from non-smokers and patients with COPD which released ~16ng/ml (Figure 5.5A). MDM from smokers released CXCL8 in a concentration-dependent manner when treated with SRM-1650B, albeit significance was not reached (Figure 5.5B). SRM-2975 also did not induce CXCL8 release from MDM (Figure 5.5C). MDM from non-smokers, smokers or patients with COPD treated with increasing concentrations of DEP-N, SRM-1650B or SRM-2975 did not release IL-6 (Figure 5.6) or TNFα (Figure 5.7) compared with non-stimulated controls.

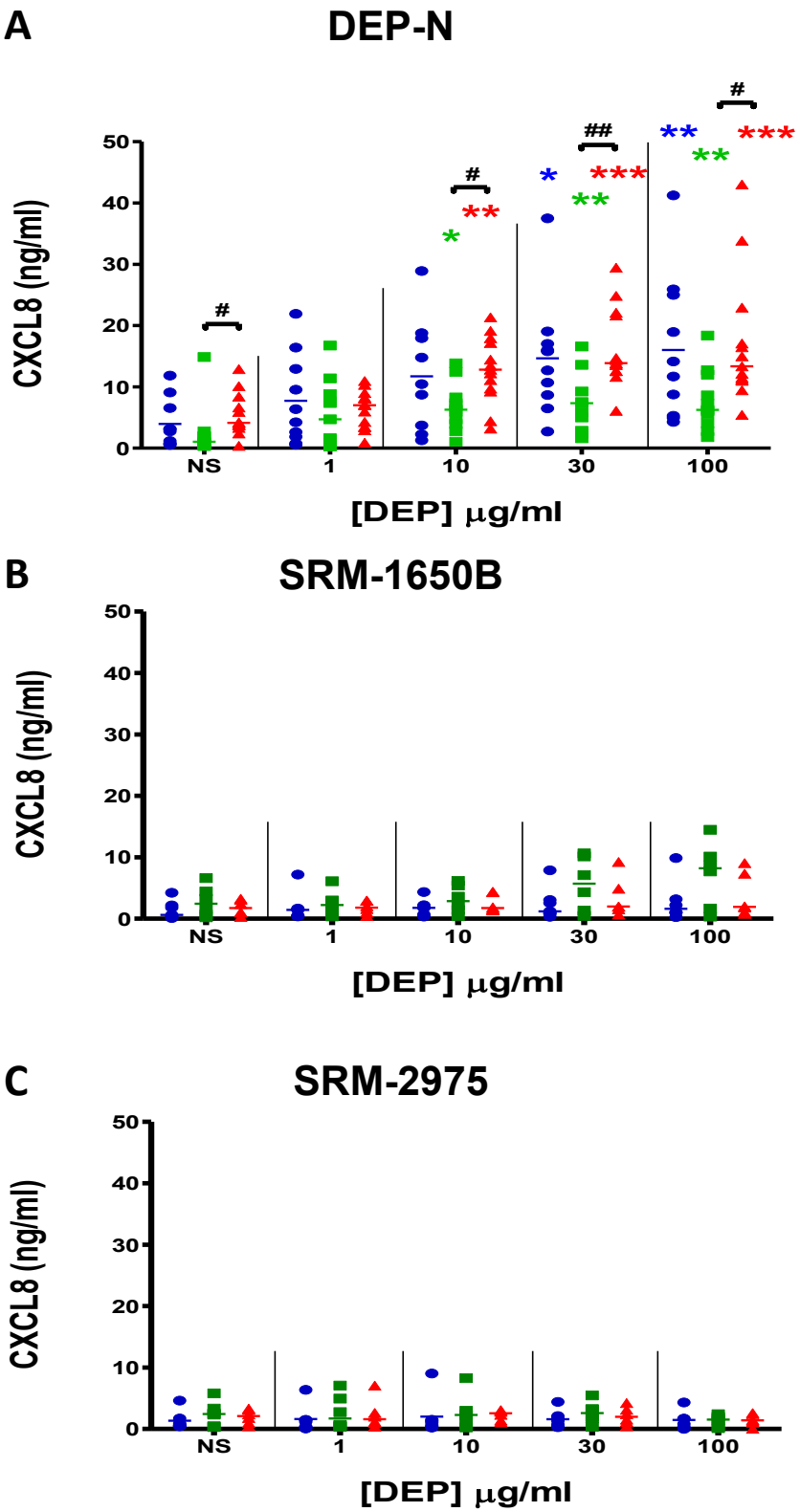

Figure 5.5. Effect of DEP-Treated MDM on CXCL8 Release.

MDM from non-smokers (●) (n=7-10), smokers (■) (n=6-11) and patients with COPD (▲) (n=6-13: ex-smokers n=3-5; current-smokers n=2-7; unknown n=1) were treated with 1-100µg/ml of (A) DEP-N, (B) SRM-1650B or (C) SRM-2975 and incubated at 5% ($^{V}/_{V}$) CO_2, at 37°C for 24h. Following incubation, supernatants were harvested and CXCL8 release was measured using ELISA. Data are expressed as medians. *p<0.05, **p<0.01, p<0.001 *vs* non-stimulated controls. #p<0.05, ##p<0.01 smokers *vs* patients with COPD.

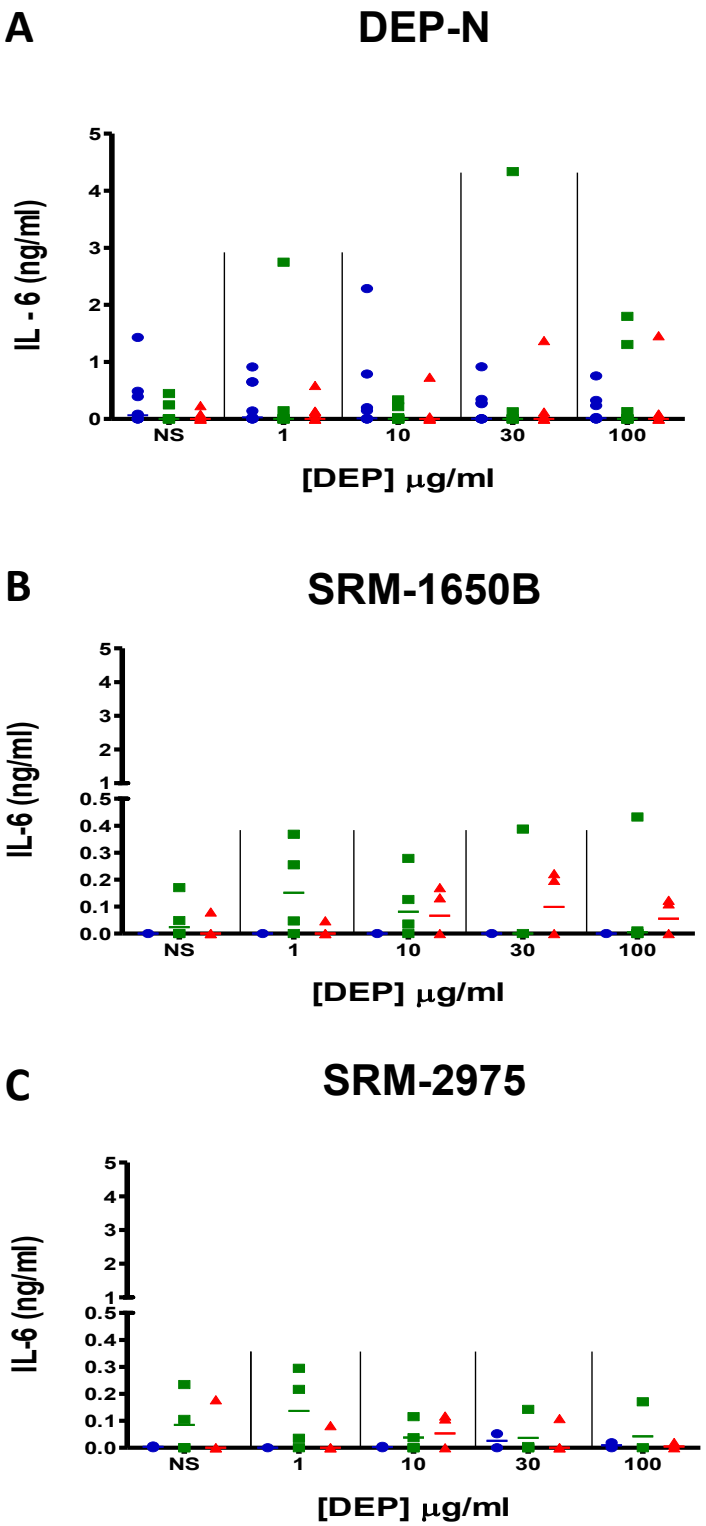

Figure 5.6. Effect of DEP-Treated MDM on IL-6 Release.

MDM from non-smokers (●) (n=2-9), smokers (■) (n=4-10) and patients with COPD (▲) (n=4-11; ex-smokers n=3-6; current-smokers n=1-3; unknown n=2) were treated with 1-100µg/ml of (A) DEP-N, (B) SRM-1650B or (C) SRM-2975 and incubated at 5% ($^{V}/_{V}$) CO_2, at 37°C for 24h. Following incubation, supernatants were harvested and IL-6 release was measured using ELISA. Data are expressed as medians. No significant differences were found.

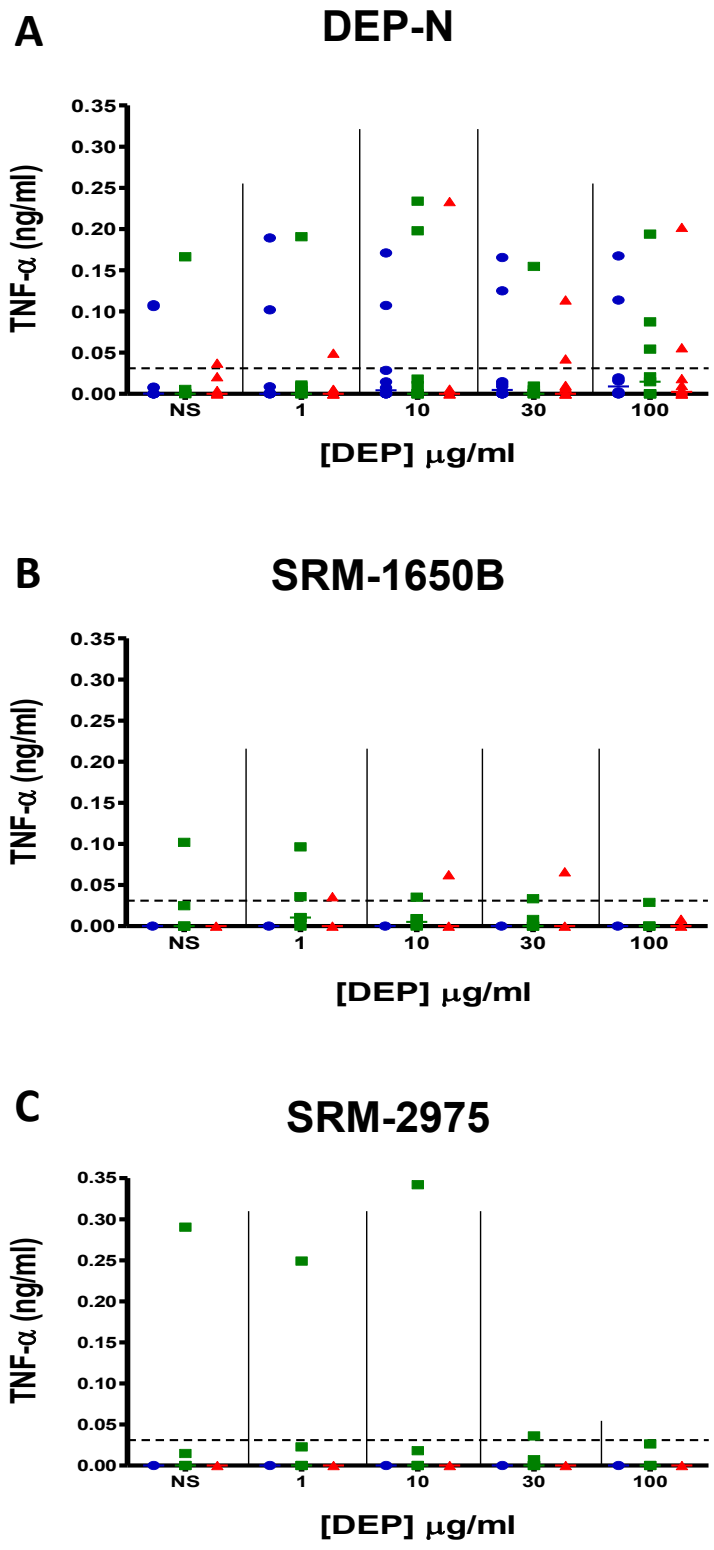

Figure 5.7. Effect of DEP-Treated MDM on TNFα Release.

MDM from non-smokers (●) (n=6-10), smokers (■) (n=6-9) and patients with COPD (▲) (n=3-11; ex-smokers n=1-4; current-smokers n=2-6; unknown n=1) were treated with 1-100μg/ml of (A) DEP-N, (B) SRM-1650B or (C) SRM-2975 and incubated at 5% ($^{V}/_{V}$) CO_2, at 37°C for 24h. Following incubation, supernatants were harvested and TNFα release was measured using ELISA. Data are expressed as medians. Dotted line represents limit of detection. Data are expressed as medians. No significant differences were found

5.3.3 Endotoxin Content of DEP samples

DEP bind a number of components to their surface, including endotoxin. As DEP-N and SRM-1650B were associated with release of CXCL8 by MDM, the DEP samples were examined for endotoxin content using the LAL assay. There was no significant difference in endotoxin content across 1-100μg/ml in DEP-N (Figure 5.8A) or SRM-1650B (Figure 5.8B) samples when compared to vehicle alone. SRM-2975 showed a higher endotoxin level at 100μg/ml compared to vehicle alone, albeit not significant.

To validate the findings of the LAL assay, DEP-N or LPS (control) was treated with or without the endotoxin scavenger polymyxin B and applied to MDM and CXCL8 output measured. Treatment of MDM with increasing concentrations of DEP-N with or without polymyxin B, did not significantly differentially release CXCL8. In contrast, MDM treated with LPS (10ng/ml) significantly released ~40ng/ml of CXCL8 compared to MDM treated with LPS and polymyxin B, which had released ~1ng/ml of CXCL8 (Figure 5.9). Treatment of MDM with DEP significantly reduced cell viability at 100μg/ml, but did not reduce viability in MDM treated in combination with DEP and polymyxin B, compared to non-stimulated controls (Figure 5.10). These data validate the findings of the LAL assay and also show that DEP-N has not adsorbed endotoxin which is therefore, unlikely to be responsible for the CXCL8 release.

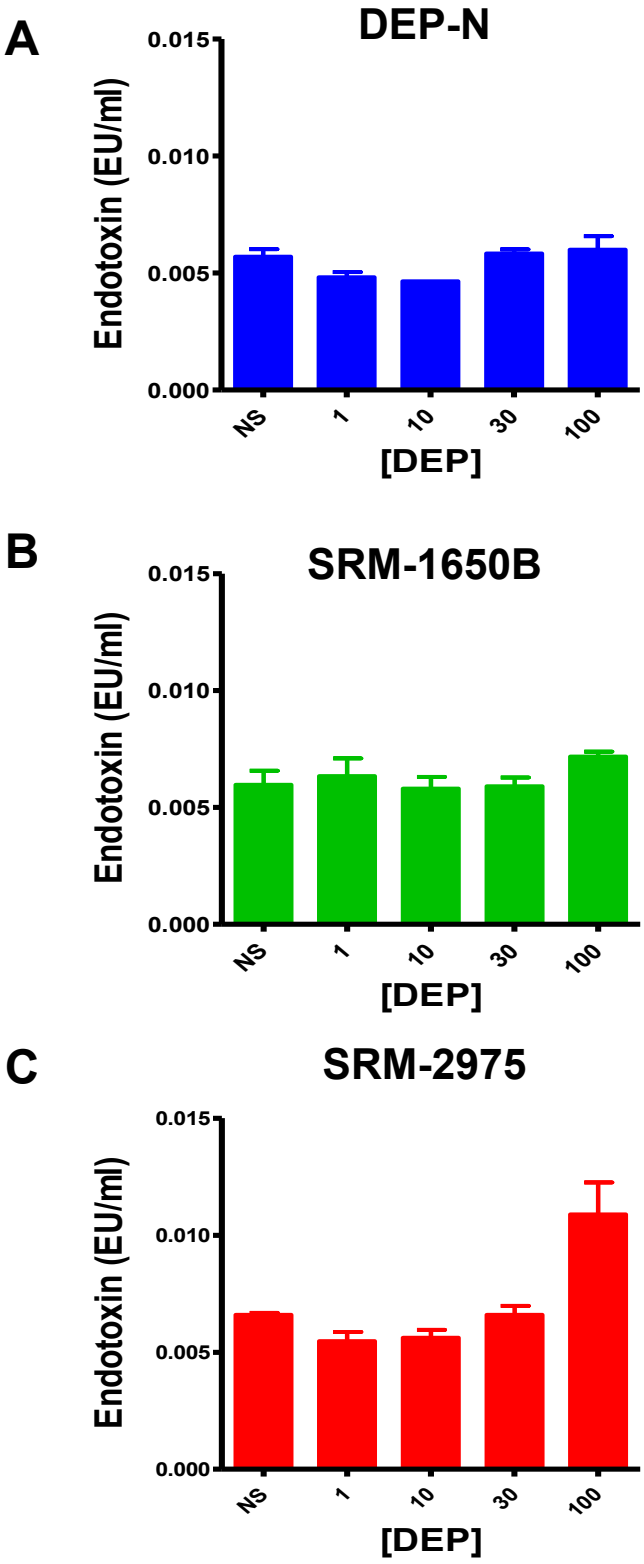

Figure 5.8. Endotoxin Content Adsorbed to the Surface of DEP

The endotoxin content of DEP samples (1-100µg/ml) was examined using LAL assay (n=1). (A) DEP-N (■), (B) SRM-1650B (■) or (C) SRM-2975 (■) were treated with LAL reagent and the reaction between endotoxin and LAL reagent produced a yellow colour, this was stopped by the addition of acetic acid. Absorbance was measured at 540nm. DEP-N, SRM-1650B and SRM-2975 samples were performed in triplicate, Data are mean ± SEM and no significant differences were found.

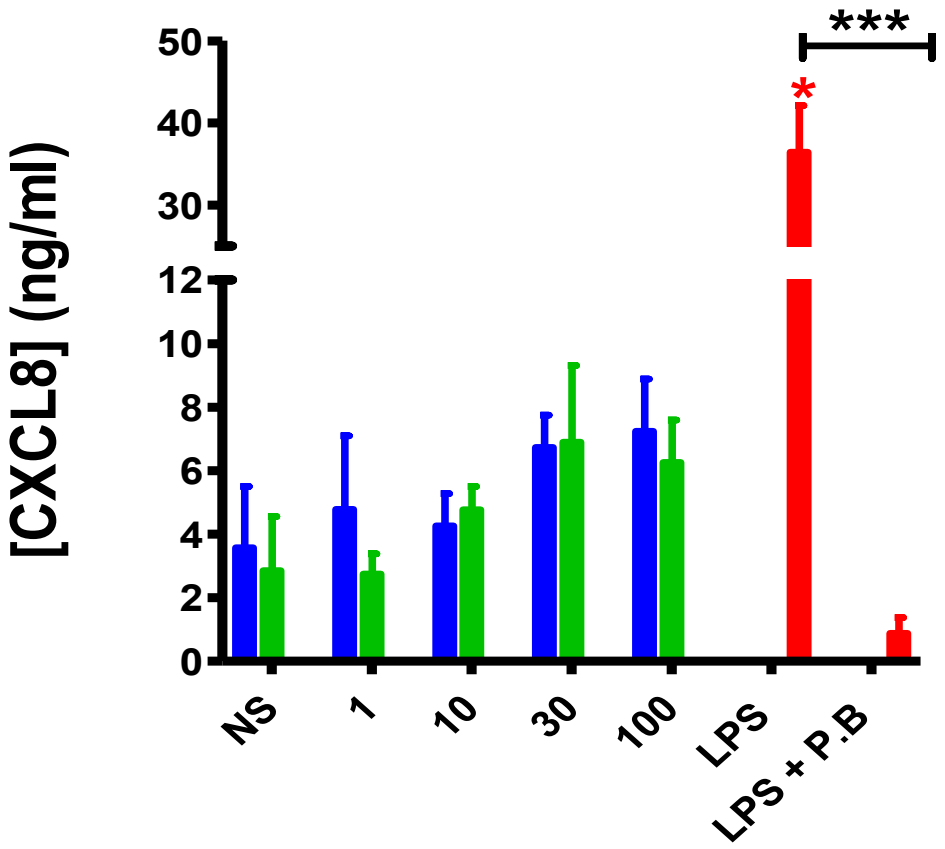

Figure 5.9. Effect of DEP-N Treatment With or Without Polymyxin B on MDM CXCL8 Release

MDM were treated with 1-100µg/ml of DEP-N (■) or LPS (10ng/ml) (■), with (■) or without polymyxin B (n=4). MDM were then incubated at 37°C, 5% ($^{V}/_{V}$) CO_2, for 24h. Following incubation, supernatants were harvested and CXCL8 release was measured using ELISA. Data are mean ± SEM. * $p<0.05$ *vs* NS, *** $p<0.001$ LPS *vs* LPS + polymyxin B.

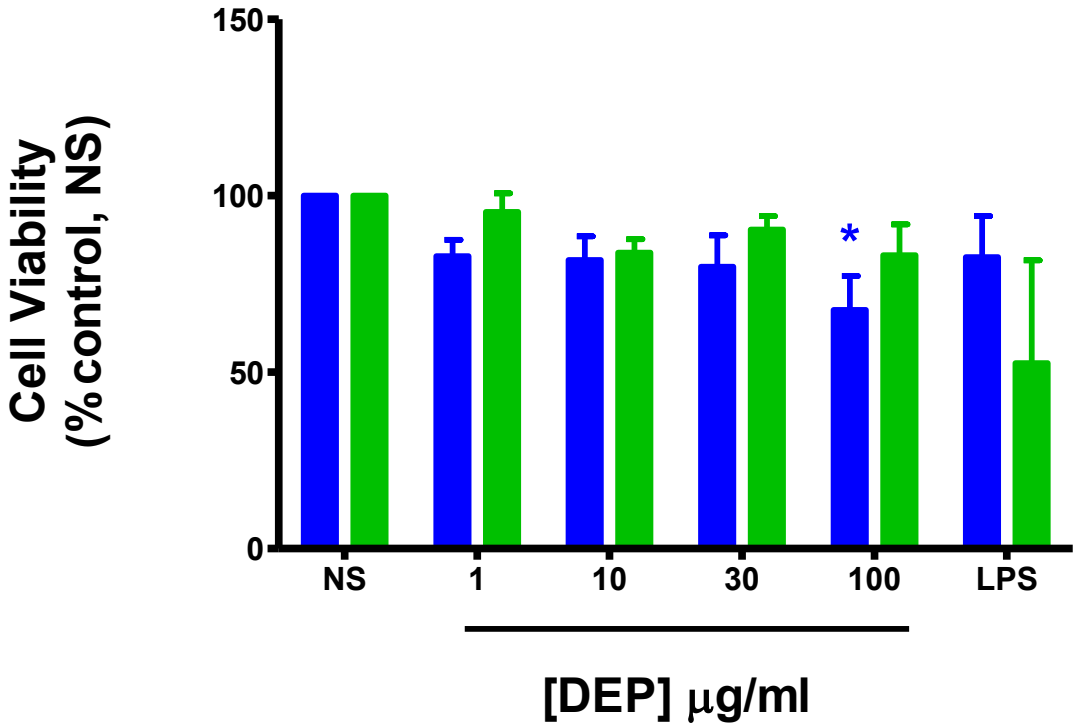

Figure. 5.10 Effect of DEP-N Treatment with or without LPS on MDM Cell-Viability.

MDM were treated with 1-100μg/ml of DEP-N (■) or LPS (10ng/ml) with or without polymyxin B (■) (n=4). Cells were incubated for 37°C, 5% ($^{V}/_{V}$) CO2 for 24h following incubation, supernatants were harvested and MTT was applied to determine cell viability. Non-stimulated (NS) cells were used as baseline controls and represented maximum cell viability (normalised data). Data are mean ± SEM of % cell viability (relative to control). No significant differences were found. * $p<0.05$ *vs* NS.

5.4 Discussion

In the present chapter the effect of DEP on MDM cytokine release was investigated and compared to release of cytokines from MDM treated with inert beads of different sizes. Treatment of MDM with inert beads, SRM-1650B or SRM-2975 did not stimulate cytokine release. MDM treated with DEP-N stimulated CXCL8 release, with no effect on IL-6 or TNFα release. The effect of DEP-N on CXCL8 release was not attributed to the presence of endotoxin on the particles, as determined by the use of LAL assay or polymixin B. Thus, the effect of DEP-N on CXCL8 release is associated with the composition, rather than size, of DEP-N particles.

The cytokines released from macrophages exposed to different samples of DEP vary from study to study (Huang et al. 2003; Becker et al. 2005; Amakawa et al. 2003), which is similar to the differential response seen herein between MDM treated with DEP-N or the SRM particles. It is considered that the difference in cytokine profile from macrophages in DEP exposure studies is attributable to the surface chemistry of the particles. Amakawa et al. 2003 showed that DEP suppress spontaneous release of IL-6 and TNFα from human and murine alveolar macrophages, which could not be attributed to loss of cell viability. To determine whether the suppression of IL-6 and TNFα was correlated to the chemical species adsorbed on the surface of the particles, macrophages were exposed to elemental carbon. Treatment of cells with carbon alone did not replicate the initial suppression of IL-6 and TNFα. However, cells treated with DEP extract suppressed IL-6 and TNFα release, suggesting that the soluble organic fraction of DEP was responsible for the effect observed.

In contrast to the findings mentioned above, other groups have suggested that release of cytokines by DEP-treated macrophages is associated to particle size (Becker et al. 2003; Hetland et al. 2005). For example Becker et al. 2003, showed that exposure of human AM to fine (<$PM_{2.5}$) particles induced a ten-fold higher release of IL-6, than macrophages exposed to ultra fine particles (<$PM_{0.1}$). In addition, Hetland et al. 2005 also showed that human AM exposed to coarse (<PM_{10}) fractions of PM induced higher levels of IL-6 and TNFα release compared to both ultrafine particles and fine particles. It was determined that even though the coarse fraction of PM had high levels of Cu, Fe, organic PAH and endotoxin, these components did not correlate to IL-6 and TNFα output. The analyses from Hetland et al. 2005 are in contrast to the findings in the present chapter. This is because, even though DEP-N, SRM-1650B and SRM-2975 displayed similar physical characteristics such as size and morphology (as determined in Chapter 3), only DEP-N was capable of stimulating the release of CXCL8, thereby suggesting that DEP size was not associated with cytokine release.

The association of DEP-N with MDM release of CXCL8 may be correlated to the metal species adsorbed on the surface of the particles. Findings from chapter 3 show that DEP-N had a high content of Cu and Fe, compared to SRM-1650B and SRM-2975. This may in part be related to the increased CXCL8 release from MDM exposed to DEP-N, rather than SRM-1650B and SRM-2975.

In addition, health effects are also associated with PM seasonal variation, with heterogeneous cytokine release being associated to the composition of DEP. For example, Becker et al. 2005, showed that treatment of human bronchial epithelial cells and AM with PM collected during winter, spring, summer and autumn, differentially induced cytokine release. PM samples collected during October were

potent inducers of IL-6 in AM, whereas PM collected in January were potent inducers of CXCL8 in bronchial epithelial cells. Analyses from Becker et al. 2005 highlight that metals such as Cu, Fe, Cr, Al and Ti were correlated to the release of IL-6 and CXCL8, which may in part reflect the findings in the present chapter. To establish whether metals bound to DEP-N were associated with the release of CXCL8, metal chelators such as ethylenediaminetetraacetic acid (EDTA), desferrioxamine (DFOA) or 2,3-dimercaprol could be used to treat DEP-N prior to MDM exposure.

The present chapter showed similarities in the release of CXCL8 between MDM from non-smokers and patients with COPD. It was speculated originally that MDM from patients with COPD would have been more sensitive to DEP-treatment and would have released a higher level of cytokines. This is because BAL macrophages from patients with COPD show a higher release of cytokines compared to healthy non-smokers (Culpitt et al. 2003; Cosio et al. 2004; Barnes 2009). It is possible that the similarity in CXCL8 response between non-smokers and patients with COPD is an effect of MDM being cultured in an external environment where they are not constantly exposed to inflammatory stimuli. The use of BAL macrophages from COPD patients maybe used to determine whether these cells are more sensitive to DEP-N exposure, as they would be acquired from an inflammatory environment.

MDM from smokers were resistant to DEP-N exposure with regards to CXCL8 release, when compared to cells obtained from non-smokers or patients with COPD. Even though statistical significance was not reached, the data herein showed that MDM from smokers were less susceptible to DEP-N stimulation. It is possible that MDM from smokers were ‘protected’ against exposure to noxious chemicals typically found in cigarettes by having augmented levels of antioxidant enzymes (McCusker & Hoidal, 1990).

Taken together, the data from this chapter reveal that DEP-N stimulated the release of CXCL8 in MDM from non-smokers, smokers and patients with COPD. Differences in response were observed in MDM from smokers, as this group was more resistant to DEP-N stimulation. Inert beads of different sizes, did not mediate similar effects, suggesting that the composition of DEP but not endotoxin was responsible for the release of CXCL8. For these reasons, the proposed hypothesis: 'Treatment of MDM with DEP will stimulate release of IL-6, TNFα and CXCL8, and the release of these mediators is more profound in MDM from patients with COPD' was not supported as only DEP-N and not SRM-1650B or SRM-2975 stimulated CXCL8 release and this effect was not greater in MDM from COPD patients.

Chapter 6:

Investigation of MAPK Signalling Pathways in DEP-Induced Cytokine Release

Chapter 6: Investigation of MAPK Signalling Pathways in DEP-Induced Cytokine Release

6.1 Introduction

The previous chapter (Chapter 5) established that DEP-N, but not SRM 1650B or SRM-2975 stimulated MDM release of CXCL8. This effect was observed in cells from non-smokers, smokers and patients with COPD. However, differences in the release of CXCL8 were observed in cells from smokers. In the present chapter the mechanism(s) associated with release of CXCL8 from DEP-N-treated MDM were examined.

DEP stimulates pulmonary cells to release pro-inflammatory mediators such as CXCL8, IL-6 and TNFα (Schwarze et al. 2013). Release of these mediators, is triggered by activation of signal transduction pathways or phosphorylation of the MAPK family. MAPK are serine/threonine protein kinases which direct extracellular signals to intracellular targets such as the transcription factor, NF-kB or AP.1, *via* interacting proteins to elicit appropriate biological responses (Hashimoto et al. 2000; Kawasaki et al. 2001). The MAPK family encompasses p38, ERK 1/2, and JNK pathways. p38 and JNK kinases are involved in the transmission of signals induced by environmental stress, heat or oxidative stress. p38 MAPK are sub-divided into four isoforms, namely p38α, p38β, p38γ or p38δ, of which p38α and p38δ are expressed in lung macrophages (Smith et al. 2006). In addition, the ERK 1/2 pathway is involved in directing mitogenic signals to intracellular targets (Chung 2011).

The composition of DEP is associated with generation of ROS in macrophages (Hiura et al. 1999). The main constituent of DEP involved in ROS production is the organic fraction which includes PAHs, nitro-PAHs and oxygenated PAHs (ketones, quinones and diones) (Li et al. 2002; Sagai et al. 1993; Kumagai & Taguchi 2007).

ROS generated by DEP are associated with MAPK signalling which leads to release of inflammatory mediators, for example, CXCL8. Methanol extraction of native DEP has shown that the organic extract and benzene components of DEP activate pathways leading to the phosphorylation of various MAPK in human airway epithelial and aortic endothelial cells (Bonvallot et al. n.d.; Tudhope et al. 2008; Li et al. 2009; Kawasaki et al. 2001). For this reason, it is hypothesised that 'DEP-N-treated MDM from patients with COPD will demonstrate, MAPK signalling leading to release of CXCL8'.

To examine this hypothesis, the following aims were investigated:

- Examine the phosphorylation of p38, ERK 1/2 and JNK in MDM treated with increasing concentrations of DEP-N.
- Examine the kinetics of DEP-N-induced phosphorylation of p38, ERK 1/2 and JNK, by conducting time course experiments.
- Examine the relationship between DEP-N induction of MAPK signalling pathways and CXCL8 release using MAPK inhibitors.
- Examine the effect of MAPK inhibitors and DEP-N treatment on MDM cell viability.

6.2 Methods

6.2.1 Treatment of MDM and Protein Collection for MAPK Analysis

In order to examine whether DEP-N induced MAPK phosphorylation in MDM, cells were treated with increasing concentrations of DEP-N and the phosphorylation of p38, ERK 1/2 and JNK was measured.

MDM were cultured in 24-well clear plates as described in Section 2.2.7.5 and treated with 500µl DEP-N (1-100µg/ml), cell culture media alone (non-stimulated control) or 10ng/ml LPS (positive control), and were incubated at 37°C, 5% ($^{V}/_{V}$) CO_2 for 1h. Following incubation, supernatants were removed and cells were immediately placed on ice. Cells were washed with 1ml ice-cold PBS followed by 15µl of 1X lysis buffer and were transferred to the MDM as described in section 2.2.13.1. Cell membranes were lysed and total protein was transferred to pre-chilled 0.5ml Eppendorf tubes. Lysates were stored at -80°C to limit protein degradation.

6.2.2 Time-Course of DEP-N on MAPK Phosphorylation

MDM were cultured in 24-well clear plates as described in section 2.2.7.6. MDM were incubated at 37°C, 5% ($^{V}/_{V}$) CO_2 in 500µl DEP-N for 0, 5, 10, 20, 40 and 60 min or LPS (10ng/ml) for 60 min. Following incubation, supernatants were removed and cells were immediately placed on ice. Cells were washed with 1ml of ice-cold PBS, followed by 15µl of 1x lysis buffer as described in Section 2.2.13.1. Cell membranes were lysed and total protein was collected using a cell scraper and transferred into pre-chilled 0.5ml Eppendorf tubes. Lysates were stored at -80°C to limit protein degradation

6.2.3 Western Blot

Total protein from cell lysates was measured using the BioRad assay as described in Section 2.2.13.2. Phosphorylation of MAPK protein by DEP-N or LPS in the concentration and time-course experiments were examined by western blot as described in Section 2.2.7.6. Blots were probed for the following MAPK: p38, ERK1/2 and JNK as described in section 2.2.13.6.

6.2.4 Effect of p38 (PF755616) Inhibiter on DEP-N induced HSP27 Phosphorylation

PF755616 (p38 inhibitor) was prepared in neat DMSO as described in Section 2.2.7.7. The p38 inhibitor was diluted by 1:10 serial dilutions to obtain a concentration range 10^{-5}–10^{-10} M. MDM were cultured in a 24-well clear plate and were pre-treated with 500µl of p38 inhibitor and incubated at 37°C, 5% ($^{V}/_{V}$) CO_2 for 30 min. Following pre-treatment, 10X DEP-N (100µg/ml) was pipetted into wells containing the p38 inhibitor and incubated at 37°C, 5% ($^{V}/_{V}$) CO_2 for 1h. Cells were then lysed as described in Section 2.2.13.1 and the downstream p38 MAPK signalling protein HSP27 was examined by western blot as described in section 2.2.13. Blots were probed for phosphorylated HSP27 as described in section 2.2.13.6.

6.2.5 Effect of MEK 1/2 (PD98059) Inhibitor on ERK 1/2 Phosphorylation

PD98059 (MEK 1/2 inhibitor) was prepared in neat DMSO as described in Section 2.2.7.8 to obtain a stock concentration of 30mM. The MEK 1/2 inhibitor was diluted 1:10 in RPMI 1650 cell culture media to obtain a working concentration of 30µM and then diluted appropriately to obtain a concentration range 0.1µM – 30µM. MDM were

pre-treated with 500µl 0.1mM - 30mM MEK 1/2 inhibitor and incubated at 37℃, 5% ($^{V}/_{V}$) CO_2 for 30 min. 500µl cell culture media was transferred to MDM (non-stimulated controls) and cells pre-treated with the MEK 1/2 inhibitor were further exposed to 10x DEP-N (100µg/ml) and incubated for 1h at 37℃, 5% ($^{V}/_{V}$) CO_2. Supernatants were removed and cells were immediately placed on ice and washed with 1ml ice-cold PBS. Cells were lysed as described in section 2.2.13.1 and western blots were probed for phosphorylated ERK 1/2 and total ERK 1/2 as described in Section 2.2.13.6.

6.2.6 Effect of p38 Inhibitor or MEK 1/2 Inhibitor on DEP-N Induced CXCL8 Release by MDM

Inhibitor compounds were prepared as described in Section 2.2.7.7 and 2.2.7.8. MDM were cultured in a 96-well black plate and were pre-treated with 150µl of the p38 or MEK 1/2 inhibitor and incubated for 1h at 37℃, 5% ($^{V}/_{V}$) CO_2.150µl of cell culture media (non-stimulated control) or DEP-N (100µg/ml) was transferred to cells with or without inhibitor pre-treatment; cells were incubated for 24h at 37℃, 5% ($^{V}/_{V}$) CO_2. Supernatants were collected and analysed for CXCL8 release by ELISA as described in Section 2.2.12.

6.2.7 Effect of p38 Inhibitor or MEK 1/2 Inhibitor of Cell Viability of MDM Treated with DEP-N

Viability of MDM treated with DEP-N with or without pre-treatment with inhibitors was assessed using the MTT assay as described in Section 2.2.10.1.

6.2.8 Statistics

Data were compared for statistical significance between subject groups by one-way ANOVA followed by Dunnett's test for multi-group comparisons. Data expressing a P value of <0.05, were considered to be statistically significant. Statistical differences were calculated using Prism V.5 (GraphPad, San Diego, USA).

6.3 Results

6.3.1 Effect of DEP-N on MAPK Phosphorylation

To determine whether DEP-N stimulated the MAPK pathway in MDM, cells were treated with increasing concentrations of DEP-N (1-100μg/ml) for 60 min and p38, ERK1/2 or JNK phosphorylation was measured.

DEP-N-treated (1-100μg/ml) MDM showed a trend to increase phosphorylation of p38 in a concentration-dependent manner in MDM from patients with COPD (Figure 6.1). Treatment of MDM with LPS (10ng/ml) increased phosphorylation of p38 in smokers only, but not in MDM from non-smokers or patients with COPD. A trend to increase phosphorylation of ERK 1/2 in a concentration-dependent manner, was also observed in MDM from non-smokers (10-100μg/ml) and patients with COPD (1-100μg/ml) although effects were not significant (Figure 6.2). MDM treated with LPS (10ng/ml) increased phosphorylation of ERK 1/2 (p44) in non-smokers and smokers. In contrast, DEP-N (1-100μg/ml) did not have any discernible effect on the phosphorylation of JNK in MDM, but did phosphorylate JNK in cells treated with LPS (10ng/ml), although effects were not significant (Figure 6.3). Since DEP-N induced phosphorylation of only p38 and ERK 1/2, examination of JNK was excluded from subsequent experiments.

6.3.2 Time Course of DEP-N on p38 and ERK 1/2 MAPK Phosphorylation

Having determined that MDM treated with DEP-N (100μg/ml) induced phosphorylation of p38 and ERK 1/2, the next step was to determine the kinetics of MAPK phosphorylation. Therefore, time-course exposure experiments were performed, whereby MDM were exposed to DEP-N (100μg/ml) for 0, 5, 10, 20, 40 or

60 min and p38 or ERK 1/2 phosphorylation was measured. LPS (10ng/ml) was used as a positive control. DEP-N induced maximal phosphorylation of p38 and ERK 1/2 at 40 min (Figure 6.4; Figure 6.5). MDM treated with LPS (10ng/ml) also induced phosphorylation of p38 and ERK 1/2 MAPK at 60 min.

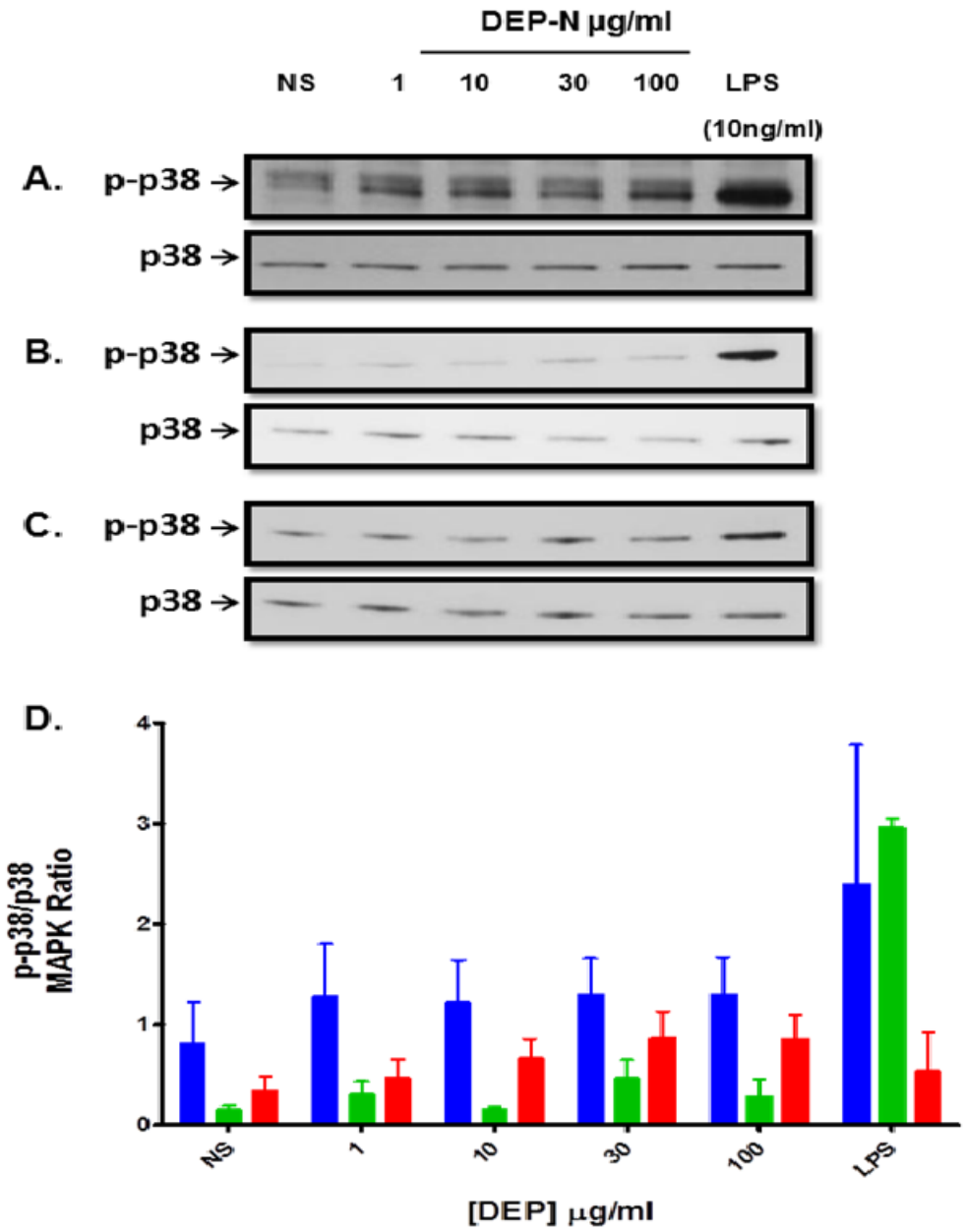

Figure 6.1 Effect of DEP-N on p38 Phosphorylation in MDM

MDM from non-smokers (■) (n=3), smokers (■) (n=2) and patients with COPD (■) (n=4; ex-smokers n=1, unknown n=3) were treated with increasing concentrations of DEP-N (1-100µg/ml) or LPS (10ng/ml) for 60 min and phosphorylation of p38 was determined by western blot. Blots of (A) non-smoker, (B) smoker and (C) COPD patients showing phosphorylated and total p38 MAPK. (D) Densitometry was used to measure the phosphorylation of p38 compared to non-stimulated controls. Data are mean ± SEM. No significant differences were found.

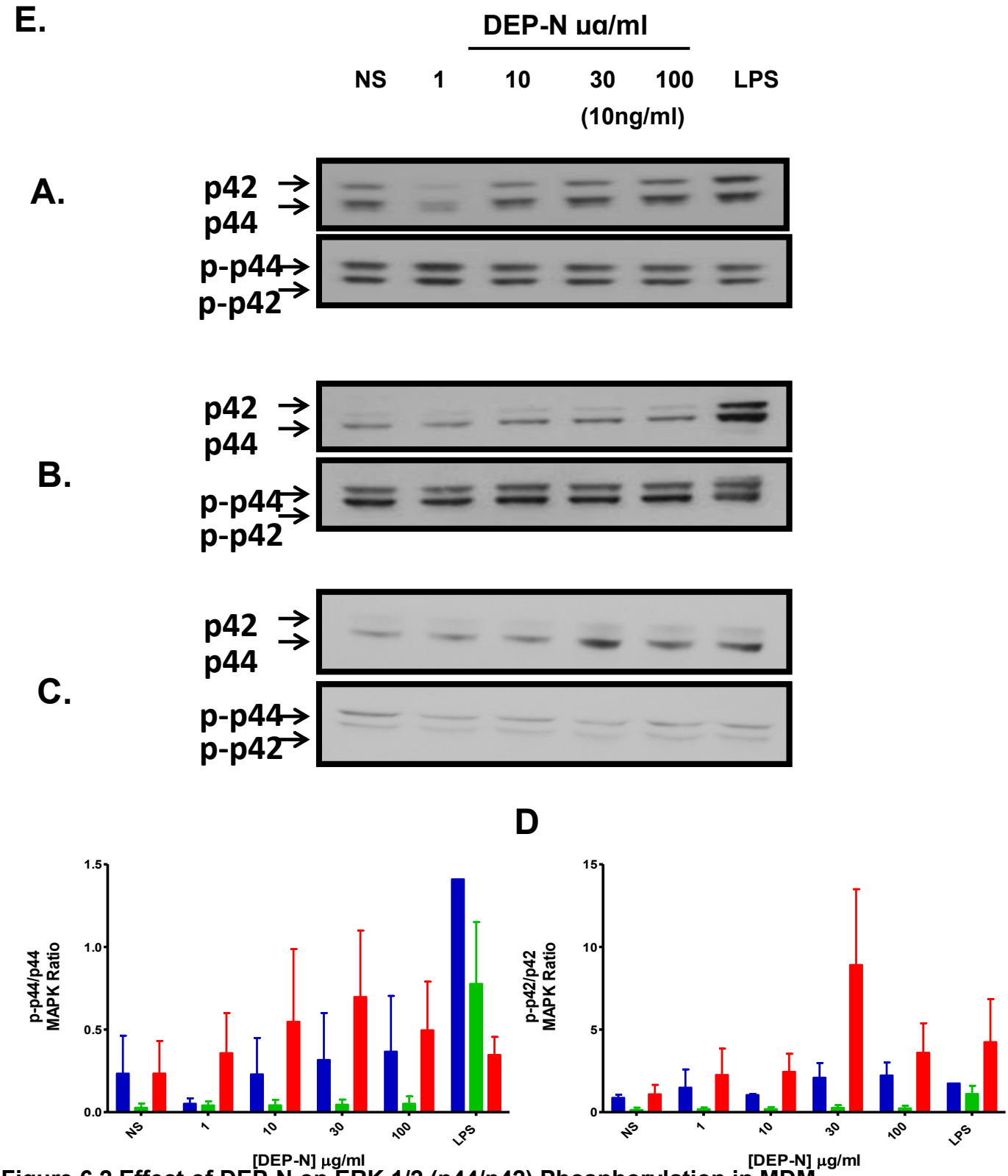

Figure 6.2 Effect of DEP-N on ERK 1/2 (p44/p42) Phosphorylation in MDM

MDM from non-smokers (■) (n=2), smokers (■) (n=2) and patients with COPD (■) (n=3; ex-smokers n=1; unknown n=2) were treated with increasing concentration of DEP-N (1-100µg/ml) or LPS (10ng/ml) for 60 min and the phosphorylation of p42/44 was determined by western blot. (A) Blots from non-smokers, (B) smokers or (C) patients with COPD showing phosphorylation of p44/p-p42 and total p44/p42. (B) Densitometry was used to measure the phosphorylation of (D) p-p44/p42 and (E) p-p42/p42 compared to non-stimulated controls. Data are mean ± SEM. No significant differences were found.

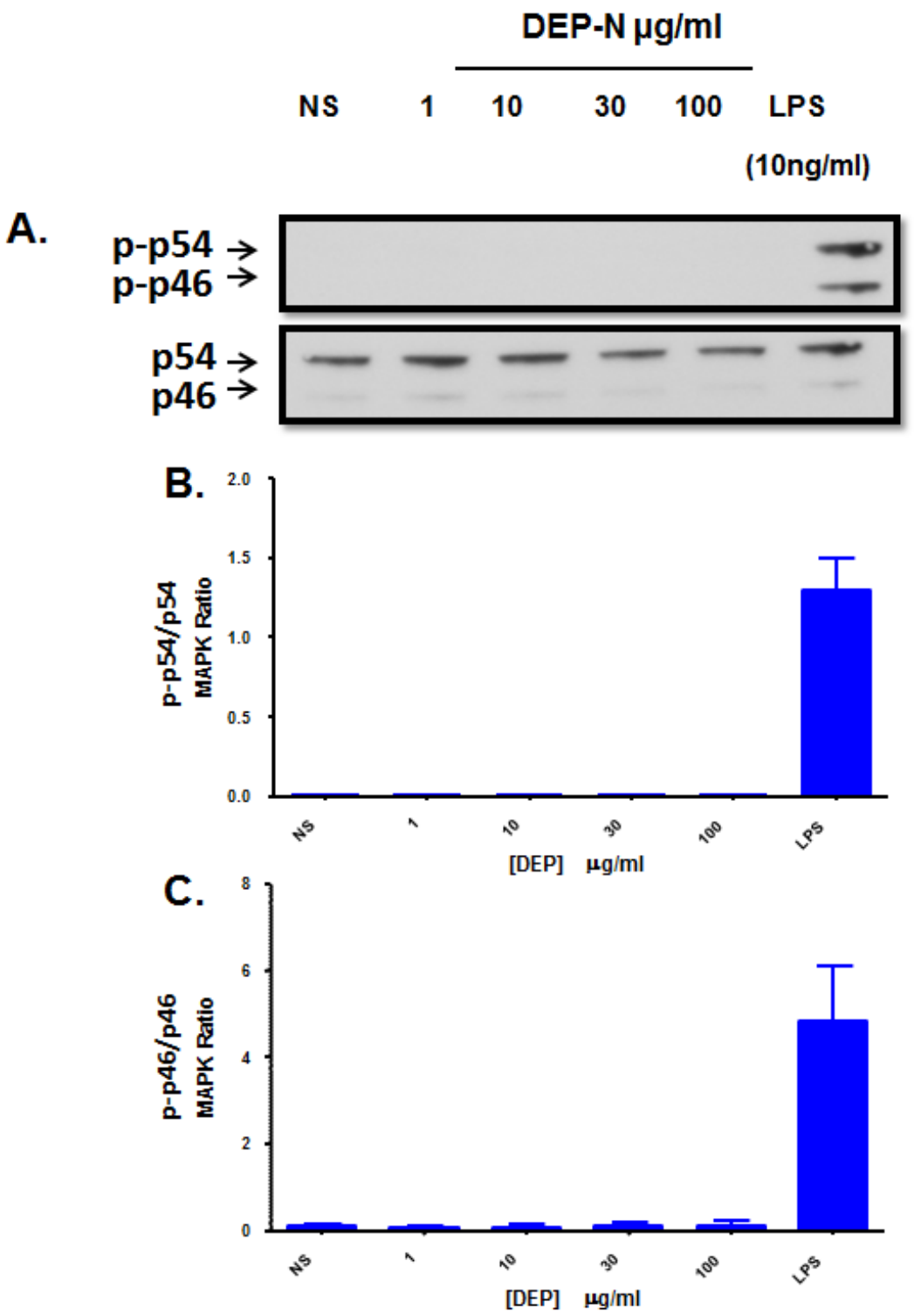

Figure 6.3 Effect of DEP-N on Phosphorylation of JNK (p54/p46)

MDM from smokers (■) (n=2) were treated with increasing concentration of DEP-N (1-100µg/ml) or LPS (10ng/ml) and the phosphorylation of p54/46 was determined by western blot. (A) Blot from smoker subject showing phosphorylation of p54/46 and total p54/46. (B) Densitometry was used to measure the phosphorylation of (B) p-p54/t-p54 and (C) p-p46/t-p46 compared to non-stimulated controls. Data are mean ± SEM.

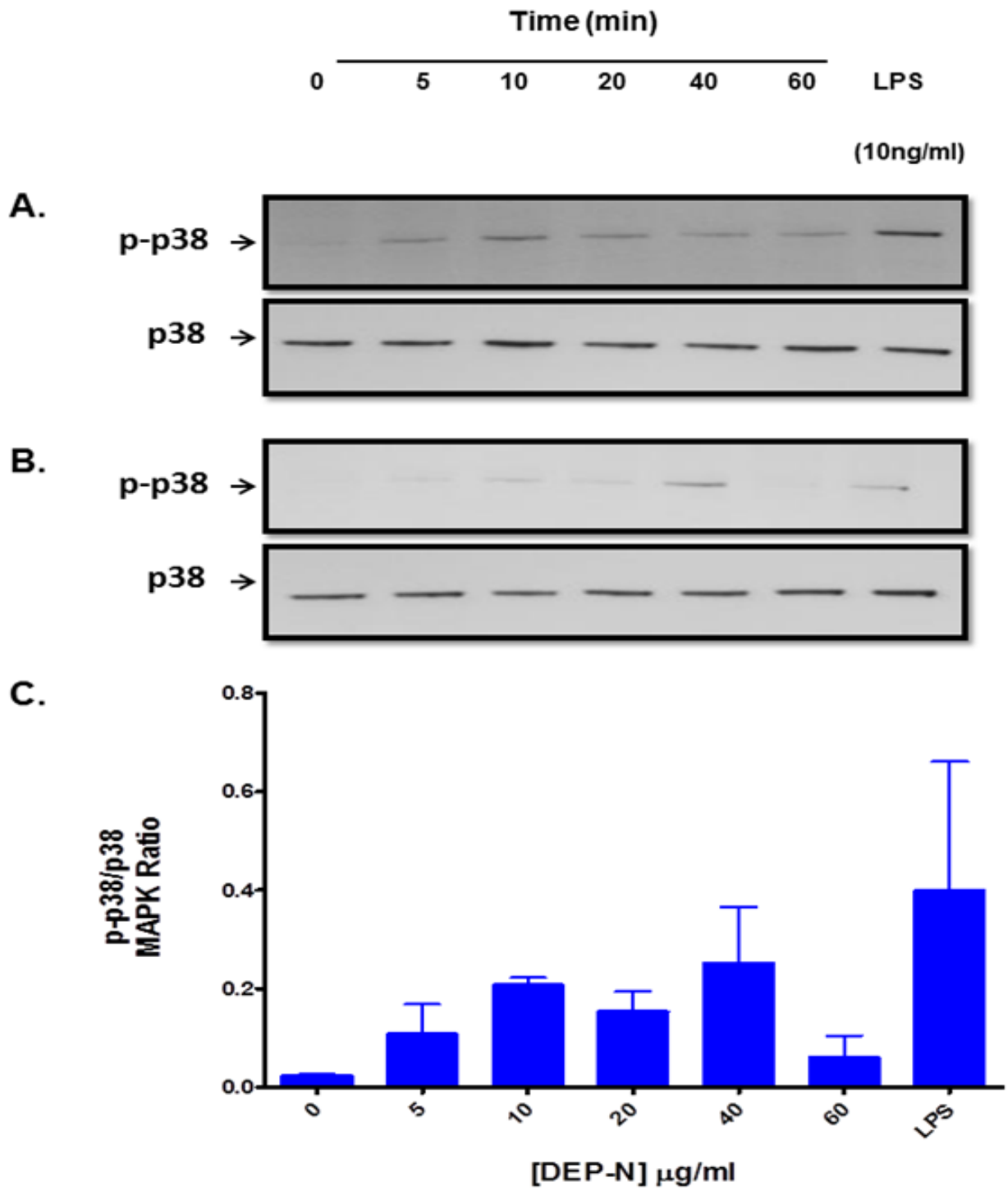

Figure 6.4 Effect of DEP-N on Kinetics of p38 Phosphorylation

The kinetics of p38 phosphorylation induced by DEP-N (100µg/ml) in MDM (■) (n=2) were determined by incubating cells at 5% ($^{V}/_{V}$) CO_2, 37℃ with DEP-N (100µg/ml) for 0, 5, 10, 20, 40 and 60 min. MDM treated with LPS (10ng/ml) were also incubated for 60 min. Phosphorylation of p38 by DEP-N-treated MDM was determined using western blot. Blots from a (A) non-smoker and (B) COPD patient showing phosphorylated and total p38. Densitometry was used to measure the phosphorylation of (C) p-p38/t-p38 compared to non-stimulated controls. Data are mean ± SEM.

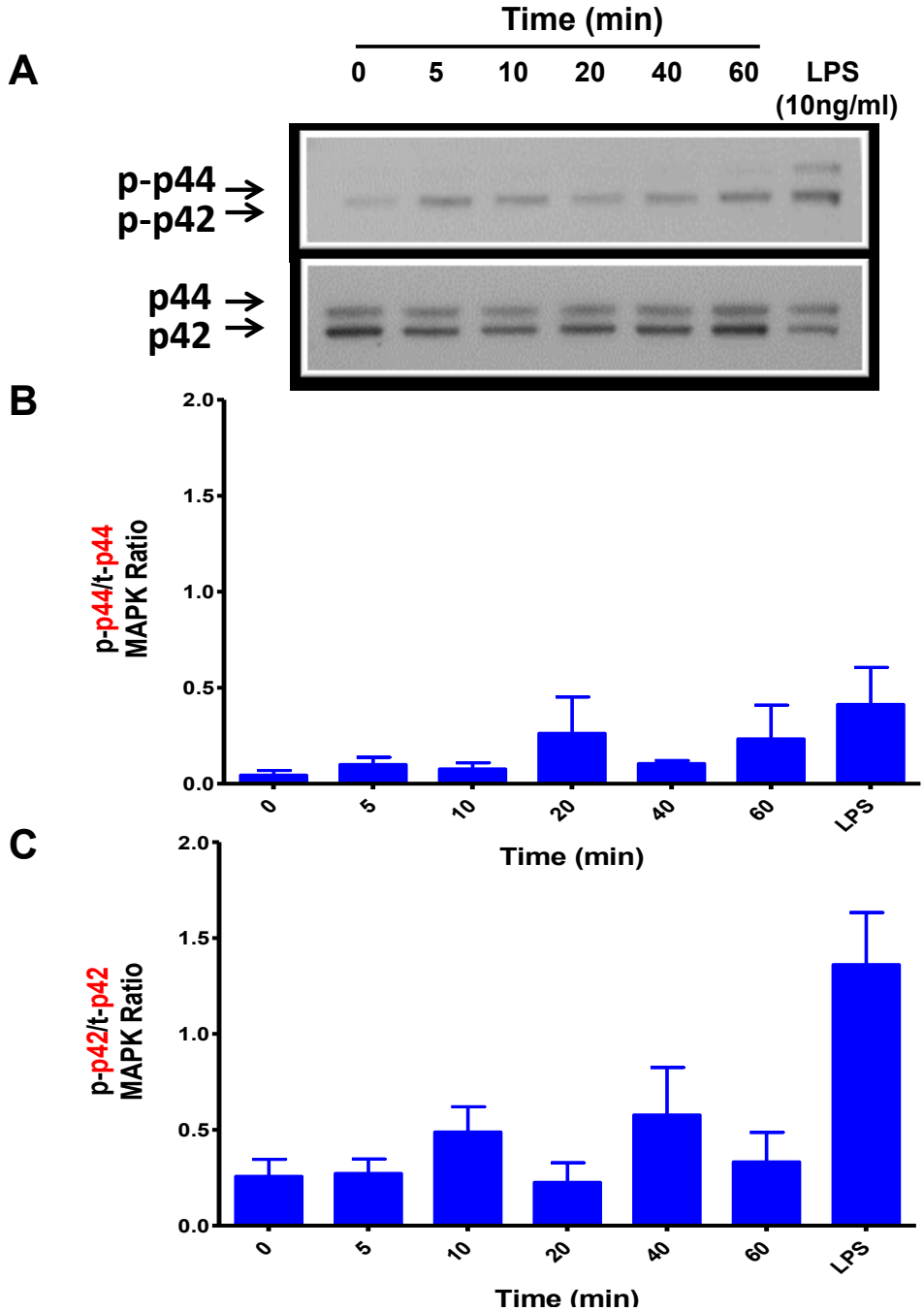

Figure 6.5 Effect of DEP-N on Kinetics of ERK 1/2 (p4/42) Phosphorylation

The kinetics of ERK 1/2 (p42/44) phosphorylation induced by DEP-N (100µg/ml), in MDM from COPD patients (■) (n=3; ex-smoker n=1, unknown n=2), were determined by incubating cells at 5% ($^{V}/_{V}$) CO_2, 37℃ with DEP-N (100µg/ml) for 0, 5, 10, 20, 40 and 60 min. MDM treated with LPS (10ng/ml) were also incubated for 60 min. Phosphorylation of (p42/44) by DEP-N treated MDM was determined using western blot. (A) Blots from a COPD patient showing phosphorylated and total p42/44. (B) Phosphorylation of p44 was normalised to total p44 and measured by densitometry. (C) Phosphorylation of p42 was normalised to total p42 and measured using densitometry. Data are mean ± SEM. *p<0.05. No significant differences were found.

6.3.3 Effect of a p38 Inhibitor (PF755616) on Phosphorylation of HSP27 in DEP-N-Treated MDM

To further determine whether DEP-N phosphorylates p38 to induce CXCL8 release, MDM were pre-treated with the p38 inhibitor, PF755616. Following pre-treatment, MDM were stimulated with DEP-N (100μg/ml) for 60 min and phosphorylation of HSP27 (downstream of p38) was assessed (Figure 6.6). DEP-N stimulated phosphorylation of HSP27 in MDM, and this signal was significantly inhibited at the highest concentration of PF755616 treatment in cells from patients with COPD (Figure 6.6). PF755616 pre-treated cells from non-smokers and smokers also showed a trend towards a concentration-dependent inhibition of HSP27 phosphorylation.

6.3.4 Effect of the p38 Inhibitor (PF755616) on DEP-N-Induced Release of CXCL8

Having determined that the PF755616 compound inhibited DEP-N induced p38 signalling, the next step was to determine whether this compound inhibited release of CXCL8 from DEP-N-treated MDM. Cells were pre-treated with the p38 inhibitor prior to stimulation with DEP-N and CXCL8 release was measured using ELISA.

DEP-N significantly induced CXCL8 release by MDM from smoker subjects and patients with COPD. DEP-N also increased the release of CXCL8 by non-smoker MDM, albeit not significantly (Figure 6.7A). PF755616 significantly inhibited release of CXCL8 in a concentration dependent manner by MDM from non-smokers, smokers and patients with COPD (Figure 6.7B). The reduction of CXCL8 release by MDM was not correlated with a reduction in cell viability (Figure 6.8). No difference was seen between MDM treated with DEP-N alone or with the p38 inhibitor and

DEP-N, with the exception of MDM from smokers pre-treated with 10^{-8} M of the PF75616 compound.

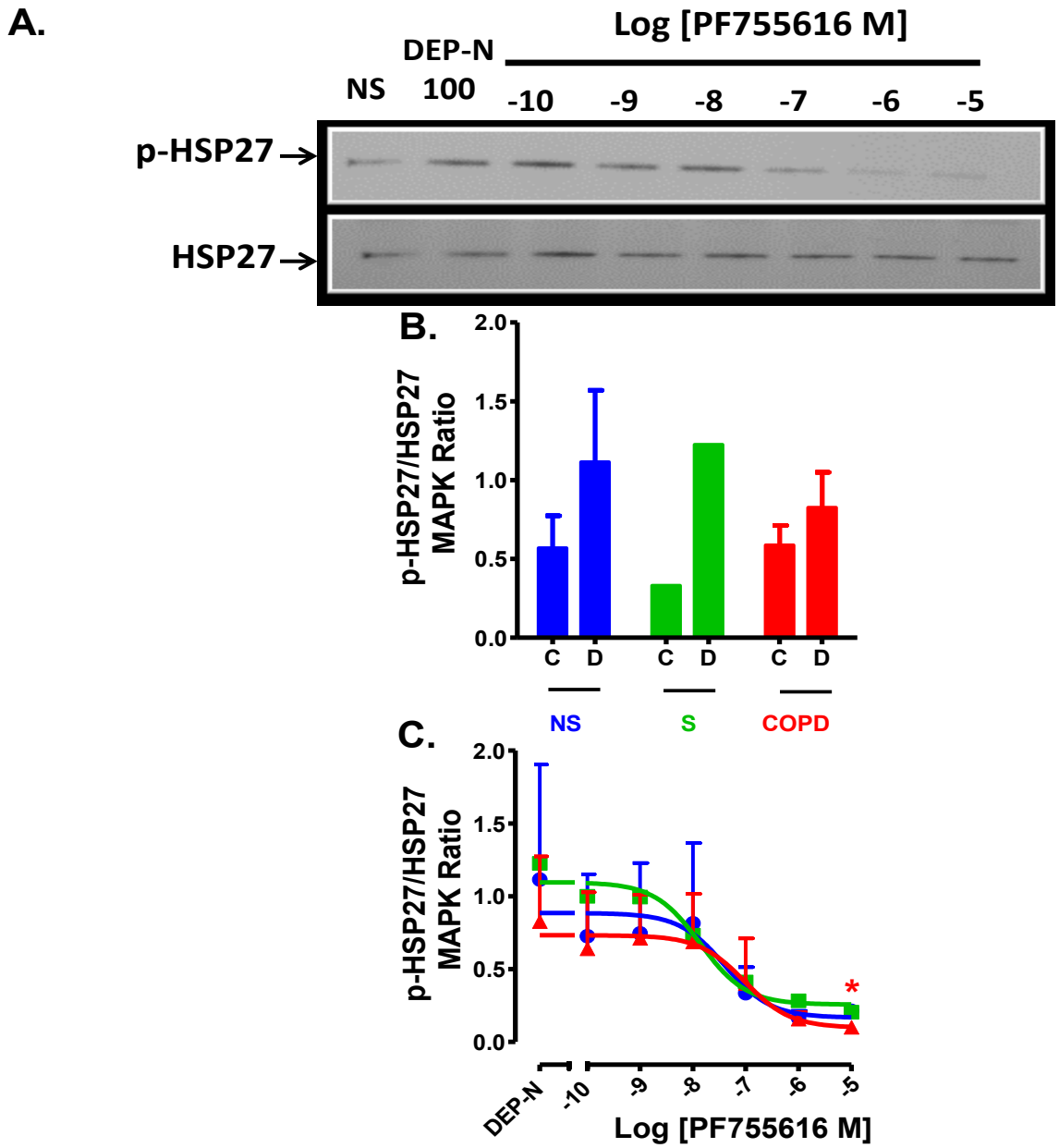

Figure 6.6 Effect of p38 Inhibitor on DEP-N Induced Phosphorylation of HSP27 in MDM

MDM from non-smokers (●) (n=3), smokers (■) (n=1) and patients with COPD (▲) (n=4; ex-smoker n=2, ex-smoker n=2) were pre-treated with increasing concentrations of the p38 inhibitor (PF755616) for 30 min. MDM were then exposed to DEP-N (100µg/ml) and incubated at 37°C, 5% ($^{V}/_{V}$) CO_2 for 1h. Following incubation, cells were lysed and phosphorylation of HSP27 was assessed. (A) Blots from a non-smoker subject showing phosphorylated and total HSP27. (B) Densitometry was used to measure phosphorylation of HSP27 in DEP-N-treated MDM (C = control and D= DEP-N). (C) Densitometry was also used to measure the effect of increasing concentrations of the p38 inhibitor on DEP-N phosphorylation of HSP27. Data are normalised to total HSP27 and are mean ± SEM. * $p<0.05$ *vs* DEP-

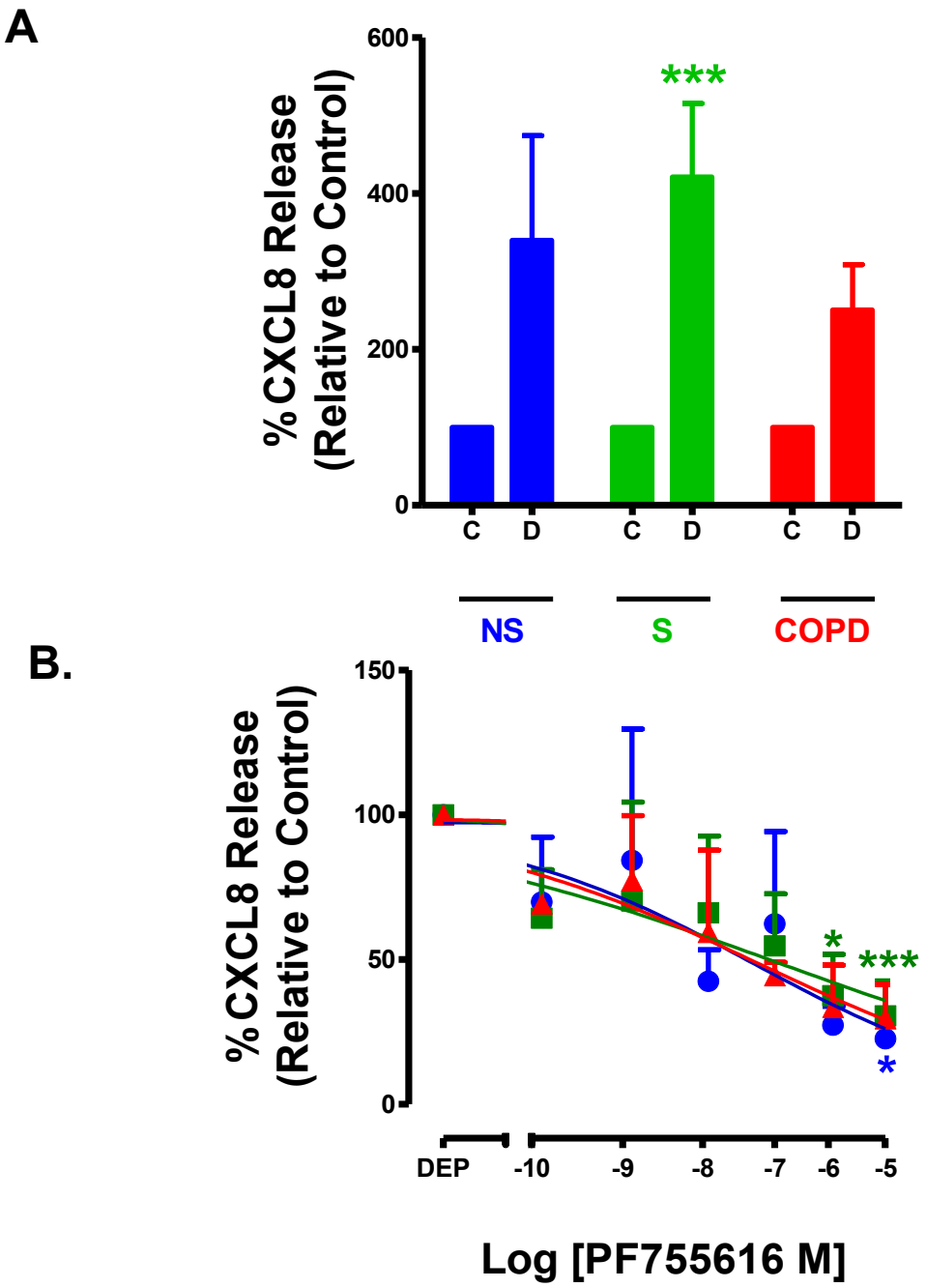

Figure 6.7 Effect of p38 Inhibitor on DEP-N-Induced Release of CXCL8 by MDM

MDM from non-smokers (■) (n=4), smokers (■) (n=7) and patients with COPD (■) (n=2; ex-smoker n=1; unknown n=1) were pre-treated with increasing concentrations of a p38 inhibitor (PF755616) and incubated 37℃, 5% ($^{V}/_{V}$) CO_2 for 1h. MDM were then exposed to DEP-N (100µg/ml) and incubated at 37℃, 5% ($^{V}/_{V}$) for 24h. Following incubation supernatants were collected and CXCL8 was measured by ELISA. (A) DEP-N stimulated release of CXCL8. (B) Release of CXCL8 from MDM pre-treated with the p38 inhibitor, followed by DEP-N stimulation, was inhibited in a concentration-dependent manner. Data are relative to controls and are mean ± SEM. *p<0.05, **p<0.01, ***p<0.001 *vs* DEP-N stimulation.

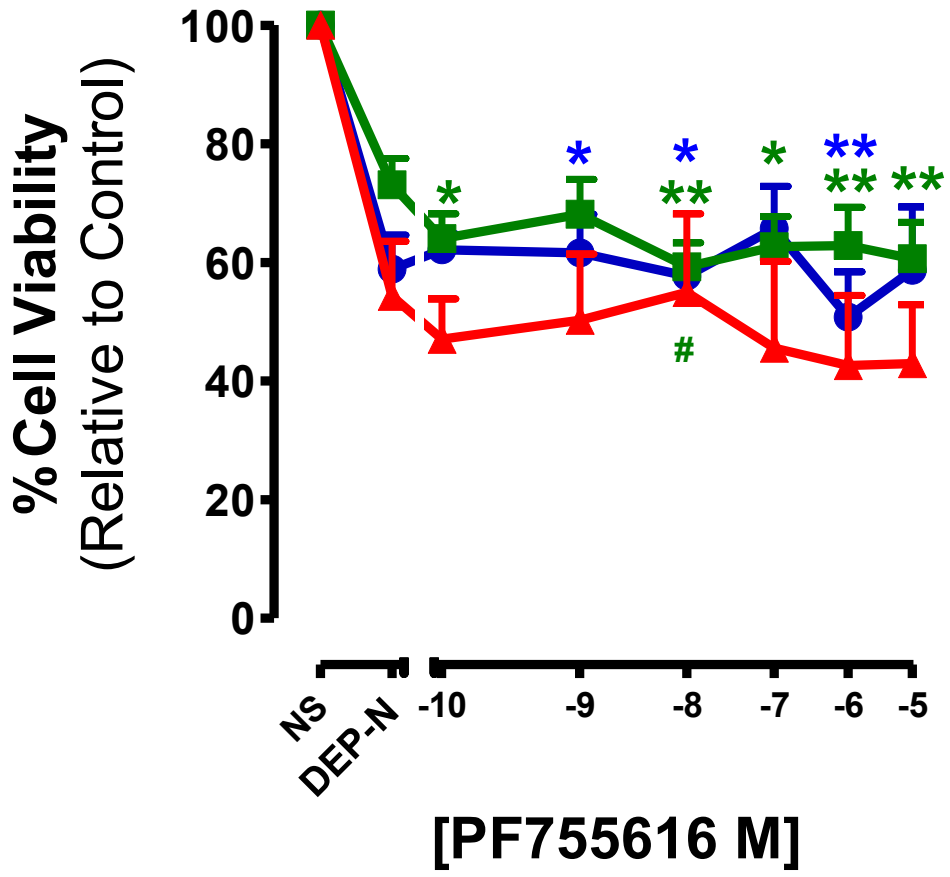

Figure 6.8 Effect of DEP-N and p38 Inhibitor on MDM Viability

MDM from non-smokers (■) (n=5), smokers (■) (n=6) and patients with COPD (■) (n=3; ex-smoker n=1, unknown n=2) were pre-treated with increasing concentrations of a p38 inhibitor (PF755616) and incubated 37℃, 5% ($^{V}/_{V}$) CO_2 for 1h. MDM were then exposed to DEP-N (100µg/ml) and incubated at 37℃, 5% ($^{V}/_{V}$) for 24h. Following incubation, supernatants were collected and cell viability was assessed by MTT assay. Cells were treated with MTT solution and incubated at 37℃, 5% ($^{V}/_{V}$) for 1h. Non-stimulated (NS) cells represented maximum cell viability (normalised data). Data are mean ± SEM of % cell viability (relative to control). *p<0.05, **p<0.01, ***p<0.001 *vs* NS controls, # p<0.05 *vs* DEP-N.

6.3.5 Effect of a MEK Inhibitor (PD98059) on Phosphorylation of ERK 1/2 in DEP-N-Treated MDM

To further determine whether DEP-N induced ERK 1/2 (p42/p44) MAPK phosphorylation, MDM were pre-treated with the MEK inhibitor PD98059 to inhibit the up-stream signalling protein MEK 1/2, thereby preventing the phosphorylation of ERK 1/2. Cells were pre-treated with the MEK 1/2 inhibitor prior to stimulation with DEP-N (100µg/ml) for 60 min and phosphorylation of ERK 1/2 measured (Figure 6.9). DEP-N stimulated ERK 1/2, albeit not significantly (Figure 6.9B), and this response showed a trend towards inhibition in concentration-dependent manner, in cells pre-treated with the MEK 1/2 inhibitor (Figure 6.9C, Figure 6.9D).

6.3.6 Effect of the ERK 1/2 inhibitor (PD98059) on DEP-N-Induced Release of CXCL8

Having determined that the MEK 1/2 inhibitor compound inhibited phosphorylation of ERK 1/2, the next step was to determine the effect of the inhibitor on CXCL8 release. Cells were pre-treated with the MEK inhibitor, followed by stimulation with DEP-N (100µg/ml) and release of CXCL8 was measured using ELISA.

DEP-N significantly induced CXCL8 release from all subject groups (Figure 6.10A). Pre-treatment of MDM with the MEK 1/2 inhibitor reduced CXCL8 release in a concentration-dependent manner, with no significant difference between MDM from non-smokers, smokers and patients with COPD (Figure 6.10B). The reduction of CXCL8 by MDM pre-treated with the MEK 1/2 inhibitor and DEP-N, was not an effect of reduced cell viability in MDM from non-smokers and smokers when compared to DEP-N alone. Viability of MEK 1/2 pre-treated cells from patients with COPD, was

significantly reduced compared to DEP-N alone at 10-30M, suggesting the combination of DEP-N and MEK 1/2 was killing the cells (Figure 6.11).

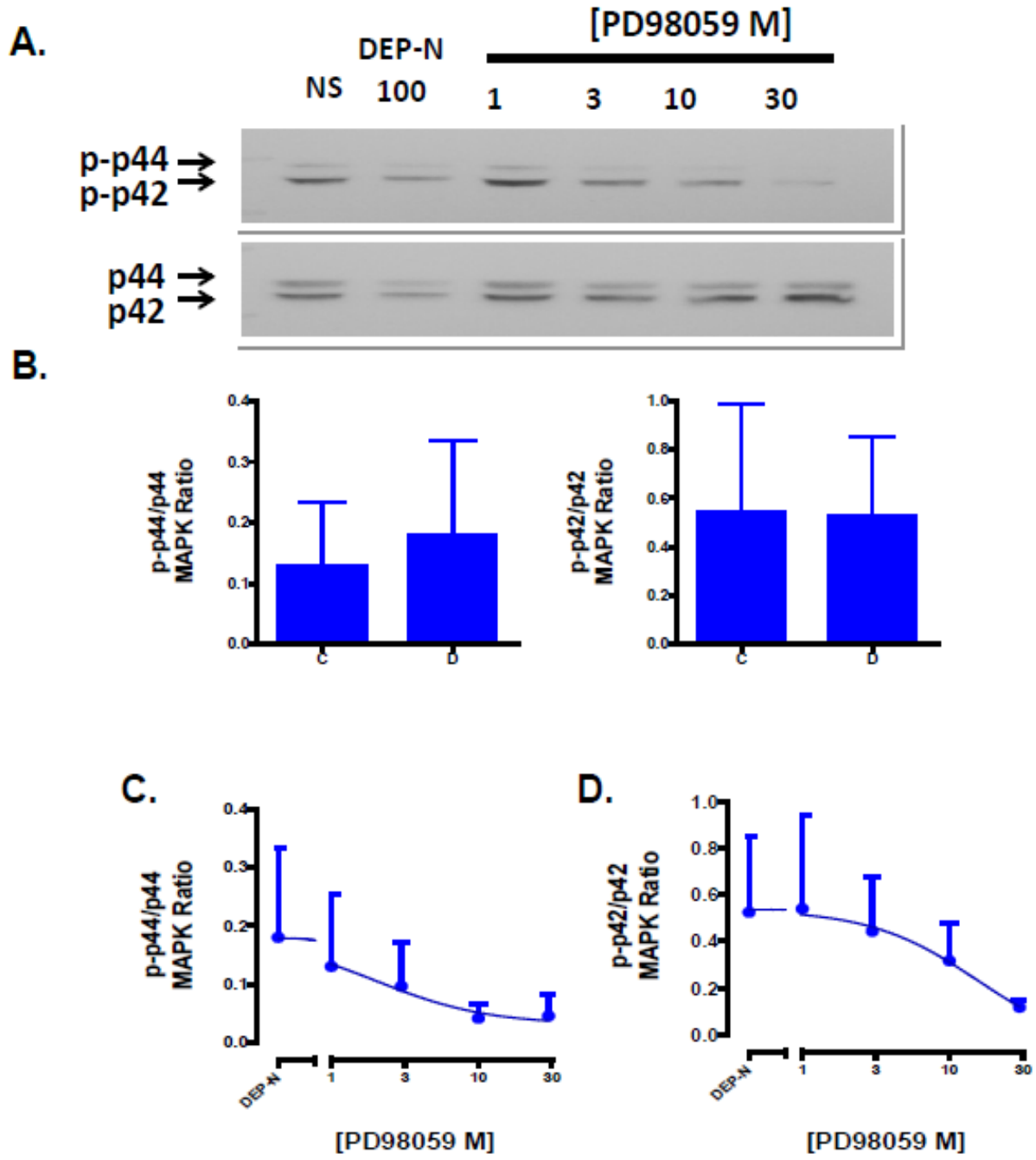

Figure 6.9 Effect of MEK 1/2 Inhibitor on DEP-N-induced Phosphorylation of ERK 1/2 (p44/p42) by MDM

MDM) were pre-treated with increasing concentrations of the MEK 1/2 inhibitor (PD98059) for 30 min (■) (n=3). MDM were then exposed to DEP-N (100µg/ml) and incubated at 37°C, 5% CO_2 ($^V/_V$) for 1h. Following incubation cells were lysed and phosphorylation of p42/44 was assessed. (A) Blots of phosphorylated and total p42/p44 from a COPD patient. (B) Densitometry was used to measure phosphorylation of p42/p44 by non-stimulated MDM (labelled as C) or cells treated with DEP-N (labelled as D). Densitometry was used to measure the effect of increasing concentrations of the MEK 1/2 inhibitor on DEP stimulation of (C) p44 (D) and p42. Data are normalised to total ERK 1/2 and data are mean ± SEM. No significant differences were found.

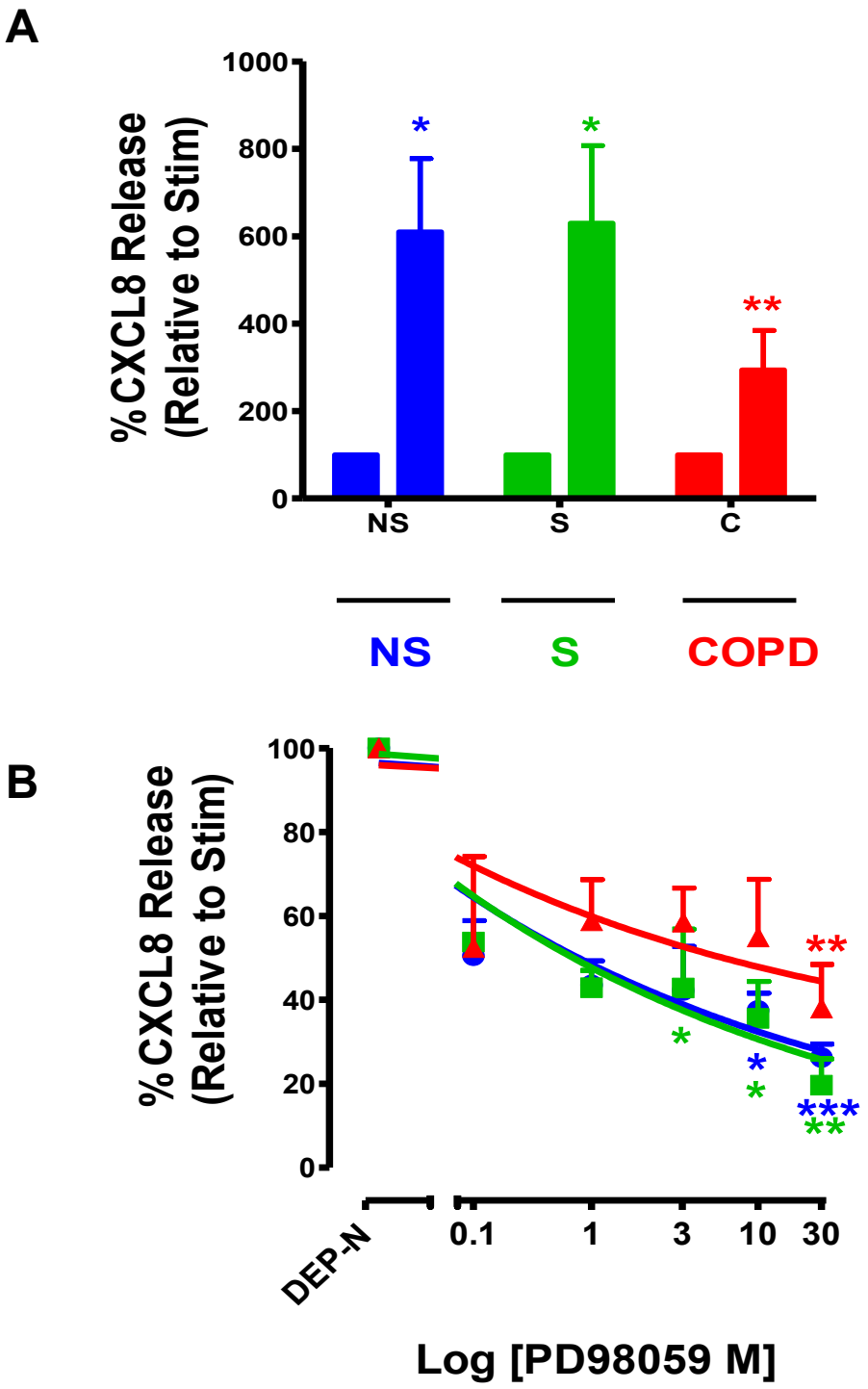

Figure 6.10 Effect of MEK 1/2 Inhibitor on DEP-N-Induced Release of CXCL8 by MDM

MDM from non-smokers (●) (n=5), smokers (■) (n=5) and patients with COPD (▲) (n=4; ex-smoker n=3, unknown n=1) were pre-treated with increasing concentrations of the MEK 1/2 inhibitor (PD98059) and incubated at 37℃, 5% ($^{V}/_{V}$) CO_2 for 1h. MDM were then exposed to DEP-N (100µg/ml) and incubated at 37℃, 5% ($^{V}/_{V}$) CO_2 for 24h. Following incubation, supernatants were collected and CXCL8 was measured by ELISA. (A) DEP-N stimulated release of CXCL8. (B) The release of CXCL8 induced by DEP-N was inhibited by MDM pre-treated with the MEK 1/2 inhibitor (0.1-30M). Data are relative to controls and are mean ± SEM. *p<0.05, **p<0.01, ***p<0.001 vs NS.

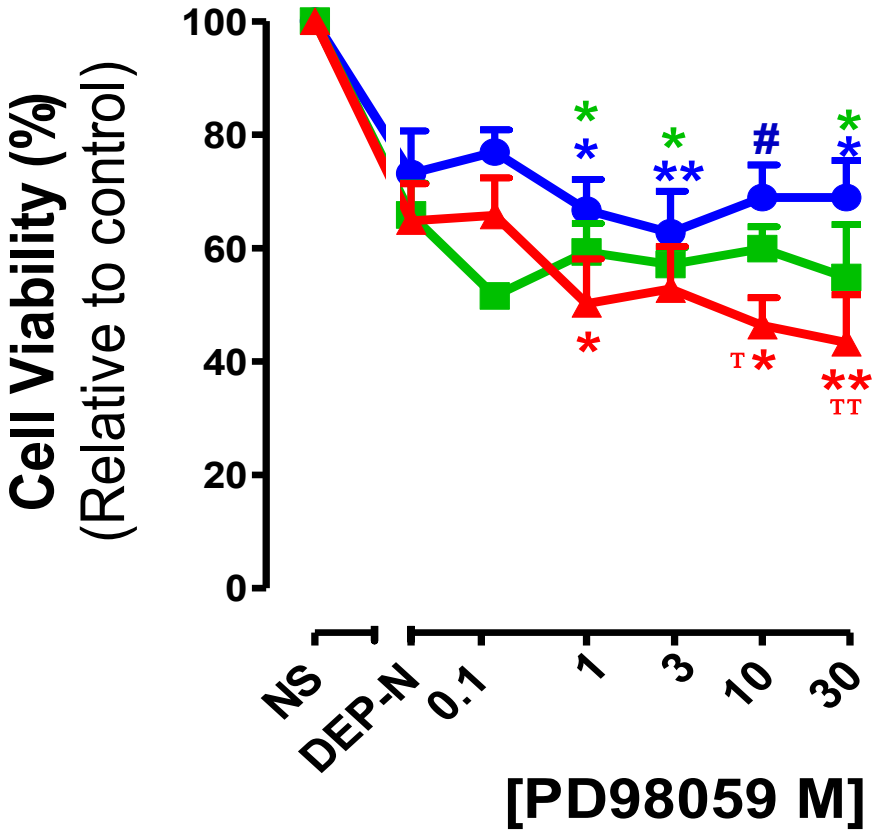

Figure 6.11 Effect of DEP-N and MEK 1/2 Inhibitor on MDM Viability

MDM from non-smokers (■) (n=5), smokers (■) (n=5) and patients with COPD (■) (n=4; ex-smoker n=3, unknown n=1) were pre-treated with increasing concentrations of a MEK inhibitor (PD98059) and incubated at 37°C, 5% ($^{V}/_{V}$) CO_2 for 1h. MDM were then exposed to DEP-N (100µg/ml) and incubated at 37°C, 5% ($^{V}/_{V}$) for 24h. Following incubation, supernatants were collected and cell viability was assessed by MTT assays. Cells were treated with MTT solution and incubated at 37°C, 5% ($^{V}/_{V}$) CO_2 for 1h. Non-stimulated (NS) cells represented maximum cell viability (normalised data). Data are expressed as mean ± SEM of % cell viability (relative to control). *p<0.05, **p<0.01, ***p<0.001 *vs* NS controls; # p<0.05 non-smokers *vs* COPD. ^{T}p<0.05, ^{TT}p<0.01 *vs* DEP-N.

6.4 Discussion

The previous chapter (Chapter 5) showed that DEP-N, but not SRM-1650B or SRM-2975, induced MDM to release CXCL8. The present chapter examined the mechanism of DEP-N induced CXCL8 release by MDM from non-smokers, smokers and patients with COPD. Cells were stimulated with DEP-N, and phosphorylation of JNK, p38 and ERK 1/2 kinases was examined.

DEP-N induced phosphorylation of p38 and ERK 1/2 but not JNK in MDM from non-smokers and COPD patients. This effect was not observed in MDM from smokers. Treatment of cells with DEP has been reported to release pro-inflammatory mediators by activating specific MAPK pathways. For example, DEP treatment of the murine JB6 P+ epidermal cell line, phosphorylated JNK but had no effect on p38 or ERK 1/2 (Ma et al. 2004), which is in contrast to the findings presented herein. Nonetheless, exposure of healthy volunteers to DEP resulted in phosphorylation of p38 and JNK, but not ERK 1/2 (Pourazer et al. 2008). The differential activation of MAPK by DEP may be associated with the complex composition of DEP. For example, the BEAS-2B bronchial epithelial cell line was exposed to different components extracted from DEP to determine activation of the CXCL8 gene. The benzene-constituent of DEP, activated p38 in a manner typically seen in cells treated with native DEP, thereby suggesting that the specific fractions of DEP composition are associated with phosphorylation of specific MAPK pathways (Kawasaki et al. 2001).

Although the composition of DEP is involved in driving phosphorylation of specific MAPK pathways, *in-vitro* studies have findings similar to the data presented herein.

For example, normal human bronchial epithelial cells (NHBEC) treated with ultrafine carbon particles, released CXCL8 *via* phosphorylation of p38 (Kim et al. 2005). Similarly, inhibition of p38 activity by the kinase inhibitor SB-202190 partially attenuated ultrafine carbon particle induced release of CXCL8 from NHBEC, thereby suggesting that p38 signalling is, at least in part, associated with CXCL8 production (Kim et al. 2005). Treatment of the THP.1 (monocyte) or RAW 264.7 (macrophage) cell lines with DEP extract also induced phosphorylation of p38 and JNK, further confirming the direct effects of DEP on macrophage functioning being associated with p38 signalling (Hiura et al. 1999).

MDM treated herein with increasing concentrations of DEP-N induced phosphorylation of p38 and ERK 1/2 pathways, although this effect was observed only in MDM from non-smokers or patients with COPD. MDM from smokers appeared less sensitive to DEP-N-induced phosphorylation of p38 and ERK 1/2. This finding reflects the data presented in Chapter 5, whereby MDM from smokers did not release similar levels of CXCL8 compared with cells from non-smokers or patients with COPD. This finding may be explained by the ROS generating capacity of DEP, on the induction of pro-inflammatory mediators (Schwarze et al. 2013). For example, it is reported that cigarette smoke exposure of primary lung macrophages or the THP.1 cell line, stimulates release of CXCL8 *via* phosphorylation of MAPK's (Birrell et al. 2008). These effects, may in part, be reversed by the antioxidant glutathione, thereby suggesting that ROS generated by DEP can be inhibited by antioxidants, thereby preventing MAPK activity and CXCL8 release. Therefore it is speculated that MDM from smokers herein, may have protective anti-oxidative mechanisms in place to clear excess ROS produced by DEP-N, thereby limiting p38 or ERK 1/2

stimulation. Nevertheless, the data suggests that the attenuated response to DEP-N by MDM from smokers is mediated upstream of p38 or ERK1/2 activation and is consistent with the reduced effect of DEP-N on CXCL8 release reported in Chapter 5. Whether this protective effect is mediated by anti-oxidants or another mechanism remains unclear but warrants further investigations.

Experiments herein investigating the kinetics of DEP-N induced phosphorylation of p38 and ERK 1/2 by time course experiments showed that maximal stimulation of p38 and ERK 1/2 was observed at 40 min. To confirm whether the trend observed for both MAPK were reproducible in cells from all subject groups, this experiment would need to be replicated.

DEP induces phosphorylation of p38 and ERK 1/2 kinases, which are involved in regulation of CXCL8 transcription factors such as NF-kB or AP.1. To determine whether p38 or ERK 1/2 signalling were involved in DEP-N -induced release of CXCL8, cells were pre-treated with either PF755616 (p38 inhibitor) or PD98059 (MEK 1/2 inhibitor) prior to exposure to DEP-N. Inhibition of both p38 and ERK 1/2 phosphorylation, resulted in similar levels of reduction in CXCL8 suggesting that the mechanism involving DEP-N induced CXCL8 release relies equally on p38 and ERK 1/2. However, it is of interest to determine which component of DEP-N is responsible for activating these kinases. Other studies have attempted to investigate this (Bonvallot et al. n.d.) For example, treatment of the 16HBE bronchial epithelial cell line with native DEP, organic extracts of DEP (OE-DEP), stripped DEP (SDEP) or carbon black (CB) particles resulted in only some components activating phosphorylation of MAPK (Bonvallot et al. n.d.). Cells treated with OE-DEP or native DEP activated the ERK 1/2 and p38 pathways. However, pre-treatment of cells with

the SB203580 p38 inhibitor reduced p38 phosphorylation but did not reduce cytokine release; thereby suggesting that other signalling pathways may be involved (Bonvallot et al. n.d.). To determine which components of DEP-N activate the p38 or ERK 1/2 kinase pathways, particles could be stripped of their surface-bound organic or metal fractions using methanol or metal chelators (i.e. EDTA) respectively. Effects between stripped and non-stripped particles on p38 or ERK 1/2 kinase pathways can then be examined by the Western blot technique.

In summary, the present chapter found that DEP-N stimulated p38 and ERK 1/2 but not JNK pathways in MDM from non-smokers and COPD patients but not cells from smokers. These two MAPK signalling pathways appear to be involved in release of CXCL8, as determined by inhibiting p38 or ERK 1/2, leading to CXCL8 release. However, because of the low ‘n’ of experiments, these investigations require further examination. Findings from the present chapter support the hypothesis that 'DEP-N treated MDM from patients with COPD will phosphorylate MAPK signalling pathways leading to MDM release of CXCL8'.

Chapter 7:

Effect of DEP on MDM Phagocytosis

7.1 Introduction

The results presented in Chapters 5 and 6 showed that DEP-N, but not SRM-1650B or SRM-2975, stimulated MDM release CXCL8 by MAPK pathways in cells from non-smokers and patients with COPD. This differential effect of the DEP appeared to be associated with composition of particles rather than size. The next step was to determine whether DEP-N, SRM-1650B or SRM-2975 had effects on any other macrophage functions therefore, the effect on phagocytosis was examined.

Inhaled DEP are targets for alveolar macrophages and may therefore, influence the capacity of macrophages to phagocytose other inhaled particles or pathogens in the lung. DEP impair phagocytosis in primary human and murine macrophages, and also macrophage cell lines (Zhou & Kobzik 2007; Lundborg et al. 2006; Yang et al. 2001). Impairment of phagocytosis may be related to the internal volume occupied by DEP, thereby inhibiting the macrophages from internalizing any further particles (Morrow et al. 1988; Tran et al. 2000). DEP also compromise the integrity of the macrophage cytoskeleton by inducing endogenous ROS. The macrophage cytoskeleton is sensitive to oxidative stress due to the presence of thiol groups leading to oxidation of cytoskeleton proteins. Cytoskeleton dysfunction impairs phagocytosis of particles and bacteria, thereby perpetuating inflammation and susceptibility to respiratory infections (Castranova et al. 2001; Möller et al. 2005; Yang et al. 2001; Li et al. 2010).

Macrophages treated with DEP of fine (<2.5μm) or ultrafine particles (<0.1μm) diameters, have elevated ROS production (Li et al. 2003). The large surface area of DEP may catalyse chemical reactions, thereby inducing ROS production, leading to oxidation of the cyotoskeleton proteins in macrophages. In addition, ultrafine

particles are not internalised by phagocytosis, and are thereby are not digested in phagolysosomes, but are retained in the cytoplasm. Retention of ultrafine particles may cause the macrophages to become replete, which prevents further ingestion of inhaled particles (Morrow et al 1988). It is unknown if impaired phagocytosis is a generic effect of DEP size or whether composition of particles may be driving this response. Therefore, examination herein of the three different DEP samples on MDM phagocytosis will be compared to MDM treated with inert beads of different sizes.

Airways are normally cleared of inhaled particles or debris by alveolar macrophages, however, in COPD macrophage phagocytosis is defective (Taylor et al. 2010; Hodge et al. 2003; Hodge et al. 2007; Berenson et al. n.d.; Donnelly & Barnes 2012) for this reason it is hypothesised that 'DEP-N, SRM-1650B or SRM-2975-treated MDM from patients with COPD will further reduce phagocytosis of fluorescent beads, compared to MDM from non-smokers or smokers'.

To examine this hypothesis, the following aims were investigated:

- Determine the effect of DEP-N, SRM-1650B or SRM-2975 on MDM phagocytosis of fluorescent beads by light microscopy.
- Determine the effect of DEP-N, SRM-1650B or SRM-2975 on MDM phagocytosis of fluorescent beads by fluorimetry.
- Examine the combination of DEP-N, SRM-1650B or SRM-2975 and fluorescent beads on MDM cell viability.
- Examine the internalisation of DEP-N-treated MDM on the phagocytosis of fluorescent beads using confocal microscopy.

- Determine the effect of 0.2μm, 10μm or 30μm sized inert beads on MDM phagocytosis of fluorescent beads by light microscopy.
- Determine the effect of 0.2μm, 10μm or 30μm sized inert beads on MDM phagocytosis of fluorescent beads by fluorimetry.
- Examine the combination of 0.2μm, 10μm or 30μm and fluorescent beads on MDM cell viability.

7.2 Methods

7.2.1 Isolation of PBMC

PBMC were isolated from whole blood obtained from non-smokers, smokers and patients with COPD (Section 2.2.2). Cells were cultured in MDM complete media (RPMI-1640, containing 10% ($^{V}/_{V}$) FCS, 10mg/ml (1% ($^{V}/_{V}$)) penicillin/streptomycin (PS), 2mM (1% ($^{V}/_{V}$)) L-glutamine) and seeded onto a 96-well black plate ($1x10^{5}$ cells/well). PBMC were incubated for 2h at 37°C, 5% ($^{V}/_{V}$) CO_2 to isolate monocytes by adherence to the plastic tissue culture plate. Monocytes were cultured in MDM complete media containing 2ng/ml GM-CSF and incubated for a further 12 days at 37°C, 5% ($^{V}/_{V}$) CO_2 to differentiate to MDM (section. 2.2.3).

7.2.2 Treatment of MDM with DEP-N, SRM-1650B or SRM-2975

DEP-N, SRM-1650B or SRM-2975 were suspended in warmed HBSS to obtain a stock concentration of 30mg/ml. DEP were sonicated for 2 min to break up large aggregates and were diluted in RPMI-1640 serum-free cell culture media to obtain the concentrations of 1-100µg/ml. MDM were treated with DEP and incubated for 24h at 37°C, 5% ($^{V}/_{V}$) CO_2. MDM incubated in media alone were used as baseline controls (Section 2.2.7.2).

7.2.3 Treatment of MDM with Inert Beads

0.2µm, 10µm and 30µm sized inert beads were re-suspended in 10X D-PBS to obtain a stock concentration of 30mg/ml. Beads were sonicated for 2 min to break up aggregates. The beads were diluted in RPMI-1640 serum-free cell culture media, to concentrations of 1-100µg/ml. MDM were treated with 1-100µg/ml inert beads and

incubated for 24h at 37°C, 5% ($^{V}/_{V}$) CO_2. MDM incubated in media alone were used as baseline controls (section 2.2.7.1).

7.2.4 Imaging of DEP- or Inert Bead-Treated MDM Incubated With Fluorescent Beads

DEP-or inert bead (1-100µg/ml)-treated MDM were incubated with fluorescent beads (phagocytic prey) and viewed under an inverted light microscope using a fluorescent lamp. Images were captured using an Olympus SLR camera fitted with a microscope compatible adaptor (Section 2.2.9.3).

7.2.5 Phagocytosis Assay

DEP-or inert bead (1-100µg/ml)-treated MDM were incubated at 37°C, 5% ($^{V}/_{V}$) CO_2 for 24h. Cells were then further exposed to 100µl fluorescent beads ($50x10^6$ beads/ml) and incubated for 4h at 37°C, 5% ($^{V}/_{V}$) CO_2 (Section 2.2.7.9). Following incubation, cells were washed with PBS and extracellular fluorescence was quenched with 1% ($^{V}/_{V}$) trypan blue for 2 min. Trypan blue was aspirated and phagocytosis of fluorescent beads by DEP-or inert bead-treated MDM was analysed by fluorimetry (Section 2.2.7.9.1).

7.2.6 Confocal Microscopy

PBMC ($2X10^5$ cells/well) were seeded onto 8-well chamber slides and incubated for 12d in the presence of GM-CSF to allow cells to fully differentiate into MDM (section 2.2.3). Cells were treated with DEP-N (1-100µg/ml) and incubated for 24h at 37°C, 5% ($^{V}/_{V}$) CO_2. Non-stimulated cells cultured in media were used as controls. DEP-N-treated MDM were incubated with fluorescent beads for 4h at 37°C, 5% ($^{V}/_{V}$) CO_2 (section 2.2.7.9). Cells were fixed by incubation in 4% ($^{W}/_{V}$) paraformaldehyde (PFA)

for 10 min at RT. The cell nuclei were stained with 2μM DAPI and incubated for 3 min at RT and the cytoplasm of cells was stained using 12.5mM Cell Tracker^{TM} Red. Chambers were removed from the slide and coverslips were affixed over the cells using citifluo and sealed with clear nail varnish. Slides were stored in the dark at 4°C (section 2.2.9.5.2).

7.2.7 Cell Viability

Viability of MDM treated with DEP or inert beads and incubated with fluorescent beads was assessed using the MTT assay (section 2.2.8.1).

7.2.8 Statistics

Data were compared for statistical significance between subject groups by one-way ANOVA followed by Dunnett's test for multi-group comparisons. Data with a P value of <0.05, were considered to be statistically significant. Statistical analysis was performed using Prism V.4 and V.5 (GraphPad, San Diego, USA).

7.3 Results

7.3.1 Imaging the effect of DEP-N, SRM-1650B or SRM-2975 on MDM Phagocytosis of Fluorescent Beads

One of the major functions of macrophages is to clear particles and debris; however, it is unknown whether cells which have been previously exposed to DEP still retain their ability to clear phagocytic prey. To examine this possibility, MDM treated with increasing concentrations of the three samples of DEP (1-100μg/ml) were further exposed to fluorescent beads, and phagocytic capacity was assessed by fluorescent microscopy. MDM that had not been previously exposed to DEP were the baseline controls.

DEP-N (Figure 7.1), SRM-1650B (Figure 7.2) or SRM 2975 (Figure 7.3) reduced phagocytosis of fluorescent beads by MDM from non-smokers, smokers and patients with COPD in a concentration-dependent manner compared to unexposed controls. At the higher concentration of DEP, large aggregates of particles could be observed within the MDM, with markedly reduced number of fluorescent beads.

7.3.2 Determining the effect of DEP-N, SRM-1650B or SRM-2975-Treated MDM on the Phagocytosis of Fluorescent Beads by Fluorimetry

Images taken using fluorescent microscopy showed that DEP-laden MDM displayed reduced phagocytosis of fluorescent beads (section 7.3.1). Fluorimetry was next used to validate these analyses, by measuring the fluorescence emitted by DEP (1-100μg/ml)-treated MDM, incubated with fluorescent beads. Base-line phagocytosis was determined in MDM not exposed to DEP but with fluorescent beads alone. DEP-N-treated MDM showed significantly reduced phagocytosis of fluorescent beads in

MDM from non-smokers, smokers and patients with COPD at the highest concentration of treatment (100µg/ml) (Figure 7.4A).

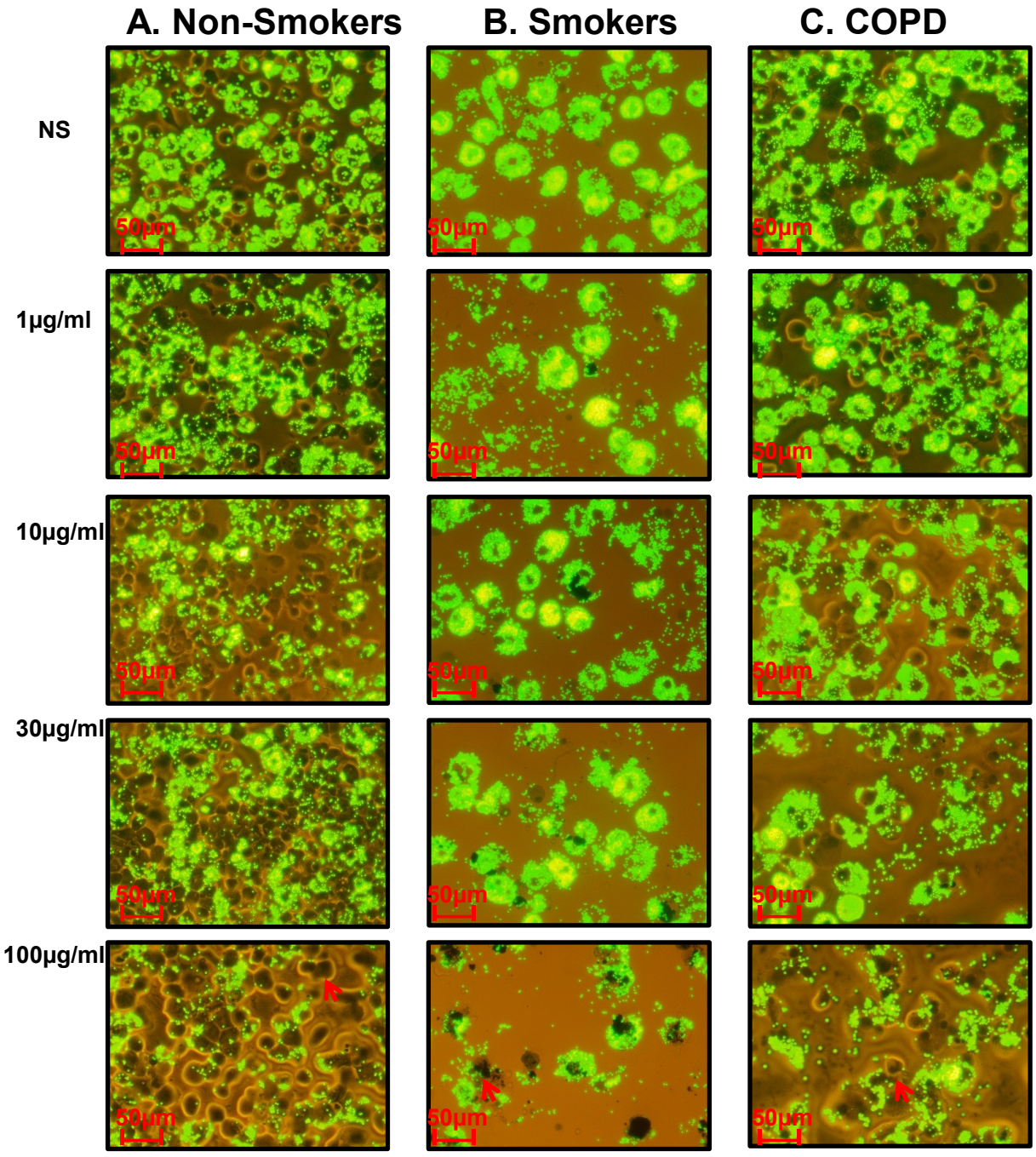

Figure 7.1. Effect of DEP-N on MDM Phagocytosis of Fluorescent Beads
DEP-N-treated MDM (1-100µg/ml) from Non-smokers (A), Smokers (B) and COPD (C) patients were incubated with fluorescent beads ($50x10^6$ beads/ml) for 4h. Non-stimulated (NS) cells were used as baseline controls and represented maximum phagocytosis by the different subject groups. A reduction in fluorescent beads (green) with increasing concentrations of DEP-N was observed in MDM from all subject groups. Red arrows indicate DEP-N-laden MDM. Cells were viewed by fluorescent microscopy and images were taken at X 20 magnification.

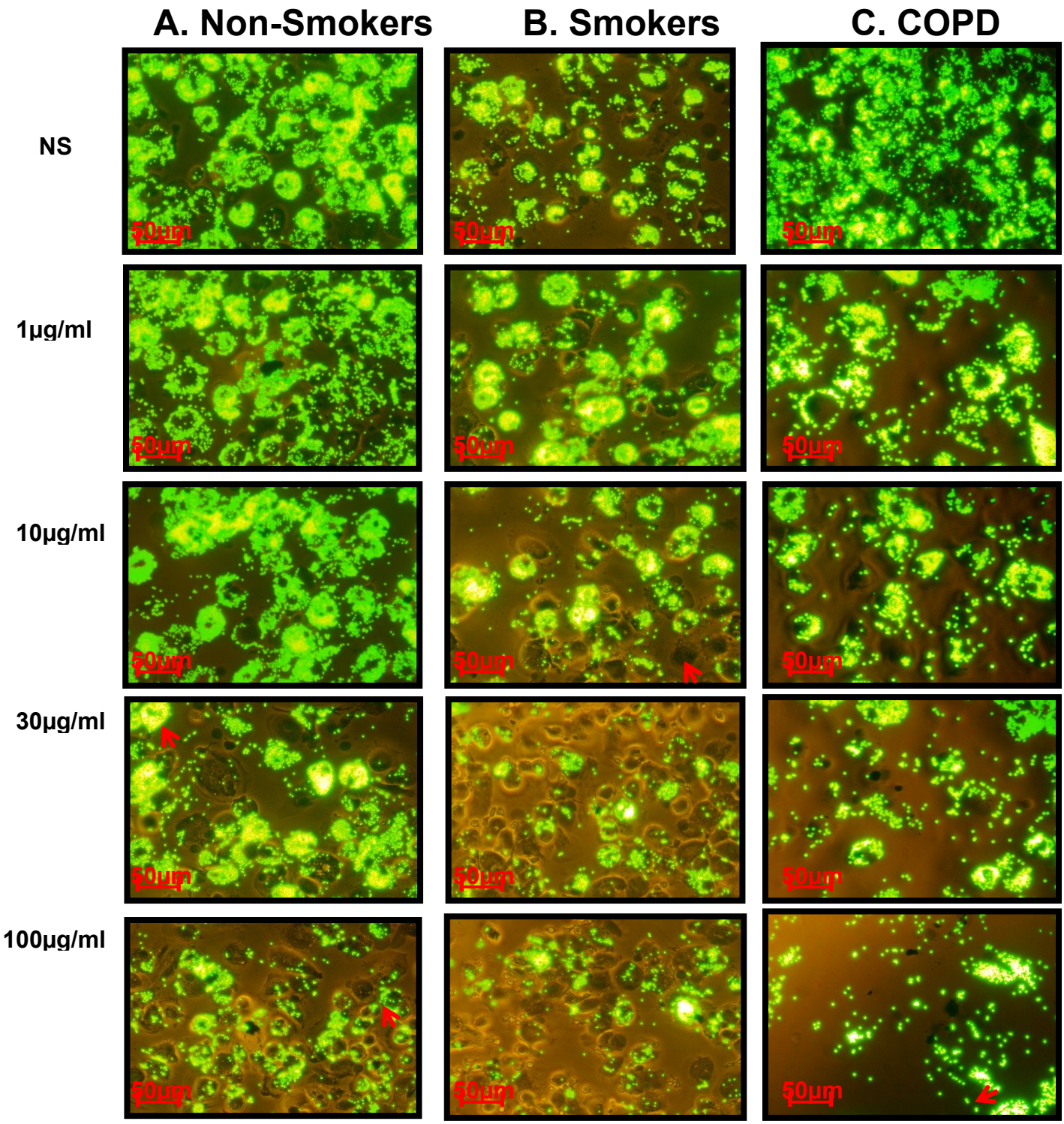

Figure 7.2 Effect of SRM-1650B on MDM Phagocytosis of Fluorescent Beads

SRM-1650B-treated MDM (1-100µg/ml) from Non-smokers (A), Smokers (B) and COPD (C) patients were incubated with fluorescent beads ($50x10^6$ beads/ml) for 4h. Non-stimulated cells were used as baseline controls (control) and represented maximum phagocytosis by the different subject groups. A reduction in fluorescent beads (green) with increasing concentrations of SRM-1650B was observed in MDM from all subject groups. Red arrows indicate SRM-1650B-laden MDM. Cells were viewed by fluorescent microscopy and images were taken at X 20 magnification.

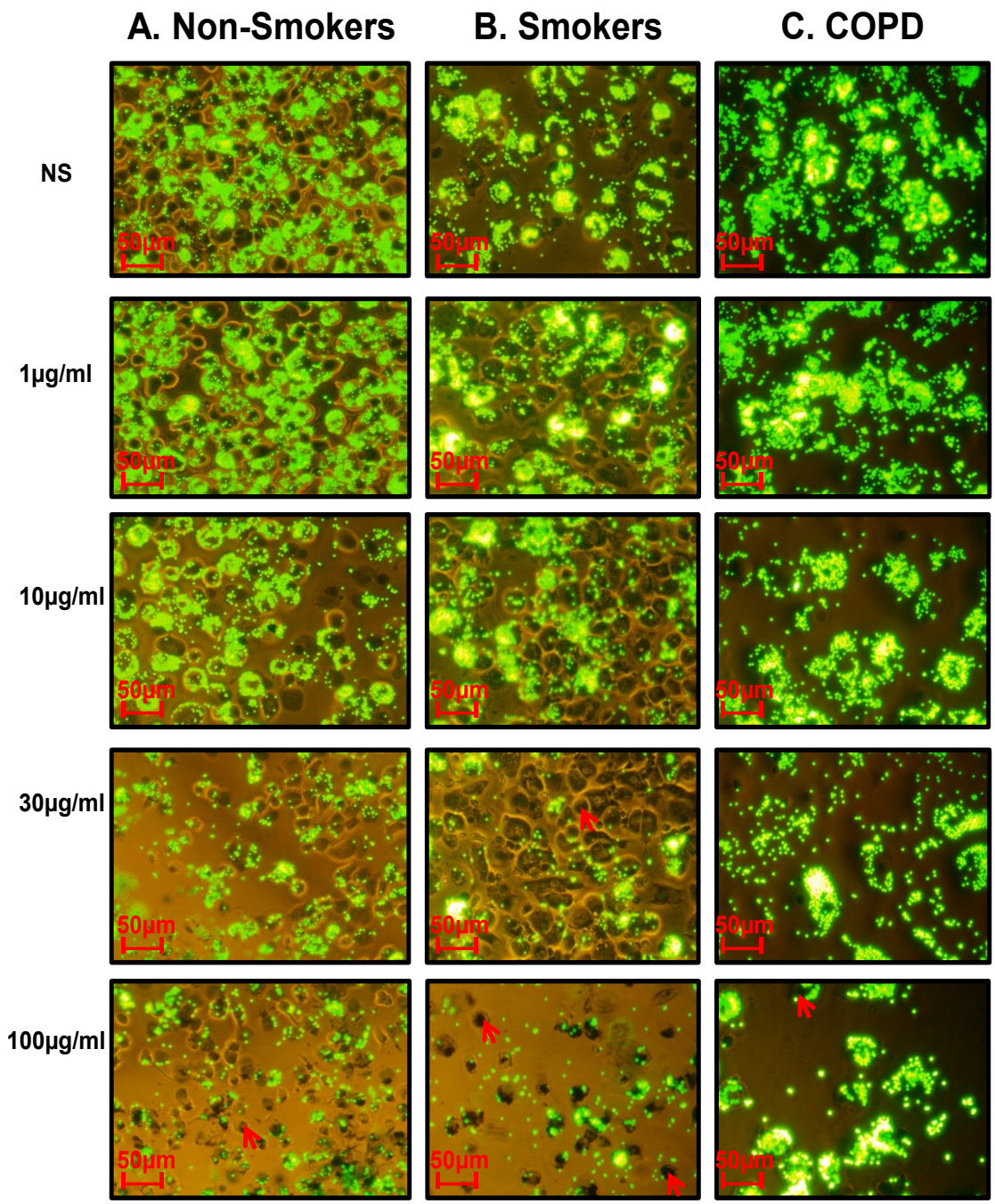

Figure 7.3 Effect of SRM-2975 on MDM Phagocytosis of Fluorescent Beads

SRM-2975-treated MDM (1-100µg/ml) from Non-smokers (A), Smokers (B) and COPD (C) patients were incubated with fluorescent beads ($50x10^6$ beads/ml) for 4h. Non-stimulated cells were used as baseline controls (control) and represented maximum phagocytosis by the different subject groups. A reduction in fluorescent beads (green) with increasing concentrations of SRM-2975 was observed in MDM from all subject groups. Red arrows indicate SRM-2975-laden MDM. Cells were viewed by fluorescent microscopy and images were taken at X 20 magnification.

However, MDM treated with SRM-1650B (Figure 7.4B) or SRM-2975 (Figure 7.4C), significantly reduced phagocytosis of fluorescent beads in non-smokers or patients with COPD but not smokers. Significant differences in phagocytosis were seen between SRM-2975-treated MDM from non-smokers and patients with COPD at 1-100µg/ml. The difference in phagocytosis between the subject groups may be associated to the high baseline values observed in non-smoker MDM.

7.3.3 Confocal imaging of the effect of DEP-N, SRM-1650B or SRM-2975 on MDM phagocytosis of Fluorescent Beads

Confocal microscopy was used to validate the fluorescent microscopy observations (section 7.3.1) and fluorimetry findings (section 7.3.2). This technique was used to differentiate whether beads were adhered to the outside of MDM or had been internalised. As DEP-N had significantly reduced phagocytosis of fluorescent beads in MDM from all volunteer groups, DEP-N was selected for confocal analysis.

DEP-N (1-100µg/ml) treated MDM from a smoker subject were exposed to fluorescent beads, and images were captured using a confocal microscope and compiled to form a z-stack (Figure 7.5). The cross hairs established that DEP-N (black pigmented material) were surrounded by cytoplasm and, thereby internalised by MDM. It was also observed that MDM were capable of internalising aggregates of various sizes as demonstrated by the areas of black pigmentation within the cell cytoplasm (Figure 7.5). In addition, MDM containing DEP-N retained the phagocytic capacity to further internalise fluorescent beads, although this became reduced as the concentration of DEP-N increased; thereby, confirming the reliability of the light microscopy images and fluorimetry data.

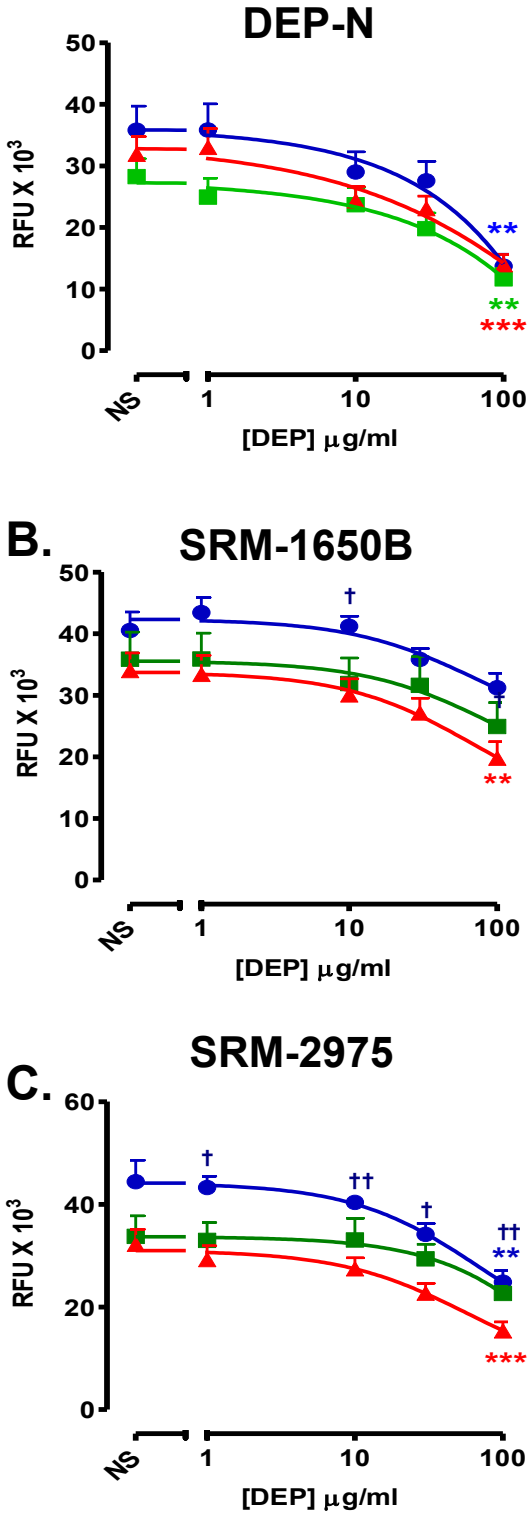

Figure. 7.4 Effect of DEP-N, SRM-1650B or SRM-2975 on MDM Phagocytosis of Fluorescent Beads.

MDM from non-smokers (●) (n=6-11), smokers (■) (n=7-12) and patients with COPD (▲) (n=13-22; ex-smoker n=11, current smoker n=9, unknown n=2) were treated with 1-100µg/ml of (A) DEP-N, (B) SRM-1650B (0.2µm) or (C) SRM-2975 (11.2µm). Particle-treated cells were incubated for 24h followed by further exposure to fluorescent beads (phagocytic prey) for 4h. Phagocytosis was measured using fluorimetry. Non-stimulated (NS) cells were baseline controls. Data are mean ± SEM of relative fluorescence units (RFU). *p<0.05, **p<0.01, ***p<0.001 *vs* non-stimulated controls. † p<0.05, †† p<0.01 non-smoker *vs* COPD.

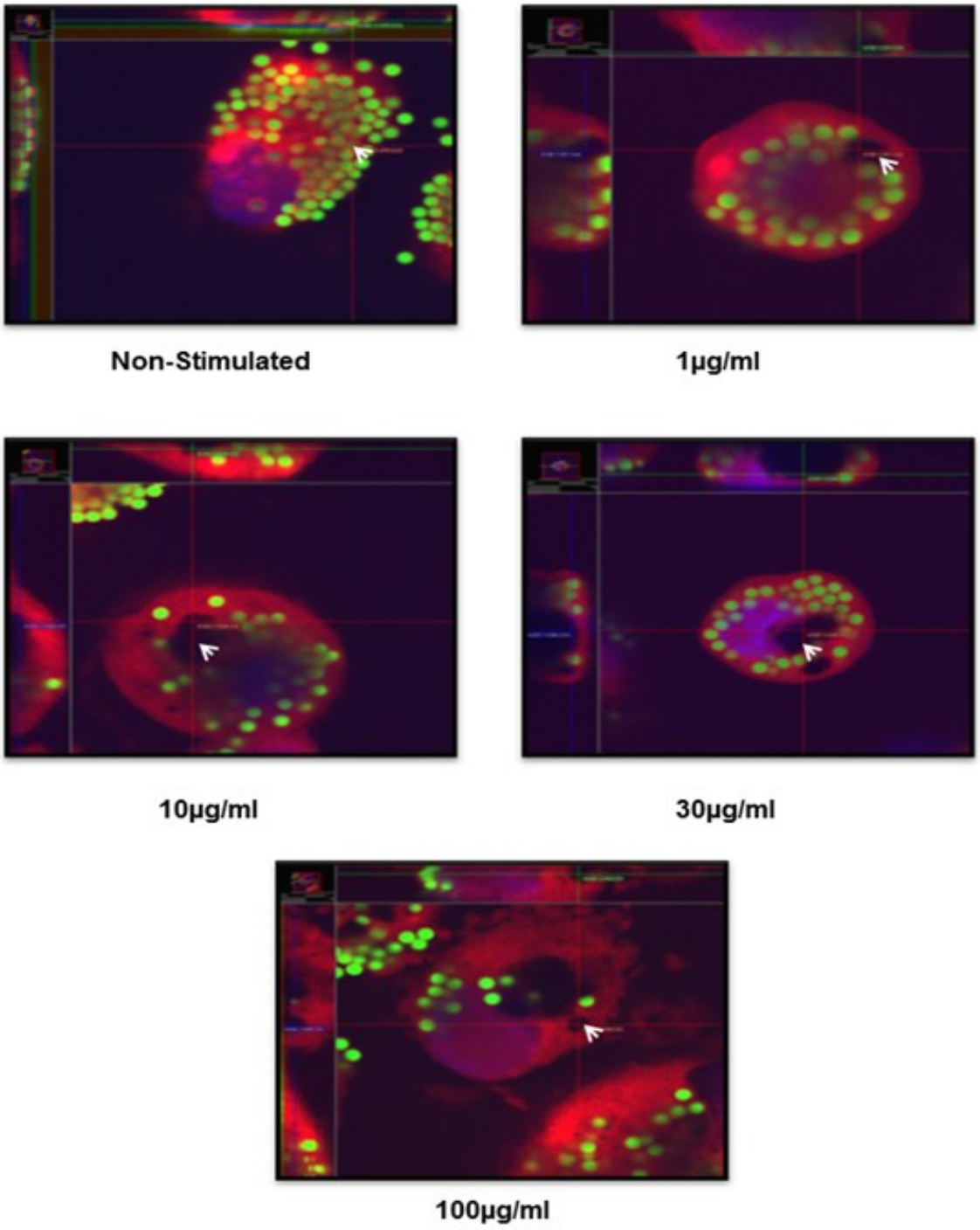

Figure 7.5 Confocal Images of DEP-N-Treated MDM Internalising Fluorescent Beads

MDM from a smoker subject were cultured on 8-well chamber slides and exposed to 100µg/ml DEP-N for 24h and viewed using confocal microscopy. Sequential images were taken through a single MDM and compiled together to form a z-stack. The nuclei is stained with DAPI (blue), the cytoplasm is stained with Cell Tracker Red (Red), fluorescent beads (green) and DEP-N (black pigmented material). Cross hairs demonstrate internalised fluorescent beads or DEP-N and white arrows indicate the bead or aggregate of DEP-N internalised by MDM.

7.3.4 Effect of DEP Samples and Fluorescent Beads on MDM Viability

Having determined that increasing concentrations of DEP-N, SRM-1650B or SRM-2975 reduced MDM-phagocytosis of fluorescent beads, the next step was to determine whether this effect was related to cell viability. MDM were incubated with DEP-N (1-100μg/ml) for 24h followed by exposure to fluorescent beads for 4h; cells were then assessed for viability by MTT assay. Cell that had not previously been exposed to DEP were the baseline controls and were considered to be 100% viable.

DEP-N (Figure 7.6A) treated MDM from COPD patients exposed to fluorescent beads significantly reduced cell viability at 1 - 100μg/ml by ~50% at the highest concentration. DEP-N also significantly reduced viability in cells from smokers at 100μg/ml by ~40%. SRM-1650B (Figure 7.6B) treated MDM exposed to fluorescent beads significantly reduced viability at 30μg/ml -100μg/ml in COPD patients by ~20% at the highest concentration. However, SRM-2975 treated MDM from COPD patients only reduced viability by ~30% at 100μg/ml (Figure 7.6C). The combination of DEP treatment and fluorescent beads did not significantly alter viability in non-smoker MDM.

7.3.5 Imaging the effect of 30μm, 10μm or 0.2μm Sized Inert Beads on MDM Phagocytosis of Fluorescent Beads

Having determined that MDM exposed to DEP-N, SRM-1650B or SRM-2975 reduced phagocytosis of fluorescent beads, the next step was to determine whether this effect was associated with DEP composition and/or size. To address this question, MDM were incubated with inert beads (1-100μg/ml) of different sizes, followed by incubation with fluorescent beads, and assessed by light microscopy and fluorimetry.

Unlike the effect of DEP on phagocytosis of fluorescent beads (Figure 7.1 -7.3), MDM from non-smokers, smokers or patients with COPD treated with increasing concentrations (1-100μg/ml) of 0.2μm (Figure 7.7), 10μm (Figure 7.8) or 30μm (Figure 7.9) sized beads did not exhibit a reduced capacity to further internalise fluorescent beads. No difference in response was observed between MDM from non-smokers, smokers or patients with COPD.

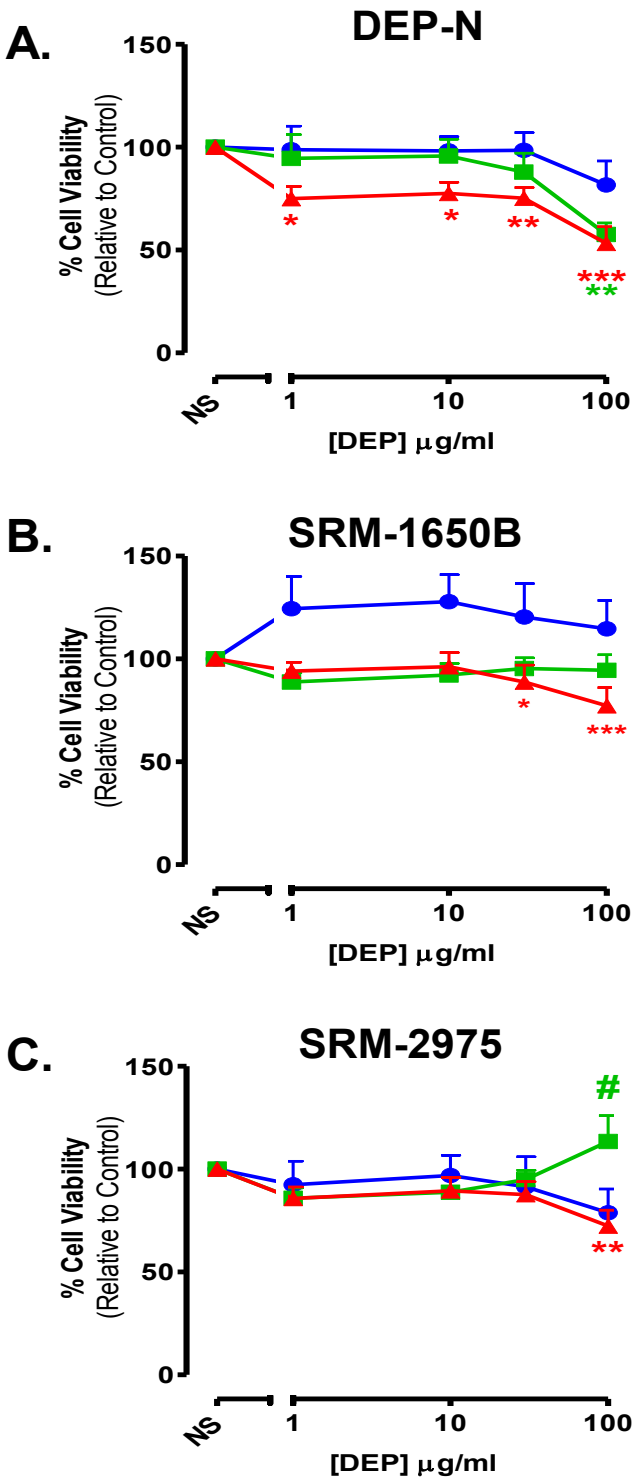

Figure. 7.6 Effect of DEP Samples and Fluorescent Beads on MDM Viability.

MDM from non-smokers (●) (n=5-6), smokers (■) (n=7-9) and patients with COPD (▲) (n=11-13; ex-smokers n=7, current smokers n=3-4, unknown n=3) were treated with 1-100µg/ml of (A) DEP-N, (B) SRM-1650B and (C) SRM-2975. DEP-treated cells were incubated for 24h followed by further exposure to fluorescent beads for 4h. Cell viability was assessed by MTT assay. Non-stimulated (NS) cells were baseline controls and represented 100% viability (normalised data). Data are mean ± SEM. * $p<0.05$, ** $p<0.01$, *** $p<0.001$ *vs* non-stimulated controls. **#** $p<0.05$ smokers *vs* COPD.

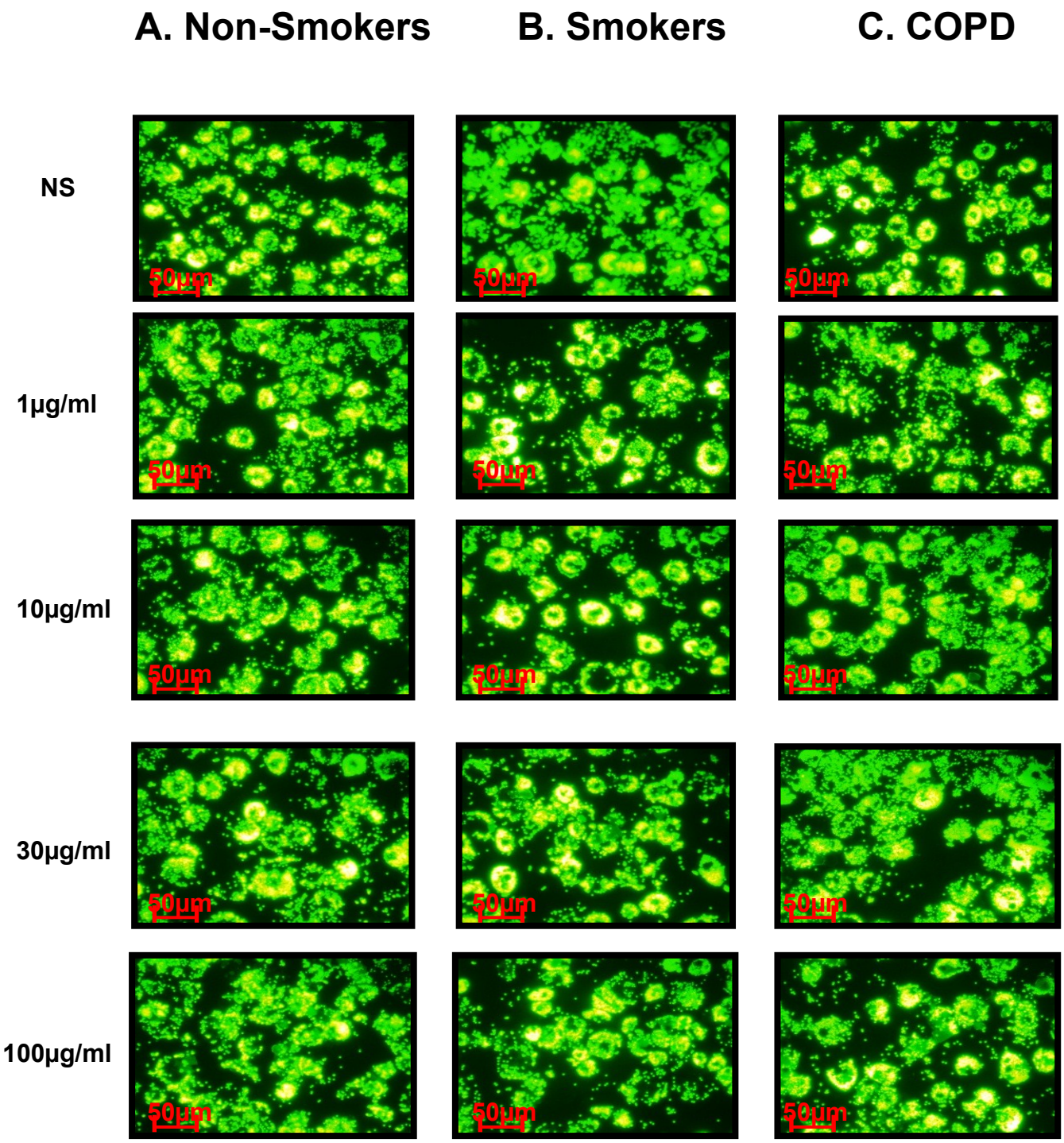

Figure 7.7 Effect of 0.2µm Sized Inert beads on MDM Phagocytosis of Fluorescent Beads

0.2µm-treated MDM (1-100µg/ml) from (A) non-smokers, (B) smokers and (C) COPD patients were incubated with fluorescent beads ($50x10^6$ beads/ml) for 4h. Cells that have not been treated with 0.2µm inert beads were used as baseline controls (controls) and represented maximum phagocytosis by the different subject groups. Cells were viewed by fluorescent microscopy and images were taken at X20 magnification. No reduction in phagocytosis of fluorescent beads (green) was observed.

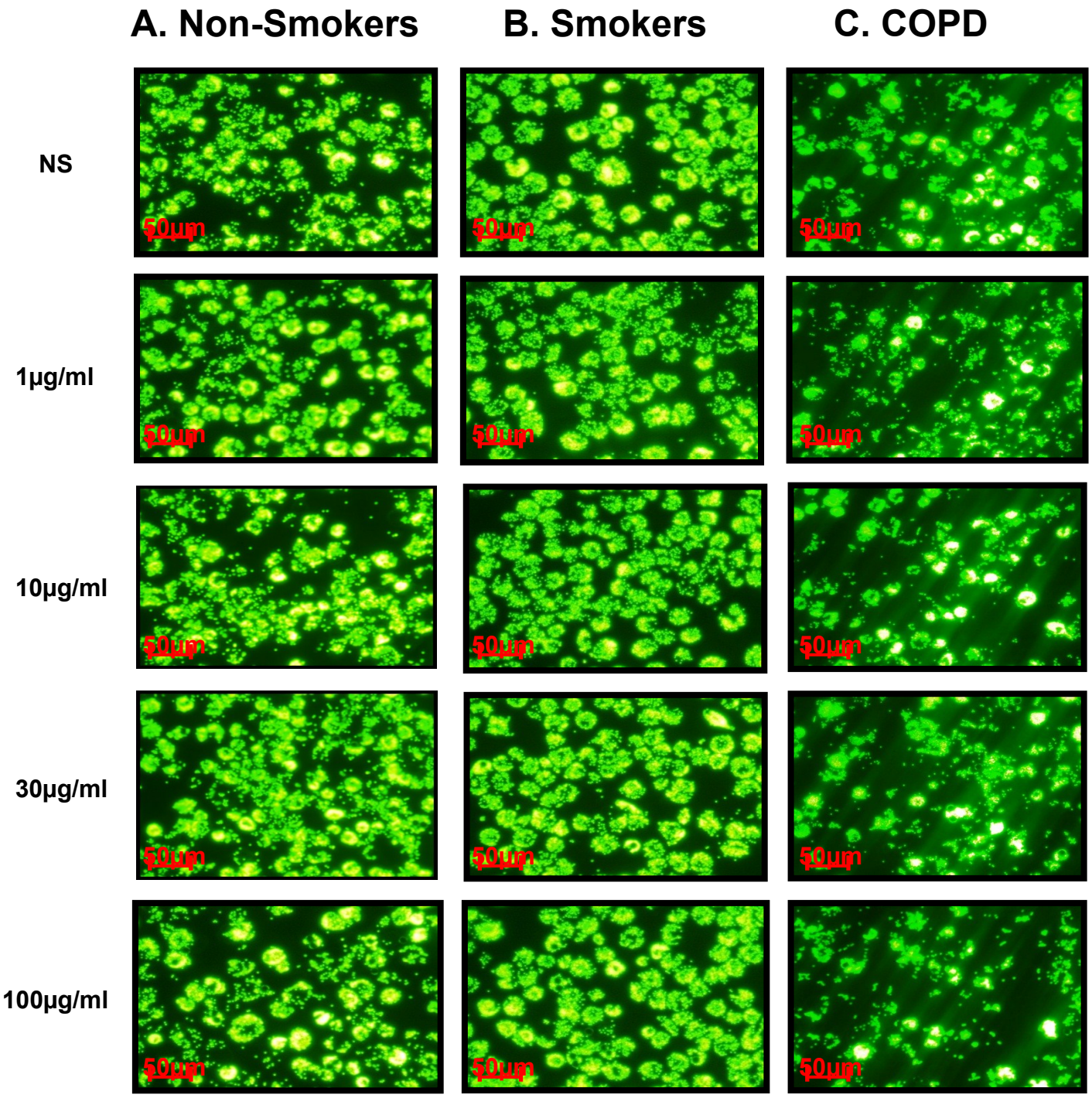

Figure 7.8 Effect of 10µm Sized Inert beads on MDM Phagocytosis of Fluorescent Beads

10µm-treated MDM (1-100µg/ml) from (A) non-smokers, (B) smokers and (C) COPD patients were incubated with fluorescent beads ($50x10^6$ beads/ml) for 4h. Cells that had not been treated with 10µm inert beads were used as baseline controls (controls) and represented maximum phagocytosis by the different subject groups. Cells were viewed by fluorescent microscopy and images were taken at X20 magnification. No reduction in phagocytosis of fluorescent beads (green) was observed.

MDM treated with increasing concentrations of 0.2μm (Figure 7.10A), 10μm (Figure 7.10B) or 30μm (Figure 7.10C) inert beads did not effect phagocytosis of fluorescent beads when compared to non-stimulated controls. No difference between response was observed in MDM from non-smokers, smokers or patients with COPD.

7.3.6 Effect of Inert Beads and Fluorescent Beads on MDM Cell Viability

Although increasing concentrations of 0.2μm, 10μm or 30μm sized inert beads did not alter subsequent MDM phagocytosis of fluorescent beads, for completeness, the effect of the combination of inert and fluorescent beads on MDM viability was assessed. Cells were incubated with increasing concentrations of 0.2μm, 10μm or 30μm inert beads for 24h and further exposed to fluorescent beads for 4h; cell viability was assessed using MTT assays. MDM treated with media alone were used as baseline controls and represented 100% viability. As might have been expected, neither 0.2μm (Figure 7.11A), 10μm (Figure 7.11B) nor 30μm (Figure 7.11C) sized beads effected MDM viability compared to baseline controls.

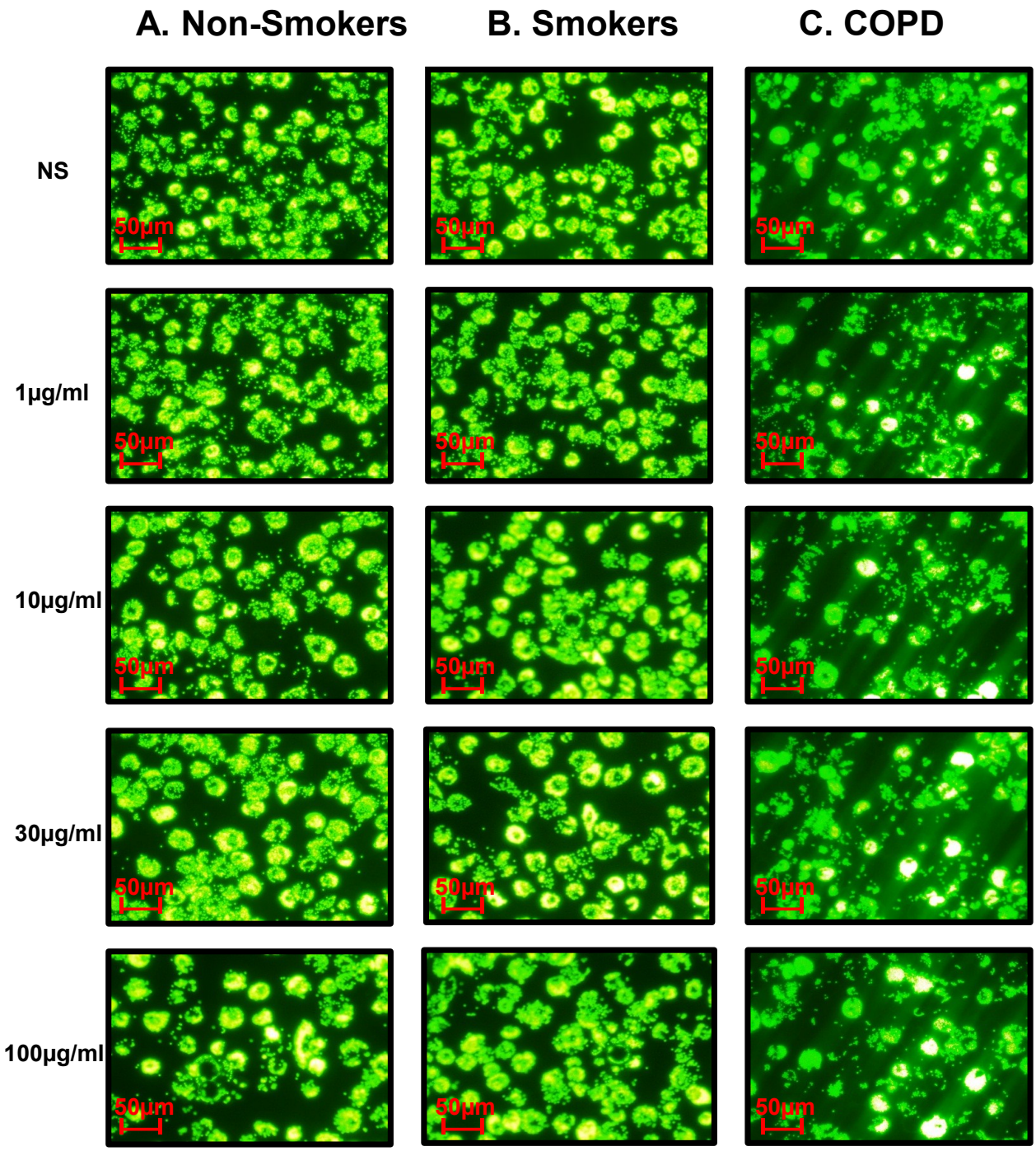

Figure 7.9 Effect of 30µm Sized Inert beads on MDM Phagocytosis of Fluorescent Beads

30µm-treated MDM (1-100µg/ml) from (A) non-smokers, (B) smokers and (C) COPD patients were incubated with fluorescent beads ($50x10^6$ beads/ml) for 4h. Cells that had not been treated with 30µm inert beads were used as baseline controls (control) and represented maximum phagocytosis by the different subject groups. Cells were viewed by fluorescent microscopy and images were taken at X20 magnification. No reduction in phagocytosis of fluorescent beads (green) was observed.

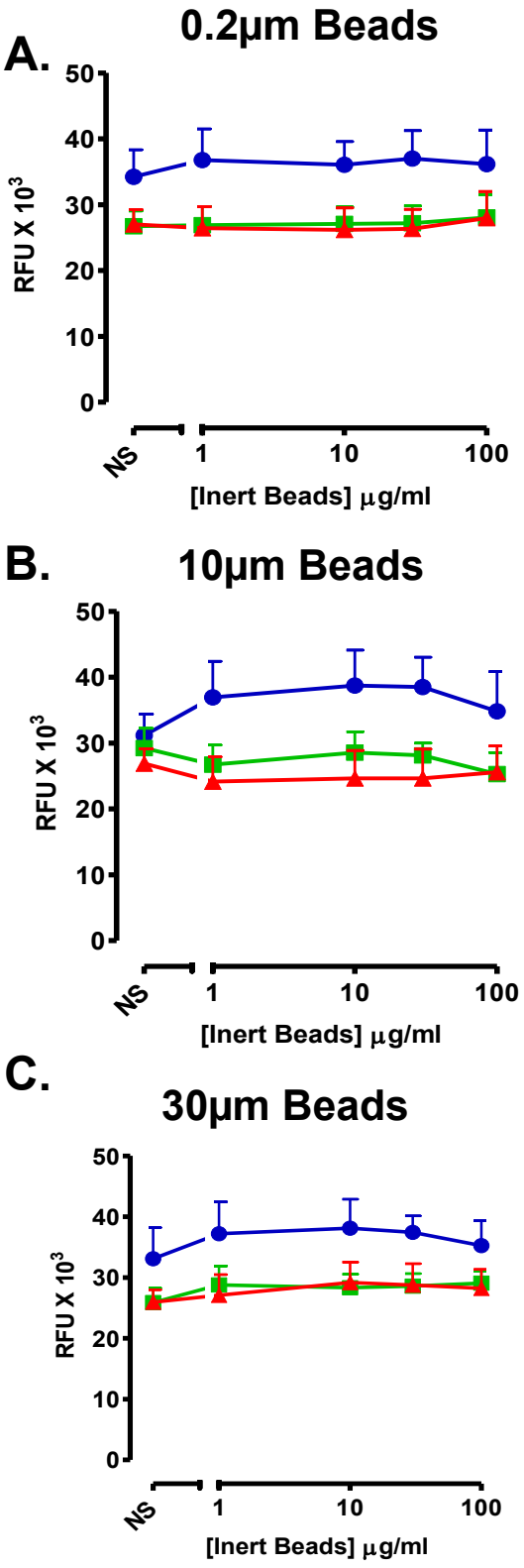

Figure. 7.10 Effect of Inert Beads on MDM Phagocytosis of Fluorescent Beads.

MDM from non-smokers (●) (n=5), smokers (■) (n=8) and patients with COPD (▲) (n=10; ex-smokers n=5, current smokers n=3, unknown n=2) were treated with 1-100µg/ml of (A) 0.2µm beads, (B) 10µm beads and (C) 30µm beads. Inert bead treated cells were incubated for 24h followed by further exposure to fluorescent beads (phagocytic prey) for 4h. Phagocytosis was measured using fluorimetery. Non-stimulated (NS) cells were baseline controls. Data are mean ± SEM relative fluorescence units (RFU).

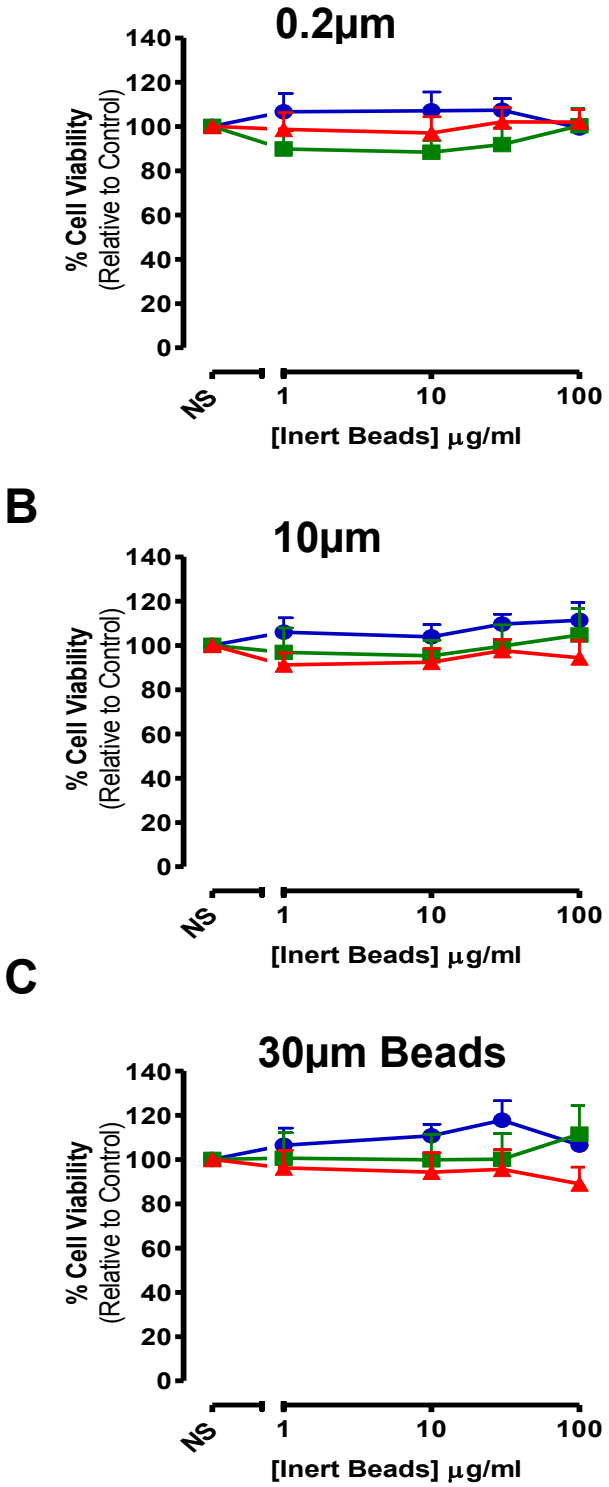

Figure. 7.11 Effect of Inert Beads of Different Sizes and Fluorescent Beads on MDM Viability.

MDM from non-smokers (●) (n=5), smokers (■) (n=8) and patients with COPD (▲) (n=10; ex-smokers n=5, current smokers n=3, unknown n=2) were treated with 1-100µg/ml of (A) 0.2µm beads, (B) 10µm beads and (C) 30µm beads. Inert bead treated cells were incubated for 24h followed by further exposure to fluorescent beads (phagocytic prey) for 4h. Phagocytosis was measured using fluorimetry, followed by treatment with MTT to determine cell viability. Cells treated with media alone were baseline controls. Data are mean ± SEM % cell viability (relative to control).

7.4 Discussion

Chapter 5 and 6 showed that DEP stimulate MDM from non-smokers and COPD patients to activate p38 and ERK 1/2 MAPK, and release CXCL8. The present chapter investigated the effect of DEP-N, SRM-1650B or SRM-2975, on MDM phagocytosis of fluorescent beads and the impact of these treatments on cell viability. Inert-bead treated MDM were also investigated for their effect on subsequent phagocytosis of fluorescent beads and cell viability, to determine whether the composition and/or size of particles effected internalisation of phagocytic prey.

The current study used qualitative (fluorescent microscopy) and quantitative (fluorimetry) techniques to validate whether cells exposed to DEP or inert beads affected the phagocytic capacity of MDM. Data from both fluorescent microscopy and fluorimetry showed that DEP-treated MDM from all subject groups reduced phagocytosis of fluorescent beads. To determine whether these analyses reflected internalisation of fluorescent beads and not fluorescence emitted by beads attached to the cell membrane, confocal microscopy was used. Sequential imaging of DEP-treated MDM showed that fluorescent beads were indeed internalised by the cells, therefore validating the data obtained using fluorescence microscopy and fluorimetry.

DEP-N significantly reduced phagocytosis of fluorescent beads in MDM from non-smokers, smokers and patients with COPD. However, MDM treated with SRM-1650B or SRM-2975 reduced phagocytosis of fluorescent beads only in non-smokers or patients with COPD. Differences in response were also observed between SRM-2975-treated MDM from non-smokers compared to cells from patients

with COPD. It is suggested that differences in phagocytosis between non-smokers and patients with COPD are associated with the viability of cells. It is possible that MDM from COPD patients are already fragile from the pre-treatment with DEP, therefore further exposing the cells to fluorescent beads will increase the burden of toxicity leading to reduced cell viability, and in part reduce phagocytosis. However, MDM from non-smokers pre-treated with SRM-2975 did not show a difference in cell viability compared to COPD patients, therefore it is suggested that the reduction of phagocytosis seen between the two subject groups is an effect of non-smokers having a higher overall baseline response compared to patients with COPD. Since non-smokers had a higher baseline phagocytic response, it is difficult to determine whether SRM-2975 induced greater inhibition of phagocytosis in patients with COPD and therefore this experiment requires further examination.

The composition of the different samples of DEP-N, SRM-1650B and SRM-2975 may be associated to the differences in phagocytic response observed in MDM. The findings observed herein are similar to findings from other *in-vitro* studies. For example, rat AM macrophages exposed to native DEP, DEP extracts (DEP-E), washed DEP (DEP-W) or carbon black (CB) were examined for their effect on phagocytic and bactericidal function on *Listeria monocytogenes.* Only native DEP or DEP-E significantly supressed AM phagocytosis and inhibited bactericidal function in these cells, whereas DEP-W reduced phagocytosis and bacterial killing to a lesser extent. In contrast, AM treated with carbon black reduced phagocytosis but did not alter bactericidal functions (Yin et al. 2007). These findings suggest that the organic components of DEP may drive suppression of phagocytosis by macrophages.

Suppression of phagocytosis following treatment of MDM with DEP may be related to a number of causes, these include, down regulation of phagocytic receptors (i.e.

MARCO) that are involved in the recognition of inhaled prey particles (Becker & Soukup, 1998; Kobzik, 1995; Palecanda et al. 1999). The occupation of macrophage cytoplasm, termed 'overload', may also prevent further internalisation of inhaled particles. For example, a particle-burden of ~2.6 - 6% of the internal volume of macrophages suppresses the clearance mechanisms of these cells (Oberdorster et al. 1994; Renwick et al. 2001; Morrow et al. 1988; Lundborg et al. 2006). In addition, occupation of 7-8% of the macrophage volume may affect the integrity of the cytoskeleton, thereby preventing clearance of particles, whilst occupation of 60% macrophage volume completely inhibits clearance (Lenhert, 1990, Dorries and Valberg, 1992, Möller, *et al*, 2002; Möller, *et al*, 2005, Lundborg*, et al,* 2006). Similarly, confocal microscopy images herein, show large aggregates of DEP-N occupying MDM volume at the highest concentration of DEP-N treatment (Figure 7.1 and Figure 7.3). However, these cells were still capable of internalising fluorescent beads, albeit less effectively compared to cells treated with low concentrations of DEP-N. In contrast to the findings of other groups (Oberdoster, et al. 1992; Dorries & Valberg 1992), the data presented herein showed that suppression of phagocytosis was not merely an effect of cells becoming replete; as inert-bead treated MDM did not reduce subsequent phagocytosis, thereby suggesting that DEP specifically inhibit phagocytosis. It was speculated (Renwick et al. 2001) that ultrafine particles (<0.1μm) and fine (<2.5μm) particles reduce macrophage phagocytosis because the larger surface area of smaller particles introduces a higher proportion of organic compounds and transition metals to cells. The DEP samples herein formed aggregates within the fine particle range. Internalisation of these particles will enable the complex composition of DEP to interact with the intracellular cytoskeleton of macrophages, thereby preventing further ingestion of fluorescent beads. Rats

instilled with a single dose of 5mg/kg of DEP or CB, followed by inoculation with *Listeria monocytogenes* demonstrated that macrophage clearance of Listeria was suppressed by DEP administration and not CB (Yang et al. 2001). This suggests that chemicals adsorbed on the surface of DEP are responsible for reduced phagocytosis.

Treatment of MDM with DEP did not supress cell viability as previously seen in Chapter 3. However, MDM treated with both DEP and fluorescent beads significantly reduced viability in smokers or patients with COPD but not cells from non-smokers. This effect suggests that treatment of MDM with DEP samples and fluorescent beads may have burdened the cells and damaged membrane integrity which may have an effect on phagocytosis.

Taken together, the findings from the present chapter data show that DEP-N, SRM-1650B or SRM-2975 pre-treatment of MDM reduce clearance of phagocytic prey. These effects are not apparently related to the DEP-treated MDM being replete, but are rather associated with the composition of the DEP-samples. Data from this Chapter does not support the hypothesis 'DEP-N, SRM-1650B or SRM-2975-treated MDM from patients with COPD will reduce phagocytosis of fluorescent beads, compared to MDM from non-smokers or smokers'. Even though MDM from COPD patients treated with SRM-2975, appeared to have reduced phagocytosis compared to MDM from non-smokers, this effect was not evident with other DEP samples. Furthermore, it is suggested that non-smoker MDM had a higher baseline phagocytosis compared to MDM from COPD patients; therefore it is difficult to discern whether SRM-2975 is responsible for the difference observed in phagocytosis between these two subject groups and requires further examination.

Chapter 8:

General Discussion

8.1 General Discussion

The overall general hypothesis of this thesis was:

"DEP modulate macrophage pro-inflammatory mediator release and phagocytosis, and this is more prominent in COPD."

The data presented herein support the first part of the hypothesis, namely that DEP modulate MDM inflammatory mediator release and phagocytosis. However, the present data did not support the second part of the hypothesis, whereby MDM from patients with COPD were not more susceptible to the effects of DEP compared with cells from non-smokers or smokers. In addition, the effects of DEP were confined to DEP-N rather than SRM-1650B and SRM-2975 particles. These observations merit some general discussion.

8.2. DEP Composition and Relevance of *In Vitro* and *In Vivo* Experiments

The composition of DEP is dependent on many factors including engine type, operating conditions or fuel type (Ono-Ogasawara & Smith 2004; Mcdonald et al. 2011). The effects observed in the experimental system used in this thesis may not reproduce similar effects *in-vivo*. This is because the composition of DEP differs between samples, and many of the cellular effects are attributed to the ROS-generating capacity of the high percentage of surface-adsorbed organics, including PAHs and nitro-PAHs (Baulig et al. 2003; Schwarze et al. 2013; Totlandsdal et al. 2013). In addition, metals, including Fe and Cu, and endotoxin adsorbed on the surface of DEP are also associated with mediating cellular effects (Imrich et al. 2007; Totlandsdal et al. 2013). The variable composition of DEP may be responsible for

activating different intracellular signalling pathways to stimulate the release of pro-inflammatory mediators, for example activation of the p38 MAPK pathway, to stimulate macrophage IL-6 release (Li et al. 2002; Totlandsdal et al. 2010; Schwarze et al. 2013).

It is also speculated that findings presented herein may differ from *in-vivo* responses as inhalation of DEP would deposit predominantly on the surface of type II pneumocytes which are covered by a layer of surfactant (Schurch et al. 1992). Surfactant proteins (SP)-A and SP-B are associated with enhancing macrophage phagocytosis by acting as opsonins (Hohlfeld et al. 1997; Benne et al. 1997). Surfactant also contains non-enzymatic anti-oxidants for example uric acid, glutathione and α-tocopherol, which protect the lung from ROS generated by DEP (Thorley & Tetley, 2007). Therefore, responses between the experiments of the present thesis may not reflect those that occur *in-vivo.*

The concentration range of DEP samples used in the experiments herein, were delivered to cells as particulate suspensions. Typical environmental levels of PM_{10} are 5-10μg/m^3, whereas biologically relevant levels are 0.2 - 20μg/cm^2 (Donaldson et al. 2005; Li et al. 2002; Li et al. 2003; Totlandsdal et al. 2010) which are comparable to those used in this thesis. It is difficult to relate inhalable doses typically found in the environment to cells treated with particulate suspensions, this is because cell culture media used to suspend particles may interfere with properties of the DEP overtime (Teeguarden et al. 2007). For example, the surface charge or chemistry, aggregation of particles and rate at which suspended particles settle on cells may be affected by the content of salts in media. To this end, it would not be feasible to determine the actual dose 'concentration' of DEP used to treat cells, as the cells would only be exposed to deposited aggregates which are large in size, but not small

particulates which would remain suspended in media (Teeguarden et al. 2007; Totlandsdal et al. 2010). The biologically relevant concentration of particulate matter is in the range of 0.2-20μg/cm^2 as determined by the calculations in Li et al. 2003 and Li et al. 2002. The biological relevance of the concentration of DEP used herein, were calculated according to the surface area of in 96-well and 24-well tissue culture plates, which are 0.32cm^2 and 3.2 cm^2 respectively. The concentration range of DEP used herein are comparable with DEP concentrations used by other groups (Chaudhuri et al. 2012; Zhou & Kobzik 2007; Saxena et al. 2008) but maybe high to be compared to exposure levels in the atmosphere. Although the findings herein cannot be extrapolated to *in-vivo* inhalation studies directly, this exposure system is effective in providing a means of testing the effect of DEP on biological parameters (Totlandsdal et al. 2012). To this end, the use of particulate suspensions allows examination of different DEP samples on macrophage function, and also allows exploration of DEP on the activation of different signalling pathways (Totlandsdal et al. 2010).

8.3. Modulation of mediator release and phagocytosis

DEP-induced release of CXCL8 by MDM from all subject groups and, contrary to the overall thesis hypothesis, this was similar between non-smokers and patients with COPD. However, in contrast, DEP-induced release of CXCL8 by MDM from smokers was reduced compared with that from MDM from non-smokers or COPD patients. DEP-N also failed to activate p38 and ERK 1/2 in MDM from smokers. Furthermore, these cells were also protected against the cytotoxic effects of DEP-N. These observations are unlikely to be a result of direct, prior cigarette smoke exposure, as MDM were differentiated outside the lung environment, thereby suggesting that this

response maybe linked to an epigenetic or genetic predisposition of these cells. Cigarette smoke consists of ~4,700 noxious chemical species, (Rahman & Macnee, 1996; Wright et al. 2012). Exposure of circulating monocytes to these chemicals may lead to activation of several anti-oxidant genes and stress related genes (Totlandsdal et al. 2012). For this reason, it is speculated that the reduced CXCL8 release, MAPK activation and cytotoxicity in MDM from smokers may be associated with increased production of anti-oxidants (Li et al. 2000). Production of these anti-oxidants may protect the cell from excess exposure to DEP-generated oxidants (Hiura et al. 1999). However, the effect of DEP-N to suppress phagocytosis was similar across MDM from all subject groups thereby suggesting the effects of DEP-N to mediate CXCL8 release and alter phagocytosis maybe via different mechanisms.

Primary BAL macrophages from COPD patients release increased levels of mediators at baseline (for example CXCL8, IL-6 or TNFα) compared to cells from non-smokers or smokers (Barnes 2009; Culpitt et al. 2003). In addition, DEP also induce release of inflammatory mediators, for example IL-6 or TNFα, by various pulmonary cells, including macrophages (Hetland et al. 2005; Totlandsdal et al. 2010; Shaw et al. 2011; Schwarze et al. 2013; Becker et al. 2005). For this reason, it was suggested that treatment of MDM with DEP would amplify release of the typical-macrophage mediators, namely CXCL8, IL-6 or TNFα, in the present experimental system. However, the findings of this thesis suggested that mediator release by DEP-treated MDM from COPD patients were not increased compared to MDM from non-smokers. It is speculated that this maybe because MDM are cultured *in-vitro* and are not constantly exposed to the underlying inflammation seen in the lungs of COPD patients (Barnes 2004; Barnes 2009). If MDM were exposed to similar

inflammatory processes present in the COPD lung, and also exposed to DEP, MDM may have further enhanced release of CXCL8, IL-6 or TNFα compared to controls.

The findings presented in this thesis may not reflect the effect of inhaled DEP on alveolar macrophages *in-vivo*. The alveolar compartment of the lung consists of numerous cells including type I/II pneumocytes, macrophages and dendritic cells. In the present *in-vitro* model of macrophage function, the effects of DEP were examined only on MDM, thereby excluding interactions of DEP with different cell types, which may in turn influence functioning of macrophages. Exposure of various cell types in the lung to DEP may stimulate immune responses and produce pro-inflammatory mediators which may go on to stimulate release of mediators by macrophages, for example IL-6 or TNFα. To investigate whether pulmonary cells exposed to DEP would modulate macrophage responses, a double cell co-culture system could be used instead of a mono-cell culture system. This could include primary human type II pneumocytes and alveolar macrophages to mimic the lung environment (Lehmann et al. 2009). A co-culture system would provide insight to the interaction of other pulmonary cells on the effect of macrophage function following DEP treatment.

Lungs of COPD patients are commonly colonised by bacteria including *Haemophilus influenzae*, *Streptococcus pneumoniae* or during an exacerbation infection with respiratory synticial virus (Donnelly & Barnes 2012; Sikkel et al. 2008). The persistence of these micro-organisms in the lung may be related to defective macrophage phagocytosis (Taylor et al. 2010; Berenson et al. 2006). The data presented herein concluded that DEP-treated MDM from COPD patients did not show reduced phagocytosis of fluorescent beads compared to non-smoker or smoker subjects. Similarly, findings by Taylor et al. 2010 also demonstrated that

MDM from COPD patients also successfully phagocytose fluorescent beads compared to non-smoker or smoker controls, but are defective in clearing fluorescently-labelled *H.influenzae* or *S.pneumoniae*. *In-vitro* experiments examining the effect of DEP on clearance of *Listeria monocytegenes* by alveolar macrophages also showed that cells were defective in internalising pathogens (Yin et al. 2007). For this reason, it is speculated that even though phagocytosis of fluorescent beads by DEP-treated MDM was similar in all subject groups, this response may be altered if DEP-treated cells were exposed to fluorescently-labelled bacteria. The latter investigation would allow examination of whether DEP reduce MDM phagocytosis significantly in patients with COPD compared to non-smoker or smoker controls. In addition, this investigation would also contribute to understanding relationship between inhalation of DEP and increased bacterial colonisation and exacerbations in COPD patients.

8.4. Clinical Implications

The data presented herein show that DEP increase pro-inflammatory mediator release and reduced phagocytosis in alveolar macrophages. These observations may explain, at least in part, the association between inhalation of DEP and their adverse effects on adverse respiratory symptoms in patients with COPD. The clinical implications associated with inhalation of DEP include deposition of these particles in the alveolar compartment of the lung where they become targets for alveolar macrophages (Figure 8.1A; Figure 8.1B). The complex composition of DEP may amplify release of the chemokine CXCL8, which is already increased in COPD (Bildberg, *et al*, 2012). The increased levels of CXCL8, may drive recruitment of neutrophils and monocytes (Behndig, *et al*, 2006), and *via* this mechanism, DEP may

increase the number of cells present in the peripheral airways (Figure 8.1D). In addition DEP are also internalised by macrophages (Figure 8.1C). The composition of DEP may prevent the clearance of other inhaled particles and bacteria, for example *S.pneumoniae* or *H.influenzae.* The defective clearance of these pathogens leads to bacterial colonisation of the lung, which contributes to the inflammatory responses observed in COPD. The combined effect of DEP on stimulation of pro-inflammatory mediator release and decreased phagocytosis of bacterial pathogens may contribute to the underlying inflammation observed in COPD, and may increase the risk of COPD exacerbations (Figure 8.1D).

The findings presented herein require further investigation to determine the mechanisms underlying DEP modulation of macrophage function. The composition of DEP-N, rather than size, is responsible for driving the increased levels of CXCL8 by activating MAPK signalling pathways, and may also be involved in the inability of macrophages to internalise fluorescent beads. This is because MDM treated with SRM-1650B or SRM-2975 and inert beads of different sizes did not replicate the increase in CXCL8. Therefore suggesting that the composition of DEP-N is associated in stimulating CXCL8 release, but this requires further examination.

Findings from the data herein and other *in-vivo* or *in-vitro* studies show that DEP are variable in composition, and health effects associated with inhalation are related to the complex constituents of these particles. Data from this study and others, show that treatment of macrophages with DEP samples stimulate the release of distinct pro-inflammatory mediator profiles. In areas of high pollution, Inhalation of DEP by healthy non-smokers may induce an inflammatory response, but these effects may not appear to damage the health of individuals. However, inhalation of DEP by

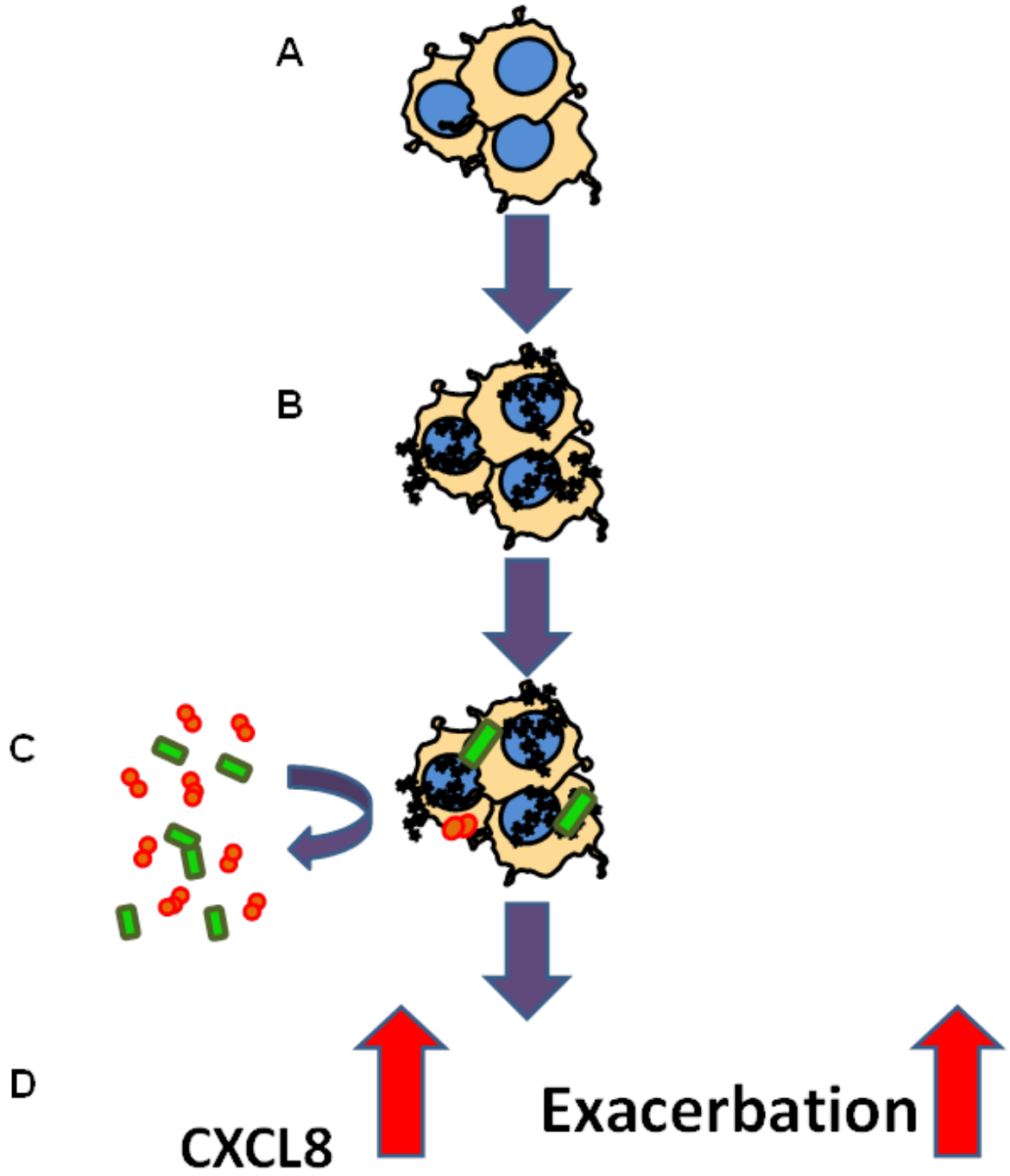

Figure 8.1 DEP-Treated Macrophages Increase CXCL8 Release and Reduce Phagocytosis

(A) AM located deep in the lung were exposed to (B) inhaled DEP. (C) AM internalise DEP, but lose their ability to internalise bacterial pathogens (curved arrow). Ineffective clearance of bacteria leads to colonisation of the lung which may (D) increase susceptibility to COPD-related exacerbations in patients. DEP also stimulate macrophages to release the chemokine, CXCL8, which is involved in the recruitment of neutrophils.

smokers or patients with COPD may aggravate the underlying inflammation seen in these individuals, which may lead to the onset symptoms (Behndig et al. 2006; Sehlstedt et al. 2010; Salvi et al. 2000).

8.5 Future Work

The observations in the present thesis indicate a number of directions for future work, as discussed below.

- MDM appear to be a suitable model of alveolar macrophage function in terms of examination and assessment of the effects of DEP in non-smokers, smokers and patients with COPD. However, it would be desirable to use primary macrophages from resected lung tissue or from BAL samples. This is because blood monocytes are differentiated into MDM by GM-CSF, meaning these cells have not been exposed to the lung environment, as would be the case if primary macrophages were used. Furthermore, using primary macrophages would mimic the effects of DEP on cells already exposed to inhaled particles or debris.

- In the present thesis, MDM from non-smokers, smokers or patients with COPD were treated with DEP and further exposed to fluorescent beads to assess the phagocytic capacity of these cells (Taylor et al. 2010). However, MDM from COPD patients are capable of internalising fluorescent beads but are defective in clearing fluorescently-labelled bacterial pathogens. To test the effect of DEP on MDM phagocytosis by COPD patients, cells could be treated with DEP and then further exposed to *H.influenzae* or *S.pneumoniae*. This experiment would examine whether DEP are capable of further reducing baseline phagocytosis by

MDM from patients with COPD, and allow comparison of data with non-smokers and smokers.

- Findings from the present thesis suggest that the composition of DEP is responsible for the increase in CXCL8 release and possibly the reduction in phagocytosis. To determine whether the composition of DEP is associated with the induction of CXCL8 or reduced phagocytosis, the samples of DEP-N could be washed with methanol to extract the adsorbed chemical species from the surface of the carbon particle. Subsequent investigations could then be performed where MDM from non-smokers, smokers or patients with COPD were treated with native-DEP, carbon black or the DEP extract, and pro-inflammatory mediator release and phagocytic ability of MDM investigated. The toxicity associated with native-DEP, carbon black or DEP extract on MDM from the different subject groups could also be assessed using MTT or flow cytometry.

- To determine whether adsorbed metals on the surface of DEP were responsible pro-inflammatory mediator release, metal chelators could be used. Subsequent experiments involving the treatment of MDM with native-DEP, carbon black or DEP-extract following metal chelation could be used to assess the effects of metals on MDM pro-inflammatory mediator release or phagocytosis. Types of metal chelators that could be used are EDTA, DFOA or 2,3-dimercaprol, which are responsible for chelating lead, iron or cadmium metals respectively (Flora and Pachauri, 2010).

- Inhaled DEP deposit in the alveolar compartment of the lung. The lung contains a number of cell types including type II pneumocytes, dendritic cells and macrophages which all will be exposed to the inhaled particles. To mimic the effects of DEP in the lung a double (i.e. MDM or macrophages with type II pneumocytes) co-culture could be used to examine the effects of DEP on type II epithelial cells, monocyte-derived dendritic cells and MDM. This will provide insight on the interaction and cross-talk between the individual cells and how this may impact the functioning of macrophages in regards to pro-inflammatory mediator release and phagocytosis.

- The effects of DEP on MDM, for example CXCL8 release, may be attributed to the generation of ROS by these particles. To determine whether DEP released CXCL8 *via* an oxidative effect, MDM can be treated with DEP in combination with anti-oxidants such as NAC. Following incubation, release of CXCL8 in the supernatant would be measured by ELISA.

- To examine whether reduced MDM phagocytosis by DEP was associated with cytoskeletal dysfunction, cells could be probed for actin integrity using phalloidin stains. Also, to assess whether DEP interfere with the cytoskeletal structure of MDM, confocal microscopy could be used.

References

Abboud, R.T. & Vimalanathan, S., 2008. Pathogenesis of COPD. Part I. The role of protease-antiprotease imbalance in emphysema. *The international journal of tuberculosis and lung disease*, 12(4): pp 361-367.

Aderem, A. & Underhill, D.M., 1999. Mechanisms of phagocytosis in macrophages. *Annual review of immunology*, 17: pp.593–623.

Agusti, A. et al., 2003. Hypothesis: does COPD have an autoimmune component? *Thorax*, 58(10): pp832 - 834.

Alessi, D.R. et al., 1995. PD 098059 is a specific inhibitor of the activation of mitogen-activated protein kinase kinase *in vitro* and *in vivo*. *The Journal of biological chemistry*, 270(46): pp 27489–27494.

Amakawa, K., et al., 2003. Suppressive effects of diesel exhaust particles on cytokine release from human and murine alveolar macrophages. *Experimental lung research*, 29(3): pp 149-64.

Anderson, H.R. et al., 1997. Air pollution and daily admissions for chronic obstructive pulmonary disease in 6 European cities: results from the APHEA project. *European Respiratory Journal*, 10(5): pp.1064–1071.

Arimoto, T. et al., 2005. Synergistic production of lung free radicals by diesel exhaust particles and endotoxin. *American journal or respiratory and critical care medicine,* 171(4): pp 379-387.

Arredouani, M.S. et al., 2004. The scavenger receptor MARCO is required for lung defense against pneumococcal pneumonia and inhaled particles. *The Journal of experimental medicine*, 200(2): pp.267–72.

Arredouani, M.S. et al., 2005. MARCO is the major binding recepto for unopsonized particles and bacteria on human alveolar macrophages. J*ournal of immunology*, 175(9): pp 6058-6064.

Atkinson, R.W. et al., 2001. Acute Effects of Particulate Air Pollution on Respiratory Admissions Results from APHEA 2 Project. *American journal of respiratory and critical care medicine*, 164(10 pt 1): pp 1860–1866.

Attfield, M.D. et al., 2012. The Diesel Exhaust in Miners study: a cohort mortality study with emphasis on lung cancer. *Journal of the National Cancer Institute*, 104(11): pp 869–83.

Backes, C.H. et al., 2013. Early life exposure to air pollution: how bad is it? *Toxicology letters*, 216(1): pp.47–53.

Barceló, B. et al., 2008. Phenotypic characterisation of T-lymphocytes in COPD: abnormal CD4+CD25+regulatory T-lymphocyte response to tobacco smoking. *The european respiratory journal*, 31(3): pp 555-562.

Baraldo, S. et al., 2012. Pathophysiology of the small airways in chronic obstructive pulmonary disease. *Respiration; international review of thoracic diseases*, 84(2): pp 89–97.

Barnes, P.J. et al., (2003). Chronic obstructive pulmonary disease: molecular and cellular mechanisms. *European respiratory journal,* 22(4): pp 672-688.

Barnes, P.J., 2010. Chronic obstructive pulmonary disease: effects beyond the lungs. *PLoS medicine*, 7(3): p.e1000220.

Barnes, P.J., 2004. Mediators of Chronic Obstructive Pulmonary Disease. *Pharmacology reviews*, 56(4): pp.515–548.

Barnes, P.J., 2008. Review series The cytokine network in asthma and chronic obstructive pulmonary disease. *The journal of clinical investigation,* 118(11): pp 3546-3556.

Barnes, P.J., 2009. The cytokine network in chronic obstructive pulmonary disease. *American journal of respiratory cell and molecular biology*, 41(6): pp 631–8.

Baulig, A. et al., 2003. Involvement of reactive oxygen species in the metabolic pathways triggered by diesel exhaust particles in human airway epithelial cells. *American journal of physiology. Lung cellular and molecular physiology*, 285(3): pp L671–9.

Baulig, A. et al., 2004. Physiochemical characteristics and biological activities of seasonal atmospheric particulate matter sampling in two locations of paris. *Environmental science & technology*, 38(22): pp 5985-92.

Becker, S. & Soukup, J.M., 1998. Decreased CD11b expression, phagocytosis, and oxidative burst in urban particulate pollution-exposed human monocytes and alveolar macrophages. *Journal of toxicology and environmental health*. Part A., 55(7): pp 455-77.

Becker, S. et al., 1987. Colony-stimulating factor-induced monocyte survival and differentiation into macrophages in serum-free cultures. *Journal of immunology,* 139(11): pp 3703-3709.

Becker, S. et al, 2003. Response of human alveolar macrophages to ultrafine, fine, and coarse urban air pollution particles. *Experimental lung research*, 29(1): pp 29-44.

Becker, S. et al., 2005. Seasonal variations in air pollution particle-iduced inflammatory mediator release and oxidative stress. *Environmental health perspectives,* 113(8): pp 1032-1038.

Behndig, A.F. et al., 2006. Airway antioxidant and inflammatory responses to diesel exhaust exposure in healthy humans. *European respiratory journal*, 27(2): pp 359–365.

Bell, M.L. & Davis, D.L., 2001. Reassessment of the lethal London fog of 1952: novel indicators of acute and chronic consequences of acute exposure to air pollution. *Environmental health perspectives*, 109(Suppl 3): pp 389–94.

Benne, C.A. et al., 1997. Surfactant protein A, but not surfactant protein D, is an opsonin for influenza A virus by rat alveolar macrophages. *European journal of immunology*, 27(4): pp 886-890.

Berenson, C.S. et al., 2013, Phagocytic dysfunction of human alveolar macrophages and severity of COPD. *The Journal of Infectious Disease*, 208(12): pp 2036-45.

Berenson, C.S. et al., 2006. Impaired phagocytosis of nontypeable Haemophilus influenzae by human alveolar macrophages in chronic obstructive pulmonary disease. *The Journal of infectious diseases*, 194(10): pp 1375–84.

Birrell, M.A., et al., 2008. Impact of tobacco-smoke on key signalling pathways in the innate immune response in lung macrophages. *The journal of cellular physiology*, 214(1): pp 27-37.

Block, M.L. et al., 2004. Nanometer size diesel exhaust particles are selectively toxic to dopaminergic neurons: the role of microglia, phagocytosis, and NADPH oxidase. *The FASEB journal,* 18(13): pp 1618-20..

Boland, S. et al., 1999. Diesel exhaust particles are taken up by human airway epithelial cells *in vitro* and alter cytokine production. *The american journal of physiology,* 276(4 pt 1): pp L604-L613.

Bonvallot, V. et al., 2001. Organic compounds from diesel exhaust particles elicit a proinflammatory response in human airway epithelial cells and induce cytochrome p450 1A1 expression. *American journal of respiratory cell and molecular biology,* 25(4): pp 515-521.

Burgel, P.R., 2011. The role of small airways in obstructive airway diseases. *European respiratory review : an official journal of the European Respiratory Society*, 20(119): pp 23–33.

Cardoso, L.S. et al. 2007. Polymyxin B as inhibitor of LPS contamination of Schistosoma mansoni recombinant proteins in human cytokine analysis. *Microbial cell factories*, 6(1): pp 1-6.

Castranova, V. et al., 2001. Effect of exposure to diesel exhaust particles on the susceptibility of the lung to infection. *Environmental health perspectives*, 109 (Suppl 4): pp 609–12.

Champion, J. A. & Mitragotri, S., 2009. Shape induced inhibition of phagocytosis of polymer particles. *Pharmaceutical research*, 26(1): pp 244–9.

Chaudhuri, N. et al., 2012. Diesel exhaust particle exposure *in vitro* alters monocyte differentiation and function. *PLOS one*, 7(12): pp e51107.

Chen, J.S.Q. & Cahill, I.M.K.T.A., 2000. Charactisation of chemical composisition and size of diesel: pp 294–298.

Chen, L.C. & Lippmann, M., 2009. Effects of metals within ambient air particulate matter (PM) on human health. *Inhalation toxicology*, 21(1): pp 1-31.

Chung, K.F., 2011. p38 mitogen-activated protein kinase pathways in asthma and COPD. *Chest*, 139(6): pp 1470–1479.

Churg, A. et al., 2006. Cigarette smoke drives small airway remodeling by induction of growth factors in the airway wall. *American journal of respiratory and critical care medicine*, 174(12): pp 1327–1334.

Churg, A. et al., 2004. Tumor necrosis factor-alpha drives 70% of cigarette smoke-induced emphysema in the mouse. *American journal of respiratory and critical care medicine*, 170(5): pp 492–498.

Cockroft, D.W., 2010. Direct challenge tests: Airway hyperresponsiveness in asthma: its measurement and clinical significance. *Chest*, 138(2 Suppl): pp 18S-24S.

Cosio, B.G. et al., 2004. Theophylline restores histone deacetylase activity and steroid responses in COPD macrophages. *The Journal of experimental medicine*, 200(5): pp 689–95.

Cosio, M.G. et al., 2009. Immunologic aspects of chronic obstructive pulmonary disease. *The New England journal of medicine*, 360(23): pp 2445–54.

Crapo, R.O. et al., 1981. Reference spirometric values using techniques and equipment that meet ATS recommendations. *The american review of respiratory disease*, 123(6): pp 659-664.

Culpitt, S. V. et al., 2003. Impaired inhibition by dexamethasone of cytokine release by alveolar macrophages from patients with chronic obstructive pulmonary disease. *American journal of respiratory and critical care medicine*, 167(1): pp 24–31.

Culpitt, S. V. et al., 2003. Inhibition by red wine extract, resveratrol, of cytokine release by alveolar macrophages in COPD. *Thorax*, 58(11): pp 942–946.

Di Stefano, A, et al., 1994. Upregulation of adhesion molecules in the bronchial mucosa of subjects with chronic obstructive bronchitis. *American journal of respiratory and critical care medicine*, 149(3): pp 803-810.

Dockery, D.W. & Pope, C. a, 1994. Acute respiratory effects of particulate air pollution. *Annual review of public health*, 15: pp 107–132.

Donaldson, K. et al., 2005. Combustion-derived nanoparticles: a review of their toxicology following inhalation exposure. *Particle and fibre toxicology*, 2: pp 10.

Donaldson, K. & Stone, V., 2003. Current hypotheses on the mechanisms of toxicity of ultrafine particles. *Annali dell'Istituto superiore di sanità*, 39(3): pp.405–10.

Donnelly, L.E. & Barnes, P.J., 2012. Defective phagocytosis in airways disease. *Chest*, 141(4): pp 1055–62.

Drost, E.M. et al., 2005. Oxidative stress and airway inflammation in severe exacerbations of COPD. *Thorax*, 60(4): pp 293–300.

Dorries, A.M. & Valberg, P.A., 1992. Heterogeneity of phagocytosis for inhaled versus instilled material. *The american review of respiratory disease,* 146(4): pp 831-837.

Dourado, V.Z. et al., 2006. Systemic manifestations in chronic obstructive pulmonary disease. *J Bras Pneumol*, 32(2): pp 161-171.

Van Eeden, S.F. et al., 2000. Neutrophils released from the bone marrow by granulocyte colony-stimulating factor sequester in lung microvessels but are slow to migrate. *The European respiratory journal*, 15(6): pp 1079–86.

Finkelstein, R. et al., 1995. Alveolar inflammation and its relation to emphysema in smokers. *American journal of respiratory and critical care medicine*, 152(5 Pt 1): pp 1666–72.

Flora, S.J.S. & Pachauri, V., 2010. Chelation in metal intoxication. *International journal of environmental research and public health*, 7(7): pp 2745-2788.

Gadgil, A. & Duncan, S.R., 2008. Role of T-lymphocytes and pro-inflammatory mediators in the pathogenesis of chronic obstructive pulmonary disease. *International journal of chronic obstructive pulmonary disease,* 3(4): pp 531-541.

Ghio, A.J. et al., 2000. Concentrated ambient air particles induce mild pulmonary inflammation in healthy human volunteers. *American journal of respiratory and critical care medicine,* 162(3 pt 1): pp 981-988.

Greenberg, S. & Grinstein, S., 2002. Phagocytosis and innate immunity. *Current opinion in immunology*, 14(1): pp 136–45.

Hart, J.E. & Laden, F., 2012. Occupational diesel exhaust exposure as a risk factor for chronic obstructive pulmonary disease. *Current opinion in pulmonary medicine*, 18(2): pp 151–4.

Hetland, R.B. et al., 2005. Cytokine release from alveolar macrophages exposed to ambient particulate matter: heterogeneity in relation to size, city and season. *Particle and fibre toxicology*, 2(4): pp 1-20.

Hiura, T.S. et al., 1999. Chemicals in diesel exhaust particles generate reactive oxygen radicals and induce apoptosis in macrophages. *The journal of immunology,* 163(10): pp 5582-5591.

Hiura, T.S. et al., 2000. The role of a mitochondrial pathway in the induction of apoptosis by chemicals extracted from diesel exhaust particles. *Journal of immunology (Baltimore, Md. : 1950)*, 165(5): pp 2703-2711.

Hodge, S. et al., 2003. Alveolar macrophages from subjects with chronic obstructive pulmonary disease are deficient in their ability to phagocytose apoptotic airway epithelial cells. *Immunology and cell biology*, 81(4): pp 289–296.

Hodge, S. et al., 2007. Smoking alters alveolar macrophage recognition and phagocytic ability: implications in chronic obstructive pulmonary disease. *American journal of respiratory cell and molecular biology,* 37(6): pp 748-755.

Hogg, J.C. et al. 2004. The nature if snall-airway obstruction in chronic obstructive pulmonary disease., *The new england journal of medicine,* 350(26): pp 2645-2653.

Hohlfeld, J. et al., 1997. The role of pulmonary surfactant in obstructive airways disease. *European Respiratory Journal*, 10(2): pp 482–491.

Holder, A.L. et al., 2008. Cellular response to diesel exhaust particles strongly depends on the exposure method. *Toxicological sciences : an official journal of the Society of Toxicology*, 103(1): pp 108–15.

Holloway, R. a & Donnelly, L.E., 2013. Immunopathogenesis of chronic obstructive pulmonary disease. *Current opinion in pulmonary medicine*, 19(2): pp 95–102.

Huang, Y.C. et al., 2003. The role of soluble components in ambient fine particles induced changes in human lungs and blood. *Inhalation toxicology*: 15(4): pp 327 -342.

Huang, S.L. et al., 2002. Contribution of endotoxin in macrophage cytokine response to ambient particles in vitro. *Journal of toxicology and environmental health. Part A,* 65(17): pp 1261-1272.

Imrich, A., et al., 2007. Alveolar macrophage cytokine response to air pollution particles: oxidant mechanisms. *Toxicology and applied pharmacology*, 218: pp 256-264.

Ishii, K.J. et al., 2008. Host innate immune receptors and beyond: making sense of microbial infections. *Cell host & microbe*, 3(6): pp 352–63.

Kafoury, R.M. & Madden, M.C., 2005. Diesel exhaust particles induce the over expression of tumour necrosis factor-alpha (TNF-alpha)gene in alveolar macrophages and failed to induce apoptosis through activation of nuclear factor-kappaB (NF-kappaB). *International research of environmental research and public health*, 2(1): pp 107-13.

Kampa, M. & Castanas, E., 2008. Human health effects of air pollution. *Environmental pollution (Barking, Essex : 1987)*, 151(2): pp 362–367.

Kawasaki, S. et al., 2001. Benzene-extracted components are important for rhe major activity of diesel exhaust particles: effect on interleukin-8 gene expression in human bronchial epithelial cells. *American journal of respiratory cell molecular biology*, 24(4): pp 419-426.

Keatings, V.M. et al., 1996. Differences in interleukin-8 and tumor necrosis factor-alpha in induced sputum from patients with chronic obstructive pulmonary disease or asthma. *American journal of respiratory and critical care medicine*, 153(2): pp 530–4.

Kim, V. & Criner, G.J., 2013. Chronic bronchitis and chronic obstructive pulmonary disease. *American journal of respiratory and critical care medicine*, 187(3): pp 228–37.

Kittelson, D.B. et al., 1999. Reviw of diesel particulate matter sampling methods.

Kittelson, D.B., 2001. Recent measurements of nanoparticle emissions from engines. Presented at the meeting on current research on diesel exhaust particles japan association of aerosol science and technology.

Kittelson, D.B., Watts, W.F. & Johnson, J.P., 2006. On-road and laboratory evaluation of combustion aerosols—Part1: Summary of diesel engine results. *Journal of Aerosol Science*, 37(8): pp 913–930.

Kobzik, L., 1995. Lung macrophage uptake of unopsonised environmental particulates. Role of scavenger-type receptors. *Journal of immunology.*, 155(1): pp 367-76.

Krivoshto, I.N. et al., 2008. The Toxicity of Diesel Exhaust : Implications for Primary Care. Journal of the american board of family medicine, 21(1): pp 55–62.

Kumagai, Y. & Taguchi, K., 2007. Toxicological effects of polycyclic aromatic hydrocarbon contaminated in diesel exhaust particles. *Asian journal of atmospheric environment*, 1(1): pp 28-35.

Lacey, D.C. et al., 2012. Defining GM-CSF- and macrophage-CSF-dependent macrophage responses by *in-vitro* models. *The american association of immunologists*, 188(11): pp 5752-5765.

Lahaye, J. & Ehrburger-Dolle, F., 1994. Mechanisms of carbon black formation. Correlation with the morphology of aggregates. *Carbon,* 32(7): pp 1319-1324.

Lehmann, A.D. et al., 2009. Diesel exhaust particles modulate the tight junction protein occludin in lung cells in vitro. *Particle and fibre toxicology*, 8(6) pp 1-14.

Lehnert, B.E., 1990. Alveolar macrophages in a particle "overload" condition. *Journal of aerosol medicine,* 3(s1): pp S9-S30.

Li, N. et al., 2002. Comparison of the pro-oxidative and proinflammatory effects of organic diesel exhaust particle chemicals in bronchial epithelial cells and

macrophages. *Journal of immunology (Baltimore, Md. : 1950)*, 169(8): pp 4531–41.

Li, N. et al., 2000. Induction of heme oxygenase-1 expression in macrophages by diesel exhaust particle chemicals and quinones via the antioxidant-responsive element. *Journal of immunology (Baltimore, Md. : 1950)*, 165(6), pp 3393–401.

Li, N. et al., 2003. Particulate air pollutants and asthma. *Clinical Immunology*, 109(3), pp 250–265.

Li, N. et al., 2003. Ultrafine particulate pollutants induce oxidative stress and mitochondrial damage. *Environmental health perspectives,* 111(4): pp 455-460.

Li, R. et al., 2010. Ultrafine particles from diesel vehicle emissions at different driving cycles induce differential vascular pro-inflammatory responses: implication of chemical components and NF-kappaB signaling. *Particle and fibre toxicology*, 7, p.6.

Libermann, T.A. & Baltimore, D., 1990. Activation of Interleukin-6 Gene Expression through the NF-KB Transcription Factor. *Molecular and cell biology*, 10(5): pp 2327-2334.

Löfdahl, J.M. et al., 2006. Different inflammatory cell pattern and macrophage phenotype in chronic obstructive pulmonary disease patients, smokers and non-smokers. *Clinical and experimental immunology*, 145(3): pp 428–37.

Løkke, A., et al., 2006. Developing COPD: a 25 year follow up study of the general population. *Thorax*, 61(11), pp.935–9.

Lopes, F.D., et al., 2009. Exposure to ambient levels of particulate matter emitted by traffic worsens emphysema in mice. *Environmental research,* 109(5): pp 544-551.

Lundborg, M. et al., 2006. Aggregates of ultrafine particles impair phagocytosis of microorganisms by human alveolar macrophages. *Environmental research*, 100(2): pp.197–204.

Ma, C. et al., 2004. Activation of nuclear factor kappa B by diesel exhaust particles in mouse epidermal cells through phophatidylinositol 3-kinase/Akt signaling pathway. *Biochemical pharmacology,* 67(10): pp1975- 983.

Ma, H., Jung, H. & Kittelson, D.B., 2008. Investigation of Diesel Nanoparticle Nucleation Mechanisms. *Aerosol Science and Technology*, 42(5): pp 335–342.

Ma, J.Y.C. & Ma, J.K.H., 2002. The dual effect of the particulate and organic components of diesel exhaust particles on the alteration of pulmonary immune/inflammatory responses and metabolic enzymes. *Journal of environmental science and health. Part C, Environmental carcinogenesis & ecotoxicology reviews*, 20(2): pp 117–47.

Macnee, W., & Donaldson, K., 2003. Mechanism of lung injury caused by PM10 and ultrafine particles with special reference COPD. *The european respiratory journal*. Supplement, 40: pp 47s-51s.

MacNee, W., 2005a. Pathogenesis of chronic obstructive pulmonary disease. *Proceedings of the American Thoracic Society*, 2(4): pp 258–66; discussion 290–1.

MacNee, W., 2005b. Pulmonary and systemic oxidant/antioxidant imbalance in chronic obstructive pulmonary disease. *Proceedings of the American Thoracic Society*, 2(1): pp 50–60.

Majo, J., Ghezzo, H. & Cosio, M.G., 2001. Lymphocyte population and apoptosis in the lungs of smokers and their relation to emphysema. *The European respiratory journal*, 17(5): pp 946–53.

Makris, D. & Bouros, D., 2009. COPD Exacerbation: lost in translation. *BMC Pulmonary medicine,* 9(6): pp 1-3.

Mcclellan, R.O., 1987. Health effects of exposure to diesel exhaust particles. *Annual review of pharmacology and toxicology*, 27: pp 279-300.

McCusker, K. & Hoidal, L., 1990. Selective increase of antioxidant enzyme activity in the alveolar macrophages from cigarette smokers and smoke-exposed hamsters. *The american review of respiratory disease,* 141(3): pp678-82.

Mcdonald, J.D. et al., 2011. Engine-Operating Load Influences Diesel Exhaust Composition and Cardiopulmonary and Immune Responses. *Environmental health perspectives,* 119(8): pp 1136–1141.

McManus, T.E. et al., 2008. Respiratory viral infection in exacerbations of COPD. *Respiratory medicine*, 102(11): pp 1575–80.

Medina-Ramón, M. et al., 2006. The effect of ozone and PM10 on hospital admissions for pneumonia and chronic obstructive pulmonary disease: a national multicity study. *American journal of epidemiology,* 163(6): pp 579-588.

Möller, W. et al., 2002. Ultrafine particles cause cytoskeletal dysfunctions in macrophages., *Toxicology and applied pharmacology,* 182(3): pp 197-207.

Möller, W. et al., 2005. Ultrafine particles cause cytoskeletal dysfunctions in macrophafes: role of intracellular calcium. *Particle and fibre toxicology,* 2(7): pp 1-12.

Morrow, P.E. et al., 1988. Possible mechanisms to explain dust overloading of the lungs. *Fundamental and applied toxicology: official journal of the society of toxicology,* 10(3): pp 369-384.

Müller, L. et al., 2010. Oxidative stress and inflammation response after nanoparticle exposure: differences between human lung cell monocultures and an advanced

three-dimensional model of the human epithelial airways. *Journal of the Royal Society, Interface / the Royal Society*, 7 Suppl 1: pp S27–40.

Murphy, S. A. et al., 1999. Bioreactivity of carbon black and diesel exhaust particles to primary Clara and type II epithelial cell cultures. *Occupational and environmental medicine*, 56(12): pp.813–9.

Murugan, V. & Peck, M.J., 2009. Signal transduction pathways linking the activation of alveolar macrophages with the recruitment of neutrophils to lungs in chronic obstructive pulmonary disease. *Experimental lung research*, 35(6): pp 439-485.

Nebreda, A.R. & Porras, A., 2000. p38 MAP kinases: beyond the stress response. *Trends in biochemical sciences,* 25(6): pp257-260.

Nightingale, J. a et al., 2000. Airway inflammation after controlled exposure to diesel exhaust particulates. *American journal of respiratory and critical care medicine*, 162(1): pp 161–166.

Nordernhäll, C. et al., 2001. Diesel exhaust enhances airway responsiveness in asthmatic subjects. *The european respiratory journal,* 17(5): pp 909-915.

Nordenhäll, C. et al., 2000. Airway inflammation following exposure to diesel exhaust: a study of time kinetics using induced sputum. *European respiratory journal,* 15(6): pp 1046-1051.

O'Donnell, D.E. & amaer, C.M., 2006. COPD exacerbations . 3: Pathophysiology. *Thorax*, 61(4): pp 354–61.

Oberdörster, G., Ferin, J. & Lehnert, B.E., 1994. Correlation between particle size, *in vivo* particle persistence, and Lung injury. *Environmental health perspectives*, 102(Suppl 4): pp 173–179.

Oberdöster, G., 2001. Pulmonary effects of inhaled ultrafine particles. *International archives of occupational and environmental health,* 74(1): pp 1-8.

Ochoa, C.E. et al., 2011. Interleukin 6, but not T helper 2 cytokines, promotes lung carcinogenesis. *Cancer prevention research (Philadelphia, Pa.)*, 4(1): pp 51–64.

Olmo, N.R.S. et al., 2011. A review of low-level air pollution and adverse effects on human health: implications for epidemiological studies and public policy. *Clinics*, 66(4): pp 681–690.

Ono-Ogasawara, M. & Smith, T.J., 2004. Diesel exhaust particles in the work environment and their analysis. *Industrial health*, 42(4): pp.389–99.

Overbeek, S. A. et al., 2013. Cigarette smoke-induced collagen destruction; key to chronic neutrophilic airway inflammation? *PloS one*, 8(1): p.e55612.

Palecanda, A. et al., 1999. Role of scavenger receptor MARCO in alveolar macrophage binding of unopsonised environmental particles. *Journal of experimental medicine.,* 189 (9): pp 1497-1506.

Park, S. et al., 2006. The role of iron in reactive oxygen species generation from diesel exhaust particles. *Toxicology in vitro: an international journal published in association with BIBRA,* 20(6): pp 851-7.

Park, E. et al., 2011. Biological Responses to Diesel Exhaust Particles (DEPs) Depend on the Physicochemical Properties of the DEPs. , 6(10): pp 1–10.

Parker, L.C. et al., 2005. The expression and roles of Toll-like receptors in the biology of the human neutrophil. *Journal of leukocyte biology,* 77(6): pp 886-892.

Pons, A. R. et al., 2005. Phenotypic characterisation of alveolar macrophages and peripheral blood monocytes in COPD. *The European respiratory journal*, 25(4): pp 647–52.

Pourazer, J. et al., 2008. Diesel exhaust increases EGFR and phosphorylated C-terminal Tyr 1173 in the bronchial epithelium. *Particle and fibre toxicology*, 5(8): pp 1-9.

Quint, J.K. & Wedzicha, J.A., 2007. The neutrophil in chronic obstructive pulmonary disease. *The Journal of allergy and clinical immunology*, 119(5): pp 1065–71.

Rahman, I. & Macnee, W, 1996. Oxidant/antioxidant imbalance in smokers and chronic obstructive pulmonary disease. *Thorax,* 51: pp 348-350.

Rahman, I., 2005. Oxidative Stress in Pathogenesis of Chronic obstructive pulmonary disease: cellular and molecular mechanims. Cell biochemistry and biphysics, 43(1): pp 167–188.

Renda, T. et al., 2008. Increased activation of p38 MAPK in COPD. *The European respiratory journal*, 31(1): pp 62–69.

Renwick, L.C., Donaldson, K. & Clouter, a, 2001. Impairment of alveolar macrophage phagocytosis by ultrafine particles. *Toxicology and applied pharmacology*, 172(2): pp 119–27.

Retamales, I. et al., 2001. Amplification of inflammation in emphysema and its association with latent adenoviral infection. *American journal of respiratory and critical care medicine*, 164(3): pp 469–73.

Rönkkö, T. et al., 2006. Effect of dilution conditions and driving parameters on nucleation mode particles in diesel exhaust: Laboratory and on-road study. *Atmospheric Environment*, 40(16): pp 2893–2901.

Rovina, N. et al., 2013. Inflammation and immune response in COPD: Where do we stand? *Mediators of inflammation*, 2013(2013): pp 413735.

Russell, R.E.K. et al., 2002. Alveolar macrophage-mediated elastolysis: roles of matrix metalloproteinases, cysteine, and serine proteases. *American journal of physiology. Lung cellular and molecular physiology*, 283(4): pp L867–73.

Rytilä, P. et al., 2006. Increased oxidative stress in asymptomatic current chronic smokers and GOLD stage 0 COPD. *Respiratory research*, 7(69): pp 1-10.

Saetta, M. et al., 2000. Goblet cell hyperplasia and epithelial inflammation in peripheral airways of smokers with both symptoms of chronic bronchitis and chronic airflow limitation. *American journal of respiratory and critical care medicine*,161(3): pp 1016-1021.

Sagai, M. et al., 1993. Biological effects of diesel exhaust particles.I. In vitro production of superoxide and in vivo toxicity in mouse. *Free radical biology and medicine*, 14(1): pp 37-47.

Sagai, M. et al., 1996. Biological effects of diesel exhaust particles (DEP). III. Pathogenesis of asthma like symptoms in mice. *Free radical biology & medicine,* 21(2): pp 199-209.

Saitoh, K. et al., 2003. Determination of elemental and ionic compositions for diesel exhaust particles by particle induced X-ray emission and ion chromatography analysis. *Analytical sciences : the international journal of the Japan Society for Analytical Chemistry*, 19(4): pp 525–8.

Salvi, S. et al., 1999. Acute inflammatory responses in the airways and peripheral blood after short-term exposure to diesel exhaust in healthy human volunteers. *American journal of respiratory and critical care medicine*, 159(3): pp 702–9.

Saxena, R.K. et al., 2008. Isolation and quantitative estimation of diesel exhaust and carbon black particles ingested by lung epithelial cells and alveolar macrophages in vitro. *Biotechniques*, 44(6): pp 799-805.

Schleimer, R.P., 2005. Innate immune responses and chronic obstructive pulmonary disease: “Terminator” or “Terminator 2”? *Proceedings of the American Thoracic Society*, 2(4), pp.342–6; discussion 371–2.

Schneider, J. et al., 2005. Nucleation particles in diesel exhaust: composition inferred from in situ mass spectrometric analysis. *Environmental science & technology*, 39(16): pp 6153–61.

Schurch, S., et al., 1992. Pulmonary surfactant: Surface properties and function of alveolar and airway surfactant. *Pure and Applied Chemistry*, 64(11): pp 1745–1750.

Schwarze, P.E. et al., 2013. Inflammation-related effects of diesel engine exhaust particles: studies on lung cells in vitro. *BioMed research international*, 2013, p.685142.

Sehlstedt, M. et al., 2010. Airway inflammatory response to diesel exhaust generated at urban cycle running conditions. *Inhalation toxicology*, 22(14): pp 1144-1150.

Seemugal, T. et al., 2001. Respiratory viruses, symptoms, and inflammatory markers in acute exacerbations and stable chronic obstructive pulmonary disease. *American journal of respiratory and critical care medicine*, 164(9): pp 1618-1623.

Seger, R. & Krebs, E.G., 1995. The MAPK signaling cascade. *FASEB Journal: Official publication of the federation of american societies for experimental biology,* 9(9): pp 726-735.

Sethi, S., 2000. Bacterial infection and the pathogenesis of COPD. *Chest.*, 117(5 Suppl 1): pp 286S-91S.

Sethi, S., 2011. Molecular diagnosis of respiratory tract infection in acute exacerbations of chronic obstructive pulmonary disease. *Clinical infectious diseases,* 52(4): pp S290-S295.

Shaw, C. A. et al., 2011. Diesel exhaust particulate--exposed macrophages cause marked endothelial cell activation. *American journal of respiratory cell and molecular biology*, 44(6): pp.840–51.

Shi, X.C., et al., 2010. Mutagenicity of Diesel Exhaust Particles from an Engine with Differing Exhaust After Treatments. *Journal of Toxicology and Environmental Health , Part A : Current Issues,* (March 2013), 73(19): pp 37–41.

Sikkel, M.S. et al., 2008. Respiratory synticial virus persistence in chronic obstructive pulmonary disease. *The paediatric infectious diesease journal,* 27(10 suppl): pp S63-70.

Sint, T., et al., 2008. Ambient air pollution particles and the acute exacerbation of chronic pulmonary disease. *Inhalation toxicology,* 20(1): pp 25-29.

Smith, S.J. et al., 2006. Inhibitory effect of p38 mitogen-activated protein kinase inhibitors on cytokine release from human macrophages. *British journal of pharmacology*, 149(4): pp 393–404.

Sonibare, J.A., 2011. A critical review of natural gas flares-induced secondary air pollutants. *Global NEST journal,* 13(1), pp 74–89.

Sunyer, J. et al., 1993. Air pollution and emergency room admissions for chronic obstructive pulmonary disease: a 5-year study. *American journal of epidemiology*, 137(7): pp 701–5.

Sunyer, J. et al., 2000. Patients with chronic obstructive pulmonary disease are at increased risk of death associated with urban particle air pollution: a case-crossover analysis. *American journal of epidemiology*, 151(1): pp 50–56.

Takano, H. et al., 2002. Diesel exhaust particles enhance lung injury related to bacterial and endotoxin through expression of proinflammatory cytoines, chemokines, and intracellular adhesion molecule-1. *American journal of respiratory and critical care medicine,* 165(9): pp 1329-1335.

Taylor, A. E. et al., 2010. Defective macrophage phagocytosis of bacteria in COPD. *The European respiratory journal : official journal of the European Society for Clinical Respiratory Physiology*, 35(5): pp 1039–47.

Taylor, P.R. et al., 2005. Macrophage receptors and immune recognition. *Annual review of immunology*, 23: pp.901–44.

Teeguarden, J.G. et al., 2007. Particokinetics in vitro: Dosimetry considerations for in vitro nanoparticle toxicity assessments. *Toxicological sciences,* 95(2): pp 300-312.

Thorley, A.J., & Tetley, T.D., 2007. Pulmonary epithelium, cigarette smoke, and chronic obstructive pulmonary disease. *International journal of chronic obstructive pulmonary disease,* 2(4): pp 409-28.

Totlandsdal, A.I. et al., 2010. Diesel exhaust particles induce CYP1A1 and pro-inflammatory responses via differential pathways in human bronchial epithelial cells. *Particle and fibre toxicology*, 7(1): pp 7-41.

Totlandsdal, A.I. et al., 2012. Differential effects of the particle core and organic extract of diesel exhaust particles. *Toxicology letters,* 208(3): pp 262-268.

Totlandsdal, A.I. et al., 2013. Differential proinflammatory responses induced by diesel exhaust particles with contrasting PAH and metal content. Environmental toxicology, [Epub ahead of print].

Tran, C.L. et al., 2000. Inhalation of poorly soluble particles. II. Influence of particle surface area on inflammation and clearance. *Inhalation toxicology,* 12(12): pp 1113-26.

Tudhope, S.J., Finney-Hayward, T.K., et al., 2008. Different mitogen-activated protein kinase-dependent cytokine responses in cells of the monocyte lineage. *The Journal of pharmacology and experimental therapeutics*, 324(1), pp.306–12.

Twigg, H.L., 2004. Macrophages in innate and acquired immunity. *Seminars in respiratory and critical care medicine*, 25(1): pp 21–31.

Twigg, H.L. & Phillips, P.R., (2009). Cleaning the air we breathe - controlling diesel particulate emissions from passenger cars. *Platinum metals review*, 53(1), pp 27-34.

Ulvestad, B. et al., 2000. Increased risk of obstructive pulmonary disease in tunnel workers. *Thorax*, 55(4): pp 277–82.

Vattanasit, U. et al., 2013. Oxidative DNA damage and inflammatory responses in cultured human cells and in humans exposed to traffic-related particles. *International journal of hygiene and environmental health*, 217(1): pp 1–11.

Vermaelen, K. & Brusselle, G., 2013. Exposing a deadly alliance: Novel insights into the biological links between COPD and lung cancer. *Pulmonary pharmacology & therapeutics*, 26(5): pp 544–54.

Vestbo, J. et al., 2012. Global Strategy for the Diagnosis, Management and Prevention of Chronic Obstructive Pulmonary Disease GOLD EXECUTIVE SUMMARY. *American journal of respiratory and critical care and medicine,* pp 1–67.

Vestbo, J. & Hogg, J.C., 2006. Convergence of the epidemiology and pathology of COPD. *Thorax,* 61(1): pp 86-88.

Vogel, C.F.A. et al., 2005. Induction of pro-inflammatory cytokines and c-reactive protein in human macrophage cell line U937 exposed to air pollution particulates. *Environmental health perspectives*, 113(11): pp 1536-1541.

Wannar, H.U., (1993). Sources of pollutants in indoor air. *IARC scientific publications*. 109: pp 19-30

Warheit, D.B & Hartsky, M.A., 1993. Role of alveolar macrophage chemotaxis and phagocytosis in pulmonary clearance responses to inhaled particles: comparisons among rodent species. *Microscopy research and technique*, 26(5): pp 412-422.

Wedzicha, J.A., & Donaldson, K., 2003. Exacerbations of chronic obstructive pulmonary disease. *Respiratory care*, 48(12): pp 1204-1213.

Wichmann, H.-E., 2007. Diesel exhaust particles. *Inhalation toxicology*, 19 (Suppl 1): pp 241–4.

Winkler, A.R. et al., 2008. In vitro modeling of human alveolar macrophage smoke exposure: enhanced inflammation and impaired function. *Experimental lung research*, 34(9): pp 599–629.

Wright, J.L. et al., 2012. Pulmonary hypertension and vascular oxidative damage in cigarette smoke exposed eNOS (-/-) mice and human smokers. *Inhalation toxicology,* 24(11): pp 732 -40.

Xia, T. et al., 2004. Quinones and aromatic chemical compounds in particulate matter induce mitochondrial dysfunction: implications for ultrafine particle toxicity. *Environmental health perspectives,* 112(14): pp1347-1358.

Xiao, G.G. et al., 2003. Use of proteomics to demonstrate a hierarchical oxidative stress response to diesel exhaust particle chemicals in a macrophage cell line. *The journal of biological chemistry*, 278(50): pp 50781-50790.

Yang, H.M. et al., 2001. Diesel exhaust particles suppress macrophage function and slow the pulmonary clearance of Listeria monocytogenes in rats. *Environmental health perspectives*, 109(5): pp 515–21.

Yin, X.J., et al., 2005. Sustained effect of diesel exhaust particles on T-lymphocyte-mediated immune responses against Listeria monocytogenes. *Toxicological studies*, 88(1): pp 73-81.

Yin, X.J. et al., 2007. Suppression of phagocytic and bactericidal functions of rat alveolar macrophages by the organic component of diesel exhaust particles. *Journal of toxicology and environmental health. Part A*, 70(10): pp 820–828.

Yoshida, T. & Tuder, R.M., 2007. Pathophysiology of cugarret smoke-induced chronic obstructive pulmonary disease. *American pysiological society,* 87(3): pp 1047-1082.

Kim, Y.M. et al., 2005. Ultrafine carbon particles induce interleukin-8 gene transcription and p38 MAPK activation in normal human bronchial epithelial cells. *American Journal of physiological society - Lung cellular and molecular physiology*, 290: pp L1028 - L1035.

Zanobetti, P., et al., 2008. Particulate air pollution and survival in COPD cohort. Environmental health. *Environmental health,* 7(48): pp 1-9.

Zhou, H. & Kobzik, L., 2007. Effect of concentrated ambient particles on macrophage phagocytosis and killing of Streptococcus pneumoniae. *American journal of respiratory cell and molecular biology*, 36(4): pp 460–465.

Web Documents:

- Global Initiative for Chronic Obstructive Lung Diseases (GOLD, 2014): http://www.goldcopd.org/uploads/users/files/GOLD_Report2014_Feb07.pdf

Image in Introduction:

- **Figure 1.4 Key Features of COPD Pathophysiology**
  http://www.pennmedicine.org/encyclopedia/em_PrintArticle.aspx?gcid=001087
  http://www.flickr.com/photos/30950973@N03/4858474968)

Appendix I:

Consent Forms

Royal Brompton & Harefield NHS Trust & National Heart and Lung Institute

FORM OF CONSENT *ADULT VOLUNTEER Healthy non- smokers*

TITLE OF PROJECT:
Macrophage Phagocytosis in COPD

EXPLANATION OF PROJECT:

Invitation:
We are inviting you to take part in a research study. We are asking you to take part in this study because you are a non-smoker. Before you decide it is important for you to understand why the research is being done and what it will involve. Please take time to read the following information carefully and discuss it with friends, relatives and your GP if you wish. Ask us if there is anything that is not clear or if you would like more information. Take time to decide whether or not you wish to take part.

Do I have to take part?
It is up to you to decide whether or not to take part. If you do decide to take part you will be given this information sheet to keep and be asked to sign a consent form. If you decide to take part you are still free to withdraw at any time and without giving a reason.

Why is the study being done?
Chronic obstructive pulmonary disease (COPD for short) involves inflammation inside the air passages of the lungs. This inflammation might be partly responsible for the shortness of breath, cough and susceptibility to chest infections that form part of COPD. We know that the inflammation involves special chemicals, or mediators, that attract white blood cells from the blood into the air passages. Once inside the air passages, the white blood cells may change (or 'differentiate') and release more mediators and attract more white cells. In COPD, one set of white cells called macrophages, appear unable to function properly. One role for these cells is to remove any inhaled particles including bacteria. In COPD, macrophages are less able to remove bacteria when compared with cells from healthy people. This may make these patients more prone to infection. We are asking you to take part in this study because you are a healthy non-smoker and do not have COPD and we would like to compare the way your white cells behave with those from COPD patients and healthy smokers. We would like to take a blood sample (which contains white cells). We will then differentiate these cells in the laboratory and then measure the way these cells remove particles. We will then see if we can improve this removal process with drugs in the laboratory. We will then identify what it is on the surface of the cells that are responsible for this. This may involve

Signed by the person in charge of the Project _____ Date 8/11/05

The Ethics Committee of the Royal Brompton & Harefield NHS Trust/National Heart & Lung Institute has approved the above statement.
Signed by the Chairman/Representative of the Committee

_____ Date 1-12-05

DOCTOR'S DECLARATION

I have explained the project to the Participant as outlined above in the presence/absence* of a Witness**

Signed _____ Date _____ Time _____

* delete as appropriate ** every effort should be made to give the explanation in the presence of a witness

Protocol Reference Number: 05/Q0404/111
Version 2

extracting ribonucleic acids or RNA from your white cells to see which genes are involved.

What the study involves

The study involves doing some tests on your lungs to find out how they are functioning. We do this by asking you to blow into a machine. We will then take a blood sample from your arm of about four tablespoons full (60ml). We may ask you for further samples at future visits.

What risks are there?

There is a risk of a small bruise from blood sampling and a small risk of fainting in a few subjects

What will happen to my blood samples?

The white blood cells will be separated from the rest of the blood sample (isolated) and then grown in the laboratory. We will then test the ability of these cells to remove particles. Some of your blood samples may be kept to isolate RNA to look for increased receptor or expression of proteins that may regulate the removal process. We would ask you to make a gift of your sample to the Institute. This means you would relinquish all rights to it for the future. After this project, we might therefore retain it for possible future research. We would not ask you for any further permission to do this, but any future testing would have received approval from a Research Ethics Committee. Your sample will be coded but not labelled with your name. Although this research study does involve the examination of genes, it does not involve a test for any specific condition. Therefore you need not declare participation in this study in any request regarding genetic testing (for example on insurance forms or mortgage application forms). No testing for serious communicable disease (for example HIV and Hepatitis B) testing will be done.

What benefits are there for you?

It is very unlikely that you will get any direct benefit from participating in this study.

What benefits may the research bring to other people?

It is possible that this research will improve our understanding of how airway inflammation in COPD can be reduced. This may be of benefit to patients in the future and may influence how we do further research into COPD.

Thank you for reading this document. You are encouraged to ask any questions you may have. Please remember that you may withdraw from this study at any time and without giving any reason. Please understand that you need not take part in this trial if you do not wish to. If you do take part, you may withdraw at any time, and need give no reason for doing so.

Imperial College holds Public Liability ("negligent harm") and Clinical Trial ("non-negligent harm") insurance policies which apply to this trial. If you can demonstrate that you experienced harm or injury as a result of your participation in this trial, you will be eligible to claim compensation without having to prove that Imperial College is at fault.
If the injury resulted from any procedure which is not part of the trial, Imperial College will not be required to compensate you in this way. Your legal rights to claim compensation for injury where you can prove negligence are not affected.

Thank you very much for your kindness in considering this project.

Signed by Chairman/Representative of the Royal Brompton & Harefield NHS Trust/N.H.L.I. Ethics Committee.

Derek Gibb

Protocol Reference Number: 05/Q0404/111

Version 2 Page2

FORM OF CONSENT

(for use by Volunteers undergoing investigations connected with clinical research)

I, _____ of _____

_____

give my consent to undergo the research procedures described overleaf. The nature, purpose and possible consequences have been fully explained to me.

Signed _____ Date _____

If you decide to take part in this project, you will be given a copy of this form for your information.

WITNESS

I am satisfied that the procedures have been fully explained to the Volunteer. The Volunteer has given consent in my presence.

Name of Witness _____ Position _____

Address _____

Signed _____ Date _____

Royal Brompton & Harefield NHS Trust & National Heart and Lung Institute

FORM OF CONSENT *ADULT VOLUNTEER Healthy smokers*

TITLE OF PROJECT:
Macrophage Phagocytosis in COPD

EXPLANATION OF PROJECT:

Invitation:
We are inviting you to take part in a research study. We are asking you to take part in this study because you are a smoker. Before you decide it is important for you to understand why the research is being done and what it will involve. Please take time to read the following information carefully and discuss it with friends, relatives and your GP if you wish. Ask us if there is anything that is not clear or if you would like more information. Take time to decide whether or not you wish to take part.

Do I have to take part?
It is up to you to decide whether or not to take part. If you do decide to take part you will be given this information sheet to keep and be asked to sign a consent form. If you decide to take part you are still free to withdraw at any time and without giving a reason.

Why is the study being done?
Chronic obstructive pulmonary disease (COPD for short) involves inflammation inside the air passages of the lungs. This inflammation might be partly responsible for the shortness of breath, cough and susceptibility to chest infections that form part of COPD. We know that the inflammation involves special chemicals, or mediators, that attract white blood cells from the blood into the air passages. Once inside the air passages, the white blood cells may change (or 'differentiate') and release more mediators and attract more white cells. In COPD, one set of white cells called macrophages, appear unable to function properly. One role for these cells is to remove any inhaled particles including bacteria. In COPD, macrophages are less able to remove bacteria when compared with cells from healthy people. This may make these patients more prone to infection. We are asking you to take part in this study because you are a smoker and do not have COPD and we would like to compare the way your white cells behave with those from COPD patients and healthy non-smokers. We would like to take a blood sample (which contains white cells). We will then differentiate these cells in the laboratory and then measure the way these cells remove particles. We will then see if we can improve this removal process with drugs in the laboratory. We will then identify what it is on the surface of the cells that are responsible for this. This may involve extracting ribonucleic acids or RNA from your white cells to see which genes are involved.

Signed by the person in charge of the Project _____ Date 18/11/05

The Ethics Committee of the Royal Brompton & Harefield NHS Trust/National Heart & Lung Institute has approved the above statement.
Signed by the Chairman/Representative of the Committee

_____ Date 1.12.05

DOCTOR'S DECLARATION

I have explained the project to the Participant as outlined above in the presence/absence* of a Witness**

Signed _____ Date _____ Time _____

* delete as appropriate ** every effort should be made to give the explanation in the presence of a witness

Protocol Reference Number: 05/Q0404/111
Version 2

What the study involves
The study involves doing some tests on your lungs to find out how they are functioning. We do this by asking you to blow into a machine. We will then take a blood sample from your arm of about four tablespoons full (60ml). We may ask you for further samples at future visits.

What risks are there?
There is a risk of a small bruise from blood sampling and a small risk of fainting in a few subjects.

What will happen to my blood samples?
The white blood cells will be separated from the rest of the blood sample (isolated) and then grown in the laboratory. We will then test the ability of these cells to remove particles. Some of your blood samples may be kept to isolate RNA to look for increased receptor or expression of proteins that may regulate the removal process. We would ask you to make a gift of your sample to the Institute. This means you would relinquish all rights to it for the future. After this project, we might therefore retain it for possible future research. We would not ask you for any further permission to do this, but any future testing would have received approval from a Research Ethics Committee. Your sample will be coded but not labelled with your name. Although this research study does involve the examination of genes, it does not involve a test for any specific condition. Therefore you need not declare participation in this study in any request regarding genetic testing (for example on insurance forms or mortgage application forms). No testing for serious communicable disease (for example HIV and Hepatitis B) testing will be done.

What benefits are there for you?
It is very unlikely that you will get any direct benefit from participating in this study.

What benefits may the research bring to other people?
It is possible that this research will improve our understanding of how airway inflammation in COPD can be reduced. This may be of benefit to patients in the future and may influence how we do further research into COPD.

Thank you for reading this document. You are encouraged to ask any questions you may have. Please remember that you may withdraw from this study at any time and without giving any reason. Please understand that you need not take part in this trial if you do not wish to. If you do take part, you may withdraw at any time, and need give no reason for doing so.

Imperial College holds Public Liability ("negligent harm") and Clinical Trial ("non-negligent harm") insurance policies which apply to this trial. If you can demonstrate that you experienced harm or injury as a result of your participation in this trial, you will be eligible to claim compensation without having to prove that Imperial College is at fault.

If the injury resulted from any procedure which is not part of the trial, Imperial College will not be required to compensate you in this way. Your legal rights to claim compensation for injury where you can prove negligence are not affected.

Thank you very much for your kindness in considering this project.

Signed by Chairman/Representative of the Royal Brompton & Harefield NHS Trust/N.H.L.I. Ethics Committee.

FORM OF CONSENT

(for use by Volunteers undergoing investigations connected with clinical research)

I, _____ of _____

_____

give my consent to undergo the research procedures described overleaf. The nature, purpose and possible consequences have been fully explained to me.

_____

Signed _____ Date _____

If you decide to take part in this project, you will be given a copy of this form for your information.

WITNESS

I am satisfied that the procedures have been fully explained to the Volunteer. The Volunteer has given consent in my presence.

Name of Witness _____ Position _____

Address _____

Signed _____ Date _____

Royal Brompton & Harefield NHS Trust & National Heart and Lung Institute

FORM OF CONSENT *ADULT PATIENT*

TITLE OF PROJECT:
Macrophage Phagocytosis in COPD

EXPLANATION OF PROJECT:

Invitation:
We are inviting you to take part in a research study. We are asking you to take part in this study because you have chronic obstructive pulmonary disease (COPD for short). Before you decide it is important for you to understand why the research is being done and what it will involve. Please take time to read the following information carefully and discuss it with friends, relatives and your GP if you wish. Ask us if there is anything that is not clear or if you would like more information. Take time to decide whether or not you wish to take part.

Do I have to take part?
It is up to you to decide whether or not to take part. If you do decide to take part you will be given this information sheet to keep and be asked to sign a consent form. If you decide to take part you are still free to withdraw at any time and without giving a reason.

Why is the study being done?
COPD involves inflammation inside the air passages of the lungs. This inflammation might be partly responsible for the shortness of breath, cough and susceptibility to chest infections that form part of COPD. We know that the inflammation involves special chemicals, or mediators, that attract white blood cells from the blood into the air passages. Once inside the air passages, the white blood cells may change (or 'differentiate') and release more mediators and attract more white cells. In COPD, one set of white cells called macrophages, appear unable to function properly. One role for these cells is to remove any inhaled particles including bacteria. In COPD, macrophages are less able to remove bacteria when compared with cells from healthy people. This may make patients more prone to infection. We are asking you to take part in this study because you have COPD and we would like to compare the way your white cells behave with those from smokers and healthy non-smokers. We would like to take a blood sample (which contains white cells). We will then differentiate these cells in the laboratory and then measure the way these cells remove particles. We will then see if we can improve this removal process with drugs in the laboratory. We will then identify what it is on the surface of the cells that are responsible for this. This may involve extracting ribonucleic acids or RNA from your white cells to see which genes are involved.

Signed by the person in charge of the Project _____ Date 18/11/05

The Ethics Committee of the Royal Brompton & Harefield NHS Trust/National Heart & Lung Institute has approved the above statement.
Signed by the Chairman/Representative of the Committee

_____ Date 1.12.05

DOCTOR'S DECLARATION

I have explained the project to the Participant as outlined above in the presence/absence* of a Witness**

Signed _____ Date _____ Time _____

* delete as appropriate ** every effort should be made to give the explanation in the presence of a witness

Protocol Reference Number: 05/Q0404/111
Version 2

What the study involves
The study involves doing some tests on your lungs to find out how they are functioning. We do this by asking you to blow into a machine. We will then take a blood sample from your arm of about four tablespoons full (60ml). We may ask you for further samples at future visits.

What risks are there?
There is a risk of a small bruise from blood sampling and a small risk of fainting in a few subjects

What will happen to my blood samples?
The white blood cells will be separated from the rest of the blood sample (isolated) and then grown in the laboratory. We will then test the ability of these cells to remove particles. Some of your blood samples may be kept to isolate RNA to look for increased receptor or expression of proteins that may regulate the removal process. We would ask you to make a gift of your sample to the Institute. This means you would relinquish all rights to it for the future. After this project, we might therefore retain it for possible future research. We would not ask you for any further permission to do this, but any future testing would have received approval from a Research Ethics Committee. Your sample will be coded but not labelled with your name. Although this research study does involve the examination of genes, it does not involve a test for any specific condition. Therefore you need not declare participation in this study in any request regarding genetic testing (for example on insurance forms or mortgage application forms). No testing for serious communicable disease (for example HIV and Hepatitis B) testing will be done.

What benefits are there for you?
It is very unlikely that you will get any direct benefit from participating in this study.

What benefits may the research bring to other people?
It is possible that this research will improve our understanding of how airway inflammation in COPD can be reduced. This may be of benefit to patients in the future and may influence how we do further research into COPD.

Thank you for reading this document. You are encouraged to ask any questions you may have. Please remember that you may withdraw from this study at any time and without giving any reason. Please understand that you need not take part in this trial if you do not wish to. If you do take part, you may withdraw at any time, and need give no reason for doing so.

Imperial College holds Public Liability ("negligent harm") and Clinical Trial ("non-negligent harm") insurance policies which apply to this trial. If you can demonstrate that you experienced harm or injury as a result of your participation in this trial, you will be eligible to claim compensation without having to prove that Imperial College is at fault.

If the injury resulted from any procedure which is not part of the trial, Imperial College will not be required to compensate you in this way. Your legal rights to claim compensation for injury where you can prove negligence are not affected.

Thank you very much for your kindness in considering this project.

Signed by Chairman/Representative of the Royal Brompton & Harefield NHS Trust/N.H.L.I. Ethics Committee.

Derek Gibb

Protocol Reference Number: 05/Q0404/111

Version 2

FORM OF CONSENT

(for use by Volunteers undergoing investigations connected with clinical research)

I, _____ of _____

_____

give my consent to undergo the research procedures described overleaf. The nature, purpose and possible consequences have been fully explained to me.

_____

Signed _____ Date _____

If you decide to take part in this project, you will be given a copy of this form for your information.

WITNESS

I am satisfied that the procedures have been fully explained to the Volunteer. The Volunteer has given consent in my presence.

Name of Witness _____ Position _____

Address _____

Signed _____ Date _____

Appendix II:

Patient Demographics

	AGE	SEX	FEV1	FEV1 %	FVC	FEV1:FVC
JiM050912	62	F	2.1	79	2.78	0.755396
MaGO120612	76	M	2.87	90.50	3.67	0.78
CLC	66	F	2.28	97	3.2	0.71
GiD	51	F	3.23	118.50	4.09	0.789731
JeL270912	64	f	2.53	94.5	3.67	0.689373
STJ260912	63	M	3.1	103.5	4.55	0.681319
ToK141009	38	M	3.34	98.6	3.26	1.02454
ChB020811	62	M	3.42	114.9	4.68	0.730769
JuB030310	54	F	1.69	94.9	2.26	0.75
NeA	44	M	3.18	79.5	3.76	0.845745
JAW161112	56	F	4.17	151.2	5.16	0.81
MaGO120612	76	M	2.87	90.50	3.67	0.78
MaBa070110	53	F	1.66	74	2.31	0.718615
LiH230311	56	F	2.6	116.2	3.28	0.792683
PaB231009	42	M	3.80	95.00	4.40	0.86
PeF181109	42	M	4.54	106.00	6.14	0.74
AnR230410	71	F	1.97	97.2	3.02	0.65
DaL211009	56	M	3.28	86.30	5.01	0.65
LaU271009	59	F	1.96	115	2.45	0.8
liF200410	63	F	2.22	90	2.81	0.790036
LoD301009	46	F	3.10	103.00	3.42	0.91
GeC	59	m	3.51	97.00	4.38	0.80
LaU021109	46	M	3.55	93	4.74	0.74
DoP040510	72	F	1.23	68.8	1.61	0.763975
MaT	70	f	2.73	112.30	3.50	0.78
MOC	57	F	2.69	103	3.49	0.770774
JAB220413	48	M	4.53	120.1	5.84	0.78
TEL230611	44	F	2.49	106.4	2.92	0.85
GAW	unknown	unknown	unknwon	unknown	unknown	unkown

Appendix II Table 1: Basic Demographics of Non-Smoker Participants Recruited for the Study.

Basic lung function data of non-smoker volunteers recruited for the study. Patient identification is anonymised. No lung function data provided for volunteer highlighted in yellow.

	AGE	SEX	FEV1	FEV1 %	FVC	FEV1:FVC	p/y	Current Smokers
AnH070311	54	F	3.18	121.9	4.41	0.7210884	40	y
AnM	56	M	3.27	118.4	3.89	0.840617	15	y
MlK110912	64	m	3.22	105.7	4.7	0.6851064		
PeC010311	63	F	1.92	98.30	2.58	0.74	68.00	y
MiV	51	M	2.4	73.8	2.4	1	24	Y
ELM190712	44	F	2.35	87.9	3.28	0.7164634	44	Y
AlF140311	53	F	2.51	93.8	3.07	0.8175896	80	y
ViV130912	59	F	3.05	109.1	4.32	0.7060185	22.5	Y
MaB170511	49	m	3.17	94.6	4.73	0.6701903	18	y
VeB080311	60	F	1.61	76.6	2.32	0.6939655	22.5	Y
DaH080311	62	M	3.28	105.4	3.96	0.8282828	20	Y
CaHu050310	57	F	2.08	92.10	2.79	0.75	25.00	Y
ChH070610	66	F	2.00	102.60	3.19	0.63	55.00	Y
JaB140711	70	f				0.7	30.00	N
JOSA200710	70	M	4.07	111.4	6.49	0.6271186		Y
KaR190710	46	f	2.26	102.10	2.78	0.81		y
RaK191109	62	M	3.15	102.80	4.56	0.69	30	y
AnS220512	59	f	1.55	63.0	2.01	0.7711443	19	y

Appendix II Table 2: Basic demographics of Smoker Participants Recruited for the Study.

Basic lung function data of smoker volunteers recruited for the study. Patient identification is anonymised.

Patients	AGE	SEX	FEV1	FEV1 %	FVC	FEV1:FVC	p/y	C.SM	EX.SM	Experiment:
AlMa040912 (AIFA)	82	M	0.71	29	1.48	0.48	23		y	**Chapter 4**: Fig 4.4A Fig 4.4B Fig 4.4C Fig 4.14A Fig 4.14B
ChD021012	75	m	0.7	22.8	2.74	0.26	60		Y	**Chapter 4**: Fig 4.4A Fig 4.4B Fig 4.4C
TELY	70	F	1.01	45.0	1.75	0.58	50	N	y	**Chapter 4:** Fig 4.8B
JaF120612	80	f	0.59	32.0	1.55	0.38	50	n	ex.	**Chapter 4** Fig 4.14A Fig 4.14B Fig 7.10A Fig 7.10B Fig 7.10C Fig. 7.11A Fig7.11B Fig7.11C
PaA180111	71	F	0.92	46.5	2.85	0.32	35	ex	ex 30y	**Chapter 5:** Fig. 5.2A Fig 5.2B Fig. 5.2C

										Fig 5.3A Fig 5.3B Fig 5.3C Fig 5.4A Fig. 5.4B Fig 5.4C Fig. 5.5A, Fig.5.5B Fig5.5C Fig. 5.6A Fig5.6B Fig 5.6C Fig 5.7A **Chapter 7:** Fig. 7.4 A Fig. 7.4 B Fig 7.4C Fig. 7.6 A Fig 7.4B Fig 7.4C Fig 7.10A Fig 7.10B Fig 7.10C Fig. 7.11A Fig7.11B Fig7.11C
BeT040810	83	M	0.83	36.0	1.97	0.42	38	n	ex	**Chapter 5:** Fig. 5.5A Fig. 5.5C

										Fig. 5.6A **Chapter 7:** Fig. 7.4 A Fig. 7.6 A
BrM240310	72	M	0.77	26.0	1.53	0.5	70	n	y	**Chapter 5:** Fig. 5.5A Fig. 5.5C Fig. 5.6A Fig 5.7A **Chapter 7:** Fig. 7.4 A
JAP010911	65	F	0.7	31.82	1.6	0.44	120		Ex.sm	**Chapter 5:** Fig. 5.5B Fig. 5.5C Fig5.6B Fig 5.6C Fig. 5.7B Fig 5.7C **Chapter 7:** Fig. 7.4 A Fig. 7.4 B Fig 7.4C Fig. 7.6 A Fig 7.4B Fig 7.4C
JuT200110	76	F	1.31	68.0	1.83	0.72	50	n	Ex.sm 7-years	**Chapter 5:** Fig. 5.5A

										Fig. 5.6A **Chapter 7:** Fig. 7.4 A Fig 5.7A
MARR310712	69	f	0.74	36.0	2.18	0.3394495	25	n		**Chapter 6:** Fig 6.10 Fig 6.11
GaH080512	58	m	0.52	15.0	1.67	0.31	25	n	y	**Chapter 6:** Figure 6.5
JuY190412	66	F	0.45	22.0	1.28		35	n	y	**Chapter 6**: Fig. 6.6
MaL250711	70	F	1.43	82.4	2.37	0.6			Y	**Chapter 5**: Fig5.6B Fig 5.6C **Chapter 6:** Fig. 6.6 **Chapter 7:** Fig. 7.4 A Fig. 7.4 B Fig 7.4C Fig. 7.6 A Fig 7.4B Fig 7.4C Fig 7.10A Fig 7.10B Fig 7.10C Fig. 7.11A Fig7.11B Fig7.11C

WiC180612	61	m	1.55	49.5	2.21	0.7	15		Y	**Chapter 6:** Fig 6.7 Fig 6.8 Fig 6.10 Fig 6.11 **Chapter 7:** Fig 7.10A Fig 7.10B Fig 7.10C
EdM080812	63	m	2.14	63.0	2.83	0.76	23	n	y	**Chapter 6:** Fig 6.10 Fig 6.11
GeWa020311	77	M	0.52		1.76	0.3	45	n	Y y	**Chapter 7:** Fig. 7.4 A Fig. 7.4 B Fig 7.4C Fig. 7.6 A Fig 7.4B Fig 7.4C
KaR290910		F	0.37	23.0	1.10	0.34	10	n	Ex.sm Y	**Chapter 7:** Fig. 7.4 A Fig. 7.4 B Fig 7.4C Fig. 7.6 A Fig 7.4B Fig 7.4C

PeR140111	60	M	2.10	55	3.60	0.58				**Chapter 7:** Fig. 7.4 A Fig. 7.4 B Fig 7.4C Fig. 7.6 A Fig 7.4B Fig 7.4C
RaD300412	67	m	1.2	40.4	2.31	0.52		never		**Chapter 6:** Fig 6.1 **Chapter 7:** Fig 7.10A Fig 7.10B Fig 7.10C Fig. 7.11A Fig7.11B Fig7.11C
JoWe030210	82	M	1.08		2.21	0.49	50	n		**Chapter 5:** Fig. 5.6A **Chapter 7:** Fig. 7.4 A
JuT200110	76	F	1.31	68.0	1.83	0.72	50	n		**Chapter 5:** Fig. 5.5A Fig. 5.6A
DaS170310	69	M	0.76	28.0	3.04	0.25	50	n		**Chapter 5:** Fig. 5.5A Fig. 5.6A Fig 5.7A

										Chapter 7: Fig. 7.4 A
CyR290512	86	m	1.68	71.0	4.16	0.4	18	n		**Chapter 5:** Fig. 5.5B Fig. 5.5C **Chapter 7** Fig. 7.4 B Fig 7.4C

Appendix II Table 3: Basic demographics of Ex-Smoker COPD Patients Recruited for the Study.

Basic lung function data of ex-smoker COPD patients recruited for the study.

Patient	**AGE**	**SEX**	**FEV1**	**FEV1 %**	**FVC**	**FEV1:FVC**	**P/Y**	**C.SM**	**EX.SM**	**Experiment:**
MaLe250912	50	f	0.87	31.6	3.59	0.24	60	y		**Chapter 4**: Fig 4.4A Fig 4.4B Fig 4.4C Fig 4.14A Fig 4.14B
LeH141111	68	m	2.36	86.8	4.33	0.55		Y		**Chapter 5**: Fig. 5.2A Fig 5.2B Fig. 5.2C Fig 5.3A Fig 5.3B Fig 5.3C Fig 5.4A Fig. 5.4B Fig 5.4C Fig. 5.5B Fig. 5.5C Fig. 5.7B Fig 5.7C **Chapter 7:** Fig. 7.4A Fig. 7.4 B Fig 7.4C Fig. 7.6A Fig 7.4B Fig 7.4C Fig 7.10A

										Fig 7.10B Fig 7.10C Fig. 7.11A Fig7.11B Fig7.11C
CaH210410	72	F	1.28	77.80	2.41	0.53	10.00	Y		**Chapter 4:** Fig. 4.8A Fig 4.8B Fig 4.8C **Chapter 6** Fig. 6.6
GoH	65	m	0.95	29.0	2.42	0.39	15	Y		**Chapter 4:** Fig. 4.8A Fig 4.8B Fig 4.8C
DEM240610	77	M	0.87	54.0	1.92	0.45	>40	Y		**Chapter 5:** Fig. 5.5A Fig 5.7A Chapter 7: Fig. 7.4 A Fig. 7.6 A
LaU151009	63	M	2.17	66%	3.11	0.7	10	y	y(ex 7 yrs)	**Chapter 5:** Fig. 5.5A Fig. 5.6A Fig 5.7A **Chapter 7:** Fig. 7.4 A
PF 005	62	F	1.11	57	1.62	0.69	24	y		**Chapter 5:**

JJ020310										Fig. 5.5A Fig. 5.6A Fig 5.7A **Chapter 7:** Fig. 7.4 A
TEB090810	63	m	0.5		1.44	0.4	70	Y		**Chapter 5:** Fig. 5.5A Fig 5.7A **Chapter 7:** Fig. 7.4 A
THWA	75	m	1.27	48	3.72	0.3	25	y		**Chapter 5:** Fig. 5.5A Fig 5.7A **Chapter 7:** Fig. 7.4 A
AIA	57	F	1.4	59	2.45	0.57	25	Y		**Chapter 5:** Fig. 5.5B Fig. 5.5C Fig5.6B Fig 5.6C Fig. 5.7B Fig 5.7C **Chapter 7:** Fig. 7.4 A Fig. 7.4 B

										Fig 7.4C Fig. 7.6 A Fig 7.4B Fig 7.4C
AlT190911	63	F	1.03	36.9	2.23	0.46	36	Y	y	**Chaoter 6**: Fig. 6.6
ClP300412	59	M	2.5	70.0	4.14	0.6	52.5	Y		**Chapter 7** Fig 7.10A Fig 7.10B Fig 7.10C Fig. 7.11A Fig7.11B Fig7.11C
GaB080512	49	M	3.11	83.1551	4.93	0.63	12	Y		**Chapter 7:** Fig. 7.4 B Fig 7.4C Fig 7.4B Fig 7.4C Fig 7.10A Fig 7.10B Fig 7.10C Fig. 7.11A Fig7.11B Fig7.11C
GeQ090211	57	M	0.92	32.00	2.50	0.37	65	y		**Chapter 5:** Fig. 5.5A Fig. 5.6A Fig 5.7A

										Chapter 7: Fig. 7.4 A
JuM240610	79	F	1.26	75.6	1.65	0.76	10	Y		**Chapter 5:** Fig. 5.5A **Chapter 7:** Fig. 7.4 A Fig. 7.6 A

Appendix II Table 4: Basic demographics of Current-Smoking COPD Patients Recruited for the Study.

Basic lung function data of current-smoking COPD patients recruited for the study.

PATIENT	AGE	SEX	FEV1	FEV1 %	FVC	FEV1:FVC	p/y	C.SM	EX.SM	Experiment:
MaCO200912	69	M	1.81	52.2	3.15	0.57				**Chapter 4:** Fig 4.4A Fig 4.4B Fig 4.4C
VEH/Hul300412	59	m	1.89	61.6	4.12	0.46	70			**Chapter 7:** Figure 7.4A Fig. 7.4 B Fig 7.4C
MaG030512	67	f	1.1		1.81	0.61	30			**Chapter 6:** Figure 6.5
SuC050512	59	F	1.09	47.6	2.53	0.43	30			**Chapter 6:** Fig 6.1 Fig 6.5
ALB190410	53	M	2.92	86.6	3.69	0.79		N		**Chapter 5:** Fig 5.6A Fig 5.7A **Chapter 7:** Fig. 7.4 A
ELP110110	58	F	1.75	73.4	2.67	0.66		n		**Chapter 5:** Fig.5.5A Fig. 5.6A **Chapter 7:** Fig. 7.4 A

AnP260512	74	m	1.72	65.4	2.63	0.65		n		**Chapter 5:** Fig. 5.2A Fig 5.2B Fig. 5.2C Fig. 5.5B Fig. 5.5C **Chapter 6:** Fig 6.7 Fig 6.8 Fig 6.10 Fig 6.11 **Chapter 7:** Fig. 7.4 B Fig 7.4C Fig 7.10A Fig 7.10B Fig 7.10C Fig. 7.11A Fig7.11B Fig7.11C
VeM030512	59	F	1.13	44.0	1.9	0.59		n		**Chapter 5:** Fig. 5.2A Fig 5.2B Fig. 5.2C

										Chapter 6: Fig 6.1 Fig 6.8 **Chapter 7**: Figure 7.4A Fig. 7.4 B Fig 7.4C Fig 7.10A Fig 7.10B Fig 7.10C Fig. 7.11A Fig7.11B Fig7.11C
RoFr	66	m	1.81	56.4	3.53	0.51		n		Chapter 4: Fig. 4.8A Fig 4.8B Fig 4.8C
ShS300412	unknown	unknown								Chapter 6: Fig 6.1

Appendix II Table 5: Basic demographics of COPD Patients Recruited for the Study.

Basic lung function data of COPD patients recruited for the study. No or limited information is provided, in regards to current smoking or ex-smoking patients recruited (only pack years given). No lung function is provided for the patient highlighted in yellow.

	COPD (Never Smoked/ Limited Information Supplied) n=9	COPD (Ex-Smoker) n=25	COPD (Current Smokers) n=15
Age (Years)	63 ± 2	71 ± 2	64 ± 2
FEV_1 (L)	2 ± 2	1 ± 0.1	1 ± 0.2
FEV_1 (% Predicted)	61 ± 5	44 ± 4	58 ± 5
FVC	3 ± 0.3	2 ± 0.1	3 ± 0.3
FEV_1:FVC	0.6 ± 0.04	0.5 ± 0.03	0.5 ± 0.04
Smoking History (Pack Years)	43 ± 13	42 ± 5	32 ± 6

Appendix II Table 6: Basic demographics of Current-Smoking and Ex-Smoking COPD Patients Recruited for the Study.

Basic demographics of current-smoking and ex-smoking COPD patients recruited for the study. Demographics of COPD patients with unknown or limited information regarding current or ex-smoking status are also provided.

Appendix III:

NIST Certificates

National Institute of Standards & Technology

Certificate of Analysis

Standard Reference Material® 1650b

Diesel Particulate Matter

This Standard Reference Material (SRM) is intended for use in evaluating analytical methods for the determination of selected polycyclic aromatic hydrocarbons (PAHs) and nitro-substituted PAHs (nitro-PAHs) in diesel particulate matter and similar matrices. In addition to certified and reference values for selected PAHs and nitro-PAHs, reference or information values are provided for percent extractable mass, particle-size distribution, and specific surface area; supplemental information on mutagenic activity is also provided. All of the chemical constituents for which certified, reference, and information values are provided are naturally present in the diesel particulate material. SRM 1650b was prepared from the same bulk diesel particulate material that was issued in 1985 as SRM 1650 [1] and in 2000 as SRM 1650a [2–4]. A unit of SRM 1650b consists of a bottle containing approximately 200 mg of diesel particulate material.

Certified Mass Fraction Values: Certified values are provided for PAHs in Table 1 and nitro-PAHs in Table 2. A NIST certified value is a value for which NIST has the highest confidence in its accuracy, in that all known or suspected sources of bias have been investigated or taken into account [5]. The certified values for the PAHs and nitro-PAHs are based on the agreement of results obtained at NIST from two or more independent analytical methods [5].

Reference Mass Fraction Values: Reference values are provided for additional PAHs in Table 3, for PAHs of molecular mass 302 in Table 4, and for additional nitro-PAHs in Table 5. In Tables 3 and 5, the reference values for some PAHs and nitro-PAHs, respectively, are listed more than once depending on the extraction conditions that are used (see "Preparation and Analysis"). A reference value for percent extractable mass is provided in Table 6. Reference values are noncertified values that are the best estimate of the true value; however, the values do not meet the NIST criteria for certification and are provided with associated uncertainties that may reflect only measurement precision, may not include all sources of uncertainty, or may reflect a lack of sufficient statistical agreement among multiple analytical methods [5].

Information Values: Information values for specific surface area, as determined by N_2 gas adsorption, and particle-size characteristics are provided in Table 7. An information value is considered to be a value that may be of use to the SRM user, but insufficient information is available to assess the uncertainty associated with the value or only a limited number of analyses were performed [5].

Expiration of Certification: The certification of **SRM 1650b** is valid, within the measurement uncertainty specified, until **31 December 2022**, provided the SRM is handled and stored in accordance with the instructions given in this certificate (see "Instructions for Handling, Storage, and Use"). However, the certification is invalid if the SRM is damaged, contaminated, or otherwise modified.

Maintenance of SRM Certification: NIST will monitor this SRM over the period of its certification. If substantive technical changes occur that affect the certification before the expiration of this certificate, NIST will notify the purchaser. Registration (see attached sheet) will facilitate notification.

Coordination of the technical measurements leading to the certification of SRM 1650b was under the leadership of M.M. Schantz and S.A. Wise of the NIST Chemical Sciences Division.

Statistical consultation was provided by N.A. Heckert and S.D. Leigh of the NIST Statistical Engineering Division.

Carlos A. Gonzalez, Chief
Chemical Sciences Division

Gaithersburg, MD 20899

Robert L. Watters, Jr, Director

Certificate Issue Date: 17 July 2013

Office of Reference Materials

Analytical measurements for the certification of SRM 1650b were performed by H.A. Bamford, B.J. Porter, D.L. Poster, M.M. Schantz, P. Schubert, and R. Zeisler of the NIST Chemical Sciences Division. Analytical measurements for PAHs and nitro-PAHs were also provided by C. Chiu of the Environmental Technology Centre, Environment Canada (Ottawa, Canada). Specific surface area and porosity measurements and confirmation measurements for 1-nitropyrene were provided by P. Scheepers of the Department of Epidemiology at Katholieke Universiteit Nijmegen (Nijmegen, The Netherlands).

Support aspects involved in the issuance of this SRM were coordinated through the NIST Office of Reference Materials.

INSTRUCTIONS FOR HANDLING, STORAGE, AND USE

Handling: This material is a naturally occurring diesel particulate material and contains constituents of known and unknown toxicities and mutagenicities; therefore, extreme caution and care should be exercised during its handling and use.

Storage: Store SRM 1650b in its original bottle at temperatures below 30 °C and keep away from direct sunlight.

Use: Prior to removal of subsamples for analysis, the contents of the bottle should be mixed thoroughly. The recommended minimum sample size is 50 mg, although smaller sample sizes have been evaluated. The evaluation of the homogeneity of SRM 1650b, at small sample sizes for PAHs, is described in "Homogeneity Assessment for PAHs" and in further detail in reference 6.

PREPARATION AND ANALYSIS[(1)]

Sample Collection and Preparation: The diesel particulate material used for the preparation of SRM 1650b was the same bulk diesel particulate material used for the preparation of SRM 1650 and SRM 1650a. This material was obtained through the Coordinating Research Council, Inc. (Atlanta, GA). The particulate material was collected from the heat exchangers of a dilution tube facility following 200 engine hours of particulate accumulation. Several direct injection four-cycle diesel engines, operating under a variety of conditions were used to generate this particulate material. Therefore, while the sample is not intended to be representative of any particular diesel engine operating under any specific conditions, it should be representative of heavy-duty diesel engine particulate emissions.

Relationship Among SRM 1650, SRM 1650a, and SRM 1650b: SRM 1650b was prepared from the same bulk diesel particulate matter used for preparation of SRM 1650; the bulk material had been stored at –20 °C since the preparation of SRM 1650 in 1984. SRM 1650b was analyzed as described below to confirm that the bulk diesel particulate matter was the same as the material used for SRM 1650 and SRM 1650a. The analyses of SRM 1650b confirmed that the material was the same and that the mass fractions of PAHs and nitro-PAHs had not significantly changed. The results of these analyses were then used to assign new certified and reference mass fractions and to increase again the number of PAHs and nitro-PAHs with values assigned. However, measurements for some properties (e.g., percent extractable mass and pore size) and some PAHs (selected methyl- and dimethyl-substituted PAHs) were not repeated on SRM 1650b; instead it was determined that the information values from SRM 1650a are applicable to SRM 1650b.

Polycyclic Aromatic Hydrocarbons (PAHs)

The general approach used for the value assignment of the PAHs in SRM 1650b consisted of pressurized fluid extraction (PFE) using dichloromethane (DCM), toluene, or a toluene/methanol mixture at two extraction temperatures (100 °C and 200 °C), cleanup of the extracts using solid phase extraction (SPE), and analysis by using gas chromatography/mass spectrometry (GC/MS) on three stationary phases of different selectivity [i.e., a relatively nonpolar phase, a 50 % (mole fraction) phenyl-substituted methylpolysiloxane phase, and a dimethyl 50 % (mole fraction) polysiloxane liquid crystalline stationary phase]. PFE was the only extraction method used at NIST; previous studies indicated that conventional Soxhlet extraction was not as effective as PFE in the removal of higher relative molecular mass PAHs [7]. Results were also obtained from Environment Canada as described in "GC/MS (Environment Canada)".

[(1)]Certain commercial equipment, instruments or materials are identified in this certificate to adequately specify the experimental procedure. Such identification does not imply recommendation or endorsement by the National Institute of Standards and Technology, nor does it imply that the materials, or equipment identified are necessarily the best available for the purpose.

Multiple sets of GC/MS results performed by the of the NIST Chemical Sciences Division, designated as GC/MS (Ia and Ib), GC/MS (IIa and IIb), GC/MS (IIIa and IIIb), GC/MS (IVa and IVb), GC/MS (Va and Vb), GC/MS (VIa and VIb), GC/MS (VII), GC/MS (VIII) and GC/MS (Environment Canada), were obtained using three columns with different selectivities for the separation of PAHs. For all PAH analyses, the mass spectrometer was operated using electron impact ionization.

GC/MS (Ia and Ib): For GC/MS (I) analyses, duplicate subsamples of 50 mg from six bottles of SRM 1650b were mixed with Hydromatrix (Isco, Lincoln, NE) and extracted with toluene using PFE at 100 °C and 13.8 MPa as described by Schantz et al. [7]. The extracts were concentrated to about 0.5 mL, solvent exchanged to hexane, placed on an aminopropylsilane SPE cartridge, and eluted with 20 mL of 2 % DCM in hexane (volume fraction). The eluant was concentrated and then analyzed by using GC/MS with a 0.25 mm i.d. × 60 m fused silica capillary column with a relatively nonpolar phase (0.25 µm film thickness; DB-XLB, J&W Scientific, Folsom, CA) and these results are denoted as GC/MS (Ia). Concentrated eluants were also analyzed on a 50 % phenyl-substituted methylpolysiloxane stationary phase (0.25 mm i.d. × 60 m, 0.25 µm film thickness; DB-17MS, J&W Scientific), and these results are designated as GC/MS (Ib).

GC/MS (IIa and IIb): For the GC/MS (IIa and IIb) analyses, 50 mg samples from six bottles of SRM 1650b were extracted with toluene using PFE at 200 °C and 13.8 MPa. The extracts were processed and analyzed as described above for GC/MS (Ia) and GC/MS (Ib) and the results are designated GC/MS (IIa) and GC/MS (IIb), respectively.

GC/MS (IIIa and IIIb): For GC/MS (IIIa and IIIb) analyses, subsamples of 50 mg to 100 mg from six bottles of SRM 1650b were mixed with clean sodium sulfate and extracted with DCM using PFE at 100 °C and 13.8 MPa. The extracts were processed as described above for GC/MS (Ia and Ib) and then analyzed by using GC/MS on fused silica capillary columns with a 50 % phenyl-substituted methylpolysiloxane stationary phase (0.25 mm i.d. × 60 m, 0.25 µm film thickness), designated as GC/MS (IIIa), and on a dimethyl 50 % polysiloxane liquid crystalline stationary phase (0.25 mm i.d. × 15 m, 0.25 µm film thickness; LC-50, J&K Environmental, Milton, Ontario, Canada), designated as GC/MS (IIIb).

GC/MS (IVa and IVb): For GC/MS (IVa and IVb) analyses, subsamples of 50 mg to 100 mg from six bottles of SRM 1650b were extracted with DCM using PFE at 200 °C and 13.8 MPa. The extracts were processed and analyzed by using GC/MS on the two columns as described above for GC/MS (IIIa and IIIb).

GC/MS (Va and Vb) and GC/MS (VIa and VIb): Additional extractions and analyses were performed in the same manner as for GC/MS (IIIa and IIIb) and GC/MS (IVa and IVb) to obtain concentrations for selected methylated PAHs. These data sets are designated as GC/MS (Va and Vb) and GC/MS (VIa and VIb).

GC/MS (VII): For the relative molecular mass (M_r) 276 and higher PAHs, additional extractions and analyses were performed in a similar manner as for GC/MS (Ib) except that the PAHs of interest were eluted from the aminopropylsilane SPE cartridge using 40 mL of 10 % DCM in hexane (volume fraction). These data are designated as GC/MS (VII).

GC/MS (VIIIa through VIIId): The effect of increasing the temperature and pressure used for PFE on the extraction efficiency for PAHs was evaluated. The solvent used was toluene, although a 9:1 toluene:methanol (volume fraction) was also evaluated. The PFE conditions used included: 100 °C with 13.8 MPa; 100 °C with 20.7 MPa; 200 °C with 13.8 MPa; and 200 °C with 20.7 MPa, methods GC/MS (VIIIa) through GC/MS (VIIId), respectively. Following an SPE step similar to that of method I above, the processed extracts were analyzed using a non-polar, extra-low bleed phase (0.25 mm i.d. × 60 m, 0.25 µm film thickness).

GC/MS Internal Standards: For all GC/MS measurements described above, except GC/MS (VIa and VIb), selected perdeuterated PAHs were added to the diesel particulate matter prior to extraction for use as internal standards for quantification purposes. For GC/MS (VIa and VIb), fluorinated PAHs were added to the diesel particulate matter prior to extraction for use as internal standards for quantification purposes.

GC/MS (Environment Canada): For PAH measurements at Environment Canada, subsamples of approximately 10 mg from each of four bottles of SRM 1650b were extracted with DCM or hexane/acetone (1:1 volume fraction) using microwave-assisted extraction at 100 °C for 20 min. The extract was filtered through sodium sulfate and concentrated to a few milliliters by rotary evaporation, solvent exchanged to cyclohexane, and then divided into two portions; one portion was processed for PAH measurements and the other portion was processed for nitro-PAH measurements (see below). The PAH fraction was isolated from the extract by using open-column chromatography on silica, with hexane followed by benzene as the mobile phase. The PAH fraction was then analyzed by using GC/MS on a DB-XLB column (0.25 mm i.d. × 30 m, 0.25 µm film thickness). Selected perdeuterated PAHs were added to the diesel particulate matter prior to extraction for use as internal standards for quantification purposes.

PAH Isomers of Relative Molecular Mass (M_r) 302: For the determination of the relative molecular mass (M_r) 302 isomers, the method used was similar to that described by Schubert et al. [8]. Two sets of samples (one set of three subsamples and one set of six subsamples) of approximately 50 mg each were extracted using PFE at 100 °C and 13.8 MPa with DCM. The extracts were then concentrated, solvent exchanged to hexane, passed through an aminopropylsilane SPE cartridge, and eluted with 40 mL of 10 % DCM in hexane (volume fraction). The processed extract was then analyzed by GC/MS using a 0.25 mm i.d. × 60 m fused silica capillary column with a 50 % phenyl-substitued methylpolysiloxane phase (0.25 µm film thickness; DB-17MS). Perdeuterated dibenzo[*a,i*]pyrene was added to the diesel particulate matter, prior to extraction, for use as an internal standard.

Homogeneity Assessment for PAHs: The homogeneity of SRM 1650b was assessed by analyzing duplicate samples of 50 mg from six bottles selected by stratified random sampling. Samples were processed and analyzed as described above for GC/MS (I). No statistically significant differences among bottles were observed for the PAHs at the 50 mg sample size. The relative homogeneity of trace levels of PAHs in SRM 1650b in the milligram sampling range was also evaluated. The subsampling contribution to the overall uncertainty varies with PAH considered. Using pyrene as an example, the subsampling error for a 10 mg sample size of SRM 1650b is 2 %, while the subsampling error for a 50 mg sample of SRM 1650b is 0.9 %. A more extensive evaluation of the homogeneity of SRM 1650b, at small sample sizes for PAHs, is described in reference 6.

Nitro-Substituted Polycyclic Aromatic Hydrocarbons (Nitro-PAHs)

SRM 1650b was analyzed at NIST and Environment Canada for the determination of nitro-PAHs. The general procedure for determination of nitro-PAHs at NIST utilizes GC with negative ion chemical ionization mass spectrometry (GC/NICI-MS) [9,10] and high-resolution mass spectrometry using negative chemical ionization (GC/NCI-HRMS). Mass fraction values for nitro-PAHs are provided in Table 2 and 5.

GC/NICI-MS (I): Subsamples of approximately 50 mg from each of six bottles of SRM 1650b were mixed with Hydromatrix (Isco, Lincoln, NE) and extracted with DCM using PFE at 100 °C and 13.8 MPa. The extracts were concentrated to about 0.5 mL, solvent exchanged to hexane, placed on an aminopropylsilane SPE cartridge, and eluted with 40 mL of 20 % DCM in hexane (volume fraction). To isolate the nitro-PAH fraction, the concentrated eluant was analyzed by normal-phase liquid chromatography (LC) using a semi-preparative amino/cyano phase column with a mobile phase of 20 % DCM in hexane [10]. The nitro-PAH fraction was analyzed by GC with GC/NICI-MS using a 0.25 mm i.d. × 30 m fused silica capillary column containing a 50 % phenyl-substituted methylpolysiloxane stationary phase (0.25 µm film thickness), and the results are designated as GC/NICI-MS (I).

GC/NICI-MS (II): A second set of four subsamples of SRM 1650b was processed and analyzed at a different time using the same procedures described above and the results are denoted as GC/NICI-MS (II).

GC/NICI-MS (IIIa through IIId): The effect of increasing the temperature and pressure used for PFE on the extraction efficiency for nitro-PAHs was evaluated. The solvent used was toluene, although a 9:1 toluene:methanol (volume fraction) was also evaluated. The PFE conditions used included: 100 °C with 13.8 MPa; 100 °C with 20.7 MPa; 200 °C with 13.8 MPa; and 200 °C with 20.7 MPa [methods GC/NICI-MS (IIIa) through GC/NICI-MS (IIId), respectively]. Following an SPE step similar to that of method I above, the processed extracts were analyzed using a non-polar, extra-low bleed proprietary phase (0.25 mm i.d. × 60 m, 0.25 µm film thickness).

GC/NCI-HRMS: For the Environment Canada measurements of nitro-PAHs, five subsamples of SRM 1650b were extracted as described above for PAH measurements. The second portion of the extract was taken to dryness and then redissolved in 1 mL of dimethyl sulfoxide (DMSO). The nitro-PAH fraction was isolated by using a liquid-liquid partition scheme involving hexane extraction of the DMSO to remove aliphatic hydrocarbons, followed by dilution of the DMSO with water and extraction of the polar fraction into cyclohexane. The nitro-PAHs were then isolated by using normal-phase LC on a silica column with a solvent gradient from 5 % DCM in hexane (volume fraction) to 100 % DCM. The nitro-PAH fraction was collected from 60 % DCM in hexane to 100 % DCM, concentrated, and analyzed by using GC on a 30 m 5 % phenyl-substituted methylpolysiloxane column (0.25 mm i.d., 0.25 µm film thickness) with detection by high-resolution mass spectrometry using negative chemical ionization (GC/NCI-HRMS).

GC/NICI-MS and GC/NCI-HRMS Internal Standards: For the GC/NICI-MS and GC/NCI-HRMS measurements described above, perdeuterated nitro-PAHs were added to the diesel particulate matter, prior to extraction, for use as internal standards for quantification purposes.

Value Assignment for PAHs and Nitro-PAHs

The value assignment of PAHs and nitro-PAHs in SRM 1650b is based on the measurements used when SRM 1650b was issued in 2006 and on recent additional measurements using different extraction temperatures. Recent studies on the extraction of PAHs and nitro-PAHs from diesel particulate matter [11–13] have shown that using PFE at 200 °C removes higher quantities of some PAHs and nitro-PAHs than using PFE at 100 °C. As a result of these studies, value assignment for specific PAHs and nitro-PAHs in SRM 1650b is based on measurements using PFE at both 100 °C and 200 °C. In cases where the quantities of the individual PAHs and nitro-PAHs do not change with the PFE temperature, the measurements were combined and the resulting values are denoted as certified values in Tables 1 and 2. When different results are obtained at 100 °C and 200 °C, the values are reported for both temperatures, and they are denoted as reference values in Tables 3 and 5. These reference values should be considered "method dependent" values, because they are dependent on the extraction method and temperature.

Percent Extractable Mass

For the determination of percent extractable mass, six subsamples of approximately 200 mg were extracted using Soxhlet extraction for 18 h with DCM. The extract was concentrated to approximately 20 mL and then filtered to remove particulate matter. Aliquots of 100 µL to 150 µL were placed in tared aluminum foil pans; the DCM was evaporated until constant mass was obtained, and then the mass of the residue remaining was determined. The percent extractable mass reference value for SRM 1650a is applicable to SRM 1650b and provided in Table 6.

Particle Size Information, Specific Surface Area, and Porosity

Particle-size distribution measurements for SRM 1650b were carried out using a laser diffraction instrument (Mastersizer 2000, Malvern Instruments, Southborough, MA) set at a refractive index of 1.5 and absorption index of 0.1 and the liquid suspension method with the instrument manufacturer's small volume sample dispersion unit (Hydro 2000 SM). A suspension of 0.1 % (mass fraction) of SRM 1650b in distilled water with 0.001 % Triton (volume fraction) was prepared by ultra-sonication for 1 h and 24 h. After the recording of the background, a portion of the suspension was added to the measurement cell to achieve an obscuration of 5 %. Three passes of the sample solution were recorded and averaged. Results were calculated using the General Purpose Model provided by the instrument manufacturer; the results obtained for the two sonication periods are shown in Figure 1. The diesel particulate matter, as-received, does not have a stable particle size because of agglomeration which is evident, as the particle-size distribution for SRM 1650b measured after the 1 h sonication period did not show a typical profile for a material from a combustion process. The subsequent 24 h sonication broke up most agglomerates, and the size distribution shows a profile typical for combustion engine emissions (see Table 7).

The specific surface area and porosity were determined based on N_2 gas adsorption measurements [14]. The gas adsorption measurements were performed on a NOVA-1200 instrument (Quantachrome Corp., Boynton Beach, FL) at 77 K after the samples were outgassed for 24 h at 120 °C under vacuum. The N_2 isotherms were analyzed using the Brunauer-Emmet-Teller (BET) equation [15] to obtain the surface area (Table 7) and the Barrett-Joyner-Halenda (BJH) method [16] to obtain the porosity. Based on the BJH method, SRM 1650b shows a wide distribution of mesopores, but with substantial outer area. The pore diameter of the particles in SRM 1650b ranges from 4 nm to 45 nm with a mean at about 25 nm.

Supplemental Information for SRM 1650b

Because SRM 1650, SRM 1650a, and SRM 1650b were all prepared from the same bulk diesel particulate matter, some measurements reported for the previous two materials have not been duplicated for SRM 1650b and the previous results are transferable to the current SRM 1650b. In addition, because SRM 1650 and SRM 1650a have been available since 1985, a considerable amount of information on the characterization of these materials has been published. A summary of some of the studies reporting characterization of this diesel particulate matter SRM is provided in Poster et al [3,4]. A description of the mutagenicity assay is provided below as supplemental information for SRM 1650b.

Mutagenicity Activity: Reference values for the mutagenic activity of a dichloromethane extract of SRM 1650 were determined as part of an international collaborative study in 1989 sponsored by the International Programme on Chemical Safety (IPCS) and supported and technically coordinated by the U.S. Environmental Protection Agency's (EPA) Office of Health Research. Twenty laboratories from North America, Europe, and Japan participated in the study for which a complete summary has been published [17,18]. Mutagenicity data were provided by J. Lewtas and L.D. Claxton of the National Health and Environmental Effects Research Laboratory, U.S. EPA (Research Triangle Park, NC).

Table 2. Certified Mass Fraction Values for Nitro-PAHs in SRM 1650b

Nitro-PAH	Mass Fraction[a] (µg/kg)
9-Nitrophenanthrene[b,c,d,e]	539 ± 24
3-Nitrophenanthrene[b,c,e]	4250 ± 50[f]
2-Nitrofluoranthene[b,c,e]	217 ± 15
3-Nitrofluoranthene[b,c,e]	65.1 ± 1.1
1-Nitropyrene[b,c,e,g]	18400 ± 300
7-Nitrobenz[*a*]anthracene[b,c,e]	943 ± 22[f]
6-Nitrochrysene[b,c,e]	46.6 ± 1.1[f]

[a] The certified mass fraction values, unless otherwise footnoted, are weighted means of the mass fractions from multiple analytical methods [19]. The uncertainty listed with each value is an expanded uncertainty about the mean [19,20] with coverage factor, $k = 2$, calculated by combining within method variances with a between method variance [21] following the ISO/JCGM Guide [22,23].

[b] GC/NICI-MS (I) on 50 % phenyl-substituted methylpolysiloxane stationary phase.

[c] GC/NICI-MS (II) on 50 % phenyl-substituted methylpolysiloxane stationary phase.

[d] GC/NCI-HRMS on 5 % phenyl-substituted methylpolysiloxane stationary phase.

[e] GC/NICI-MS (III) on 50 % phenyl-substituted methylpolysiloxane phase after PFE with toluene at two temperatures and two pressures (100 °C with 13.8 MPa; 100 °C with 20.7 MPa; 200 °C with 13.8 MPa; and 200 °C with 20.7 MPa).

[f] The certified value is a weighted mean of average mass fractions, with one average from each of two or more analytical methods [19,20]. The expanded uncertainty is the half width of a symmetric 95 % parametric bootstrap confidence interval [24], which is consistent with the ISO/JCGM Guide [22,23] with an effective coverage factor, *k*, equals 2.

[g] Certified value for 1-nitropyrene confirmed original SRM 1650 certified value, which included measurements by two other independent techniques [2,25].

Table 3. Reference Mass Fraction Values for PAHs in SRM 1650b
Based on Extraction Method and Conditions

Extraction Conditions	Mass Fractions (mg/kg)[a]
PFE at temperatures between 100 °C and 200 °C	
1-Methylnaphthalene[b,c,d,e,f]	1.71 ± 0.26[g]
2-Methylnaphthalene[b,c,d,e,f]	3.71 ± 0.21
Acenaphthene[c,e,f,h]	0.233 ± 0.021
1,7-Dimethylphenanthrene[e,f,i,j]	17.2 ± 0.7
4H-Cyclopenta[*def*]phenanthrene[e,f]	3.35 ± 0.18
Cyclopenta[*def*]phenanthrone[k,l]	15.6 ± 0.8
Cyclopenta[*cd*]pyrene[b,h]	0.349 ± 0.068
1-Methylfluoranthene[e,f,i,j,m]	3.17 ± 0.11
3-Methylfluoranthene[e,f,i,j,m]	6.09 ± 0.83
1-Methylpyrene[e,f,i,j]	2.05 ± 0.14
3-Methylchrysene[e,f,i,j,n,o]	2.17 ± 0.10
6-Methylchrysene[e,f,i,j,n,o]	1.57 ± 0.04[g]
Coronene[e,f,p]	9.48 ± 0.28

Extraction Conditions	Mass Fractions (mg/kg)[a]
PFE at 100 °C	
Naphthalene[e,h,q]	5.16 ± 0.48[g]
Biphenyl[e,h,k,q]	0.965 ± 0.035
Acenaphthylene[c,e,q]	0.365 ± 0.019
Fluorene[e,h,k,q]	0.762 ± 0.029
Anthracene[e,h,k,q,r,s]	1.56 ± 0.20[g]
2-Methylanthracene[h,q]	0.60 ± 0.11
Dibenzothiophene[e,h,q]	9.54 ± 0.56
1,2-Dimethylphenanthrene[t]	6.3 ± 0.5
1,6-, 2,5-, and 2,9-Dimethylphenanthrene[t]	38 ± 3
1,8-Dimethylphenanthrene[t]	4.5 ± 0.5
2,6-Dimethylphenanthrene[t]	29 ± 2
2,7-Dimethylphenanthrene[t]	20 ± 2
3,6-Dimethylphenanthrene[t]	23 ± 2
8-Methylfluoranthene[i,j]	3.60 ± 0.12[g]
2-Methylpyrene[i,j,n,o]	5.8 ± 1.4
4-Methylpyrene[i,j,n]	5.14 ± 0.63
1-Methylchrysene[n,o]	1.46 ± 0.05
2-Methylchrysene[i,j,n,o]	2.50 ± 0.26[g]
1-Methylbenz[*a*]anthracene[o]	0.355 ± 0.010
2-Methylbenz[*a*]anthracene[i,j]	0.43 ± 0.19
6-Methylbenz[*a*]anthracene[o]	5.28 ± 0.17
9- and 3-Methylbenz[*a*]anthracene[i,j]	0.61 ± 0.17
11-Methylbenz[*a*]anthracene[i,j]	0.36 ± 0.15
PFE at 200 °C	
Naphthalene[f]	7.29 ± 0.38
Biphenyl[b,c,f,l]	3.47 ± 0.17
Acenaphthylene[b,c,d,f]	1.36 ± 0.04
Fluorene[b,c,d,f]	1.27 ± 0.04
Anthracene[b,c,d,f,m]	7.58 ± 0.35
2-Methylanthracene[b,c]	5.88 ± 0.46
Dibenzothiophene[f,l,m]	20.9 ± 1.5

[a] The reference values, unless otherwise footnoted, are weighted means of the mass fractions from multiple analytical methods [19]. The uncertainty listed is an expanded uncertainty about the mean [19,20], with coverage factor, $k = 2$, calculated by combining within method variances with a between method variance [21] following the ISO/JCGM Guide [22,23].

[b] GC/MS (IIa) on a proprietary relatively nonpolar phase after PFE at 200 °C and 13.8 MPa with toluene.

[c] GC/MS (IIb) on 50 % phenyl-substituted methylpolysiloxane phase same extract as GC/MS (IIa).

[d] GC/MS (IVa) on 50 % phenyl-substituted methylpolysiloxane phase after PFE at 200 °C and 13.8 MPa with DCM.

[e] GC/MS (VIII) on non-polar extra low bleed proprietary phase after PFE with toluene at 100 °C and two pressures (13.8 MPa and 20.7 MPa).

[f] GC/MS (VIII) on non-polar extra low bleed proprietary phase after PFE with toluene at 200 °C and two pressures (13.8 MPa and 20.7 MPa).

[g] The reference value is a weighted mean of average mass fractions, with one average from each of two or more analytical methods [19,20]. The expanded uncertainty is the half width of a symmetric 95 % parametric bootstrap confidence interval [24], which is consistent with the ISO/JCGM Guide [22,23]. The effective coverage factor, k, = 2.

[h] GC/MS (Ia) on a proprietary relatively nonpolar phase after PFE at 100 °C and 13.8 MPa with toluene.

[i] GC/MS (Va) on 50 % phenyl-substituted methylpolysiloxane phase after PFE at 100 °C with DCM.

[j] GC/MS (VIa) on 50 % phenyl-substituted methylpolysiloxane phase after PFE at 100 °C with DCM.

[k] GC/MS (IIIa) on 50 % phenyl-substituted methylpolysiloxane phase after PFE at 100 °C and 13.8 MPa with DCM.

[l] GC/MS (IVa) on 50 % phenyl-substituted methylpolysiloxane phase after PFE at 200 °C and 13.8 MPa with DCM.

[m] GC/MS (IVb) on dimethyl 50 % polysiloxane liquid crystalline stationary phase with same extract as GC/MS (IVa)

[n] GC/MS (VIb) on dimethyl 50 % polysiloxane liquid crystalline stationary phase with same extract as GC/MS (VIa).

[o] GC/MS (Vb) on dimethyl 50 % polysiloxane liquid crystalline stationary phase with same extract as GC/MS (Va).

[p] GC/MS (VII) on 50 % phenyl-substituted methylpolysiloxane phase after PFE at 100 °C with DCM.

[q] GC/MS (Ib) on 50 % phenyl-substituted methylpolysiloxane phase same extract as GC/MS (Ia).

[r] GC/MS (Environment Canada) on a proprietary relatively nonpolar phase.

[s] GC/MS (IIIb) on dimethyl 50 % polysiloxane liquid crystalline stationary phase with same extract as GC/MS (IIIa).

[t] Reference values based on GC/MS analyses on 5 % and/or 50 % phenyl-substituted methylpolysiloxane phase after PFE at 100 °C and 13.8 MPa with DCM from SRM 1650a.

Table 4. Reference Mass Fraction Values for PAHs of Relative Molecular Mass 302 in SRM 1650b

PAH	Mass Fractions[a,b] (mg/kg)
Dibenzo[*b*,*e*]fluoranthene	0.375 ± 0.034
Naphtho[1,2-*b*]fluoranthene	2.31 ± 0.21
Naphtho[1,2-*k*]fluoranthene and Naphtho[2,3-*j*]fluoranthene	1.71 ± 0.17
Naphtho[2,3-*b*]fluoranthene	0.427 ± 0.048
Dibenzo[*b*,*k*]fluoranthene	1.68 ± 0.17
Dibenzo[*a*,*k*]fluoranthene	0.148 ± 0.009
Dibenzo[*j*,*l*]fluoranthene	1.31 ± 0.09
Dibenzo[*a*,*l*]pyrene	0.137 ± 0.024
Naphtho[2,3-*e*]pyrene	0.770 ± 0.073
Dibenzo[*a*,*e*]pyrene	1.13 ± 0.049
Naphtho[2,1-*a*]pyrene	0.818 ± 0.052
Dibenzo[*e*,*l*]pyrene	0.770 ± 0.095
Benzo[*b*]perylene	0.125 ± 0.013

[a] The reference values are weighted means of the mass fractions from multiple analytical methods [19]. The uncertainty listed with each value is an expanded uncertainty about the mean [19,20], with coverage factor, $k = 2$, calculated by combining within method variances with a between method variance [21] following the ISO/JCGM Guide [22,23].
[b] GC/MS on 50 % phenyl-substituted methylpolysiloxane phase after PFE at 100 °C and 13.8 MPa with DCM.

Table 5. Reference Mass Fraction Values for Selected Nitro-PAHs in SRM 1650b Based on Extraction Method and Conditions

Extraction Conditions	Mass Fractions[a] (µg/kg)
PFE at temperatures between 100 °C and 200 °C	
1-Nitronaphthalene[b,c,d,e]	85.6 ± 1.1
2-Nitronaphthalene[b,c,d,e]	236 ± 5
2-Nitrobiphenyl[b,c,d,e]	16.1 ± 0.7[f]
3-Nitrobiphenyl[b,c,d,e]	57.3 ± 1.6
5-Nitroacenaphthene[b,c,d,e]	36.8 ± 0.6[f]
2-Nitrofluorene[b,c,d,e]	46.0 ± 1.5
PFE at 100 °C	
9-Nitroanthracene[b,c,d,g]	5940 ± 90[f]
4-Nitrophenanthrene[b,c]	152 ± 3
1-Nitrofluoranthene[b,c]	272 ± 4[f]
8-Nitrofluoranthene[b,c]	112 ± 6[f]
4-Nitropyrene[b,c]	137 ± 4[f]
6-Nitrobenzo[*a*]pyrene[b,c,g]	1420 ± 26[f]
3-Nitrobenzo[*e*]pyrene[b,c]	79.8 ± 6.7[f]
1,3-Dinitropyrene[b,c,g]	45.5 ± 1.6[f]
1,6-Dinitropyrene[b,c]	83.3 ± 2.3[f]
PFE at 200 °C	
9-Nitroanthracene[e]	6930 ± 210[f]

[a] The reference values, unless otherwise footnoted, are weighted means of the mass fractions from multiple analytical methods [19]. The listed uncertainty is an expanded uncertainty about the mean [19,20], with coverage factor, $k = 2$, calculated by combining within-method variances with a between-method variance [21] following the ISO/JCGM Guide [22,23].
[b] GC/NICI-MS (I) on 50 % phenyl-substituted methylpolysiloxane stationary phase.
[c] GC/NICI-MS (II) on 50 % phenyl-substituted methylpolysiloxane stationary phase.
[d] GC/NICI-MS (III) on 50 % phenyl-substituted methylpolysiloxane phase after PFE with toluene at 100 °C and two pressures (13.8 MPa and 20.7 MPa).
[e] GC/NICI-MS (III) on 50 % phenyl-substituted methylpolysiloxane phase after PFE with toluene at 200 °C and two pressures (13.8 MPa and 20.7 MPa).
[f] The reference value is a weighted mean of the average mass fractions, with one average from each of two or more analytical methods [19,20]. The expanded uncertainty is the half width of a symmetric 95 % parametric bootstrap confidence interval [24], which is consistent with the ISO/JCGM Guide [22,23] with an effective coverage factor, *k*, equals 2.
[g] GC/NCI-HRMS on 5 % phenyl-substituted methylpolysiloxane stationary phase.

Table 6. Reference Value for Percent Extractable Mass for SRM 1650b[a]

	Mass Fractions[b] (%)
Percent Extractable Mass	20.2 ± 0.4

[a] Reference value for percent extractable mass reported for SRM 1650a is applicable to SRM 1650b.
[b] Reference value is the mean of results obtained using one analytical technique. The expanded uncertainty, U, is calculated as $U = ku_c$, where u_c is one standard deviation of the analyte mean, and the coverage factor, $k = 2$, is determined from the Student's t-distribution corresponding to the associated degrees of freedom and 95 % confidence level for each analyte.

Table 7. Information Values for Particle-Size Characteristics and Specific Surface Area for SRM 1650b[a]

Mean Particle Diameter, d(0.5)[b]	0.18	µm
Particle Diameter, d(0.1)[c]	0.12	µm
Particle Diameter, d(0.9)[d]	0.33	µm
Volume Weighted Mean[e]	0.22	µm
Specific Surface Area (S)[f]	108	m^2/g

[a] These values are provided for informational purposes only. The values have not been confirmed by an independent analytical technique as required for certification. See Figure 1 for particle-size distribution for SRM 1650b after 1 h and 24 h sonication.
[b] d(0.5) is the particle-size distribution parameter indicating the particle size below which 50 % of the volume is present.
[c] d(0.1) is the particle-size distribution parameter indicating the particle size below which 10 % of the volume is present.
[d] d(0.9) is the particle-size distribution parameter indicating the particle size below which 90 % of the volume is present.
[e] The volume weighted mean is the particle size in a uniform distribution.
[f] Specific surface area determined by multi-point N_2 gas adsorption BET equation [15].

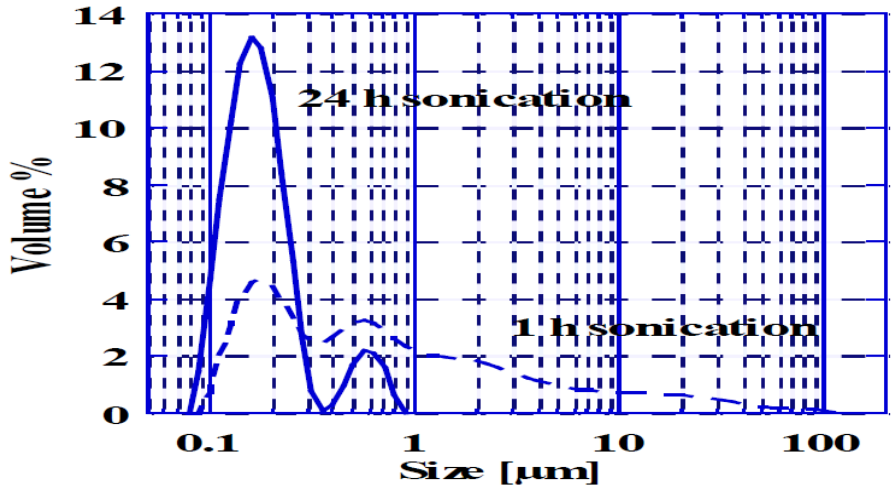

Figure 1. Particle-size distribution for SRM 1650b after 1 h and 24 h sonication.
See "Particle Size Information, Specific Surface Area, and Porosity" section for additional information.

REFERENCES

[1] SRM 1650; *Diesel Particulate Matter*; National Institute of Standards and Technology; U.S. Department of Commerce: Gaithersburg, MD (1985).

[2] SRM 1650a; *Diesel Particulate Matter*; National Institute of Standards and Technology; Department of Commerce: Gaithersburg, MD (2000).

[3] Poster, D.L.; Lopez de Alda, M.J.; Schantz, M.M.; Sander, L.C.; Vangel, M.G.; Wise, S.A.; *Development and Analysis of Three Diesel Particulate-Related Standard Reference Materials for the Determination of Chemical, Physical, and Biological Characteristics*; Polycyclic Aromat. Compd., Vol. 23, pp. 141–191 (2003).

[4] Poster, D.L.; Benner, B.A., Jr.; Schantz, M.M.; Sander, L.C.; Vangel, M.G.; Wise, S.A.; *Determination of Methyl-Substituted Polycyclic Aromatic Hydrocarbons in Diesel Particulate-Related Standard Reference Materials*; Polycyclic Aromat. Compd., Vol. 23, pp. 113–139 (2003).

[5] May, W.; Parris, R.; Beck II, C.; Fassett, J.; Greenberg, R.; Guenther, F.; Kramer, G.; Wise, S.; Gills, T.; Colbert, J.; Gettings, R.; MacDonald, B.; *Definitions of Terms and Modes Used at NIST for Value-Assignment of Reference Materials for Chemical Measurements*; NIST Special Publication 260-136; U.S. Government Printing Office: Washington, DC (2000); available at: http://www.nist.gov/srm/publications.cfm (accessed July 2013).

[6] Lippa, K.A.; Schantz, M.M.; *Microhomogeneity Evaluation of Polycyclic Aromatic Hydrocarbons in Particulate Standard Reference Materials*; Anal. Bioanal. Chem., Vol. 387, pp. 2389–2399 (2007).

[7] Schantz, M.M.; Nichols, J.J.; Wise, S.A.; *Evaluation of Pressurized Fluid Extraction for the Extraction of Environmental Matrix Reference Materials*; Anal. Chem., Vol. 69, pp. 4210–4219 (1997).

[8] Schubert, P.; Schantz, M.M.; Sander, L.C.; Wise, S.A.; *Determination of Polycyclic Aromatic Hydrocarbons with Molecular Mass 300 and 302 in Environmental-Matrix Standard Reference Materials by Gas Chromatography-Mass Spectrometry*; Anal. Chem., Vol. 75, pp. 234–246 (2003).

[9] Bezabeh, D.Z.; Bamford, H.A.; Schantz, M.M.; Wise, S.A.; *Determination of Nitrated Polycyclic Aromatic Hydrocarbons in Diesel Particulate-Related Standard Reference Materials by Using Gas Chromatography/Mass Spectrometry With Negative Ion Chemical Ionization*; Anal. Bioanal. Chem., Vol. 375, pp. 381–388 (2003).

[10] Bamford, H.A.; Bezabeh, D.Z.; Schantz, M.M.; Wise, S.A.; Baker, J.E.; *Determination and Comparison of Nitrated-Polycyclic Aromatic Hydrocarbons Measured in Air and Diesel Particulate Reference Materials*; Chemosphere, Vol. 50, pp. 575–587 (2003).

[11] Schantz, M.M.; McGaw, E.; Wise, S.A.; *Pressurized Liquid Extraction of Diesel and Air Particulate Standard Reference Materials: Effects of Extraction Temperature and Pressure*; Anal. Chem., Vol. 84, pp. 8222–8231 (2012).

[12] Bergvall, C.; Westerholm, R.; *Determination of 252–302 Da and Tentative Identification of 316–376 Da Polycyclic Aromatic Hydrocarbons in Standard Reference Materials 1649a Urban Dust and 1650b and 2975 Diesel Particulate Matter by Accelerated Solvent Extration - HPLC-GC-MS*; Anal. Bioanal. Chem., Vol. 391, pp. 2235–2248 (2008).

[13] Masala, S.; Ahmed, T.; Bergvall, C.; Westerholm, R.; *Improved Efficiency of Extraction of Polycyclic Aromatic Hydrocarbons (PAHs) from the National Institute of Standards and Technology (NIST) Standard Reference Material Diesel Particulate Matter (SRM 2975) using Accelerated Solvent Extraction*; Anal. Bioanal. Chem., Vol. 401, pp. 3305–3315 (2011).

[14] Gregg, S.J.; Sing, K.S.W.; *Adsorption, Surface Area and Porosity*; 2nd, Academic Press, London (1982).

[15] Brunauer, S.; Emmett, P.; Teller, E.; *Adsorption of Gases in Multimolecular Layers*; J. Am. Chem. Soc., Vol. 60, pp. 309–319 (1938).

[16] Barrett, E.P.; Joyner, L.G.; Halenda, P.P.; *The Determination of Pore Volume and Area Distributions in Porous Substances. I. Computations for Nitrogen Isotherms*; J. Am. Chem. Soc., Vol. 73, pp. 373–380 (1951).

[17] Lewtas, J.; Claxton, L.D.; Rosenkranz, H.S.; Schuetzle, D.; Shelby, M.; Matsushita, H.; Wurgler, F.E.; Zimmermann, F.K.; Lofroth, G.; May, W.E.; Krewski, D.; Matsushima, T.; Ohnishi, Y.; Gopalan, H.N.G.; Sarin, R.; Becking, G.C.; *Design and Implementation of a Collaborative Study of the Mutagenicity of Complex Mixtures in Salmonella Typhimurium*; Mutat. Res., Vol. 276, pp. 3–9 (1992).

[18] Claxton, L.D.; Douglas, G.; Krewski, D.; Lewtas, J.; Matsushita, H.; Rosenkranz, H.; *Overview, Conclusions, and Recommendations of the IPCS Collaborative Study on Complex Mixtures*; Mutat. Res., Vol. 276, pp. 61–80 (1992).

[19] Dersimonian, R.; Laird, N.; *Meta-Analysis in Clinical Trials*; Control Clin. Trials, Vol. 7, pp. 177–188 (1986).

[20] Rukhin, A.L.; *Weighted Means Statistics in Interlaboratory Studies*; Metrologia, Vol. 46, pp. 323–331 (2009).

[21] Horn, R.A.; Horn, S.A.; Duncan, D.B.; *Estimating Heteroscedastic Variance in Linear Models*; J. Am. Stat. Assoc., Vol. 70, pp. 380–385 (1975).

[22] JCGM 100:2008; *Evaluation of Measurement Data - Guide to the Expression of Uncertainty in Measurement*; (GUM 1995 with Minor Corrections), Joint Committee for Guides in Metrology (JCGM) (2008); available at http://www.bipm.org/utils/common/documents/jcgm/JCGM_100_2008_E.pdf (accessed July 2013); see also Taylor, B.N.; Kuyatt, C.E.; *Guidelines for Evaluating and Expressing the Uncertainty of NIST Measurement Results*; NIST Technical Note 1297, U.S. Government Printing Office: Washington, DC (1994); available at http://www.nist.gov/pml/pubs/index.cfm (accessed July 2013).

[23] JCGM 101:2008; *Evaluation of Measurement Data – Supplement 1 to the "Guide to the Expression of Uncertainty in Measurement" - Propagation of Distributions using a Monte Carlo Method*; JCGM (2008); available at http://www.bipm.org/utils/common/documents/jcgm/JCGM_101_2008_E.pdf (accessed July 2013).

[24] Efron, B.; Tibshirani, R.J.; *An Introduction to the Bootstrap*; Chapman & Hall (1993).

[25] MacCrehan, W.A.; May, W.E.; Yang, S.D.; Benner, B.A., Jr.; *Determination of Nitro Polynuclear Aromatic Hydrocarbons in Air and Diesel Particulate Matter Using Liquid Chromatography With Electrochemical and Fluorescence Detection*; Anal. Chem., Vol. 60, pp. 194–199 (1988).

National Institute of Standards & Technology

Certificate of Analysis

Standard Reference Material® 2975

Diesel Particulate Matter (Industrial Forklift)

This Standard Reference Material (SRM) is intended for use in evaluating analytical methods for the determination of selected polycyclic aromatic hydrocarbons (PAHs) in diesel particulate matter and similar matrices. In addition to certified, reference, and information values for selected PAHs and nitro-subsituted PAHs, reference or information values are provided for total extractable mass, particle-size distribution, and specific surface area. All of the chemical constituents for which certified, reference, and information values are provided in SRM 2975 are naturally present in the particulate material. A unit of SRM 2975 consists of a bottle containing 1 g of the diesel particulate matter collected from an industrial diesel-powered forklift.

Diesel particulate matter from the same lot of material that was used to prepare SRM 2975 was also used to prepare SRM 1975 *Diesel Particulate Extract* [1], which is a dichloromethane extract of the diesel particulate matter. A second diesel particulate material, SRM 1650b *Diesel Particulate Matter* [2], which was originally issued in 1985, is representative of heavy-duty diesel engine particulate emissions.

Certified Concentration Values: Certified values for concentrations, expressed as mass fractions, are provided for 11 PAHs in Table 1. A NIST certified value is a value for which NIST has the highest confidence in its accuracy, in that all known or suspected sources of bias have been investigated or accounted for by NIST [3]. The certified values for the PAHs and nitro-substituted are based on the agreement of results obtained at NIST from two or more independent analytical methods.

Reference Concentration Values: Reference values for concentrations, expressed as mass fractions, are provided for 28 additional PAHs (some in combination) in Table 2 and for 17 nitro-substituted PAHs in Table 3. Reference values for total extractable mass and the particle-size distribution are provided in Tables 4 and 5, respectively. Reference values are noncertified values that represent best estimates of the true value; however, the values do not meet the NIST criteria for certification and are provided with associated uncertainties that may reflect only measurement precision, may not include all sources of uncertainty, or may reflect a lack of sufficient statistical agreement among multiple analytical methods.

Information Concentration Values: Information values are provided for the concentrations, expressed as mass fractions, of 11 PAHs of molecular mass 302 in Table 6 and for specific surface area as determined by gas adsorption in Table 7. An information value is considered to be a value that may be of use to the SRM user, but insufficient information is available to assess the uncertainty associated with the value or only a limited number of analyses were performed.

Expiration of Certification: The certification of SRM 2975 is valid, within the measurement uncertainties specified, until **31 January 2018,** provided the SRM is handled and stored in accordance with the instructions given in this certificate. However, the certification is nullified if the SRM is damaged, contaminated, or otherwise modified.

Maintenance of SRM Certification: NIST will monitor this SRM over the period of its certification. If substantive technical changes occur that affect the certification before the expiration of this certificate, NIST will notify the purchaser. Registration (see attached sheet) will facilitate notification.

Stephen A. Wise, Chief
Analytical Chemistry Division

Robert L. Watters, Jr, Chief
Measurement Services Division

Gaithersburg, MD 20899
Certificate Issue Date: 19 March 2009
See Revision History on Last Page

The coordination of the technical measurements leading to the certification of SRM 2975 was under the leadership of S.A. Wise of the NIST Analytical Chemistry Division.

Analytical measurements for the certification of SRM 2975 were performed at NIST by H.M. Bamford, D. Bezabeh, M. Lopez de Alda, D.L. Poster, L.C. Sander, M.M. Schantz, P. Schubert, and L. Walton of the NIST Analytical Chemistry Division. Specific surface area, porosity, and 1-nitropyrene measurements were provided by P. Scheepers of the Department of Epidemiology at Katholieke Universiteit Nijmegen, Nijmegen, The Netherlands. The particle-size distribution data were provided by Honeywell, Inc., Clearwater, FL.

The diesel particulate material was provided by M.E. Wright of the Donaldson Company, Inc., Minneapolis, MN.

Consultation on the statistical design of the experimental work and evaluation of the data were provided by S.D. Leigh and M.G. Vangel of the NIST Statistical Engineering Division.

Support aspects involved in the issuance of this SRM were coordinated through the NIST Measurement Services Division.

NOTICE AND WARNING TO USERS

Storage: SRM 2975 should be stored in its original bottle at temperatures less than 30 °C and away from direct sunlight.

Handling: This material is a naturally occurring diesel particulate material and contains constituents of known and unknown toxicities and mutagenicities. Therefore, appropriate caution and care should be exercised during its handling and use.

INSTRUCTIONS FOR USE

Prior to removal of subsamples for analysis, the contents of the bottle should be mixed.

PREPARATION AND ANALYSIS[1]

Sample Collection and Preparation: The diesel particulate material used to prepare SRM 2975 was obtained from M.E. Wright of the Donaldson Company, Inc., Minneapolis, MN. The material was collected from a filtering system designed specifically for diesel-powered forklifts [4]. This diesel particulate material was selected based on a recommendation by J. Lewtas, US Environmental Protection Agency, Research Triangle Park, NC. The diesel particulate material was received at NIST in a 55-gal drum. The material was removed from the drum and homogenized in a V-blender for 1 h and then stored in polyethylene bags. A total of 13.7 kg of diesel particulate material was homogenized; a total of 5.65 kg of material was extracted for preparation of SRM 1975 [1] and the remaining diesel particulate material was bottled for distribution as SRM 2975.

Polycyclic Aromatic Hydrocarbons (Tables 1 and 2): The general approach used for the value assignment of the PAHs in SRM 2975 was similar to that reported for the recent certification of several environmental matrix SRMs [5–8] and consisted of combining results from analyses using various combinations of different extraction techniques and solvents, cleanup/isolation procedures, and chromatographic separation and detection techniques. This approach consisted of Soxhlet extraction and pressurized fluid extraction (PFE) using dichloromethane (DCM) or toluene/methanol mixture, cleanup of the extracts using solid phase extraction (SPE), followed by analysis using the following techniques: (1) reversed-phase liquid chromatography with fluorescence detection (LC-FL) analysis of isomeric PAH fractions isolated by normal-phase LC (i.e., multidimensional LC) and (2) gas chromatography/mass spectrometry (GC/MS) analysis of the PAH fraction on three stationary phases of different selectivity (i.e., a 5 % [mole fraction]) phenyl-substituted methylpolysiloxane phase, a 50 % phenyl-substituted methylpolysiloxane phase, and a smectic liquid crystalline stationary phase.

Seven sets of GC/MS results, designated as GC/MS (Ia and Ib), GC/MS (II), GC/MS (III), and GC/MS (IVa, IVb, and IVc), were obtained using three columns with different selectivities for the separation of PAHs. For GC/MS (I) analyses, duplicate subsamples of 100 mg from eight bottles of SRM 2975 were extracted with toluene:methanol (1:1 by volume) using PFE (excess volume in the PFE cells was filled with clean sodium sulfate) as described by

[1]Certain commercial equipment, instrumentation, or materials are identified in this report to adequately specify the experimental procedure. Such identification does not imply recommendation or endorsement by National Institute of Standards and Technology nor does it imply that the materials or equipment identified are necessarily the best available for the purpose.

Schantz et al. [9]. The extracts were concentrated to about 0.5 mL and placed on an aminopropylsilane SPE cartridge and eluted with 20 mL of 2 % DCM in hexane. The eluant was concentrated and then analyzed by GC/MS using a 0.25 mm i.d. × 60 m fused silica capillary column with a 5 % (mole fraction) phenyl-substituted methylpolysiloxane phase (0.25 µm film thickness) (DB-5 MS, Agilent Technologies, [Wilmington, DE]) [GC/MS (Ia)]. A subset of 8 of the 16 extracts from GC/MS (Ia) were also analyzed on a 50 % (mole fraction) phenyl-substituted methylpolysiloxane stationary phase (0.25 mm i.d. × 60 m, 0.25 µm film thickness) (DB-17MS, Agilent Technologies) [GC/MS (Ib)]. For the GC/MS (II) analyses, 100 mg samples of SRM 2975 were extracted with DCM using PFE; the extracts were processed and analyzed as described above for GC/MS (Ia). GC/MS (III) was identical to GC/MS (II) except that Soxhlet extraction with DCM for 18 hours was used instead of PFE. For the GC/MS (IV) analyses, subsamples of 40 mg to 100 mg of SRM 2975 were extracted with DCM using PFE and the extracts processed as for GC/MS (I). The processed extracts were then analyzed by GC/MS using three different columns: 5 % phenyl methylpolysiloxane [GC/MS (IVa)], 50 % phenyl methylpolysiloxane [GC/MS (IVb)], and a 0.2 mm i.d. × 25 m (0.15 µm film thickness) smectic liquid crystalline phase (SB-Smectic, Dionex, Lee Scientific Division, [Salt Lake City, UT]) [GC/MS (IVc)].

For the LC-FL results, subsamples of approximately 200 mg from each of six bottles of SRM 2975 were Soxhlet extracted for 20 hours using 200 mL of DCM. The extracts were concentrated and processed through aminopropylsilane SPE cartridges as described above for the GC/MS analyses. The processed extract was further fractionated using normal-phase LC on a semi-preparative aminopropylsilane column (µBondapak NH_2, 9 mm i.d. × 30 cm, Waters Associates, [Milford, MA]) to isolate isomeric PAH fractions as described previously [10–12]. Four fractions were collected containing PAHs of molecular mass: 178 and 202 (fraction 1), 228 (fraction 2), 252 and 276 (fraction 3) and 278 (fraction 4). All of PAH fractions were analyzed using a 5-µm particle-size polymeric octadecylsilane (C_{18}) column (4.6 mm i.d. × 25 cm, Hypersil-PAH, Keystone Scientific, Inc., [Bellefonte, PA]) with wavelength programmed fluorescence detection [11–13]. For all of the GC/MS and LC-FL measurements described above, selected perdeuterated PAHs were added to the diesel particulate samples prior to solvent extraction for use as internal standards for quantification purposes.

Homogeneity Assessment for PAHs: The homogeneity of SRM 2975 was assessed by analyzing duplicate samples of 100 mg each from eight bottles selected by stratified random sampling. Samples were processed and analyzed as described above for GC/MS (I). Statistically significant differences among bottles were observed for the PAHs at the 100 mg sample size, and this source of variability has been incorporated in the calculation of the uncertainty associated with the assigned values.

PAH Isomers of Molecular Mass 302 (Table 6): For the determination of the molecular mass 302 isomers, samples of approximately 100 mg each were extracted using PFE with DCM as the extraction solvent. The extracts were then concentrated with a solvent change to hexane and passed through an aminopropyl SPE cartridge and eluted with 40 mL of 10 % DCM in hexane (volume fraction). The processed extract was then analyzed by GC/MS using a 0.25 mm i.d. × 60 m fused silica capillary column with a 50 % phenyl-substitued methylpolysiloxane phase (0.25 µm film thickness) (DB-17MS, Agilient Technologies). Perdeuterated dibenzo[*a,i*]pyrene was added to the diesel particulate matter prior to extraction for use as an internal standard.

Nitro-Substituted PAHs (Table 3): SRM 2975 was analyzed at NIST and one other laboratory for the determination of nitro-substituted PAHs. At NIST, three sets of three, five, and four samples of SRM 2975 (~100 mg each) were spiked with the following perdeuterated nitro-PAHs for use as internal standards: 9-nitroanthracence-d_9, 3-nitrofluoranthene-d_9, 1-nitropyrene-d_9, and 6-nitrochrysene-d_{11}. The samples were extracted using PFE with DCM as the extraction solvent. Following concentration, each sample was processed through an aminopropylsilane SPE cartridge using 40 mL of 20 % DCM in hexane. The concentrated eluant was then subjected to normal-phase LC using a semi-preparative amino/cyano phase column with a mobile phase of 20 % DCM in hexane to isolate the nitro-PAH fraction. The nitro-PAH fraction was analyzed by GC with negative chemical ionization mass spectrometry (GC/NCI-MS) using a 0.25 mm i.d. × 30 m fused silica capillary column containing a 5 % diphenyl-substituted dimethylsiloxane phase, 0.25 µm film thickness or a 50 % phenyl-subsituted methylpolysiloxane phase, 0.25 µm film thickness.

The concentration of 1-nitropyrene was also measured at the Department of Epidemiology at Katholieke Universiteit Nijmegen, Nijmegen, The Netherlands using the GC/MS method [14].

Mutagenicity: The mutagenicity of solvent extracts of SRM 2975 has not been determined; however, the mutagenicity values for SRM 1975 should be applicable to extracts of SRM 2975. The diesel particulate of SRM 2975 was used for the preparation of SRM 1975 *Diesel Particulate Extract*, a DCM extract of the SRM 2975 diesel particulate matter. SRM 1975 was prepared by Soxhlet extraction using DCM of multiple samples of SRM 2975.

Reference values for mutagenic activity for SRM 1975 are reported in the Certificate of Analysis for SRM 1975 [1] and in detail in reference 15.

Percent Extractable Mass (Table 4): For the determination of percent extractable mass, six subsamples of approximately 1 g to 2 g of SRM 2975 were extracted using Soxhlet extraction for 18 h with DCM. The extract was concentrated to approximately 20 mL and then filtered to remove particulate matter. Aliquots of 100 µL to 150 µL were placed in tared aluminum foil pans; the DCM was evaporated until constant mass was obtained and then the mass of the remaining residue was determined.

Particle-Size Information (Table 5): Dry particle-size distribution measurements for SRM 2975 were obtained as part of a collaborative effort with Honeywell, Inc., Clearwater, FL. A Microtrac® particle analyzer, which makes use of light-scattering techniques, was used to measure the particle-size distribution of SRM 2975. Briefly, a reference beam is used to penetrate a field of particles and the light that scatters in the forward direction from the field is measured and the particle size as a volume distribution is derived via a computer-assisted analysis. From these data, the total volume, average size, and a characteristic width of the particle-size distribution are calculated. The system has a working range from 0.7 µm to 700 µm.

Specific Surface Area and Porosity (Table 6): The specific surface area and porosity were determined based on nitrogen gas adsorption measurements [16]. The gas adsorption measurements were performed on a NOVA-1200 instrument, Quantachrome Corp., Boynton Beach, FL at 77 K after the samples were outgassed for 24 h at 120 EC under vacuum. The nitrogen isotherms were analyzed using the Brunauer-Emmet-Teller (BET) equation [17] to obtain the surface area (Table 6) and the Barrett-Joyner-Halenda (BJH) method [18] to obtain the porosity. Based on the BJH method, SRM 2975 shows a wide distribution of mesopores, but with substantial outer area. The pore diameter of the particles in SRM 2975 range from 4 nm to 35 nm with the greater number of particles at about 20 nm.

Table 1. Certified Concentrations for Selected PAHs in SRM 2975

	Mass Fractions (mg/kg)[a]
Phenanthrene[b,c,d,e,f,g]	17.0 ± 2.8
Fluoranthene [b,c,,d,e,f,g]	26.6 ± 5.1
Pyrene[b,c,d,e,f,g]	0.90 ± 0.24
Benz[*a*]anthracene[b,c,d,e,f,g,h]	0.317 ± 0.066
Chrysene[g,h]	4.56 ± 0.16
Triphenylene[g,h]	5.22 ± 0.20
Benzo[*j*]fluoranthene [h,i]	0.82 ± 0.11
Benzo[*k*]fluoranthene[c,d,e,f,g,h,i]	0.678 ± 0.076
Benzo[*e*]pyrene[b,c,d,e,f,h]	1.11 ± 0.10
Benzo[*a*]pyrene[e,f,g,h]	0.0522 ± 0.0053
Benzo[*ghi*]perylene[b,c,e,f]	0.498 ± 0.044

[a] Each set of results is expressed as the certified value ± the expanded uncertainty. Each certified value is a mean of the means from two or more analytical methods. For results from two methods, the certified value is the equally weighted mean; for results from three or more methods, the certified value is the mean weighted as described in Paule and Mandel [19]. Each uncertainty, computed according to the CIPM approach as described in the ISO and NIST Guides [3], is an expanded uncertainty at the 95 % level of confidence, which includes random sources of uncertainty within each analytical method and among methods, as well as uncertainty due to the variation among the bottles. The expanded uncertainty defines a range of values within which the true value is believed to lie, at a level of confidence of approximately 95 %

[b] GC/MS (Ia) on 5 % phenyl-substituted methylpolysiloxane phase after PFE with toluene:methanol mixture

[c] GC/MS (II) on 5 % phenyl-substituted methylpolysiloxane phase after PFE with DCM

[d] GC/MS (III) on 5 % phenyl-substituted methylpolysiloxane phase after Soxhlet extraction with DCM

[e] GC/MS (IVa) on 5 % phenyl-substituted methylpolysiloxane phase after PFE with DCM

[f] GC/MS (IVb) on 50 % phenyl-substituted methylpolysiloxane phase of same extracts as GC/MS (IVa)

[g] LC-FL of isomeric PAH fractions after Soxhlet extraction with DCM

[h] GC/MS (IVc) on a smectic liquid crystalline phase of same extracts as GC/MS (IVa)

[i] GC/MS (Ib) on 50 % phenyl-substituted methylpolysiloxane phase of selected extracts from GC/MS (Ia)

Table 2. Reference Concentrations for Selected PAHs in SRM 2975

	Mass Fractions (mg/kg)[a]
1-Methylphenanthrene[b,c,d,e,f]	0.89 ± 0.11
2-Methylphenanthrene[b,c,d,e,f]	2.0 ± 0.2
3-Methylphenanthrene[b,c,d,e,f]	1.0 ± 0.2
4- and 9-Methylphenanthrene[b,c,d,e,f]	0.44 ± 0.09
1,2-Dimethylphenanthrene[e,f]	0.05 ± 0.02
1,6-, 1,7-, 2,5-, and 2,9-Dimethylphenanthrene[e,f]	0.57 ± 0.08
1,8-Dimethylphenanthrene[e,f]	0.06 ± 0.02
2,6-Dimethylphenanthrene[e,f]	0.25 ± 0.05
2,7-Dimethylphenanthrene[e,f]	0.23 ± 0.05
3,6-Dimethylphenanthrene[e,f]	0.18 ± 0.02
Anthracene[e,g]	0.038 ± 0.008
Benzo[*ghi*]fluoranthene[h]	10.2 ± 0.5
8-Methylfluoranthene[f]	0.068 ± 0.004
1-, 3-, and 7-Methylfluoranthene[e]	0.53 ± 0.03
2-Methylpyrene[e,f]	0.040 ± 0.008
4-Methylpyrene[e,f]	0.022 ± 0.005
Benzo[*c*]phenathrene [b,c,d,e,f,i]	1.0 ± 0.4
Benzo[*a*]fluoranthene[f,i]	0.06 ± 0.02
Benzo[*b*]fluoranthene[f,h,i]	11.5 ± 3.6
Perylene[g]	0.054 ± 0.009
Indeno[1,2,3-*cd*]pyrene[e,f]	1.4 ± 0.2
Indeno[1,2,3-*cd*]fluoranthene[f]	1.1 ± 0.2
Dibenz[*a,j*]anthracene[e]	0.37 ± 0.07
Dibenz[*a,c*]anthracene/Dibenz[*a,h*]anthracene[e]	0.52 ± 0.08
Pentaphene[e]	0.038 ± 0.007
Benzo[*b*]chrysene[e,f]	0.08 ± 0.03
Picene[e,f]	1.0 ± 0.2
Coronene[e]	1.1 ± 0.2

[a] Each set of results is expressed as the reference value ± the expanded uncertainty. Each reference value is the mean from one analytical method or a mean of the means from two or more analytical methods. For results from two methods, the certified value is the equally weighted mean; for results from three or more methods, the certified value is the mean weighted as described in Paule and Mandel [19]. Each uncertainty, computed according to the CIPM approach as described in the ISO and NIST Guides [3], is an expanded uncertainty at the 95 % level of confidence, which includes random sources of uncertainty within each analytical method and among methods, as well as uncertainty due to the variation among the bottles. The expanded uncertainty defines a range that contains the estimate of the true value at a level of confidence of approximately 95 %.

[b] GC/MS (Ia) on 5 % phenyl-substituted methylpolysiloxane phase after PFE with toluene:methanol mixture

[c] GC/MS (II) on 5 % phenyl-substituted methylpolysiloxane phase after PFE with DCM

[d] GC/MS (III) on 5 % phenyl-substituted methylpolysiloxane phase after Soxhlet extraction with DCM

[e] GC/MS (IVa) on 5 % phenyl-substituted methylpolysiloxane phase after PFE with DCM

[f] GC/MS (IVb) on 50 % phenyl-substituted methylpolysiloxane phase of same extracts as GC/MS (IVa)

[g] LC-FL of isomeric PAH fractions after Soxhlet extraction with DCM

[h] GC/MS (IVc) on a smectic liquid crystalline phase of same extracts as GC/MS (IVa)

[i] GC/MS (Ib) on 50 % phenyl-substituted methylpolysiloxane phase of selected extracts from GC/MS (Ia)

Table 3. Reference Concentrations for Selected Nitro-Substituted PAHs in SRM 2975

	Mass Fractions (mg/kg)[a]
1-Nitronaphthalene[b]	0.041 ± 0.005
2-Nitronaphthalene[b]	0.112 ± 0.017
9-Nitroanthracene[c]	2.97 ± 0.45
9-Nitrophenanthrene[c]	0.444 ± 0.047
3-Nitrophenanthrene[b]	0.185 ± 0.017
1-Nitrofluoranthene[b]	0.182 ± 0.056
2-Nitrofluoranthene[b]	0.205 ± 0.053
3-Nitrofluoranthene[c]	3.74 ± 0.59
8-Nitrofluoranthene[b]	0.593 ± 0.090
4-Nitropyrene[b]	0.182 ± 0.021
1-Nitropyrene[c]	34.8 ± 4.7
7-Nitrobenz[*a*]anthracene[c]	3.46 ± 0.78
6-Nitrochrysene[c]	2.22 ± 0.45
6-Nitrobenzo[*a*]pyrene[c]	1.36 ± 0.27
1,3-Dinitropyrene[c]	1.18 ± 0.29
1,6-Dinitropyrene[c]	2.36 ± 0.39
1,8-Dinitropyrene[b]	3.10 ± 0.57

[a] The reference value is an unweighted mean of the results from two or three data sets. The uncertainty listed with each value is an expanded uncertainty about the mean, with coverage factor 2 (approximately 95 % confidence), calculated by combining a between-method variance [20] with a pooled, within-method variance following the ISO and NIST Guides [3].
[b] Reference value is based on two data sets from methods performed at NIST.
[c] Reference value is based on three data sets from methods performed at NIST.

Table 4. Reference Value for Total Extractable Mass for SRM 2975

Total Extractable Mass[a]	2.7 % ± 0.2 % Mass Fraction[b]

[a] Extractable mass as determined from Soxhlet extraction using DCM

[b] The results are expressed as the reference value ± the expanded uncertainty. The reference value for the total extractable mass is the mean value of six measurements. The uncertainty, computed according to the CIPM approach as described in the NIST and ISO Guides [3], is an expanded uncertainty at the 95 % level of confidence. The expanded uncertainty defines a range that contains the best estimate of the true value at a level of confidence of approximately 95 %.

Table 5. Reference Values for Particle-Size Characteristics for SRM 2975

Particle Measurement	Value[a]
Mean diameter (volume distribution, MV, µm)[b]	31.9 ± 0.6
Mean diameter (area distribution, µm)[c]	11.2 ± 0.1
Mean diameter (number distribution, µm)[d]	1.62 ± 0.01
Surface Area (m^2/cm^3)[e]	0.538 ± 0.006

The following data show the percent of the volume that is smaller than the indicated size:

Percentile	Particle Diameter (µm)[a]
95	110 ± 3
90	70 ± 2
80	44.9 ± 0.8
70	32.4 ± 0.6
60	24.8 ± 0.4
50[f]	19.4 ± 0.3
40	15.2 ± 0.2
30	11.7 ± 0.2
20	8.5 ± 0.1
10	5.3 ± 0.1

[a] Each reference value is the mean value of measurements from the analysis of subsamples from four bottles. Each uncertainty, computed according to the CIPM approach as described in the NIST and ISO Guides [3], is an expanded uncertainty at the 95 % level of confidence. The expanded uncertainty defines a range that contains the best estimate of the true value at a level of confidence of approximately approximately 95 %.

[b] The mean diameter of the volume distribution represents the center of gravity of the distribution and compensates for scattering efficiency and refractive index. This parameter is strongly influenced by coarse particles.

[c] The mean diameter of the area distribution, calculated from the volume distribution with less influence from the presence of coarse particles than the MV parameter.

[d] The mean diameter of the number distribution calculated from the volume distribution.

[e] Calculated specific surface area assuming solid, spherical particles. This is a computation and should not be interchanged with an adsorption method of surface area determination (see Table 6) as this value does not reflect porosity or topographical characteristics.

[f] Median diameter (50 % of the volume is less than 19.4 µm)

Table 6. Information Concentrations of Selected PAHs of Molecular Mass 302 in SRM 2975[a]

	Mass Fraction (mg/kg)
Dibenzo[*b,e*]fluoranthene	2.7
Naphtho[1,2-*b*]fluoranthene	7.3
Naphtho[1,2-*k*]fluoranthene and Naphtho[2,3-*j*]fluoranthene	2.6
Naphtho[2,3-*b*]fluoranthene	0.37
Dibenzo[*b,k*]fluoranthene	2.7
Dibenzo[*a,k*]fluoranthene	0.71
Dibenzo[*j,l*]fluoranthene	2.3
Naphtho[2,3-*e*]pyrene	0.56
Dibenzo[*a,e*]pyrene	0.57
Dibenzo[*e,l*]pyrene	3.4

[a] These concentrations are provided as information values because the results have not been confirmed by an independe analytical technique as required for certification. These values are provided for information only.

Table 7. Information Value for Specific Surface Area of SRM 2975 as Determined by Gas Adsorption

Specific Surface Area (S)[a]	91 m^2/g

[a] Specific surface area determined by multi-point N_2 adsorption BET method.

REFERENCES

[1] SRM 1975; *Diesel Particulate Extract*; National Institute of Standards and Technology; U.S. Department of Commerce: Gaithersburg MD, 07 November 2000.

[2] SRM 1650b; *Diesel Particulate Matter*; National Institute of Standards and Technology; U.S. Department of Commerce: Gaithersburg MD, 27 September 2006.

[3] ISO; *Guide to the Expression of Uncertainty in Measurement*, ISBN 92-67-10188-9, 1st ed.; International Organization for Standardization: Geneva, Switzerland, (1993); see also Taylor, B.N.; Kuyatt, C.E., *Guidelines for Evaluating and Expressing Uncertainty of NIST Measurement Results*; NIST Technical Note 1297, U.S. Government Printing Office: Washington DC (1994); available at http://physics.nist.gov/Pubs/.

[4] Wright, M.E.; Klein, A.D. Jr.; Stesniak, E.J.; *A Diesel Exhaust Filter System for Industrial Diesel Forklifts*; SAE Technical Paper Series 911852: Warrendale, PA (1991).

[5] Wise, S.A.; Schantz, M.M.; Benner, B.A. Jr.; Hays, M.J.; Schiller, S.B.; *Certification of Polycyclic Aromatic Hydrocarbons in a Marine Sediment Standard Reference Material*; Anal. Chem. Vol. 67, pp 1171-1178 (1995).

[6] Wise, S.A.; Schantz, M.M.; Hays, M.J.; Koster, B.J.; Sharpless, K.S.; Sander, L.C.; Schiller, S.B.; *Certification of Polycyclic Aromatic Hydrocarbons in Mussel Tissue Standard Reference Materials*; Polycyclic Aromat. Compd. Vol. 12, pp 21–26, (1997).

[7] Poster, D.L.; Lopez de Alda, M.J.; Schantz, M.M.; Sander, L.C.; Vangel, M.G.; Wise, S.A.; *Certification of a Diesel Particulate Related Standard Reference Material (SRM 1975) for PAHs*; Polycyclic Aromat. Compd. Vol. 14/15, pp 23–31 (1999).

[8] Wise, S.A.; Sander, L.C.; Schantz, M.M.; Hays, M.J.; Benner, B.A. Jr.; *Recertification of Standard Reference Material (SRM) 1649 Urban Dust for the Determination of Polycyclic Aromatic Hydrocarbons (PAHs)*; Polycyclic Aromat. Compd. Vol. 13, pp. 419–456 (2000).

[9] Schantz, M.M.; Nichols, J.J.; Wise, S.A.; *Evaluation of Pressurized Fluid Extraction for the Extraction of Environmental Matrix Reference Materials*; Anal. Chem. Vol. 69, pp. 4210–4219 (1997).

[10] Wise, S.A.; Chesler, S.N.; Hertz, H.S.; Hilpert, L.R.; May, W.E.; *Chemically-Bonded Aminosilane Stationary Phase for the High Performance Liquid Chromatographic Separation of Polynuclear Aromatic Hydrocarbons*; Anal. Chem. Vol. 49, pp 2306–2310 (1977).

[11] May, W.E.; Wise, S.A.; *Liquid Chromatographic Determination of Polycyclic Aromatic Hydrocarbons in Air Particulate Extracts*; Anal. Chem. Vol. 56, pp 225–232 (1984).

[12] Wise, S.A.; Benner, B.A. Jr.; Byrd, G.D.; Chesler, S.N.; Rebbert, R.E.; Schantz, M.M.; *Determination of Polycyclic Aromatic Hydrocarbons in a Coal Tar Standard Reference Material*; Anal. Chem. Vol. 60, pp 887–894 (1988).

[13] Wise, S.A.; Deissler, A.; Sander, L.C.; *Liquid Chromatographic Determination of Polycyclic Aromatic Hydrocarbon Isomers of Molecular Weight 278 and 302 in Environmental Standard Reference Materials*; Polycyclic Aromat. Compd. Vol. 3, pp 169–184 (1993).

[14] Scheepers, P.T.J.; Velders, D.D.; Martens, M.H.J.; Noordhoek, J.; Bos, R.P.; *Gas Chromatographic-Mass Spectrometric determination of Nitro Polycyclic Aromatic Hydrocarbons in Airbourne Particulate Matter from Workplace Atmospheres Contaminated with Diesel Exhaust*; J. Chromatogr. Vol. 677, pp. 107–121 (1994).

[15] Hughes, T.J; Lewtas, J.; Claxton, L.D.; *Development of a Standard Reference Material for Diesel Mutagenicity in the Salmonella Plate Incorporation Assay*; Mutat. Res. Vol. 391, pp. 243–258 (1997).

[16] Gregg, S.J.; Sing, K.S.W.; *Adsorption, Surface Area and Porosity*, 2nd ed., Academic Press, London (1982).

[17] Brunauer, S.; Emmett, P.H.; Teller, E.; *Adsorption of Gases in Multimolecular Layers*; J. Amer. Chem. Soc. Vol. 60, pp 309–319 (1938).

[18] Barrett, E.P.; Joyner, L.G.; Halenda, P.P.; *The Determination of Pore Volume and Area Distributions in Porous Substances. I. Computations for Nitrogen Isotherms*; J. Amer. Chem. Soc. Vol. 73, pp. 373–380 (1951).

[19] Paule, R.C.; Mandel, J.; *Consensus Values and Weighting Factors*; J. Research NBS Vol. 87, pp. 377–385 (1982).

[20] Levenson, M.S.; Banks, D.L.; Eberhardt, K.R.; Gill, L.M.; Guthrie, W.F.; Liu, H.K.; Vangel, M.G.; Yen, J.H.; Zhang, N.F.; *An Approach to Combining Results From Multiple Methods Motivated by the ISO GUM*; J. Res. Natl. Inst. Stand. Technol., Vol. 105, pp. 571–579 (2000).

Certificate Revision History: 19 March 2009 (Addition of reference and information values and update of expiration date); 10 April 2008 (Update of expiration date and editorial changes); 07 November 2000 (Original certificate date).

Users of this SRM should ensure that the certificate in their possession is current. This can be accomplished by contacting the SRM Program at: (301) 975-2200; fax (301) 926-4751; e-mail srminfo@nist.gov; or via the Internet http://www.nist.gov/srm.